The role of BAHD acyltransferases in poplar (*Populus* spp.) secondary metabolism and synthesis of salicinoid phenolic glycosides.

by

Russell James Chedgy
B.Sc., University of Exeter, 1999
M.Sc., University of British Columbia, 2006

A Dissertation Submitted in Partial Fulfillment
of the Requirements for the Degree of

DOCTOR OF PHILOSOPHY

in the Department of Biology

Supervisory Committee

The role of BAHD acyltransferases in poplar (*Populus* spp.) secondary metabolism and synthesis of salicinoid phenolic glycosides.

by

Russell James Chedgy
B.Sc., University of Exeter, 1999
M.Sc., University of British Columbia, 2006

Supervisory Committee

Dr. C. Peter Constabel, Supervisor
(Department of Biology)

Dr. Jürgen Elthing, Departmental Member
(Department of Biology)

Dr. Rachael Scarth, Departmental Member
(Department of Biology)

Dr. Chris Upton, Outside Member
(Department of Biochemistry)

Abstract

Supervisory Committee

Dr. C. Peter Constabel, Supervisor
(Department of Biology)

Dr. Jürgen Elthing, Departmental Member
(Department of Biology)

Dr. Rachael Scarth, Departmental Member
(Department of Biology)

Dr. Chris Upton, Outside Member
(Department of Biochemistry)

The salicinoids are phenolic glycosides (PGs) characteristic of the Salicaceae family and are known defenses against insect herbivory. Common examples are salicin, salicortin, tremuloidin, and tremulacin, which accumulate to high concentrations in the leaves and bark of willows and poplars. Despite their important role in plant defense, their biosynthetic pathway is not known, although recent work has suggested that benzyl benzoate acts as a possible biosynthetic intermediate. We identified three candidate genes encoding BAHD-type acyltransferases that are predicted to produce benzylated secondary metabolites, named *PtACT47*, *PtACT49*, and *PtACT54*.

Expression of *PtACT47* and *PtACT49* generally correlated with PG content in a variety of tissues and organs of wild type hybrid poplar plants. This correlation was also found in transgenic hybrid poplar where PG content varied with the level of expression of the condensed tannin regulator MYB134 transcript. In these plants, a suppression of *PtACT47* and *PtACT49* expression was correlated with lower PG content. In contrast, *PtACT54* exhibited very low expression in all tissues tested, and this level of expression was not affected in MYB134 plants.

In order to better understand their possible biochemical functions, cDNA cloning, heterologous expression, and *in vitro* functional characterization was performed on these three BAHD acyltransferases. Recombinant PtACT47 exhibited a low substrate selectivity and could utilize acetyl-CoA, benzoyl-CoA, and cinnamoyl-CoA as acyl donors with a variety of alcohols as acyl acceptors. This enzyme showed the greatest

K_m/K_{cat} ratio (45.8 nM^{-1} sec^{-1}) and lowest K_m values (45.1 μM) with benzoyl-CoA and salicyl alcohol, and was named benzoyl-CoA:salicyl alcohol *O*-benzoyltransferase (PtSABT). Recombinant PtACT49 utilized a narrower range of substrates, specifically benzoyl-CoA and acetyl-CoA and a limited number of alcohols. Its highest K_m/K_{cat} (31.8 nM^{-1} sec^{-1}) and lowest K_m (55.3 μM) was observed for benzoyl-CoA and benzyl alcohol, and it was named benzoyl-CoA:benzyl alcohol *O*-benzoyltransferase (PtBEBT). Both enzymes were also capable of synthesizing plant volatile alcohol esters at trace levels, for example hexenyl benzoate. Recombinant PtACT54 shares low sequence identity with PtSABT (52.3%) and PtBEBT (52.5%) and exhibited only moderate BEBT-like properties. PtSABT and PtBEBT appear to be paralogs based on their high sequence identity (90.6%) and closely related yet distinct biochemical functions. They likely arose from gene duplication and subsequent functional diversification possibly by neofunctionalization.

Wounding experiments showed that abiotic damage stimulated the synthesis of specific PGs, notably salicin and salicortin within 24-48hrs. This was accompanied by a proportional increase in the expression of *PtSABT* and *PtBEBT*. Furthermore, experiments using transgenic RNAi lines with knock-down suppression of *PtBEBT*, and *PtSABT*, and both genes simultaneously, provided the first direct evidence that BAHD acyltransferases are important in PG production. *PtSABT* suppression, both individually and in the double knock-down suppression, significantly lowered salicortin content, particularly in mature leaves. However, a reduced level of *PtBEBT* expression did not have a significant effect on the PGs measured. This could indicate that BEBT-like activity may be a shared function among closely related BAHDs. The suppression of multiple *BEBT*-like genes may be necessary to further delineate their functions.

Table of Contents

List of Tables

List of Figures

List of Abbreviations

^{o}C	Degrees Celsius
bp	Base pairs
CAS #	Chemical abstracts service number
cm	Centimeters
CoA	Coenzyme A
C_t	Cycle threshold
CT	Condensed tannins (proanthocyanidins)
dry wt	Dry weight
fr. wt	Fresh weight
g	Grams
GC-MS	Gas chromatography with mass spectrometry
HPLC	High performance liquid chromatography
hrs	Hours
I.S.	Internal standard
K_{cat}	Enzyme turnover number
kDa	Kilodaltons
kHz	Kilohertz
K_m	Michaelis–Menten constant (μM)
K_m/K_{cat}	Enzyme specificity ratio
L	Litre
LC-MS	Liquid chromatography with mass spectrometry
LOD	Limit of detection
mins	Minutes
mL	Milliliter
mm	Millimeter
MYB	Myeloblastosis family of transcription factors
nm	Nanometers
PCR	Polymerase chain reaction
PG	Phenolic glycosides
PtACT	*Populus trichocarpa* acyltransferase
PtBEBT	*Populus trichocarpa* benzoyl-CoA:benzyl alcohol *O*-benzoyltransferase
PtSABT	*Populus trichocarpa* benzoyl-CoA:salicyl alcohol *O*-benzoyltransferase
qPCR	Quantitative polymerase chain reaction
RNAi	RNA interference
SDS–PAGE	Sodium dodecyl sulfate polyacrylamide gel electrophoresis
T_R	Retention time
UV	Ultraviolet
Vmax	Enzyme maximum velocity (μM sec^{-1})
μg	Microgram

μL	Microliter
μm	Micrometer

Acknowledgements

I would like to thank, first and foremost, my graduate supervisor, Dr. C. Peter Constabel, for his guidance and support throughout this work. I would also like to thank members of my graduate committee, Dr. Jürgen Elthing, Dr. Rachael Scarth, Dr. Chris Upton, and Dr. Martin Boulanger for their advice and help with this project. Thank you to Dr. Eran Pichersky, University of Michigan, for supplying the *Clarkia breweri* BEBT plasmid; Dr. John D'Auria, Texas Tech University for helpful discussions on BAHD assays; Dr. Tobias G. Köllner, Max Planck Institute for Chemical Ecology, Jena, Germany for GC-MS analysis; Mr. Cuong Le and Mr. Darryl Hardie, UVic Genome BC Proteomics Centre for LC-MS analysis; Mr. Philip-Edouard Shay, University of Victoria, for his assistance with statistical analyses; and Mr. Brad Binges, Glover Greenhouse Facility, University of Victoria, for help with plant care. I would like to thank Dr. Vincent Walker for his advice regarding HPLC analysis of plant phenolic extracts and to Dr. Kazuko Yoshida for her advice with molecular cloning work. This work was funded by the Natural Sciences and Engineering Research Council of Canada (Discovery Grants and Accelerator Supplements to C.P.C. and a Postgraduate Scholarship to myself). I would also like to thank my family, friends and colleagues for their years of support.

Co-authorship Statement

The majority of the work and writing presented in this thesis is my own. In places, portions of text are taken from Chedgy *et al*. (2015). This article was a collaborative effort between Dr. C. Peter Constabel, Dr. Tobias G. Köllner, and myself. The majority of the writing responsibilities for this publication were taken by Dr. Constabel and myself, while Dr. Köllner provided valuable editorial input. The sections where text is included from this publication are clearly stated at the beginning of each chapter.

For the confirmation of enzyme products by mass spectroscopy shown in section 3.3 and Figures 3.8 and 3.9, the GC-MS analysis was carried out by Dr. Tobias G. Köllner at the Max Planck Institute for Chemical Ecology, Jena, Germany, and the LC-MS by Mr. Cuong Le and Dr. Darryl Hardie at the UVic Proteomics Centre, Victoria. For both types of analysis, I performed the preparative steps by first conducting the enzyme assays using recombinant proteins, and for GC-MS I extracted the chemical products in hexane before samples were sent for analysis, for the LC-MS analysis I was present during the analysis. The text for the method descriptions of these analyses shown in section 2.14 was partially written by Dr. Tobias G. Köllner for GC-MS, and Mr. Cuong Le for LC-MS.

Dr. Constabel offered advice and input into the content of this thesis and performed editing duties throughout the writing process. Figures that are redrawn, updated or taken from other researchers' publications are clearly stated as such in the figure titles.

Chapter 1. Introduction and research objectives

Some portions of text in Sections 1.1; 1.2; and 1.3 were taken from Chedgy *et al*. (2015).

1.1. Phytochemistry of *Populus*

The genus *Populus* is widely distributed throughout the northern hemisphere, and individual species are adapted to diverse ecosystems ranging from desert to riparian to the alpine (Lindroth and St. Clair, 2013). They are fast-growing forest trees subject to attack by a variety of vertebrate and invertebrate herbivores, including several insect species that manifest large-scale population outbreaks (Mattson *et al*., 2001). The success of *Populus* is in part due to their phenotypic plasticity and phytochemical diversity. *Populus* trees typically accumulate large amounts of phenolic compounds, including condensed tannins (CTs, proanthocyanidins), hydroxycinnamic acids, and salicinoid phenolic glycosides (PGs) (Hwang and Lindroth, 1997; Constabel and Lindroth, 2010). The salicinoids are found only in the Salicaceae which comprises *Salix* (willows) and *Populus* (poplars, aspens, and cottonwoods), and they can accumulate to high concentrations in leaves, bark, buds and extrafloral nectaries (Boeckler *et al*., 2011; Constabel and Lindroth, 2010; Young *et al*., 2010*a*). They are composed of a core of glucose and salicyl alcohol, either of which is typically esterified with phenolic or hydroxycinnamic acids. The most common examples of PGs include salicin (1), salicortin (2), tremuloidin (3), and tremulacin (4) but many additional related structures are known (Boeckler *et al*., 2011). A summary of the chemical structures and related information of the majority of the PGs identified to date, as well as degradation products of interest is shown in Figure 1.1 and Table 1.1. The chemicals shown have been identified from a variety of species within the *Populus* and *Salix* genera. Many of the compounds shown are not ubiquitous within the Salicaceae, and are unique to individual species or to a limited number of species. However, PGs such as salicin (1) and salicortin (2) are prevalent among the Salicaceae. Some examples of these compounds can accumulate to significant levels, for example trembling aspen (*P. tremuloides*) can exhibit a foliar PG content of up to 19% dry wt. (Donaldson *et al*., 2006*a*). However, there is tremendous genotype-specific variation in phytochemical content, including the PGs, in poplar (Hwang and Lindroth, 1997). This variation is illustrated in Table 1.2 that

Table 1.1. Common names, chemical structures and relevant literature for selected salicinoid PGs of the Salicaceae and degradation products of interest.

Common name	CAS #	Chemical structure	Formula	Relevant literature
(1) Salicin	138-52-3	*β*-D-Glucopyranoside,2-(hydroxymethyl)phenyl	$C_{13}H_{18}O_7$	Braconott, 1830; Thieme, 1963, 1964*a*, 1964*b*, 1965*a*, 1965*b*, 1965*c*, 1965*d*.
(2) Salicortin	29836-41-7	β-D-Glucopyranoside,2-[[[(1-hydroxy-6-oxo-2cyclohexen-1-yl)carbonyl]oxy]methyl]phenyl	$C_{20}H_{24}O_{10}$	Pearl and Darling, 1971*a*, 1971*b*, 1971*c*; Thieme, 1964*c*, 1965*d*
(3) Tremuloidin	529-66-8	*β*-D-Glucopyranoside,2-(hydroxymethyl)phenyl,2-benzoate	$C_{20}H_{22}O_8$	Pearl and Darling, 1959; Thieme, 1965*d*
(4) Temulacin	29836-40-6	*β*-D-Glucopyranoside,2-[[[(1-hydroxy-6-oxo-2-cyclohexen-1-yl)carbonyl]oxy]methyl]phenyl,2-benzoate	$C_{27}H_{28}O_{11}$	Pearl and Darling, 1971*c*; Thieme and Richter, 1966
(5) Arbutin	497-76-7	*β*-D-Glucopyranoside, 4-hydroxyphenyl	$C_{12}H_{16}O_7$	Kolehmainen *et al*., 1995
(6) Helicin	618-65-5	Salicylaldehyde *β*-D-glucoside	$C_{13}H_{16}O_7$	Thieme, 1963
(7) 2′-*O*-acetylsalicin	143885-60-3	*β*-D-Glucopyranoside, 2-(hydroxymethyl)phenyl, 2-acetate	$C_{15}H_{20}O_8$	Julkunen-Tiitto and Meier, 1992; Reichardt *et al*., 1992
(8) Salicyloylsalicin	27968-78-1	*β*-D-Glucopyranoside,2-[[(2-hydroxybenzoyl)oxy]methyl]phenyl	$C_{20}H_{22}O_9$	Charaux and Rabate, 1942
(9) 2′-*O*-acetylsalicortin	113270-30-7	*β*-D-Glucopyranoside,2-[[[(1-hydroxy-6-oxo-2-cyclohexen-1-yl)carbonyl]oxy]methyl]phenyl,2-acetate	$C_{22}H_{26}O_{11}$	Meier *et al*., 1987; Meier *et al*., 1988
(10) 3′-*O*-acetylsalicortin	n/a	β-D-Glucopyranoside,3-[[[(1-hydroxy-6-oxo-2-cyclohexen-1-yl)carbonyl]oxy]methyl]phenyl,2-acetate	$C_{22}H_{26}O_{11}$	Poukens-Renwart *et al*., 1993
(11) 6′-*O*-acetylsalicortin	n/a	β-D-Glucopyranoside,6-[[[(1-hydroxy-6-oxo-2-cyclohexen-1-yl)carbonyl]oxy]methyl]phenyl,2-acetate	$C_{22}H_{26}O_{11}$	Lee *et al*., 2013
(12) 2′,6′-*O*-acetylsalicortin	n/a	β-D-Glucopyranoside,2,6-[[[(1-hydroxy-6-oxo-2-cyclohexen-1-yl)carbonyl]oxy]methyl]phenyl,2-acetate	$C_{24}H_{29}O_{12}$	Lee *et al*., 2013
(13) HCH-salicortin	157072-22-5	*β*-D-Glucopyranoside,2-[[[(1-hydroxy-6-oxo-2-cyclohexen-1-yl)carbonyl]oxy]methyl]phenyl,6-(1-hydroxy-6-oxo-2-cyclohexene-1-carboxylate)	$C_{27}H_{30}O_{13}$	Picard *et al*., 1994
(14) 2′-Cinnamoylsalicortin	143183-59-9	*β*-D-Glucopyranoside,2-[[[(1-hydroxy-6-oxo-2-cyclohexen-1-yl)carbonyl]oxy]methyl]phenyl,2-[(2*E*)-3-phenyl-2-propenoate]	$C_{29}H_{30}O_{11}$	Nichols-Orians *et al*., 1992
(15) Salicyloyltremuloidin	10059-19-5	*β*-D-Glucopyranoside,2-[[(2-hydroxybenzoyl)oxy]methyl]phenyl,2-benzoate	$C_{27}H_{26}O_{10}$	Pearl and Darling, 1959
(16) Chaenomeloidin	138101-84-5	*β*-D-Glucopyranoside,2-(hydroxymethyl)phenyl,3-benzoate	$C_{20}H_{22}O_8$	Mizuno *et al*., 1991

Table 1.1. (Continued) Common names, chemical structures and relevant literature for selected salicinoid PGs of the Salicaceae and degradation products of interest.

Common name	CAS #	Chemical structure	Formula	Relevant literature
(17) Deltoidin	31025-54-4	*β*-D-Glucopyranoside,2-(hydroxymethyl)phenyl,2-(2-hydroxybenzoate)	$C_{20}H_{22}O_9$	Pearl and Darling, 1971*a*
(18) Fragilin	19764-02-4	*β*-D-Glucopyranoside,2-(hydroxymethyl)phenyl,6-acetate	$C_{15}H_{20}O_8$	Thieme, 1963*a*
(19) Grandidentatin	28876-24-6	*β*-D-Glucopyranoside,2-hydroxycyclohexyl, 2-[3-(4-hydroxyphenyl)-2-propenoate] (9CI)	$C_{21}H_{28}O_9$	Pearl and Darling, 1962
(20) Isograndidentatin A	n/a	*cis*-2-hydroxycyclohexyl-4′-*O*-*p*-coumaroyl-*β*-glucopyranoside	$C_{21}H_{28}O_9$	Si *et al*., 2009
(21) Isograndidentatin B	n/a	*cis*-2-hydroxycyclohexyl-6′-*O*-*p*-coumaroyl-*β*-glucopyranoside	$C_{21}H_{28}O_9$	Si et al., 2009
(22) Lasiandrin	144398-33-4	*β*-D-Glucopyranoside,2-[[[(1-hydroxy-6-oxo-2-cyclohexen-1-yl)carbonyl]oxy]methyl]phenyl,2-acetate 6-(1-hydroxy-6-oxo-2-cyclohexene-1-carboxylate)(9CI)	$C_{29}H_{32}O_{14}$	Reichardt *et al*., 1992
(23) Nigracin	18463-25-7	*β*-D-Glucopyranoside,4-hydroxy-2-(hydroxymethyl)phenyl,6-benzoate	$C_{20}H_{22}O_9$	Fukui, 1954; Thieme and Benecke, 1967
(24) Populin	99-17-2	*β*-D-Glucopyranoside,2-(hydroxymethyl)phenyl,6-benzoate	$C_{20}H_{22}O_8$	Bridel, 1919; Richtmyer and Yeakel, 1934
(25) Populoside	26632-35-9	*β*-D-Glucopyranoside,2-[[[(2E)-3-(3,4-dihydroxyphenyl)-1-oxo-2-propen-1-yl]oxy]methyl]phenyl	$C_{22}H_{24}O_{10}$	Erickson *et al*., 1970; Gird *et al*., 2001; Zhang *et al*., 2006
(26) Populoside A	913254-38-3	*β*-D-Glucopyranoside,4-hydroxy-2-[[[(2*E*)-3-(4-hydroxyphenyl)-1-oxo-2-propen-1-yl]oxy]methyl]phenyl	$C_{22}H_{24}O_{10}$	Zhang *et al*., 2006
(27) Populoside B	913253-98-2	*β*-D-Glucopyranoside,2-[[[(2*E*)-3-(4-hydroxyphenyl)-1-oxo-2-propen-1-yl]oxy]methyl]phenyl	$C_{22}H_{24}O_9$	Zhang *et al*., 2006
(28) Populoside C	913254-00-9	*β*-D-Glucopyranoside,2-[[[(2*E*)-3-(4-hydroxy-3-methoxyphenyl)-1-oxo-2-propen-1-yl]oxy]methyl]phenyl	$C_{23}H_{26}O_{10}$	Zhang *et al*., 2006
(29) Salireposide	16955-55-8	*β*-D-Glucopyranoside,2-[(benzoyloxy)methyl]-4-hydroxyphenyl	$C_{20}H_{22}O_9$	Thieme, 1963, 1964*a*, 1964*b*, 1965*a*, 1965*b*, 1965*c*, 1965*d*
(30) Trichocarposide	17063-94-4	*β*-D-Glucopyranoside,2-(hydroxymethyl)phenyl,6-[(2*E*)-3-(4-hydroxyphenyl)-2-propenoate]	$C_{22}H_{24}O_9$	Thieme, 1965*d*
(31) Salicyl alcohol	90-01-7	2-(Hydroxymethyl)phenol	$C_7H_8O_2$	Erdmann, 1841
(32) Catechol	120-80-9	Benzene-1,2-diol	$C_6H_6O_2$	Allen, 1889
(33) 6-Hydroxy-2-cyclohexen-on-oyl moiety (6-HCH moiety)	n/a	6-Hydroxy-2-cyclohexen-on-oyl moiety	$C_7H_{10}O_4$	Mattes *et al*., 1987
(34) Cyclohexen-1,2 dione	n/a	Cyclohexan-1,2 dione	$C_6H_5O_2$	Mattes *et al*., 1987
(35) (+)-6-Hydroxy-2-cyclohexenone (6-HCH)	n/a	(+)-6-Hydroxy-2-cyclohexenone	$C_6H_5O_2$	Mattes *et al*., 1987

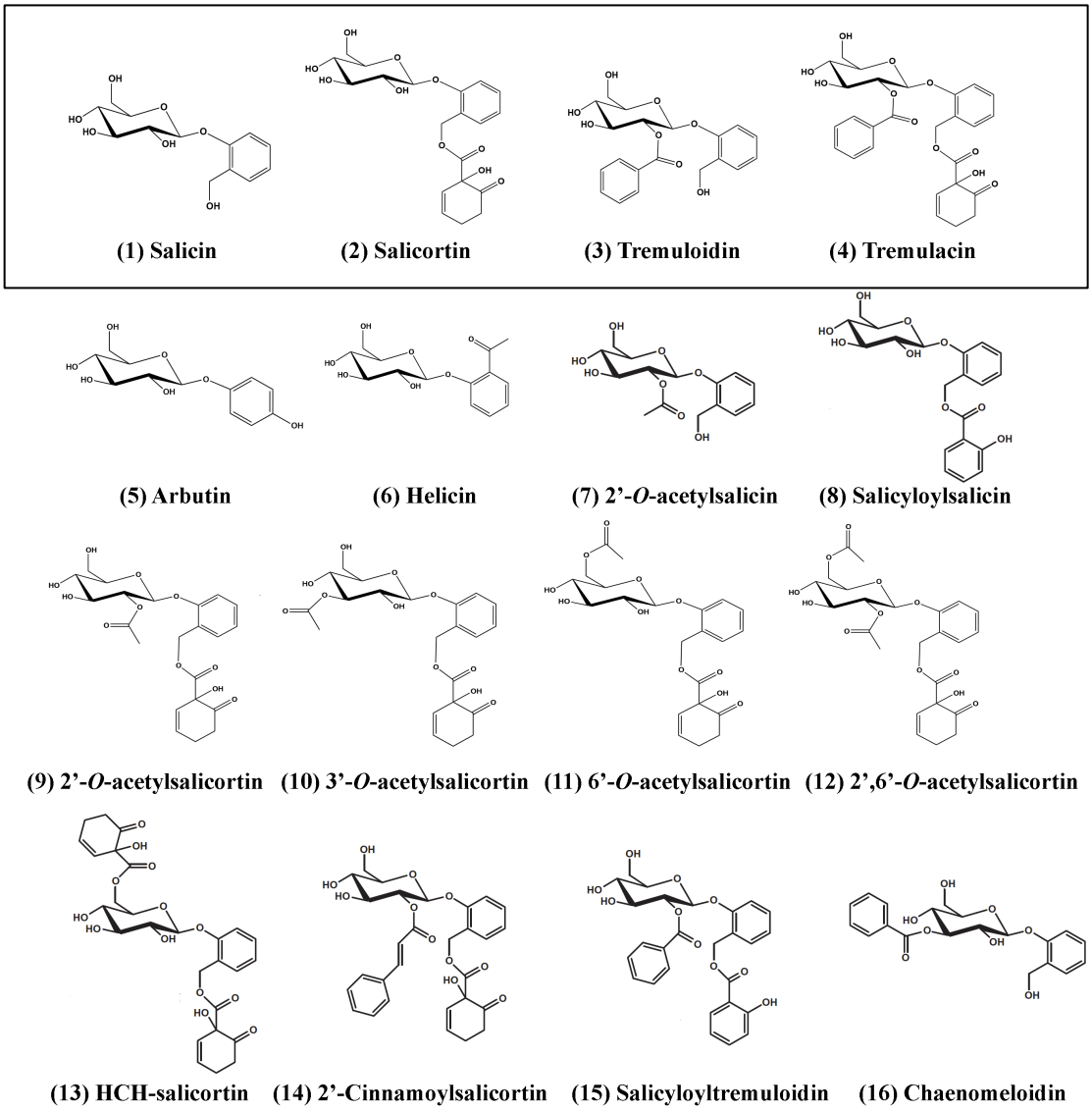

Figure 1.1. The structures and common names of salicinoid PGs of the Salicaceae and degradation products of interest.

Note: highlighted chemicals 1-4 represent the main focus of chemical analysis for this study.

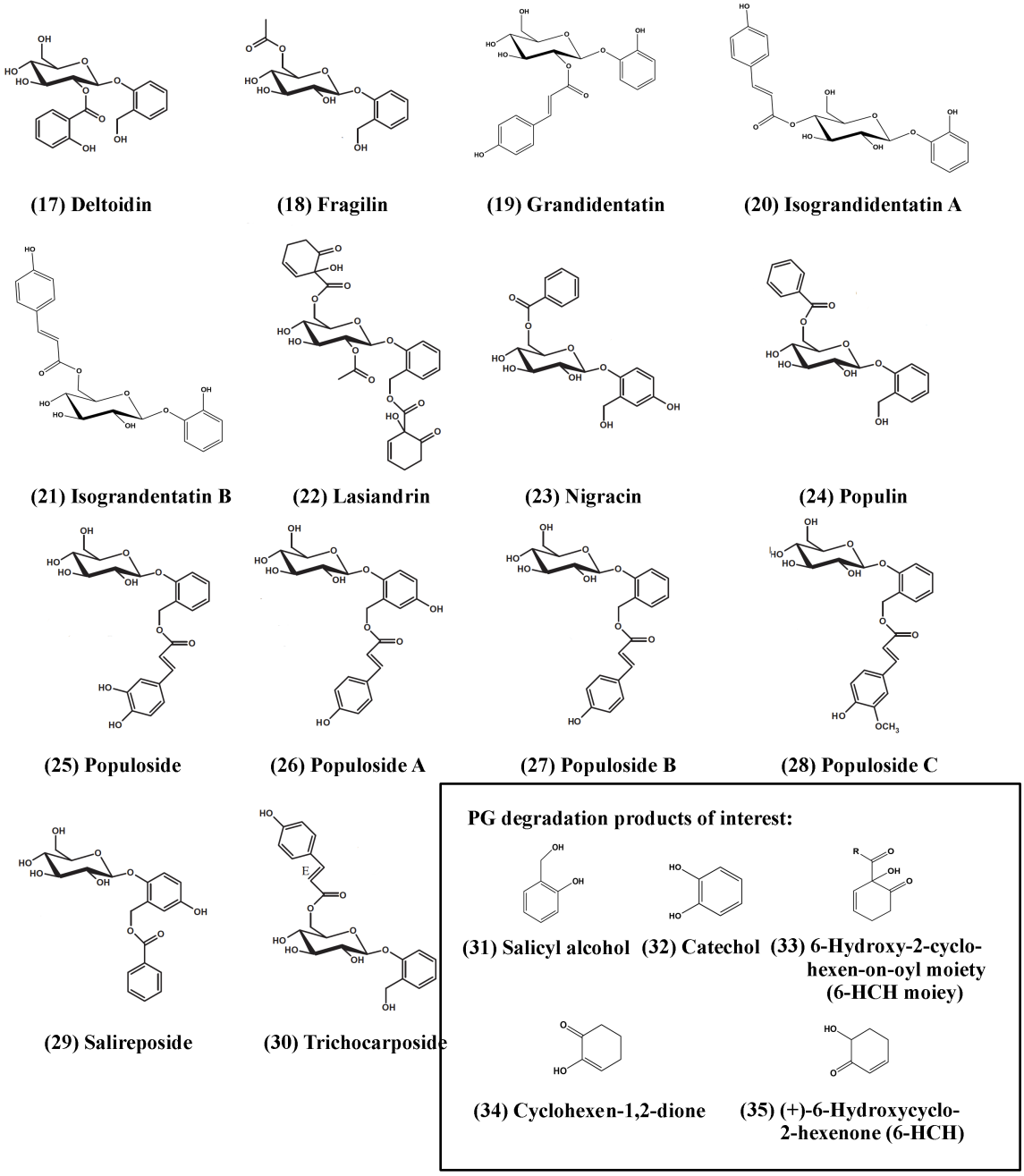

Figure 1.1. (Continued) The structures and common names of salicinoid PGs of the Salicaceae and degradation products of interest.

Note: highlighted chemicals 31-34 are PG degradation products of interest, potentially important in conferring anti-herbivory properties.

Table 1.2. A summary of the *in planta* distribution of salicinoid PGs in common *Populus* species as found in the literature.

	Mean salicinoid PG concentration (mg g^{-1} DW)			
Tissue	Salicin (1)	Salicortin (2)	Tremulacin (3)	Tremuloidin (4)
Buds	-	19.4 (12.1)[a] (*n*=8)[b]	16.6 (11.7) (*n*=7)	-
Leaves	12.2 (12.9) (*n*=7)	32.7 (27.2) (*n*=11)	28.4 (21.7) (*n*=8)	5.95 (7.8) (*n*=5)
Bark	19.3 (6.0) (*n*=2)	26.5 (4.9) (*n*=2)	-	-
Roots	-	-	-	-

Note: limited to species *P. alba*, *P. deltoides*, *P. nigra*, *P. tremula P. tremuloides*, and *P. trichocarpa*.

[a] Numbers in parenthesis represent standard deviation, [b] the number of values used to generate the mean represented by *n*. Source publications: Benedec *et al*., 2014; Clausen *et al*., 1992; Clausen *et al*., 1989; Donaldson *et al*., 2006*a*; English *et al*., 1991; Hemming and Lindroth, 2000; Hemming and Lindroth, 1999; Hwang and Lindroth, 1997; Jakubas *et al*., 1989; Julkunen-Tiitto, 1986; Julkunen-Tiitto and Sorsa, 2001; Lindroth and Kinney, 1998; Lindroth and Koss, 1996; Lindroth and Pajutee, 1987; Lindroth *et al*., 1987; Lindroth *et al*., 1988; Lindroth *et al*., 1999; Lindroth *et al*., 2001; Palo, 1984; Warren *et al*., 2003; Young *et al*., 2010*a*.

shows the *in planta* distribution of four major PGs, salicin (1), salicortin (2), tremuloidin (3), and tremulacin (4) which together can account for >90% of the total PG content in *P. trichocarpa*, and other of *Populus* species (Boeckler *et al*., 2011; Clausen *et al*., 1992; Donaldson *et al*., 2006*a*; Lindroth *et al*., 1987; Lindroth *et al*., 1999; Lindroth and Hwang, 1996), The PGs have been implicated in defense against lepidopteran herbivores (Boeckler *et al*., 2011; Hwang and Lindroth, 1997). While the synthesis of other classes of phenolic metabolites such as CTs is well documented to be responsive to herbivory and other environmental stresses (Boeckler *et al*., 2013; Hwang and Lindroth, 1997; Osier and Lindroth, 2001), the evidence for the inducibilty of PGs is somewhat ambiguous (Boeckler *et al*., 2013; Clausen *et al*, 1989; Young *et al*., 2010*b*) and historically they have been considered as standing or constitutive defenses (Boeckler *et al*., 2013).

1.2. Biosynthesis of the salicinoid phenolic glycosides

In *Populus*, the biosynthesis of flavonoids, CTs, and phenolic acids is well characterized (Figure 1.2). In contrast, the biosynthetic pathway of salicinoids is very poorly understood. However, several *in vivo* stable isotope-labeling studies have offered some insight. In other plant species, benzenoid metabolism has been shown to be derived from the amino acid L-phenylalanine (Phe, F) (Jarvis *et al*., 2000), a product of the shikimate pathway (Wegrzyn *et al*., 2010), and involves compounds such as benzaldehyde and benzyl benzoate that may also be intermediates in PG synthesis (Babst *et al*., 2010; Boatright *et al*., 2004; Jarvis *et al*., 2000; Zenk, 1967). Early work by Zenk (1967) suggested that benzaldehyde may be a key intermediate in salicin (1) production in *Salix purpurea*. Two pathways were proposed, benzoic acid ⇒ benzaldehyde ⇒ salicylaldehyde ⇒ helicin ⇒ salicin; and *trans*-cinnamic acid ⇒ *o*-coumaric acid ⇒ salicylaldehyde ⇒ helicin ⇒ salicin. Interestingly, labeled salicyl alcohol (2-hydroxybenzyl alcohol) was shown not to be a direct precursor of salicin (Zenk, 1967). In *Cucumis sativus* and *Nicotina attenuata*, Jarvis *et al*. (2000) demonstrated that benzenoid metabolites are derived from the amino acid L-Phe, since 3-hydroxy-3-phenylpropanoic acid was shown to be a metabolite of L-Phe that is subsequently incorporated into benzoic acid and salicylic acid via *trans*-cinnamic acid. The enzyme phenylalanine

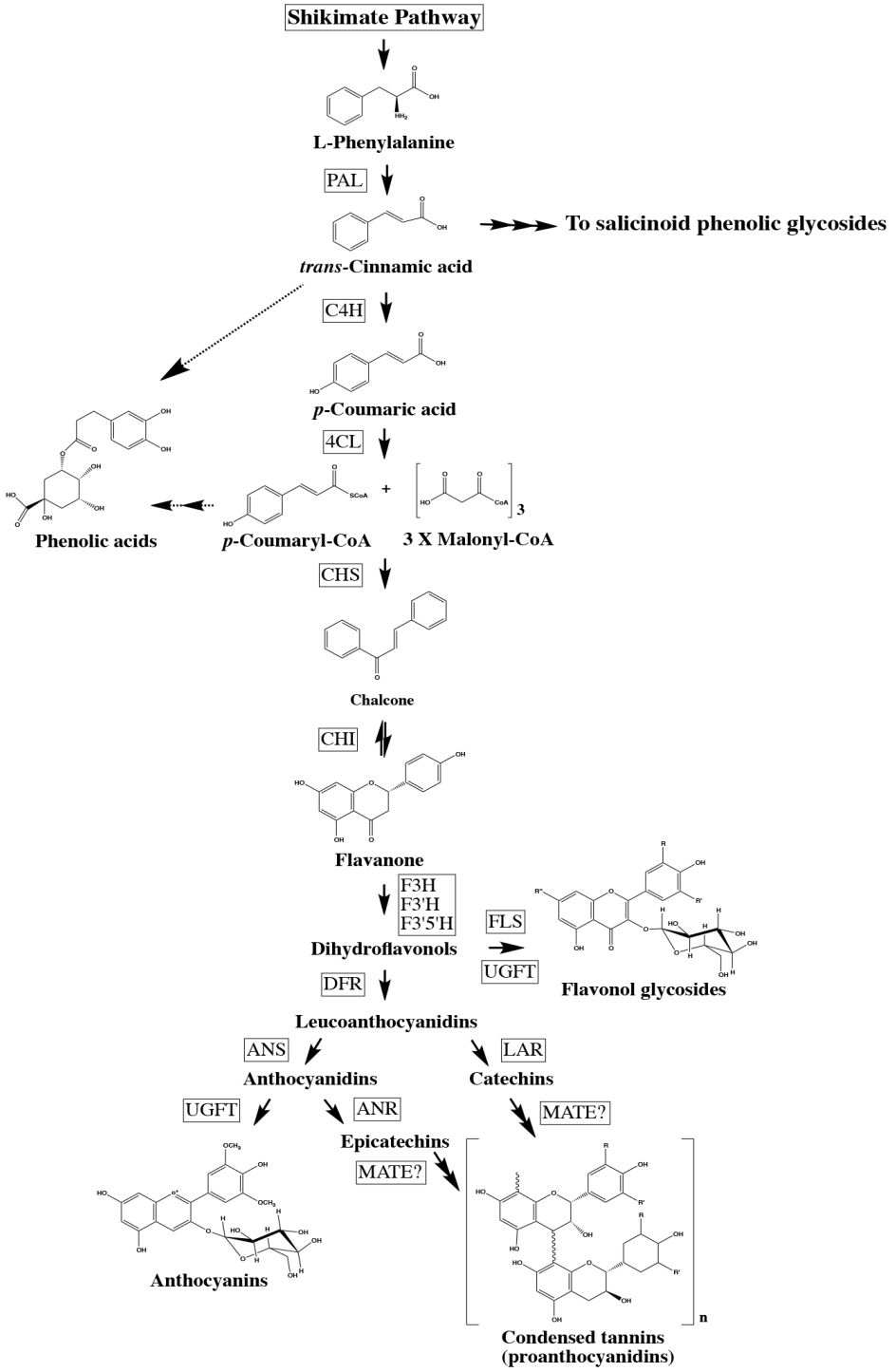

Figure 1.2. A model for phenlypropanoid metabolism in poplar (redrawn from Mellway *et al.*, 2009). PAL, Phe ammonia-lyase; C4H, cinnamate 4-hydroxylase; 4CL, 4-coumarate CoA-ligase; CHS, chalcone synthase; CHI, chalcone isomerase; F3H, flavanone 3-hydroxylase; F3'H, flavonoid 3'-hydroxylase; F3'5'H, flavonoid 3'5'-hydroxylase; DFR, dihydroflavonol reductase; FLS, flavonol synthase; LAR, leucoanthocyanidin reductase; ANS, anthocyanidin synthase; ANR, anthocyanidin reductase; MATE, multidrug and toxic compound extrusion transporter; UFGT, UDP-Glc flavonoid glucosyltransferase.

ammonia lyase (PAL) is known to catalyze the deamination of Phe to *trans*-cinnamic acid (Camm and Towers, 1973), and this marks the entry point in phenylpropanoid metabolism. Here, *trans*-cinnamic acid can either be converted to *p*-coumaric acid by the cytochrome P_{450} monooxygenase, cinnamate 4-hydroxylase (C4H) (Ro *et al*., 2001) and enter several well characterized pathways ultimately leading to phenolic acids, flavonol glycosides, anthocyanins, and CTs (Chen *et al*., 2009; Constabel and Lindroth, 2010) (Figure 1.2). Alternatively, in the Salicaceae, *trans*-cinnamic acid may be converted to benzoic acid and salicylic acid (2-hydroxybenzoic acid), marking an entry point into the pathway(s) potentially leading to PGs. The role of PAL in salicylate synthesis was further demonstrated by Ruuhola and Julkunen-Titto (2003*a*) using micropropagated *Salix pentandra* plants that had been treated with the PAL inhibitor 2-aminoindan-2-phosphonic acid (AIP). This resulted in plants with significantly reduced salicylate levels. Furthermore, exogenous application of benzoic acid, salicylic acid, and helicin increased production of some salicylates in AIP-treated plants. The researchers suggested that salicin (1) production may proceed via benzoyl-glucose, an intermediate in the synthesis of salicylic acid.

In *Cucumis sativus* and *Nicotiana attenuata*, Jarvis *et al*. (2000) observed that radio-labeled 3-hydroxy-3-phenylpropanoic acid was not incorporated into benzaldehyde, indicative of alternate pathways in which *trans*-cinnamic acid is converted to benzoic acid by a shortening of the C_3 side chain by two carbons. This side chain shortening can occur either by a CoA-dependent *β*-oxidative pathway in which benzoyl-CoA is an intermediate (Hertweck *et al*., 2001; Jarvis *et al*., 2000), or via a CoA-independent non–*β*-oxidative pathway where benzaldehyde is the intermediate (Abd El-Mawla and Beerhues, 2002; Long *et al*., 2009). Using deuterium-labeled L-Phe in *Petunia hybrida*, Boatright *et al*. (2004) observed that the flux of L-Phe through the non-*β*-oxidative pathway is twice that through the CoA-dependent *β*-oxidative pathway, signifying that both routes play a role. The researchers also predicted that benzyl benzoate may also be a key intermediate for salicylates. In addition, feeding of benzoic acid has been shown to induce accumulation of higher-order PGs in various tissues of *Salix* spp. (Ruuhola and Julkunen-Tiitto, 2003), confirming its importance in PG synthesis.

Babst *et al*. (2010) measured isotopic incorporation of ^{13}C labeled cinnamic acid,

benzoates, and salicylates into salicin (1) and salicortin (2) using *P. nigra* leaf discs. The researchers suggest that the pathways leading to salicin (1) and salicortin (2) may be separate and potentially antagonistic braches in PG metabolism. They showed that labeled benzyl alcohol was incorporated into the salicyl moiety of salicortin (2) but not salicin (1). Conversely, labeled salicyl alcohol and salicyl aldehyde were readily converted to salicin but not salicortin, and moreover, appeared to inhibit salicortin production. A metabolic grid model of PG biosynthesis was proposed by Babst *et al*. (2010) (Figure 1.3) in which benzyl benzoate is also placed as a key intermediate leading to salicortin formation. Very little is known about the PG pathway to date, including the origins of the 6-HCH moiety (33) present in PGs such as salicortin (2) and tremulacin (4), and the role of salicyl alcohol shown by Babst *et al*. (2010) to be readily converted to salicin (1), an observation that is at odds with Zenk (1967) who suggest it is not a direct precursor of salicin (1).

Given that all PGs contain glucosyl moieties, it is likely that glycosyltransferases (GTs) are involved, and it follows that the availability of carbohydrates may influence PG accumulation. There is evidence that both PG and CT accumulation demand substantial amounts of carbohydrates (Arnold *et al*., 2004). Payyavula *et al*. (2009; 2011) showed that in poplar the group-3 sucrose transporter/sucrose carrier (SUT/SUC) protein called PtSUT4 (Genbank, ADW94617.1), a tonoplast localized protein, might be important in PG synthesis. Using *in vitro* cell suspension cultures of the aspen grown in the dark, feeding cells with salicyl alcohol, salicylaldehyde and helicin, but not benzoic acid, benzyl alcohol, benzylaldehyde, salicylic acid, cinnamic acid or *o*-coumaric acid, led to increased salicin (1) and isosalicin. Interestingly, this was accompanied by a significant up-regulation of *PtSUT4* expression. This trend was most notable during the exponential and stationary phases of cell growth. Also of interest was a reciprocal reduction in CT content by up to 35% at 96 h, possibly a result of competition for the carbon resources between growth, CT and salicin synthesis. However, higher order PGs such as salicortin (2) and tremulacin (4) were not detected in cell cultures at any stage of the experiment, but were present in leaves of plant that propagated from the calli. This absence of complex PGs in cell culture may be a result of differences in compartmentalization between culture cells and fully formed plant tissues. In addition to the up-regulation of

PtSUT4, two abundant GT transcripts, *PtGT1-2* (ADL67596.1) and *PtGT1-246* (XM_002304986.2), also exhibited increased expression following feeding of salicylates. Given the glycosylated nature of PGs, GTs likely play a role in PG synthesis and genes such as these warrant further investigation.

Payyavula *et al*. (2009; 2011) also manufactured transgenic RNAi hybrid poplar (INRA 717-IB4 *P. tremula* x *P. alba*) lines with reduced *PtSUT4* expression (68% less than wild type plants). Down-regulation of *PtSUT4* resulted in the decreased abundance of both salicortin (2) and tremulacin (4) in young shoot organs, including shoot tips, young leaves, mature leaves and primary stems. Sucrose and glucose levels were higher in source leaves of PtSUT4 transgenics than wild type plants. Transgenic plants were also exposed to two growth regimes, N-depleted and N-abundant conditions. Under N deficiency, PGs decreased in wild type plants, but not in *PtSUT4* plants; notably salicortin (2) increased in shoot tips and primary stems of transgenics. Similarly, tremulacin (4) decreased in nearly all shoot organs of the wild type plants, but was sustained at levels in transgenics that were comparable to wild type plants in optimal growing conditions. In N-abundant conditions, transgenic plants showed lower levels of PGs than wild type plants. The researchers suggest that PtSUT4 may participate in the transport of sucrose from the vacuole to the cytosol where it can undergo hydrolysis by SuSy (sucrose synthase) to yield UDP-glucose (Koch, 2004), a common sugar utilized by most GTs for glycosylation (Hostel, 1981; Jones and Vogt, 2001) that could be donated to salicinoid compounds for PG production downstream. The researchers also suggest that PtSUT4 may partly regulate N-level dependent PG-CT homeostasis by differential carbohydrate allocation. See Figure 1.3 for a summary of this information and the predicted pathway leading to PG formation. For a complete model of predicted phenylpropanoid synthesis including flavonoids and PGs see Appendices Figure A1.1.1.

To date, no enzymes specific for the production of PGs have been identified, yet the nature of many of the predicted intermediate compounds offer clues as to the types of enzymes potentially involved. In particular, benzenoid intermediates such as benzyl benzoate are hypothesized to be pivotal in PG metabolism. A precedent for the production of such compounds has been set by several examples of BAHD acyltransferase which have been functionally characterized in other plants species.

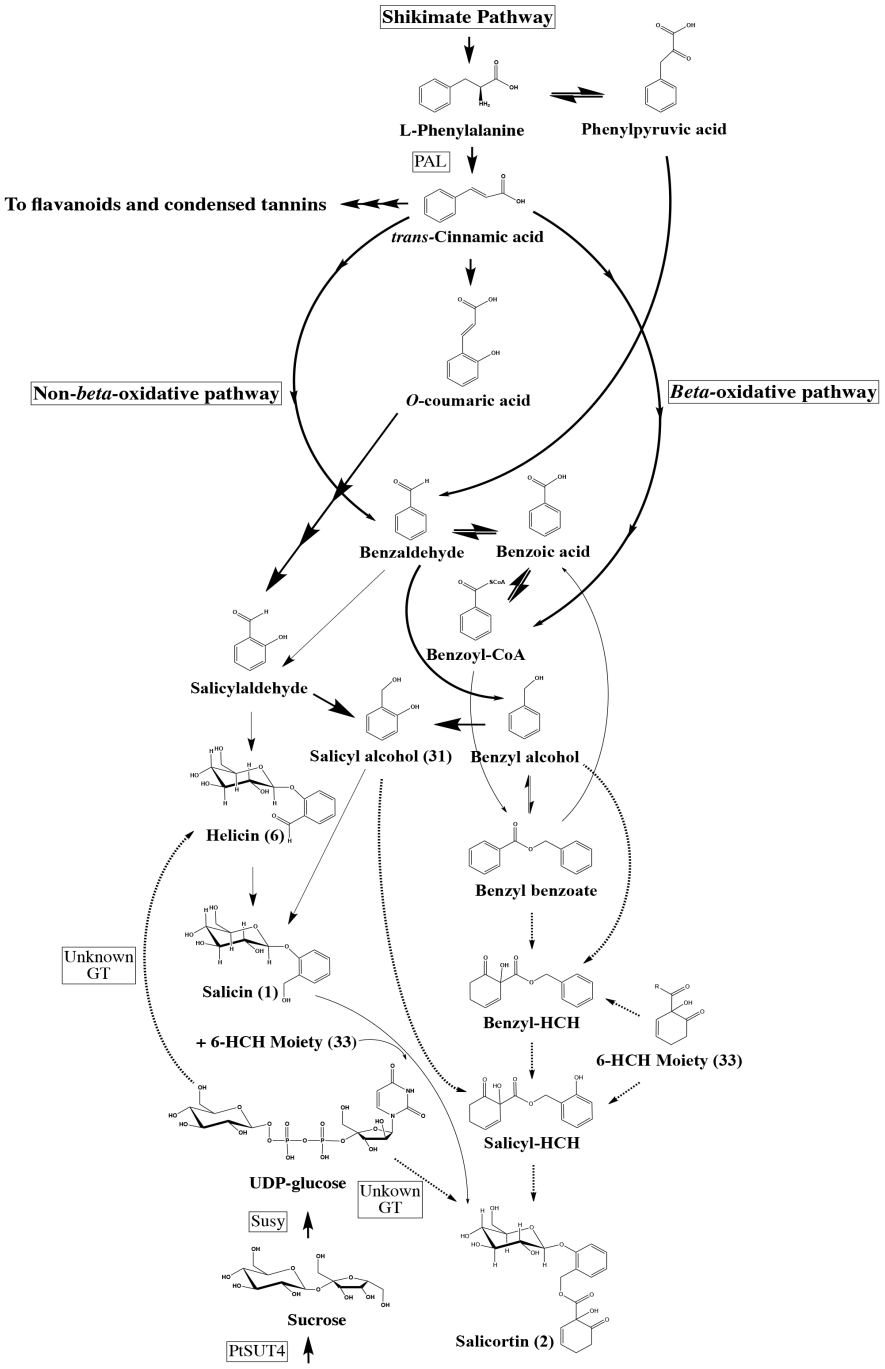

Figure 1.3. A proposed model for salicinoid PG synthesis in poplar (redrawn and updated from Babst *et al*., 2010). Based on data from Babst *et al*., 2010; Boatright *et al*., 2004; Jarvis *et al*., 2000; Long *et al*., 2009; Orlova *et al*., 2006; Pierpont, 1994; Payyavula *et al*. (2009; 2011); Ruuhola and Julkunen-Tiitto, 2003; Zenk, 1967. Solid black bold arrows indicate reactions catalyzed by functionally characterized enzymes. Solid black un-bolded arrows indicate pathways proposed previously in willow, tobacco, petunia and snapdragon. Dashed black arrows indicate hypothesized pathways based in part on r isotope-labeling feeding studies.

1.3. BAHD acyltransferases and their potential roles in salicinoid metabolism

The acronym BAHD refers to the first letter of the first four enzymes that were discovered to belong to this family. The first letter 'B' refers to benzyl alcohol *O*-acetyltransferase (BEAT), an acetyltransferase from the California wild flower *Clarkia breweri*, also known as 'Fairy Fans' and as 'Brewer's Clarkia'. It is required for synthesis of the floral volatile benzyl acetate in this species (Dudareva *et al*., 1998). The letter 'A' refers to anthocyanin *O*-hydroxycinnamoyltransferase (AHCT), a benzoyl/hydroxycinnamoyl-CoA acyltransferase identified in *Gentiana triflora* and is believed to be involved in the synthesis of acylated anthocyanins responsible for floral pigmentation (Fujiwara *et al*., 1997, 1998). 'H' represents N-hydroxycinnamoyl/benzoyltransferase (HCBT), also a benzoyl/hydroxycinnamoyl-CoA acyltransferase identified in carnation (*Dianthus caryophyllus*). It is thought to be required for synthesis of a class of phytoalexins known as anthramides (Yang *et al*., 1997). Finally, 'D' corresponds to deacetylvindoline 4-*O*-acetyltransferase (DAT), an acetyltransferase of the species *Catharanthus roseus* also known as 'Madagascar Periwinkle'. This enzyme is involved in the synthesis of the alkaloid vindoline (St. Pierre *et al*. 1998). A key example of a BAHD capable of synthesizing compounds relevant to the proposed models for salicinoid PGs is benzoyl-CoA:benzyl alcohol *O*-benzoyltransferase (CbBEBT) from *Clarkia breweri* (D'Auria *et al*., 2002) which produces benzyl benzoate from benzyl alcohol and benzoyl-CoA. However, it is not known if similar enzymes are present in poplar, as predicted by Babst *et al*. (2010).

The BAHDs are CoA-dependent enzymes that transfer acylated moieties (RC(O)R') of an acyl-activated CoA thioester donor to an alcohol acceptor molecule (D'Auria, 2006). Phylogenetic analysis using full-length amino acid sequences of functionally characterized BAHD enzymes by D'Auria (2006) and Stewart *et al*. (2005) shows that they form five distinctive clades that correlate to general function (Figure 1.4). BAHDs typically have low substrate selectivity, and can use a variety of CoA thioester and alcohol co-substrates. CbBEBT can utilize acetyl-CoA, benzoyl-CoA or cinnamoyl-CoA with a range of alcohols which include benzyl alcohol, 3-hydroxybenzyl alcohol, 4-hydroxybenzyl alcohol, and cinnamyl alcohol (D'Auria *et al*., 2002); BEAT uses acetyl-CoA with either benzyl alcohol, cinnamyl alcohol or 2-naphthaleneethanol (Dudareva *et*

al., 1998); and VlAMAT, anthraniloyl-CoA:methanol acyltransferase from *Vitis labrusca* uses acetyl-CoA, anthraniloyl-CoA, or benzoyl-CoA with a variety of alcohols (Wang and De Luca, 2005).

BAHDs are involved in the production of a wide range of biologically important phenolic metabolites. For example anthocyanins that are important for attraction of floral pollinators and animal vectors for seed dispersal via ripened fruits. Anthocyanidin 3-*O*-glucoside coumaroyl-CoA transferases At3AT1 and At3AT2 from *A. thaliana* are capable to utilizing *p*-coumaroyl-CoA with a variety of anthocyanins such as pelargonidin 3-glucoside, cyanidin 3-glucoside, and malvidin 3-glucoside to yield pelargonidin 3-*O*-(coumaroyl) glucoside, cyanidin 3-*O*-(coumaroyl) glucoside, and malvidin 3-*O*-(coumaroyl) glucoside respectively (Lou *et al*., 2007). There are multiple examples of BAHDs that are involved with the production of plant volatiles that can have diverse roles as pollinator attractants, in plant to plant signaling, and in tritrophic defense mechanisms. For example, the alcohol acyltransferases CmAAT1, from Charentais melon (*Cucumis melo*) can synthesize a variety of plant volatiles such as (E)-2-hexenyl acetate from (E)-2-hexen-1-ol + acetyl-CoA; hexyl hexanoate from hexanol + hexanoyl-CoA; and benzyl acetate from benzyl alcohol + acetyl-CoA (El-Sharkawy *et al*., 2005). BAHDs have also been implicated in the production of phenolic compounds that are important for lignin and other important plant structural compounds. For example, AtHCT, hydroxycinnamoyl-CoA:shikimate/quinate hydroxycinnamoyltransferase in *A. thaliana* that can synthesize *p*-coumaroyl-shikimate from *p*-coumaroyl-CoA and shikimate (Hoffmann *et al*., 2003; Muroi *et al*., 2009).

The primary structure of all BAHD enzymes is characterized by two highly conserved amino acid motifs, HXXXD, corresponding to histidine (His, H), followed by three interchangeable positions, then a single aspartic acid (Asp, D) residue; and the second motif is DFGWG, Asp, Phe, glycine (Gly, G), trytophan (Trp, W), and Gly (St. Pierre and De Luca, 2000). In addition, a third motif, YFGNC, tyrosine (Tyr,Y), Phe, Gly, asparagine (Asn, N), and cysteine (Cys, C), has been observed to be present in BAHDs responsible for acylating anthocyanins/flavonoids (Nakayama *et al*., 2003). The structure of one BAHD, vinorine synthase was solved by Ma *et al*. (2005) (Figure 1.5). It was shown to be a two-domain structure with the HXXXD motif located at the active site

located at the interface of both domains, this is also true of several other families of acyltransferases that utilize CoA thioesters as acyl donors. These include type I, II, and III chloramphenicol acetyltransferases (CAT) as well as choline/carnitine-*O*-acyltransferases (St Pierre and De Luca, 2000). The DFGWG motif is positioned near the carboxyl terminus (C-terminus) of the protein, far away from the HXXXD site and may have a structural role (Figure 1.6). Modification or deletion of these residues by site-directed mutagenesis leads to a significantly reduction or complete loss of activity (Bayer *et al*., 2004; Susuki *et al*., 2003). Yu *et al*. (2008) observed that BAHDs which use malonyl-CoA as an acyl donor and catalyze the malonylation of a range of isoflavone 7-*O*-glucosides (MtMaT1) in *Medicago truncatula*, were incapacitated when a 110 amino acid section was removed from the C-terminus which includes the DFGWG motif. This deletion led to improper folding of the protein and impaired the cellular localization of the enzyme. The researchers concluded that the DFGWG motif may play a role in protein stabilization at specific pHs.

Further to this, El-Sharkawy *et al*. (2005) demonstrated that in a naturally occurring mutation in a non-functional version of the alcohol acyltransferse CmAAT, changing the Ala residue in position 268 to Tyr was sufficient to recuperate enzyme activity. Conversely, reversion of Tyr 268 back into Ala abolished this activity. However, this point mutation did not occur in either of the two characteristic motifs. The two characteristic BAHD motifs may be catalytic sites important for general acyltransfer ability, and may work in conjunction with other residues or motifs located elsewhere in order to confer enzymatic activity and determine substrate specificity. Yu *et al*. (2009) identified 94 putative BAHDs within the *P. trichocarpa* genome. To date, just one of these has been functionally characterized, a hydroxyl acid/fatty alcohol hydroxycinnamoyltransferase 1 (PtFHT1) (Cheng *et al*., 2013).

1.4. Mechanisms by which PGs confer anti-herbivory properties

The PGs have been implicated as anti-herbivory cues for mammals such as mountains hares (*Lepus timidus*), field voles (*Microtus agrestis*) and elk (*Cervus elaphus*) in multiple studies where an inverse correlation exists between tissue PG content and their

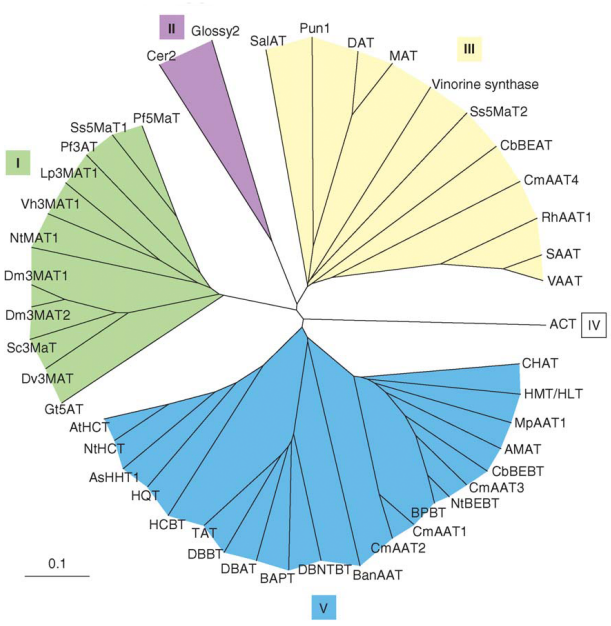

Figure 1.4. A phylogeny of BAHD acyltransferases (taken from D'Auria, 2006). The 5 major clades having shared function are labeled, I) modification of anthocyanins; II) synthesis of long-chain epicuticular waxes; III) utilization of alcohol substrates typically with acetyl-CoA; IV) amide synthesis; V) benzenoid ester production including enzymes from *Taxus* spp. involved in paclitaxel production, and synthesis of hydroxycinnamoyl quinate/shikimate esters. For GenBank accession numbers of proteins see section 2.4.

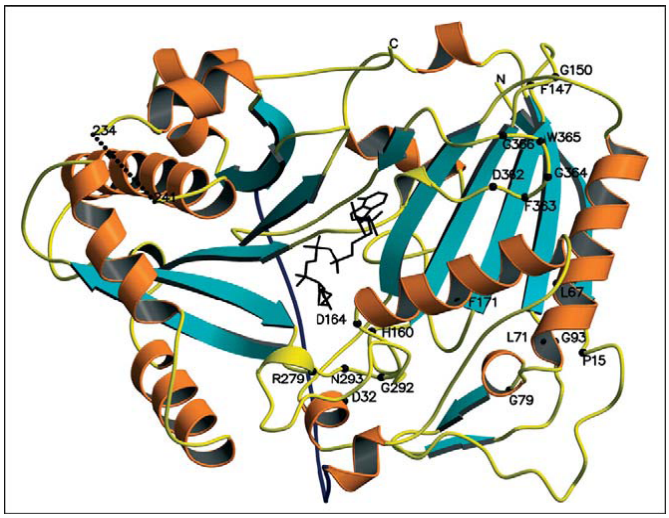

Figure 1.5. A ribbon diagram of vinorine synthase crystal structure (taken from Ma *et al.*, 2004). CoA molecule is depicted in black.

consumption (Bailey *et al*., 2007; Bryant and Kuropat, 1980; Heiska *et al*., 2007; Tahvanainen *et al*., 1985*a*; Wooley *et al*., 2008). Several studies have shown PGs to act as feeding deterrents against generalist lepidopteran herbivores by reducing their fitness by restricting growth of adults and larvae, and limiting progeny size (Hwang and Lindroth, 1997; Lindroth and Peterson, 1988; Tahvanainen *et al*., 1985*b*). An important example of this is the gypsy moth caterpillar (*Lymantria dispar*) for which host quality appears to be driven by PG concentrations (Hwang and Lindroth, 1997; 1998; Osier *et al*., 2000; Hemming and Lindroth, 1995). In contrast to these generalists, however, specialist herbivores can sequester PGs and utilize them for their own defense. Examples include the viceroy butterfly (*Limenitis archippus*, Nymphalidae) and larvae of the coleopterans, *Chrysomela populi* and *Phratora vitellinae* (Prudic *et al*., 2007; Rowell-Rahier and Pasteels, 1990).

In plants, phytochemicals such as PGs are often sequestered in specialized cells or organelles such as the central vacuole to prevent their oxidation (Marrs *et al*., 1995). Herbivory, abiotic and physical stresses can result in tissue damage, rupturing cellular compartmentalization, leading to their release and potential degradation either by foliar enzymes or enzymes and pH conditions within in the digestive tract of herbivores (Raven *et al*., 1999). Many studies have focused on the degradation products of PGs that may act as feeding deterrents, or they may simply be toxic substances to generalist herbivores (Scriber and Slansky, 1981). Mattes *et al*. (1987) first identified cyclohexenone compounds such as cyclohexen-1,2 dione (34) and (+)-6-hydroxy-2-cyclohexenone (6-HCH) (35) in the buds and internodes of Balsam poplar (*P. balsamifera* L.) and suggested that are degradation products of PGs such as salicortin (2). Mattes *et al.* (1987) proposed a degradation pathway (Figure 1.6) that involves ester hydrolysis of salicortin (2) to yield salicin (1) and 6-hydroxy-2-cyclohexen-on-oyl moiety (6-HCH moiety) (33) likely due to esterase activity from foliar sources. The 6-HCH moiety (33) then decarboxylates to catechol (32) which becomes the intermediate precursor of cyclohexen-1,2 dione (34) and (+)-6-hydroxy-2-cyclohexenone (6-HCH) (35). The researchers suggest that such compounds are potent anti-herbivory agents.

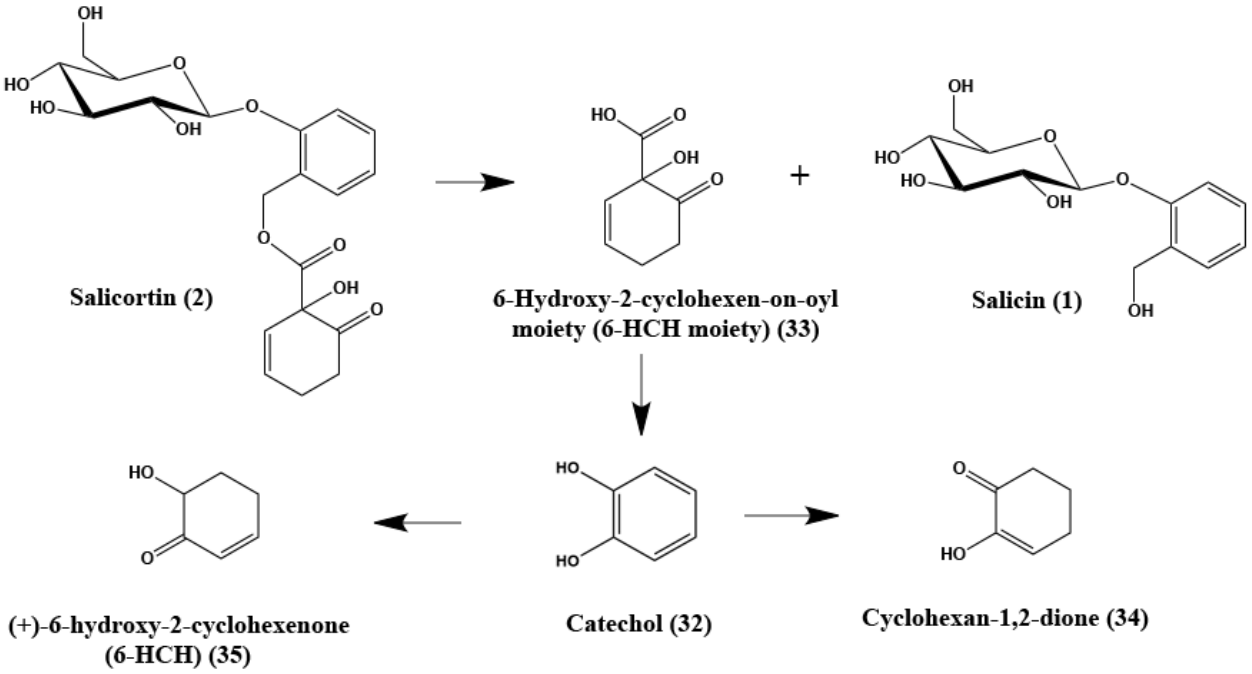

Figure 1.6. The degradation of salicortin into cyclohexenone compounds by foliar esterases (Redrawn from Mattes *et al*., 1987).

Further to this, Haruta *et al*. (2001) studied the effects of wounding of *P. tremuloides* on the induction and expression of polyphenol oxidases (PPOs) that may be correlated to defense responses. The researchers detected catechol (32) in ethanol extracts taken from damaged tissues as determined by electron spin resonance (ESR) measurements. The researchers suggested that catechol (32) might be derived by mechanisms (Figure 1.7) where salicortin (2) degrades into Salicin (1) and a 6-HCH moiety (33) through the action of esterases or in the presence of a strong base. In the alkaline insect gut, 6-HCH (35) can be converted to catechol (32) and the semiquinone is formed by the action of PPO.

Clausen *et al*. (1989) studied the degradation of PGs from *P. tremuloides* leaves following abiotic wounding. *In situ* experiments were conducted on leaves of standing plants that were torn at their periphery to mimic the damage caused by third to fifth instar larvae of the large aspen tortrix (Lepidoptera, *Choristoneura conflictana*). Leaves were collected 24 hrs later and subjected to chemical analysis by HPLC and GC. *In vitro*

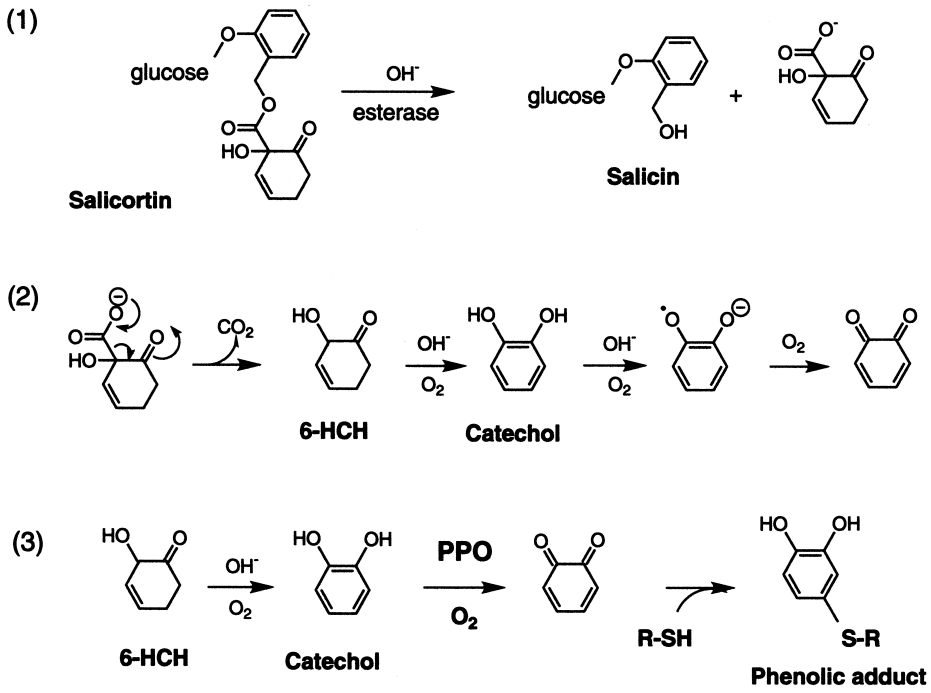

Figure 1.7 The production of catechol from salicortin and its oxidation during ESR experiments and defense reactions (taken from Haruta *et al*., 2001).

(1) Salicortin is hydrolyzed by a strong base, or by an esterase during tissue maceration and herbivory. (2) Catechol and its semiquinone are formed from unstable intermediates by strong base (pH>10) during ESR experiments. The semiquinone is detected based on characteristic ESR spectra. (3) Reactions proposed to occur during insect feeding in lepidopteran guts (pH≈10). 6-HCH is converted to catechol, which is subsequently oxidized by PPO. The resulting o-quinone alkylates a free sulfhydryl group, for example, a cysteine residue within polypeptides, resulting in a protein with one or more phenolic adducts. Free amino groups on amino acids and proteins may also be alkylated (not shown).

studies were also conducted in which fresh leaves were divided along the mid-vein and one half was homogenized and extracted in methanol immediately, while the other was crushed to simulate wounding and allowed to sit for 30 minutes before extraction. After an additional 24 hrs both sets of samples were chemically analyzed. In standing plants, the researchers observed a significant increase in PG levels following wounding. *In vitro* studies showed that salicortin (2) and tremulacin (4) were readily converted to 6-HCH (35) in wounded tissue, possibly by foliar esterases. The researcher also noted that 6-HCH (35) could be further degraded to catechol (32), observations that corroborate the conclusions of Mattes *et al*. (1987). In a third experiment the researchers fed salicortin

(2), tremulacin (4), 6-HCH (35), and catechol (32) to *C. conflictana* larvae in their second to fifth instars as part of an artificial diet and measured pupae weight. All four of these compounds were observed to significantly reduce the mean pupea weight by 30-50%. The researchers also postulate that within the herbivore gut, 6-HCH (35) is converted to catechol (32) and phenol that may reduce the food value of aspen leaves to defoliators.

Two publications by Ruuhola *et al*. (2001 and 2003*b*) studied the anti-herbivory effects of leaf extracts from three chemically divergent willow species, *S. phylicifolia, S. pentandra*, and *S. myrsinifolia,* containing low to high levels of salicylates (respectively), on the generalist moth, *Operophtera brumata* (Lepidoptera, Geometridae). They observed an inverse correlation between salicylate levels and larval growth, with the greatest inhibition of growth observed when larvae were fed with *S. myrsinifolia* leaves which contained the highest PG content. This effect was not due to the anti-nutritive effects of salicylates as no significant differences in the assimilation of carbon or nitrogen from material ingested by the larvae was observed between the leaves of the three species tested. The researchers also monitored salicylate degradation the digestive tract of larvae and constructed a possible PG degradation pathway (Figure 1.8). They observed that salicortin (2) and 2′-*O*-acetylsalicortin (9) and their derivatives are initially degraded by foliar esterases released by cell rupturing to salicin (1) and a 6-hydroxy-2-cyclohexen-on-oyl moiety (6-HCH moiety) (33). A slow conversion of salicin (1) to salicyl alcohol (31) was potentially due to *β*-glucosidases. In agreement with the findings of Mattes *et al*. (1987) and Clausen *et al*. (1989), the 6-HCH moiety (33) that is cleaved from salicortin (2) can be further converted to catechol (32), however the biochemical steps that lead to catechol (32) formation differ somewhat from previously published works. Ruuhola *et al*. (2001) suggest that the 6-HCH moiety (33) is converted first to cyclohexen-1,2 dione (34) which can degrade to catechol (32) and then to *o*-quinone via the action of polyphenol oxidase/catechol oxidase (PPO). Catechol (32) is a known substrate of PPOs and the resulting *o*-quinone is known bind to nucleophilic NH_2 and SH groups of amino acids and proteins (Constabel, 1999) and lowering nutritive value of the protein (Felton *et al*., 1989, 1992). It is interesting that PPO was also found to be an inducible defense protein in poplar (Wang and Constabel, 2003). In addition, PPO-generated quinones may under go redox cycling to produce oxidative stress in the gut lumen in Lepidoptera, or be

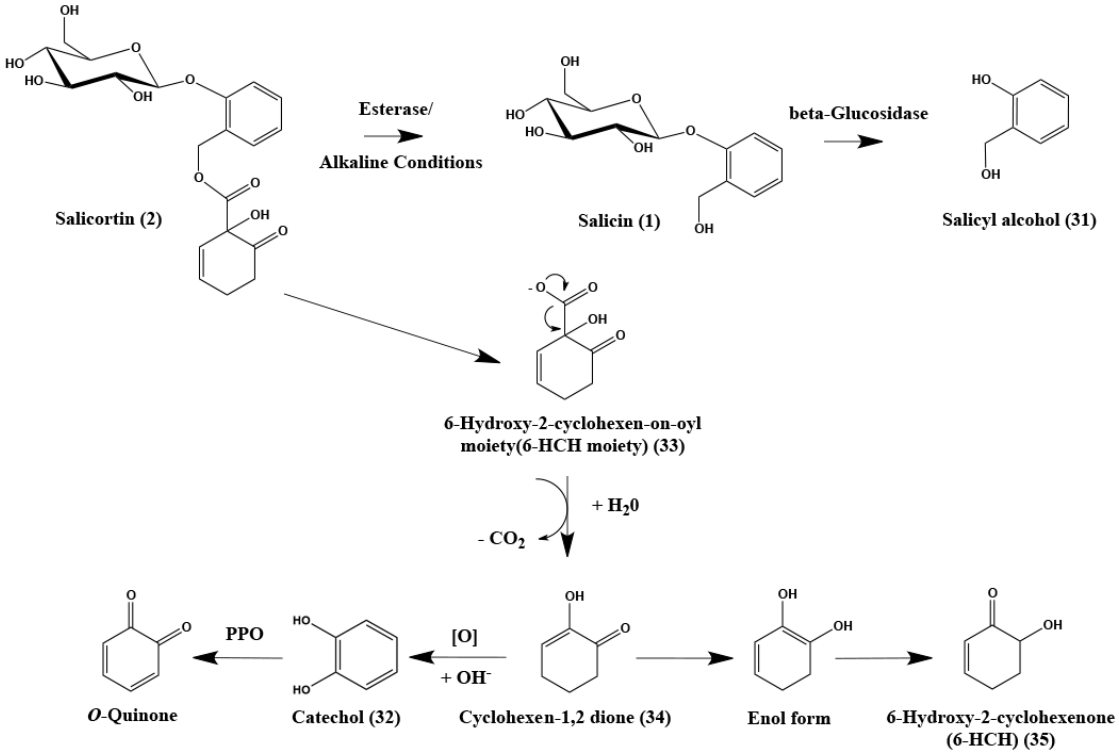

Figure 1.8. A model of salicortin break down in insect guts, leading to toxic products (redrawn from Ruuhola *et al*., 2003*b*).

absorbed and produce other toxic effects on mammalian herbivores (Constabel and Barbehenn, 2008). Cyclohexen-1,2 dione (34) may also be tautomerized to the enol form and further to the ketoform, (+)-6-hydroxy-2-cyclohexenone (6-HCH) (35).

Ruuhola *et al*. (2001) also conducted artificial diet experiments by rearing 4th instar *O. brumata* larvae on artificial diets with four different concentrations of chlorogenic acid, catechol (32), salicin (1), or salicyl alcohol (31). Catechol and salicyl alcohol were observed to significantly reduce larval growth, while salicin and chlorogenic acid had no effect. Salicyl alcohol has previously been reported to be a toxic agent of salicylates, potentially causing gut lesions in Southern Armyworm (*Spodoptera eridania*, Lepidoptera, Noctuidae) (Lindroth and Peterson, 1988). The formation of *o*-quinone-related degradation products from PGs have also been implicated as being bioactive against pests by Zhu *et al*. (1998). The researchers showed that degradation products of salicortin (2) selectively inhibited *β*-glucosidases of *Agrobacterium faecalis*. *β*-

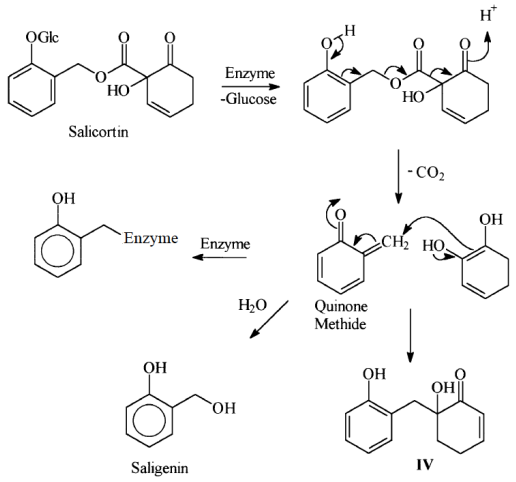

Figure 1.9. The fate of salicortin on enzymic hydrolyses of the glycosidic bond (taken from Zhu *et al*., 1998).

-glucosidases are key enzymes in cellulose degradation, catalyzing the final step that converts cellobiose to glucose and such enzymes may facilitate bacterial infections in the plant (Shewale, 1982). Enzymatic hydrolysis of salicortin (2) produces an aglycone that fragments in to *o*-quinone methide (Figure 1.9). A small percentage of *o*-quinone methide reacts with H_2O to form salicyl alcohol, a minor product of the reaction. A portion of the *o*-quinone methide may react with nucleophiles at or near the active site of *β*-glucosidase which is believed to lead to the formation of modified enzymes with decreased activity and modified substrate selectivity. Based on this data, it is feasible that PGs such as salicortin (2) may be able to decrease the activity of *β*-glucosidases required in the digestion processes of herbivores and lower the nutritive value of the plant tissue that has been consumed.

Overall it is clear that PGs content strongly influences the herbivores choice as to which tissues to consume. PGs are prone to degradation both at the site of tissue damage by the release of foliar esterases, or during the digestion process in the gut of the herbivore. Evidence suggests that degradation products of PGs rather than intact PGs confer the anti-herbivory effects. In particular, degradation products such as catechol (32), 6-HCH (35) and the 6-HCH moiety (33) appear to confer the most potent effects on generalist herbivores.

1.5. Is PGs synthesis inducible?

In the 1970's and early 1980's several hypotheses were established in order to articulate the strategies employed by plants to resist herbivory such as the 'optimal defense hypothesis' (McKey, 1974; Rhoades, 1979). The underlying assumption was that plants with an evolutionary history of high herbivory prioritize secondary metabolite production, even at the expense of growth. This led to the evolution of secondary metabolites with the costs of defense paid in order to maximize plant fitness. The defense of young leaves is also predicted by this model, as immature leaves are of greater value to a plant, representing more potential lifetime carbon assimilation than older leaves. In many plant species, herbivory can induce increased production of phytochemicals in order to mitigate further damage to the remaining tissues (Karban and Baldwin, 1997). Induction of carbon-rich phytochemicals such as PGs incur tradeoffs between resource allocation, growth, and enhanced resistance (Rhoades, 1979; Strauss *et al*., 2002). One such tradeoff was demonstrated by Ruuhola and Julkunen-Titto (2003) in *Salix pentandra* cultured in the presence of 2-aminoindan-2-phosphonic acid (AIP), a powerful inhibitor of the PAL enzyme. AIP plants exhibited significantly increased plant growth and reduced levels of salicylates compared to wild type plants. This trade-off between PG production and growth was also demonstrated by Donaldson *et al*. (2006*b*) who showed that growth of *P. tremuloides* was negatively correlated with PG concentrations when grown in conditions of low fertility with increased competition from other plants. The researchers also observed a similar negative correlation with foliar CT content and tree mass. Results from this study further support the hypothesis if a tradeoff between growth and defense which is mediated by resource availability. Furthermore, Osier and Lindroth (2006) observed that in *P. tremuloides*, PG allocation appeared to be costly in terms of growth, but only under resource-limiting conditions.

In order to assess the degree of carbon allocation that is funneled in to PG synthesis, Massad *et al*., (2014) exposed *P. trichocarpa* saplings to $^{13}CO_2$ at the beginning and end of the growing season and monitored its incorporation into various metabolites. *P. trichocarpa* appears to follow the optimal defense strategy, investing ^{13}C into PGs in expanding leaves directly after labeling. PG production continued throughout the season, illustrating their value in terms of the fitness benefit as herbivory defenses. Furthermore,

leaf damage occurring early in the growing season induced salicin production, in keeping with the criteria of the optimal defense strategy.

An important aspect of phytochemical induction is the time frame involved, for example short-term induction, defined here as occurring within 48 hrs, versus long-term induction (>48 hrs). As detailed above, Clausen *et al.* (1989) provided evidence of the short-term induction of PGs within 24hrs of abiotic wounding in *P. tremuloides* leaves. Long-term induction of PG (after 1 week) was observed in work by Ruuhola *et al*. (2001*b*) who studied induction of salicylates in *Salix myrsinifolia* (dark-leaved willow) following wounding by *Phratora vitellinae* L. (Lepidoptera, Chrysomelidae) a specialist leaf-beetle. The researchers observed that salicylate induction was systemic following wounding. Salicylate concentration increased in unwounded young, immature and mature leaves, but no significant changes in salicylate levels were observed in wounded leaves. In particular, salicortin (2) and an unresolved salicortin derivative showed significant increases, whereas salicin (1), a diglucoside of salicin, and salicyl alcohol (31) did not show significant changes. In addition, the levels of three aromatic amino acids, L-Phe, Tyr and Trp increased in immature leaves following herbivory. The researchers suggest that this may be indicative of shikimate pathway-associated enzymes being induced, and that the observed increase in salicylates may be due to an increased rate of biosynthesis rather than accumulation of PGs through translocation.

Long-term induction of PGs (11 days) was observed by Young *et al*. (2010*b*) who monitored the effect of epidermal leaf mining by the aspen serpentine leafminer (*Phyllocnistis populiella*) on the leaf chemistry of *P. tremuloides*. Levels of PGs salicortin (2) and tremulacin (4) increased significantly eleven days after the onset of leaf mining compared with leaves treated with insecticide to reduce mining damage. The researchers observed that leaves with extrafloral nectaries (EFNs) exhibited significantly higher PG levels, both constitutive and induced compared with leaves where EFNs were not present. However, there was no difference in the ability of both types of leaves to induce PG production with the onset of mining. For example in leaves without EFNs that were treated with insecticide showed [PG] (salicortin and tremulacin combined) of ≈ 19(±2) mg g^{-1} dry wt compared with ≈ 40(±9) mg g^{-1} dry wt following leaf mining. In

leaves with EFNs present, [PG] in insecticide-treated leaves was ≈ 23(±6) mg g^{-1} dry wt and ≈ 50(±11) mg g^{-1} dry wt in response to mining.

In contrast, several studies have observed no significant changes in PGs, or only slow, long term changes in levels following the onset of stress. Stevens and Lindroth (2005) subjected 12 genotypes of *P. trichocarpa* to two levels of abiotic defoliation and soil nutrient levels, then measured the foliar PG (salicortin (2) and tremulacin (4)) and CT content. Two assay time points were selected, damaged leaves harvested one week after defoliation to examine rapid and local induction, and undamaged leaves harvested eight weeks after defoliation in order to assess systemic induction. The researchers observed that CTs were induced while PGs showed no significant induction one week post-defoliation. However, accumulation of PGs was observed under longer-term induction conditions, following a pattern of 'intermediate-delayed induced resistance' (IDIR), while CTs followed a 'rapid induced resistance' (RIR) pattern.

Boeckler *et al*. (2013) exposed old-growth *P. nigra* to gypsy moth caterpillar (*Lymantria dispar*) herbivory in field experiments and then profiled the foliar PG levels. In one experiment PG levels in a single tree were measured after one week of herbivory, and in a second, larger trial using 20 trees after four weeks. No significant changes in PGs in the single tree trial were observed one week after herbivory. In the larger scale herbivory trial, the PG content actually declined by up to 40% in damaged leaves and adjacent undamaged leaves of herbivore-exposed treese compared to controls. These data suggest that in *P. nigra*, PGs may act as constitutive defenses. However, in the same study other classes of phenolics such as flavonol glycosides, low molecular weight flavan-3-ols, and CTs were also found not to be affected by herbivory in the larger trial, data that is at odds with other researchers' findings (Osier and Lindroth, 2004). In the single tree experiment, after 1 week CTs increased by 10–20 %, and low molecular weight flavan-3-ols decreased by 10 % in the leaves but increased by 10 % in the bark. It is known that phenolic levels are subject to high variation between genotypes of the same species (Lindroth *et al*., 1999; Osier and Lindroth, 2001), which may account for some of the variation in the observed data from different studies.

In a wider context that extends beyond plant chemical ecology, many PGs have been shown to confer properties that have a variety of biotechnological, industrial, and pharmaceutical applications. These properties are examined in Appendices section A2.1.

1.6. Rationale

In order to address the major gap in our knowledge of poplar PG biochemistry and chemical ecology, we identified two putative genes that encode BAHD-like acyltransferases, *PtACT47* (Potri.013G074500) and *PtACT49* (Potri.019G043600). These genes are similar in amino acid sequence to CbBEBT, a BAHD acyltransferases known to synthesize benzyl benzoate from benzoyl-CoA and benzyl alcohol in *Clarkia breweri* (D'Auria *et al*., 2002). The expression of *PtACT47* and *PtACT49* has been shown to be repressed in transgenic hybrid poplar that overexpress the CT regulator MYB134 protein (Mellway *et al*., 2009). Microarray analysis of the transcriptome in MYB134 plants showed that *PtACT47* and *PtACT49* have significantly lowered expression (0.28 and 0.27 respectively) compared to wild type plants (Mellway *et al*., 2009). In addition, increased CT content and significantly lower PG levels (Mellway *et al*., 2009) observed in these plants provided a correlation between lowered expression of *PtACT47* and *PtACT49*. Based on these data, genes *PtACT47* and *PtACT49* are ideal candidates for further investigation in terms of their functional characterization *in vitro* and roles *in planta* that may have links with PG synthesis.

These and other similar genes have also been implicated as having a defense-related role in work by Levée *et al*. (2009) who conducted expression profiling of transgenic hydrid poplars (*P. tremula x P. alba*) overexpressing *PtWRKY23*, an ortholog of the *Arabidopsis thaliana* WRKY23 transcription factor, a key regulator in defense responses against pathogens. Following exposure to *Melampsora* rust fungi, microarray analysis showed that expression of *PtACT47* and *PtACT49* was significantly up-regulated by 4.7 and 3.3 times respectively compared to wild type plant lines, although PG content was not measured in this work. In addition, three other putative BAHD genes showed significant mis-regulation, *PtACT45* (Potri.013G074400.1, expression fold change, 4.36); *PtACT46* (Potri.013G074300.1, 2.07); and *PtACT54* (Potri.001G448000.1, 0.24). A cursory examination of the amino acid sequences of all five genes reveals that the two

characteristic BAHD motifs are identical in all of them as HTMSD and DFGWG, with the exception of *PtACT54* which has HPMSD and DYGWG. The work will focus on three of these genes, *PtACT47*, *PtACT49*, and *PtACT54*. The intriguing observation that *PtACT47* and *PtACT49* expression correlates to PG content in MYB134 poplars justifies further investigation into their activities and potential roles in poplar phenolic metabolism. Further examination of the role of *PtACT54* would be of interest given that its expression appears to be reactive to the onset of fungal infestations. Based on its contrasting BAHD motifs, it may provide an interesting comparison to PtACT47 and PtACT49 for *in vitro* functional characterization studies and potentially offer insight into the biochemical roles of the amino acid residues within these motifs.

1.7. Core research objectives

The core objective of this work is to test the hypothesis that BAHD acyltransferases contribute to salicinoid PG formation in *Populus* spp. Research Question One examines the biochemical activity of BAHDs proteins PtACT47, PtACT49 and PtACT54 *in vitro*. Several approaches will be taken in order to answer this; a bioinformatic approach using phylogenetic analysis would allow for comparison of their amino acid sequences with functionally characterized BAHDs from other plant species. Their positioning within the five major BAHD clades previously delineated (D'Auria, 2006; Stewart *et al*., 2005) may offer some insight into their potential activities. Given the low substrates selectivity of BAHD enzymes, molecular approaches for the *in vitro* functional characterization of these enzymes must also be employed. These will include cDNA cloning, heterologous expression of recombinant protein, protein purification, and assays to test and measure enzyme activity of each gene product *in vitro*.

Question Two asks how is *PtACT47* and *PtACT49* expression related to PG metabolism *in planta*. Firstly, a more detailed analysis of the correlation between PG content and expression of *PtACT47* and *PtACT49* in MYB134 overexpressing hybrid poplar is required. Gene expression can be measured for each gene using qPCR, and the concentration of specific PGs (salicin, salicortin, tremuloidin, and tremulacin) can be quantified using an HPLC-based approach. It will also be valuable to examine this relationship from leaves of different developmental stages to test if levels of individual

PGs change with leaf age. If so, the order in which they accumulate may provide indirect evidence of their positions up- or downstream in PG synthetic pathways. Secondly, the production of transgenic poplars with RNA interference (RNAi) knock-down suppression of these genes of interest will be important in order to delineate their effects on PG content. If these genes are important in PG metabolism, a decrease in PG concentration should be evident. The nature of changes to the phenolic profiles may potentially indicate the relative position of these genes, up- or down-stream in the PG pathways. Microarray analysis of the RNAi transcriptome may reveal other genes that are down-regulated that share co-expression patterns with the genes of interest which may also play a role in PG production.

Chapter 2. Methods and materials

Some portions of text in Sections 2.1-2.14 were taken from Chedgy *et al*. (2015).

2.1. Chemicals and solvents

HPLC-grade acetonitrile (≥99.9%, CAS # 75-05-8), HPLC-grade hexane (≥ 97.0%, CAS # 110-54-3), phosphoric acid (≥ 85 wt. % in H_2O, CAS # 7664-38-2), salicyl alcohol (31) (97%, CAS # 90-01-7), trifluoroacetic acid (TFA, CAS # 76-05-1) were purchased from Fisher Scientific (Ottawa, ON, Canada). 2-acetonaphthone (99% pure, CAS # 93-08-3), 5-bromo-4-chloro-indolyl-β-$_D$-galactopyranoside (> 99%, CAS # 7240-90-6), 5-hexen-1-ol (CAS # 821-41-0), acetyl-CoA sodium salt (> 93%, CAS # 102029-73-2), benzyl acetate (≥ 99.7%, CAS # 140-11-4), benzyl benzoate (≥ 99.1%, CAS # 120-51-4), benzyl alcohol (≥ 99.5%, CAS # 100-51-6), benzoyl-CoA lithium salt (≥ 90%, CAS # 102185-37-5), carbenicillin (CAS # 4697-36-3), cefotaxine (CAS # 24316-19-6), cinnamyl alcohol (98%, CAS # 104-54-1), *cis*-3-hexen-1-ol (≥ 98%, CAS # 928-96-1), coniferyl alcohol (98%, CAS # 458-35-5), D-(-)-salicin (1) (> 99%, CAS # 138-52-3), gentamicin (CAS # 1403-66-3), indole-3-butyric acid (> 99%, CAS # 133-32-4), isopropyl β-$_D$-1-thiogalactopyranoside (> 99%, CAS # 367-93-1), kanamycin (CAS # 59-01-8), linalool (97%, CAS # 78-70-6), *myo*-inositol (> 99%, CAS # 87-89-8), rifampicin (CAS # 13292-46-1) were purchased from Sigma-Aldrich (Oakville, ON, Canada). Caffeoyl-CoA (> 85%, CAS # 53034-79-0), cinnamoyl-CoA (> 90%, CAS # 76109-04-1), *p*-coumaroyl-CoA (> 80%, CAS # 119785-99-8) and *p*-coumaryl alcohol (> 90%, CAS # 3690-05-9) were purchased from TransMIT GmbH (Giessen, Germany).

2.2. Plant material and growing conditions

Poplar hybrid clones from the French National Institute for Agricultural Research (INRA) were used in this work, these were INRA 353-38 (*P. tremula* x *P. tremuloides*) and INRA 717-1-B4 (*P. tremula* x *P. alba*) available in the Constabel lab. These hybrid lines are referred to as '353' and '717' respectively here after. In addition, MYB134 transgenic 353 lines (Mellway *et al*., 2009) were used. Plants were maintained in the

University of Victoria's Bev Glover Greenhouse with supplemental fertilizer and light as described (Major and Constabel, 2006).

For maintenance of sterile plant lines used for transformations and other manipulations, plants were micro-propagated in sterile conditions using nutrient enriched agar media in clear polypropylene 'magenta' boxes (approx. 8 cm^3) and typically grown in light conditions with a diurnal cycle (12 hrs light, 12 hrs darkness) at 21^oC. McCown's woody plant media (WPM) was used containing WPM basal salt mixture (McCown and Lloyd, 1981), 0.23 % wt vol^{-1}; *myo*-inositol, 100 mg L^{-1}; sucrose, 4 % wt vol^{-1}, Murashige and Skoog (MS) vitamins (Murashige and Skoog, 1962), indole-3-butyric acid (IBA), 0.5 μM; and solidified with 3% (wt vol^{-1}) Phytoagar (Sigma-Aldrich) and 1.1% (wt vol^{-1}) Phytagel (Sigma-Aldrich), pH to 5.7–5.8. Plants were grown for twelve weeks or until six fully unfolded leaves had developed before being micro-propagated into MS media or being transferred to greenhouse conditions. For greenhouse specimens, plants were transferred into a soil medium (Sunshine Mix 4, SunGro Horticulture, Agawam, MA, USA) and placed in a humidity controlled growth room at ≥ 70% humidity under natural light conditions and acclimated for four weeks. Plants were then transferred to fertilizer-supplemented soil (per 2.4 L of soil, micromax, 2.9 g; dolomite lime, 11.4 g; Acer mix, 21.4 g; superphosphate 1.1 g), and placed in to a growth room with ambient humidity and natural light conditions (temperate region, Victoria, BC, Canada). Plants were grown for an additional twelve weeks or until sixteen fully unfolded leaves had developed before being harvested. Typically, leaf harvesting consisted of excising leaves at the petiole-leaf border using scissors, the leaf mid-vein was excised and discarded, the remaining tissue was immediately frozen in liquid nitrogen and stored at -80^oC until analyzed.

2.3. RNA extraction and analysis of gene expression

Leaves of three different age classes were used, based on the leaf plastochron index (LPI), young leaves were defined as LPI 1-5; medium leaves, LPI 6-10; and old leaves, LPI 11-15. Leaves were harvested from twelve-week-old plants and pooled for each age class for individual plants, and four biological replicates of each plant type were used. Frozen leaves were homogenized and total RNA was extracted using a phenol-chloroform extraction protocol (Jaakola *et al*., 2001). For qPCR analysis, 25 ng of total

RNA was treated with DNase I (Invitrogen, Burlington, ON, Canada) according to the manufacturer's instructions. 5 ng of DNase I-treated RNA was used for reverse transcription with SuperScript II reverse transcriptase (Invitrogen). Following validation experiments, qPCR analysis was performed using an Mx3005P machine (Stratagene). Reactions (15 mL) consisted of the QuantiTect SYBRGreen mix (Qiagen, Toronto, ON, Canada) with 0.67 mM gene-specific primers and 6.25 ng of cDNA template per reaction. Primers used were as follows, *PtACT47* sense primer 5'-AATGCTATATACGGCGGGGC -3' and antisense primer 5'-AGCTGGCCCTTCAACATACC -3' with an amplification efficiency of 99.4% at an optimal annealing temperature of 60^{o}C and yielding a 179 bp amplicon; *PtACT49* sense primer 5'- AAGGTGGGGTTGGCGCCATC -3' and antisense primer 5'-GGACTTAGTTTGCGCGCTAACTG -3' with an amplification efficiency of 98.4% at an optimal annealing temperature of 59^{o}C and yielding a 179 bp amplicon; and *PtACT54* sense primer 5'- GCTATTCGAGGAGTTGACCAAG -3' and antisense primer 5'-ATATCTAACACCAGAAAGGGATAAGGA -3' with an amplification efficiency of 101.6% at an optimal annealing temperature of 60^{o}C and yielding a 268 bp amplicon. Appendices section A1.1 shows the qPCR amplicon nucleotide sequence information for *PtACT47*, *PtACT49* and *PtACT54*, primer amplification efficiency curves for at their optimal amplification temperatures, dissociation curves, and amplification plots. The amplification protocol was 95^{o}C for 10 mins, 40 cycles of (95^{o}C 30 s, annealing temperature 30 s, 72^{o}C 30 s), 95^{o}C 1 min, annealing temperature 30 s, 95^{o}C 30 s. Dissociation curves were obtained and reaction products visualized using agarose gel electrophoresis to confirm that a single, specific product was produced in each reaction. Cycle threshold (C_t) values were determined by Mx4000 software at a manually set fluorescence threshold of 0.019, and relative transcript abundances (22DCt). Relative transcript abundance values were determined after normalization to geometric mean levels of constitutively expressed, 'house keeping' genes ubiquitin (*UBQ10*) gene (sense primer 5'-ACCAAGCCCAAGAAGATCAAGCA-3' and antisense primer 5'-CCAGCACCGCACTCAGCA-3') with an optimal annealing temperature of 64^{o}C; and elongation factor (*ELF4*) gene (sense primer 5'-TGGGGCCTCTATTTAGCATGGAT-3', and antisense primer 5'-CTGCACCCGAAATGGGATTGACC-3') with an optimal

annealing temperature of 64^{o}C. Differences in gene expression were calculated as $\Delta C_T = C_{Tgene} - C_{Tgeomean}$.

2.4. Nucleotide and amino acid sequence analysis

Sequence data for *PtACT47* (Potri.013G074500), *PtACT49* (Potri.019G043600) and *PtACT54* (Potri.001G448000) was downloaded from Phytozome v10 (http://*www.phytozome.net/*) and all other sequence information was obtained from the NCBI (http://*www.ncbi.nlm.nih.gov/*). FASTA sequence files were generated using BioEdit software (v7.2.3) (http://*www.mbio.ncsu.edu/bioedit/bioedit.html*) (Hall, 1999) and aligned using Clustal W multiple sequence alignment software (Version 2.1) (http://www.genome.jp/tools/clustalw/) (Larkin *et al*., 2007). For the full-length amino acid sequence comparison, a neighbor-joining phylogeny was generated using MEGA 5 software (Build# 5110426) (Tamura *et al*., 2011). The following proteins were used and listed with their corresponding Genbank accession numbers, enzyme name, plant species and associated reference: AcAT16-HO772640, acyltransferase, *Actinidia chinensis* (Beuning *et al*., 2004); AdAT9-HO772637, acyltransferase, *Actinidia deliciosa* (Beuning *et al*., 2004); AMAT-AAW22989, anthraniloyal-CoA:methanol anthraniloyal transferase, *Vitis labrusca* (Wang and De Luca, 2005); AsHHT1-BAC78633, hydroxyanthranilate hydroxycinnamoyltransferase, *Avena sativa* (Yang *et al*., 2004); At5MAT-Q9LJB4, Malonyl-CoA:anthocyanidin 5-*O*-glucoside-6″-*O*-malonyltransferase, *Arabidopsis thaliana* (D'Auria *et al*., 2007); AtACT-Q9FNP9, agmatine coumaroyltransferase, *A. thaliana* (Muroi *et al*., 2009); AtHCT-NP_199704, hydroxycinnamoyl-CoA shikimate/quinate hydroxycinnamoyl transferase, *A. thaliana* (Hoffmann *et al*., 2004); AtHHT1-ACY78659, omega-hydroxyacid hydroxycinnamoyltransferase, *A. thaliana* (Gou *et al*., 2009); AtSCT-Q8VZU3, Sinapoylglucose-choline *O*-sinapoyltransferase, *A. thaliana* (Shirley *et al*., 2001); AtSDT-NP_179932, spermidine disinapoyl acyltransferase, *A. thaliana* (Luo *et al*., 2009); AtSHT-AEC06845, spermidine hydroxycinnamoyl transferase, *A. thaliana* (Grienenberger *et al*., 2009); BanAAT-CAC09063, alcohol acyltransferase, *Musa sapientum* (Beekwilder *et al*., 2004); BAPT-AAL92459, Baccatin III-*O*-phenylpropanoyltransferase - *Taxus Canadensis* (Walker *et al*. 2002*b*); BPBT-AAU06226, benzoyl-CoA:benzyl alcohol/phenylethanol

benzoyltransferase, *Petunia* x *hybrida* (Boatright *et al*., 2004); CbBEAT-AAF04787, benzylalcohol acetyltransferase, *Clarkia breweri* (Nam *et al*., 1999); CbBEBT-AAN09796, benzoyl-CoA:benzylalcohol-*O*- benzoyltransferase, *C. breweri* (D'Auria *et al*., 2002); CbRAS-CAK55166, Rosmarinic acid synthase, *Solenostemon scutellarioides* (Berger *et al*., 2006); CcHCT-DQ104740, hydroxycinnamoyl-CoA:quinate hydroxycinnamoyltransferase, *Cynara cardunculus* (Comino *et al*., 2007); CcHCT1-EF137954, hydroxycinnamoyl-CoA shikimate/quinate hydroxycinnamoyltransferase, *Coffea canephora* (Lepelley *et al*., 2007); Cer2-AAB17946, eceriferum 2, *A. thaliana* (Negruk *et al*., 1996, Xia *et al*., 1996); CHAT-AAN09797, (Z)-3-hexen-1-ol-*O*-acetyltransferase, *A. thaliana* (D'Auria *et al*., 2002; Hoffmann, *et al*., 2003); CmAAT1-CAA94432, alcohol acyltransferase, *Cucumis melo* (El-Sharkawy *et al*., 2005); CmAAT2-AAL77060, alcohol acyltransferase, *C. melo* (El-Sharkawy *et al*., 2005); CmAAT3-AAW51125, alcohol acyltransferase, *C. melo* (El-Sharkawy *et al*., 2005); CmAAT4-AAW51126, alcohol acyltransferase, *C. melo* (El-Sharkawy *et al*., 2005); CsHCT-AEJ88365, hydroxycinnamoyltransferase, *Cucumis sativus* (Varbanova *et al*., 2011); CsHQT-DQ915589, hydroxycinnamoyl-CoA:quinate hydroxycinnamoyltransferase, *Cynara scolymus* (Comino *et al*., 2009); DAT-AAC99311, deacetylvindoline-4-*O*-acetyltransferase - *Catharanthus roseus* (St Pierre *et al*., 1998); DBAT-AAF27621, 10-deacetylbaccatin III-10-O-acetyl transferase, *Taxus canadensis* (Walker and Croteau, 2000*a*); DBBT-Q9FPW3, 2-debenzoyl-7,13-diacetylbaccatin III-*O*-benzoyltransferase, *T. canadensis* (Walker and Croteau, 2000*b*); DBNTBT-AAM75818, 3*'*-N-debenzoyl-2*'*-deoxytaxol N-benzoyltransferase, *T. canadensis* (Walker *et al*., 2002*a*); Dm3MAT1-AAQ63615, anthocyanidin 3-*O*-glucoside-6*″*-*O*-malonyltransferase - *Chrysanthemum* x *morifolium* (Suzuki *et al*., 2004*a*); Dm3MAT2-AAQ63616, anthocyanidin 3-*O*-glucoside-3*″*,6*″*-*O*-dimalonyltransferase - *Chrysanthemum* x *morifolium* (D'Auria *et al*., 2002); Dm3MAT3-BAF50706, anthocyanin malonyltransferase, *Chrysanthemum* x *morifolium* (Unno *et al*., 2007); Dv3MAT-Q8GSN8, Malonyl-CoA:anthocyanin 3-*O*-glucoside-6*″*-*O*-malonyltransferase, *Dahlia pinnata* (Suzuki *et al*., 2002); EcHQT-AFF19202, hydroxycinnamoyl-CoA:quinate hydroxycinnamoyltransferase, *Erythroxylum coca* (D'Auria, 2012); Glossy2-DAA36076, *Zea mays* (Tacke *et al*., 1995); Gt5AT-Q9ZWR8, anthocyanin 5-

aromatic acyltransferase - *Gentiana triflora* (Fujiwara *et al*., 1998); HCBT-CAB06430, anthranilate N-hydroxycinnamoyl/benzoyltransferase, *Dianthus caryophyllus* (Yang *et al*., 1997); HcHCT-JQ779021, hydroxycinnamoyl-CoA shikimate/quinate hydroxycinnamoyl transferase, *Hibiscus cannabinus* (Chowdhury *et al*., 2012); HMT-BAD89275, (-)-13alpha-hydroxymultiflorine/(+)-13alpha-hydroxylupanine *O*-tigloyltransferase, *Lupinus albus* (Okada *et al*., 2005); HvACT-AAO73071, agmatine coumaroyltransferase, *Hordeum vulgare* (Burhenne *et al*., 2003); LaAT-AB581532, acyltransferase, *Lupinus angustifolius* (Bunsupa *et al*., 2011); LaAT1-DQ886904, alcohol acyltransferase, *Lavandula angustifolia* (Landmann *et al*., 2011); LaAT2-DQ886905, alcohol acyltransferase, *Lavandula angustifolia* (Landmann *et al*., 2011); Lp3MAT1-AAS77404, quercetin 3-*O*-glucoside-6″-*O*-malonyltransferase, *Lamium purpureum* (Suzuki *et al*., 2004*b*); MAT-A8HYU5, minovincinine 19-hydroxy-*O*-acetyltransferase, *C. roseus* (Laflamme *et al*., 2001); MoRAS-RAS_MELOI, rosmarinate synthase, hydroxycinnamoyl-CoA:hydroxyphenyllactate hydroxycinnamoyltransferase, *Melissa officinalis* (Weitzel and Petersen, 2011); MpAATI-AAU14879, alcohol acyl transferase, *Malus domestica* (Souleyre *et al*., 2005); NtBEBT-AAN09798, benzoyl coenzyme A:benzyl alcohol benzoyl transferase, *Nicotiana tabacum* (D'Auria *et al*., 2002); NtHCT-CAD47830, hydroxycinnamoyl transferase, *Nicotiana tabacum* (Hoffmann *et al*., 2003); NtHQT-CAE46932, hydroxycinnamoyl-CoA quinate transferase, *Nicotiana tabacum* (Niggeweg *et al*., 2004); NtMAT1-2XR7_A, malonyltransferase, *Nicotiana tabacum* (Manjasetty *et al*., 2012); OsAT10-LOC_Os06g39390; OsMaT1-BAD21952, quercetin 3-*O*-glucoside-6″-*O*-malonyltransferase, *Oryza sativa* (Sasaki *et al*., 2002); OsMaT2-NP001046855, quercetin 3-*O*-glucoside-6″-*O*-malonyltransferase, *Oryza sativa* (Ohyanagi *et al*., 2006); Pf3AT-Q9MBC1, anthocyanin acyltransferase, *Perilla frutescens* (Yonekura-Sakakibara *et al*., 2000); Pf5MaT-Q9LJB4, malonyl-CoA:anthocyanin 5-*O*-glucoside-6‴-*O*-malonyltransferase – *P. frutescens* (Suzuki *et al*., 2001); PhCFAT-ABG75942, coniferyl alcohol acyltransferase, *Petunia* x *hybrida* (Dexter *et al*., 2007); PtFHT1-XP_002298644, hydroxyl acid/fatty alcohol hydroxycinnamoyltransferase 1, *Populus trichocarpa* (Cheng *et al*., 2013); Pun1-ADN97116, acyltransferase, *Capsicum annuum* (Stewart *et al*., 2005); RhAAT1-AAW31948, acetyl-CoA geraniol/citronellol acetyltransferase, *Rosa* hybrid cultivar

(Shalit *et al*., 2003); SAAT-AAG13130, alcohol acyltransferase, *Fragaria* x *ananassa* (Aharoni *et al*., 2000); SalAT-Q94FT4, salutaridinol 7-*O*-acetyltransferase, *Papaver somniferum* (Grothe *et al*., 2001); Sc3MaT-AAO38058, malonyl-CoA:anthocyanidin 3-*O*-glucoside-6″-*O*-malonyltransferase, *Pericallis cruenta* (*Senecio cruentus*) (Suzuki *et al*., 2003*a*); ScSlAT2-AFM77971, Ss5MaT1-Q8W1W9, malonyl-CoA:anthocyanin 5-*O*-glucoside-6‴-*O*-malonyltransferase, *Salvia splendens* (Suzuki *et al*., 2001); Ss5MaT2-AAR26385, anthocyanin 5-*O*-glucoside-4‴-*O*-malonyltransferase, *S. splendens* (Suzuki *et al*., 2004*c*); StFHT-FJ825138, feruloyl transferase, *Solanum tuberosum* (Serra *et al*., 2010); TAT-AAF34254, taxa-4(20),11(12)-dien-5 alpha-ol-*O*-acetyl transferase, *T. canadensis* (Walker *et al*., 2000); TpHCT2-ACI16631, malate *O*-hydroxycinnamoyl transferase, *Trifolium pratense* (Sullivan, 2009); VAAT-AX025504, alcohol acyl transferase, *Fragaria vesca* (Aharoni *et al*., 2000); Vh3MAT1-AAS77402, quercetin 3-*O*-glucoside-6″-*O*-malonyltransferase, *Glandularia* x *hybrid* (Suzuki *et al*., 2004*b*); VhBEBT-BAE72881, benzoyl-CoA benzoic acid benzoyltransferase, *Glandularia* x *hybrida* (Togami *et al*., 2006); Vinorine synthase-CAD89104, *Rauvolfia serpentine* (Ma *et al*., 2005).

2.5. Amplification of *PtACT47*, *PtACT49*, and *PtACT54*

Leaf tissue was harvested from the *P. trichocarpa* 'Nisqually 1' clone. This plant was originally derived from a female genotype located on the banks of the Nisqually river (WA, USA) used for genome sequencing by Tuskan *et al*. (2006). mRNA was purified from total RNA using the Oligotex® mRNA Mini Kit (Qiagen), and cDNA was produced as described above. Primers were designed to be complementary to *P. trichocarpa* full length cDNA clones *PtACT47*, *PtACT49*, and *PtACT54* using Vector NTI® Express Designer Software (Life Technologies Inc., Burlington, ON, Canada). The *PtACT47* sequence was amplified by PCR using primers 5'-GCGGATCCTTA*ATG*GCTTCATCACCC-3' (the start codon is shown in italics and the *Bam*HI restriction site is underlined) and 5'-GCCCCGGGAAC*TTA*TAAGGAAGACGCG-3'; *PtACT49* was amplified using primers 5'-GCGGATCCTACAATA*ATG*GCATCATCACCC-3' and 5'-

GCCCCGGG*TTA*TAGGGAAGATACAATAAATTTGG-3' (the stop codon is shown in italics and the *Xma*I restriction site is underlined); and *PtACT54* by 5'-GCGGTACC*ATG*CCAACTCCTACTTCCTTA-3' (with the start codon of *PtACT54* is shown in italics and the *Kpn*I site is shown by underlining) and 5'-GCCCCGGG*TCA*AAGCCTGTGTCTTATAGG-3' (with the stop codon of *PtACT54* shown in italics and the *Xma*I site is shown by underlining). PCR amplification conditions were 98^{o}C 3 mins, 35 repetitions of (98^{o}C 30 s, 58^{o}C 30 s, 72^{o}C 45 s), 72^{o}C 10 mins, using Phusion® high-fidelity DNA Polymerase (New England Biolabs Inc., Ipswich, MA, USA). Since proofreading enzymes produce 'blunt end' amplicons in which both the 5'-3' stand and the 3'-5' strand are exactly equal in length, this lowers ligation efficiency. Therefore a 5' A overhang was added to the amplicon (Clark, 1988). Amplicons were incubating with regular TAQ polymerase in the presence of dATP (deoxyadenosine triphosphate) at 70^{o}C for 30 mins. The amplified fragments were then ligated into the pGEM®-T Easy vector (Figure 2.1) (Promega Corp., Madison, WI, USA). Ligation mixes were used to transform XL1-Blue *E. coli* electro-competent cells (Agilent Technologies Inc., Mississauga, ON, Canada) to facilitate blue/white screening of successfully transformed bacterial colonies.

2.6. Generation of a PtACT49-H166A mutant protein

In order to alter the conserved HXXXD motif in the PtACT49 protein from HTMSD to ATMSD, the basic histidine (H) residue in position 166 was replaced with the non-polar alanine (A), sense and antisense primers were designed that overlapped the motif for PCR-site directed mutagenesis. Primers were as follows, sense primer 5'-GCTCCGCCTGAACGCTACCATGAGTGAT-3'(bases encoding alanine are underlined) and antisense primer 5'-GCATCACTCATGGTAGCGTTCAGGCGGA-3'). These primers were used in conjunction with *PtACT49* sense and antisense primers used previously to amplify the *PtACT49* coding sequence in two segments using the pGEM®-T Easy-PtACT49 plasmid as a template. This resulted in two amplicon fragments, one for the fragment spanning the start codon ATG to the end of the HXXXD motif at position 170, and the other fragment spanning positions 62 to 460. Both fragments were purified by agarose gel electrophoresis and gel extraction, mixed in equal part and used as a PCR

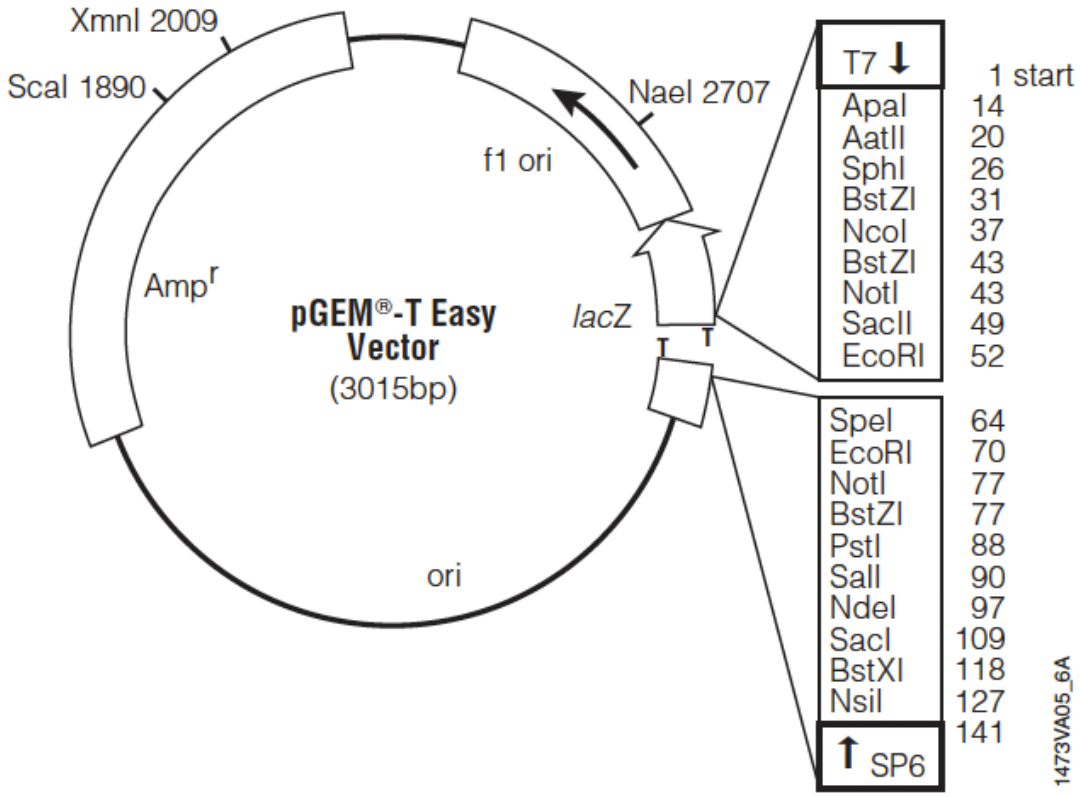

Figure 2.1. pGEM®-T Easy vector map and sequence reference points (taken from the Promega technical manual TM042, 2010).

Important restriction sites and nucleotide positions, T7 RNA polymerase transcription initiation site, position 1; multiple cloning region, 10–128; SP6 RNA polymerase promoter (–17 to +3), 139–158; SP6 RNA polymerase transcription initiation site, 141; pUC/M13 reverse sequencing primer binding site, 176–197; *lac*Z start codon, 180; *lac* operator, 200–216; β-lactamase coding region, 1337–2197; phage f1 region, 2380–2835; *lac* operon sequences, 2836–2996, and 166–395; pUC/M13 forward sequencing primer binding site, 2949–2972; T7 RNA polymerase promoter (–17 to +3), 2999–3. Inserts can be sequenced using the SP6 promoter primer, T7 promoter primer, pUC/M13 forward primer, or pUC/M13 reverse primer.

template to amplify the full-length H166A mutant sequence using *PtACT49* sense and antisense primers. The product was then cloned into the pGEM®-T Easy vector, and sequenced to confirm the mutation and absence of spurious PCR-generated errors.

2.7. Transformation of XLI-Blue *E. coli* cells and blue/white screening

Vectors such as pGEM®-T Easy and recombinant protein expression vectors utilize the *lac* operon present in *Escherichia coli* (Davies and Jacob, 1968; Sambrook *et al*.,1989). See Appendices section A1.2 for full details. The pGEM®-T Easy vector can be used in conjunction with XLI-Blue *E. coli* electro-competent cells to facilitate blue/white screening of successfully transformed bacterial colonies. XLI-Blue cells were transformed with the pGEM-T Easy constructs by electroporation using an Eppendorf electroporator 2510 (Eppendorf AG, Hamburg, Germany) at a charging voltage of 1500 volts, and a pulse length of 5 msec. Transformed cells were then incubated for 12 hrs at 37^{o}C on lysogeny broth (LB) agar plates supplemented with 100 μg mL^{-1} carbenicillin (CAS # 4697-36-3), 80 μg mL^{-1} X-gal and 0.5 mM IPTG (isopropyl β-$_{D}$-1-thiogalactopyranoside, CAS# 367-93-1) a non-fermentable analog of lactose that inactivates the *lac*Z repressor (Barkley and Bourgeois, 1978) and induces transcription of the *lac* operon. White bacteria colonies were then selected and subjected to colony PCR using -21 M13F (5' TGTAAAACGACGGCCAGT 3') and -28 M13R (5' AGGAAACAGCTATGACCAT 3') primers with TAQ polymerase. Successfully transformed colonies were grown in 3 mL liquid cultures of LB with appropriate antibiotics for 12 hours at 37^{o}C and shaking at 200 rpm using a MaxQ 4000 bench top orbital shaker (Thermo Scientific, Ottawa, ON, Canada). Plasmid DNA was extracted and purified using EZ-10 Spin Column Plasmid DNA Kit (Bio Basic Canada Inc., Markham, ON, Canada). The sequences were verified by DNA sequencing, all manufacture of primers and sequencing were performed by Eurofins Genomics (Huntsville, AL, USA).

2.8. Heterologous expression in *E. coli* and purification of recombinant protein

PtACT47, *PtACT49*, *PtACT49*-H166A and *PtACT54* sequences were excised from the pGEM®-T Easy vector using *Bam*HI and *Xma*I, then cloned between the *Bam*HI and

*Xma*I sites of vectors pQE-30 or pQE-31 (Qiagen). The pQE vector expression system utilizes the bacteriophage T5 promoter transcription–translation system and belongs to the pDS family of plasmids (Bujard *et al*., 1987) that are derived from plasmids pDS56/RBSII and pDS781/RBSII-DHFRS (Stüber *et al*., 1990). The pQE-30 and pQE-31 vectors (Figure 2.2) are low-copy plasmids with promoter–operator element consisting of phage T5 promoter which is recognized by the *E. coli* RNA polymerase. It has two *lac* operator sequences which increase *lac* repressor binding to ensure efficient repression of the T5 promoter. The vectors have a synthetic ribosomal binding site, RBSII, for high translation rates and two strong transcriptional terminators, t0 from phage lambda (Schwarz *et al*., 1978) and T1 from the rrnB operon of *E. coli*, to prevent read-through transcription and to ensure stability of the expression construct. The vectors also have the ColE1 origin of replication (Sutcliffe, 1979) as well as the *β*-lactamase gene (*bla*) that confers resistance to ampicillin (Sutcliffe, 1979) at 100 μg ml^{-1}. The pQE-30 and pQE-31 overexpression vectors facilitate the production of N-terminally His-tagged recombinant proteins.

Vector construction design was achieved using Vector NTI® Express Designer Software (Life Technologies Inc.). Ligation of the full-length gene sequences into pQE vectors resulted in the pQE-30-*PtACT47* construct which contains the sequence encoding MRGSHHHHHHGS-PtACT47; pQE-31-*PtACT49* construct which contains the sequence encoding MRGSHHHHHHTD-PTIPtACT49; pQE-30-*PtACT49*-H166A construct which contains the sequence encoding MRGSHHHHHHGS-PTACT49-H166A; and pQE-30-PtACT54 construct which contains the sequence encoding MRGSHHHHHHGS-*PtACT54*, all under the control of a T5 promoter (Figure 2.3). These plasmids were moved into *E. coli* BL21 codon plus RP, pREP4, GroES/GroEL cells (Stratagene, Agilent Technologies, Santa Clara, CA, USA) for recombinant protein production. Codon plus RP allows for expression of genes encoding tRNA for rare argenine (Arg, R) and proline (Pro, P) amino acid codons**.** Since the pQE vectors do not carry the *lac*I gene which encodes *lac* repressor, to ensure tightly-regulated expression, the host strain contains the pREP4 helper plasmid which contains the *lac*I gene. GroES/GroEL is a molecular chaperone complex that enhances the correct folding of recombinant protein (Braig *et al*., 1994; Tilly *et al*., 1981; Xu *et al*., 1997).

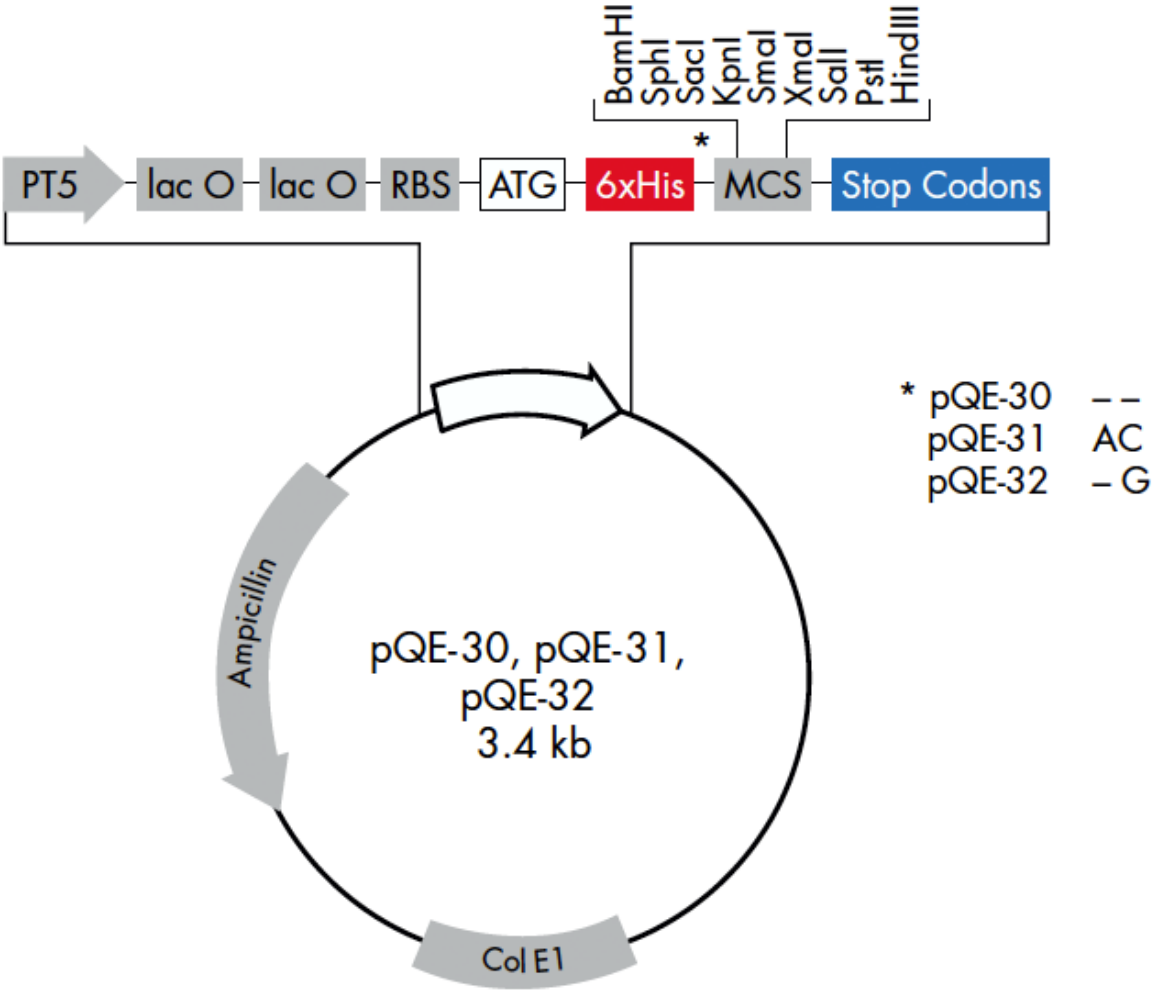

Figure 2.2. Vector maps of pQE-30, pQE-31, and pQE-32 for overexpression of N-terminus His-tagged recombinant protein (taken from the QiaExpressionist Manual, Qiagen, 2001).

Abbreviations are as follows, PT5, T5 promoter/*lac* operator element; ATG, start codon; 6xHis, 6xHis-tag coding sequence; MCS, multiple cloning site; Col E1, ColE1 origin of replication.

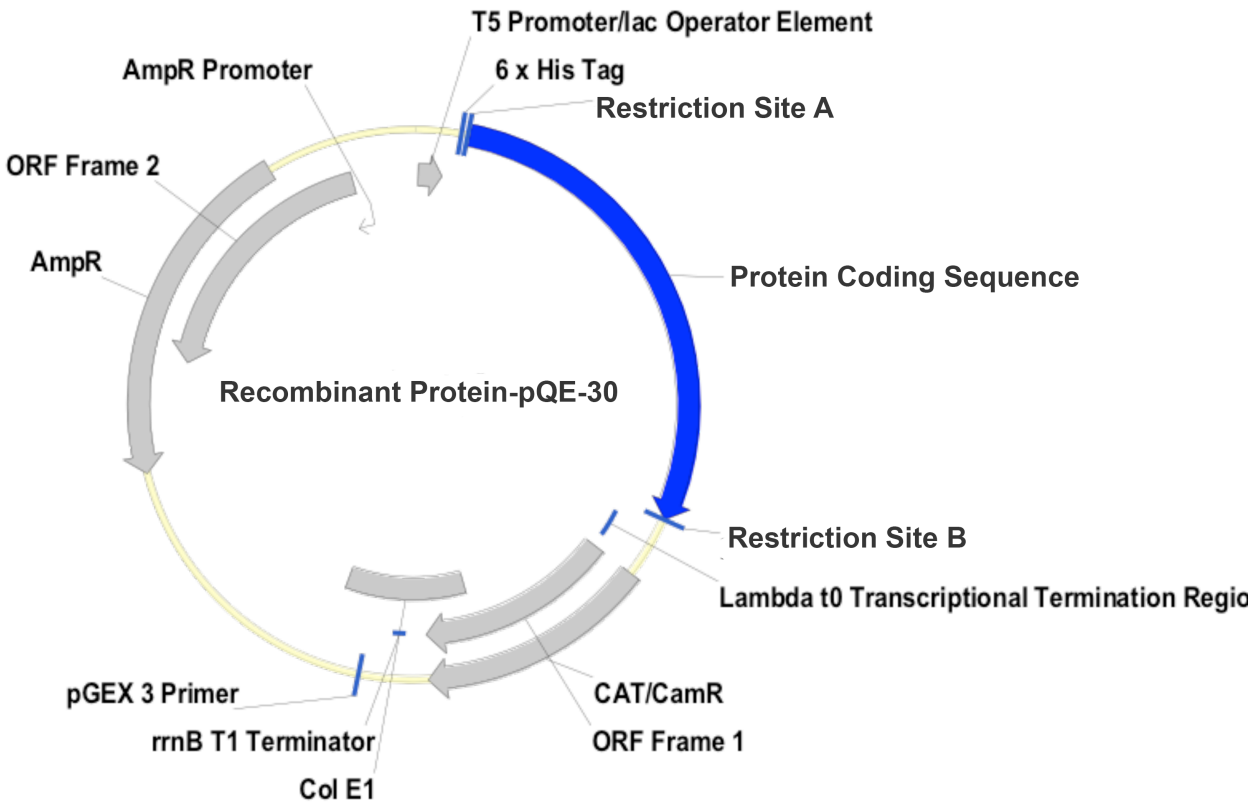

Figure 2.3. A general vector map for recombinant protein-pQE-30. The full coding sequence of *PtACT47, PtACT49, PtACT49-H166A, or PtACT54* (shown in blue) is flanked by restriction sites A and B. Diagram drawn using Vector NTI® Express Designer Software (Life Technologies Inc.)

E. coli BL21 harboring the constructs were cultured at 18^{o}C for 24 hrs at 220 rpm in overnight express^{TM} instant terrific broth (TB) auto-induction medium (Novagen, EDM Millipore, Etobicoke, ON, Canada) containing 100 µg mL^{-1} carbenicillin. Auto-induction media exploits the sequential utilization of glucose and lactose by *E. coli* in two distinct growth phases, known as diauxie (Studier, 2005). Protein expression is regulated by the antagonistic effects of glucose and lactose on the *lacUV5* promoter. Glucose prevents lactose-mediated activation the *lacUV5* promoter because its presence prevents uptake of lactose into the cell by *β*-galactoside permease (a.k.a. lactose permease). High glucose levels inside the cell triggers a mechanism known as 'carbon catabolite repression' in which a form of Enzyme II A (EIIA) specifically responsible for glucose transport and part of the phosphotransferase system, exists in its unphosphorylated form which leads to repression of *lacY* (Inada *et al*., 1996; Kimata *et al*., 1997; Meadow *et al*., 1990; Postma *et al*., 1996; Saier *et al*., 1996). Depletion of glucose reverses the carbon catabolite repression mechanism, and the use of other carbon sources such as lactose is stimulated, which in turn initiates the expression of *lacY* and *β*-galactoside permease production. Auto-induction medium contains a high glucose:lactose concentration ratio; glucose stimulates rapid cell growth while repressing protein expression. High-density cell growth and glucose depletion is followed by a spontaneous induction of protein expression. The media is rich in amino acids which also promotes high cell density growth while simultaneously preventing induction by lactose during the log-phase growth, and high rates of aeration at low lactose concentrations (Studier, 2005). Auto-induction is advantageous when compared to traditional IPTG induction due to its simplicity, increased final bacterial culture density, and concentration of target protein per volume of culture (Studier, 2005).

2.9. Purification of recombinant protein

E. coli cells were grown overnight in auto-induction media in order to overexpress recombinant protein. Cells were then pelleted by centrifugation at 4000 rpm for 20 mins at 4^{o}C then resuspended in 1/3 volume of the original culture in binding buffer (20 mM Tris, 1M NaCl, 30 mM imidazol, 10 mM *β*-mercaptoethanol). The pH of all the buffers

used was determined according to each protein's isoelectric point (pI), the pH at which the protein carries no net electrical charge. Proteins are more likely to aggregate at their pI which can decrease protein yield, to mitigate this, the pH was set at one pH unit higher that the protein pI. pI was calculated based on amino acid sequence using the Compute pI/Mw tool on the ExPASy Bioinformatics Resource Tool Portal (http://web.expasy.org/compute_pi/) (Swiss Institute of Bioinformatics, Lausanne, Switzerland). The theoretical pI values and molecular weights (kDa) for each recombinant protein purified, including the His-tag, were as follows, PtACT47, pI 7.7 / 51.9 kDa; PtACT49, 7.2, 52.6; PtACT49-H166A, 7.6, 52.2; PtACT54, 8.0, 53.6) (Appendices Figure A2.1).

In order to maximize protein yield and purification efficiency, prior to cell lysis, a protease inhibitor cocktail (set I, animal free, 30 μL per liter of original culture volume) (Calbiochem, EDM Millipore) was added to prevent protein degradation by cellular proteases. In addition, deoxyribonuclease I (DNase I) (Roche Diagnostics Corp., Indianapolis, IN, USA) was added at 50 μL of DNase I (2500 units mL^{-1}) per liter of original culture. This degrades unwanted single- and double-stranded DNA from the cell lysate to improve protein extraction efficiency. The cell suspension was then lysed by ultrasonication using a sonic dismembrator model 500 (Fisher Scientific, Nepean, ON, Canada) equipped with a CE Converter 102C probe (Branson Ultrasonics, Danbury, CT, USA). Samples were placed on ice to mitigate the heat generation and prevent protein denaturing. A regime of 10 x 15 s pulses at 30% amplitude, with a 30 s pause between pulses to allow for cooling. Samples were centrifuged at 10,000 g at 4^{o}C for 30 mins. The soluble protein is contained in the supernatant while the pellet is predominantly composed of insoluble protein, inclusion bodies and cell debris. The supernatant was then incubated with Ni-NTA Superflow™ nickel charged resin (Qiagen Inc., Toronto, ON), 1 mL resin per liter of original culture, incubated for 2 hours at 4^{o}C, and shaken at 150 rpm. This resin has a capacity to bind 6xHis-tagged protein at 5–10 mg mL^{-1} (QIAexpressionist manual, 2001). Resin was then loaded onto a gravity-flow column at 4^{o}C and washed with 20 mL of wash buffer (20 mM Tris, 1M NaCl, 40mM imidazol, and 10 mM β-mercaptoethanol). The initial flow-through fraction and the wash fraction are retained to maximize protein yield, Ni-NTA resin was added to these fractions and

incubated for another hour, mixing gently at 4°C. Elution of 6xHis-tagged recombinant protein was achieved by washing with 1mL of elution buffer (20 mM Tris, 1M NaCl, 300 mM imidazol, and 10 mM β-mercaptoethanol). In high concentrations, imidazole competes with 6xHis-tagged protein for the resin binding sites resulting in protein elution.

The protein concentration (μg mL^{-1}) of the eluent was determined using the Bradford protein assay (Bradford, 1976) in conjunction with a BSA (bovine serum albumin) standard curve. Further concentration of protein was achieved using Centricon 50 or 60 centrifuge filters (EMD Millipore) since all proteins of interest are >50 and <60. This size exclusion process also removes unwanted proteins that fall outside of this size range. The concentration of purified protein was adjusted to 0.5 mg mL^{-1} in 50% glycerol and 100 μL aliquots were placed into micro centrifuge tubes and stored at -80°C until future use.

2.10. SDS-PAGE and immunoblotting

Sodium dodecyl sulfate polyacrylamide gel electrophoresis (SDS-PAGE) gels (12%) were loaded with semi-purified recombinant protein (20 μg) and proteins were separated using the Mini Protean II cells kit (Bio-Rad, Mississauga, ON, Canada). SDS–PAGE was performed according to Laemmli (1970) and stained using Coomassie brilliant blue G-250. A replicate gel was electro-blotted onto polyvinylidene fluoride (PVDF) membrane (Bio-Rad). Detection of His-tagged protein was achieved by immunoblotting (Burnette, 1981) with sequential incubation of blots with a 1:3000 dilution of a mouse monoclonal antibody against 6xHis tag (GE Healthcare Life Science) followed by a 1:3000 dilution of a goat anti-Mouse IgG horseradish peroxide conjugate (Bio-Rad) in tween tris-buffered saline (TTBS) solution containing 1% bovine serum albumin (BSA), 20mM Tris, 150 mM NaCl, and 0.05% Tween-20, at pH 7.5 as described in Sambrook *et al*. (1989). Blots were then developed colorimetrically using a 3,3'-diaminobenzidine tetrahydrochloride (DAB) development kit (Sigma-Aldrich).

2.11. Enzyme activity analysis

The reaction buffer consisted of 50 mM Tris-HCl, 300 mM NaCl, 1 mM dithiothreitol (DTT) at pH 7. For standard reactions, 500 μM of each substrate was incubated with 2.5

μg of purified recombinant protein in a total volume of 42.5 μL. Reactions were carried out for 30 seconds at 30^{o}C in 200 μL PCR tubes and a PCR thermal cycler, and stopped by flash-freezing in liquid nitrogen followed by the addition of 2.5 μL of 1% trifluoroacetic acid (TFA) prior to thawing. Before analysis by HPLC, the reaction mixture was centrifuged and filtered using a nylon 0.45μm syringe filter to remove particulates. Determination of Michaelis–Menten constants (K_m, μM) and maximum velocity (V_{max}, μM sec^{-1}) was determined by nonlinear regression analysis (with 95% confidence intervals) of the substrate concentration versus reaction rate data fitted into the Michaelis-Menten equation $Y = V_{max}X[K_m + S]^{-1}$, using SAS JMP Version 7.0 (SAS institute Inc.) software with the Michaelis-Menten nonlinear model (2P) preset function (Michaelis and Menten, 1913). For determination of kinetic parameters for each substrate, its concentration in the assay mixture was varied from its limit of detection (LOD) up to 2000 μM usually in 12 concentration increments at saturating concentration of the other substrate (2500 μM). The LOD was defined as the concentration of analyte required to produce a chromatographic signal equal to three times the peak-to-peak noise. All kinetic parameters were the means of three separate experiments and were reproducible to within ±10% of the mean value.

Three negative controls were used for the activity assays, 1) boiled PtACT47, PtACT49, and PtACT54 recombinant proteins which are denatured and void of activity; 2) the active site mutant PtACT49-H166A recombinant protein; and 3) a characterized *Populus* UDP-glycosyltransferase recombinant protein *Pt*UGT78L1, an enzyme not related to BAHD acyltransferases, shown to catalyze an unrelated reaction in which UDP-galactose is donated to the flavonols quercetin, kaempferol and cyaniding (Veljanovski and Constabel, 2013). This protein should not exhibit activity with CoA-thioesters. Expressing and purifying this protein as a control for assays may provide insight into any impurities, or potential thioesterase contamination derived from the *E. coli* host strain. A positive control used was CbBEBT (D'Auria *et al*., 2002) supplied by Prof. Eran Pichersky, University of Michigan. This enzyme is known to convert benzyl alcohol and benzoyl-CoA to benzyl benzoate and CoA-SH, it was used to aid the optimization of purification and enzyme assay protocols.

2.12. Extraction of phenolic phytochemicals from leaf tissue for HPLC analysis

Leaf tissue (50 mg) was steeped in 1.5 mL HPLC-grade methanol (100 %) with two steel ball bearings (2 mm in diameter) and homogenized using a Precellys 24 homogenizer (Bertin technologies, Toulouse, France) at 2 x 45 s, 5500 rpm. Samples were then exposed to a frequency of 40 kHz generated by a VWR model 75 T ultrasonic bath (VWR, Mississauga, ON, Canada) for 10 mins, followed by centrifugation at 1500 rpm for 5 mins. The supernatant was removed and the tissue sample was re-extracted two more times in an identical manner in order to maximize the extraction of phenolic compunds. The combined supernatant was dried using a SC110A SpeedVac® plus (Thermo Savant, Waltham, MA, USA) and weighed and the mass of the leaf extracts was estimated (mg). Dried extracts were then re-suspended in 300 μL methanol (HPLC-grade) and the chlorophyll was removed using a StrataX^{TM} 33 μm polymeric sorbent cartridge (8B-S100-FBL, Phenomenex, Torrance, CA, USA) according to the manufacturer's instructions. Eluent was dried, weighed and re-suspended in methanol to a concentration of 10 mg mL^{-1}, then filtered using a 0.22 μm nylon syringe filter to remove particulates. Typically 20 μL was used for reverse-phase high pressure liquid chromatography (RP-HPLC) analysis.

2.13. HPLC analysis

To quantify products of BAHD enzyme assays, products were separated using an ODS3 C-18 RP column (3 μm, 4.6 mm x 150 mm) (Intersil Corp., Milpitas, CA, USA) using a System Gold® HPLC equipped with a 126 solvent module, a 168 detector fitted with a deuterium UV lamp that has a wavelength range of 190-600 nm and a 508 auto-sampler (Beckman Coulter, Mississauga, ON, Canada). Typically reaction products of 50 μL were injected on to the column at room temperature. The liquid phase consisted of a mixture of solvent A, distilled H_2O with 1.5% phosphoric acid; and solvent B, 100% HPLC-grade acetonitrile. Chemicals were separated within 28 mins using the following gradient, 0 mins, 10% solvent B; 2 mins 45% B; 12 mins, 50% B; 16 mins, 50% B; 20 mins, 95% B; 28 mins 95% B; 34 mins 10% B. Products or substrates were quantified by comparing analyte response with the response factor of an internal standard (I.S.) 2-acetonaphthone using a single-point calibration with UV detection. 2-acetonaphthone was selected as the

I.S. because its peak retention time (T_R) did not overlap the other chemical peaks and its UV absorbance range is analogous to the other chemicals of interest. Quantification was performed at 194 nm for benzoic and benzoyl esters, and at 260 nm for CoA-thioesters.

In order to generate response factors for each chemical analyzed, pure chemical standards were prepared in either H_2O or 50% ethanol and serially diluted to produce a concentration range. Samples were subjected to chromatographic analysis until the LOD could be estimated to within 10 µM. A six-point concentration gradient was established for each chemical of interest ranging from its LOD to a maximum of 2000 μM. To each sample, the I.S. was added, typically 5 µL of I.S. (2 mg mL^{-1}) was added to each 45 µL reaction mixture before analysis. The final I.S. concentration was 200 μg mL^{-1} or 1200 µM which produced a clear signal peak with a size comparable to other peaks.

Six additional solutions were prepared in which the chemical of interest was maintained at a constant concentration of 500 μM and the I.S. concentration was varied from its LOD to a maximum of 2000 μM and analyzed. A twelve-point scatter plot was constructed (y-axis, chemical peak area/standard peak area; x-axis, chemical/standard concentration (μM)). This process was repeated three times and a scatter plot of mean data was obtained. The data were then submitted to statistical regression analysis in order to produce a unique response factor for each chemical of interest relative to I.S. This response factor was then used to accurately quantify chemical concentration (μM). Response factor equations relative to the I.S. for each of the chemicals of interest were then generated and are shown in Table 2.1.

For HPLC analysis of leaf extracts a Kinetex C-18 100Å (2.6 μm, 4.6 mm x 150 mm) column (Phenomenex) was used for separation of leaf phenolic extracts with the HPLC equipment as described above. Typically 20 μL of methanol extract was injected at a column temperature of 25^{o}C. The liquid phase consisted of a mixture of solvent A, distilled H_2O with 0.4% formic acid; and solvent B, HPLC-grade acetonitrile with 0.4% formic acid. Chemicals were separated within 42 mins using the following gradient program, 0 mins, 5% solvent B; 5 mins, 14% B; 11 mins, 38% B; 40 mins, 100% B; 42 mins, 100% B; 47 mins 5% B. Estimation of individual PG concentration was achieved by comparing peak T_R and integrated peak areas at 280 nm with pure standards of salicin, salicortin, tremuloidin and tremulacin. Standard curves were generated for each PG of

Table 2.1. Response factors for the estimation of chemical concentration relative to an I.S.

Chemical	Range (μg mL^{-1})	Wavelength (nm)	Linear formula	R^2
3-Hydroxybenzyl alcohol	1.6-62.1	194	y = 0.9149x + 1.19	0.99
Acetyl-CoA	1.1-404.8	260	y = 0.0471x + 0.21	0.98
Benzyl acetate	1.9-75.0	194	y = 0.5164x + 0.58	0.98
Benzyl alcohol	1.4-54.1	194	y = 0.8335x + 0.63	0.98
Benzyl benzoate	2.7-106.1	194	y = 0.5579x + 0.75	0.98
Benzoyl-CoA	1.8-433.8	260	y = 0.0939x + 0.21	0.99
Cinnamyl alcohol	1.2-58.7	194	y = 0.4496x + 0.87	0.99
Cinnamoyl-CoA	1.8-433.8	260	y = 0.0704x + 0.02	0.98
Coniferyl alcohol	1.3-61.3	194	y = 0.2399x + 0.82	0.99
Caffeoyl-CoA	1.7-423.4	260	y = 0.0705x + 0.02	0.98
CoA-SH	1.6-383.7	260	y = 0.0539x + 0.02	0.99
p-Coumaryl alcohol	1.5-58.1	260	y=1.004x + 0.76	0.99
Salicyl alcohol	1.6-62.1	194	y = 1.0933x + 0.33	0.99

Note: 2-acetonaphthone was the I.S. used. The linear formula for each analyte was used as the response factor when estimating concentration.

interest by measuring the peak areas of pure PG standards over a range of concentrations (LOD-2000 μg mL^{-1}). Response factors were as follows where y = UV absorbance at 280 nm, x = PG concentration (μg mL^{-1}), salicin (1), y=1185.1x, R^2 = 0.99; salicortin (2), y = 578.5x, R^2 = 0.97; tremuloidin (3), y=2637.7x, R^2 = 0.99; tremulacin (4), y = 539.5x, R^2 = 0.99.

2.14. Mass spectrometric analysis

Liquid chromatography - mass spectrometry (LC-MS) analysis to confirm enzyme products was performed using an Acquity ultra performance LC (Waters, Milford, MA, USA) coupled with a Quadrupole mass time of flight (Q-TOF) MS (Synpart) with MassLynx software v4.1 SCN704 (Waters). This analysis was performed at the UVic Genome BC Proteomics Centre, Victoria, BC, Canada by Mr Cuong Le and Mr. Darryl Hardie. Typically, 20 μL of enzyme product was injected in to a Acquity UPLC CSH Phenyl-Hexyl, 130Å, (1.7 µm, 2.1 mm X 50 mm) column (Waters), at 30^{o}C with a flow rate of 0.2 μL min^{-1}, over a linear gradient from 0% acetonitrile to 100% in 15 mins, and analysis was performed in negative ion mode. For more detailed analysis, the peaks of interest were purified by collecting the eluent at the appropriate T_R and then manually injecting the fraction in to the Orbitrap Fusion MS (Thermo Scientific, Waltham, MA USA) with electron transfer dissociation (ETD) equipped with 'Fusion tune' application software ver1.0.727.28 (Thermo Scientific). Samples were dissolved in 70% acetonitrile and fragmented with quadrapole selection in negative ion mode, and collision induced-dissociation (CID) of 35 volts.

Gas chromatography - mass spectrometry (GC-MS) was conducted by Dr. Tobias G. Köllner at the Max Planck Institute for Chemical Ecology, Jena, Germany, using an Agilent 6890 Series gas chromatograph (Agilent Technologies GmbH, Waldbronn, Germany) coupled to an Agilent 5973 quadrupole mass selective detector (interface temp, 270°C; quadrupole temp, 150°C; source temp, 230°C; electron energy, 70 eV). The compounds were separated using a DB5-MS column (30 m x 0.25 mm x 0.25 µm; Agilent, Santa Clara, CA, USA) and He (2 mL min^{-1}) as carrier gas. The sample (1 µL) was injected without split (injector temperature, 230°C) at an initial oven temperature of 70°C. The temperature was held for 3 min and then increased to 280°C with a gradient of

7°C min^{-1}, followed by a further increase to 330°C with 100°C min^{-1} and a hold for 1 min. Compounds were tentatively identified by comparison of mass spectra to those of reference spectra in the Wiley and National Institute of Standards and Technology libraries.

2.15. Manufacture of RNAi vectors for transgenic plants

The RNA interference (RNAi) pathway is a RNA-dependent gene silencing process that leads to post-transcriptional gene silencing by initiating the degradation of the gene specific mRNAs, and preventing their translation into polypeptides (Fire *et al*., 1998; Latterich, 2008). It has physiological roles as a defense against parasitic nucleotide sequences from viruses and transposons that exploit the host's gene expression and translation infrastructure in order to replicate, as well as a developmental role by controlling temporal gene expression (Latterich, 2008).

Introduction of double stranded RNA (dsRNA) in the form of hairpin RNA (hpRNA) activates the 'dicer' enzyme which cleaves long dsRNA molecules into shorter fragments of ~20 nucleotides long known as small interfering RNA (siRNA). These are unwound into two single-stranded RNAs (ssRNA), the 'passenger' and 'guide' strands. The passenger strand is degraded while and the guide strand is incorporated into the RNA-induced silencing complex (RISC). Post-transcriptional gene silencing occurs when the guide strand binds with complementary mRNA molecules inducing their cleavage by 'Argonaute', the catalytic component of the RISC (Latterich, 2008).

The hairpin structures for the target sequences was synthesized using the pKannibal vector system (Figure 2.7) (Wesley *et al*., 2001) that constitutively expresses hpRNA under the control of a cauliflower mosaic virus 35 S promotor (CaMV 35S) driven cassette. The pKannibal cassettes were then cloned into pART27 (Gleave, 1992) to form a binary vector that can be used with *Agrobacterium* spp. in order to introduce the construct into the hybrid poplar genome.

Agrobacterium tumefaciens (family, Rhizobiaceae) is a Gram negative bacteria that causes crown gall disease in a wide range of eudicotyledon angiosperms. This disease is characterized by tumor-like growths at the junction between the root and the shoot, they are induced by the conjugative transfer of a DNA segment (transfer DNA, T-DNA) from

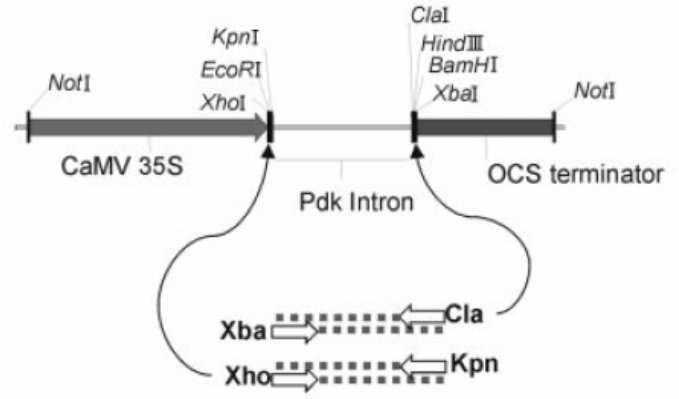

Figure 2.4. The RNAi cassette of the pKannibal vector (taken from Wesley *et al*., 2001).

PCR products from the target gene are cloned into the polylinkers of pKannibal; restriction sites added by the PCR primers ensure the correct orientation of the resulting sense and anti-sense arms. Abbreviations, CaMV 35S, cauliflower mosaic virus 35 S promotor; PdK Intron, pyruvate dehydrogenase kinase intron; OCS terminator, the octopine synthase terminator.

the bacterial tumour-inducing (Ti) plasmid which is integrated semi-randomly into the plant genome (Nester *et al*., 2005). We used a disarmed strain of *A. tumefaciens* with a Ti plasmid lacking the tumor-causing DNA sequences. The pKannibal-pART27 binary vector confers kanamycin resistance that is used for selection of transformed plants.

The pKannibal vector system (Figure 2.4) is designed such that a given PCR fragment can be inserted in the sense orientation into the *Xho*I/*EcoR*I/*Kpn*I polylinker and in the anti-sense orientation in the *Cla*I/*Hind*III/*Bam*HI/*Xba*I polylinker to produce hpRNA. A section of the gene of interest (approximately 200 bp in length) was selected and amplified from 717 hybrid (*P. tremula* x *P. alba*) leaf cDNA by two separate PCR reactions with the appropriate linker sites introduced with each primer. To achieve highly specific gene down-regulation, the nucleotide sequence must be unique to the gene of interest. Sequence regions near the 3' un-translated region (3' UTR) were selected as they are typically the least conserved (Hawkins, 1996). For all of the pKannibal constructs used in this work, the sense orientation sequence insertion was flanked by *Xho*I (5' end) and *Kpn*I (3' end), the anti-sense orientation, *Xba*I (5' end) and *Bam*HI (3' end)

restriction sites. All constructs were designed using Vector NTI® Express Designer Software (Life Technologies Inc.).

In order to check the specificity of the gene sequences selected for hairpins and the RNAi vector, the full genomic nucleotide sequences of *PtACT47* and *PtACT49* were used as bait sequences and BLAST searched against the *P. trichocarpa* genome database using Phytozome (*http://www.phytozome.net/*) and NCBI (*http://www.ncbi.nlm.nih.gov/*). Putative genes *PtACT45* (Potri.013G074400), *PtACT46* (Potri.013G074300), were found to have high sequence similarities with *PtACT47* and *PtACT49*. *PtACT54* (Potri.001G448000) was also included in this analysis for completeness, despite sharing relatively low sequence identity with *PtACT47* and *PtACT49*. In addition, an expressed sequence tag (EST) with GenBank Accession no. BU837657.1 collected from the T104C07 *Populus* apical shoot cDNA library *P. tremula* x *P. tremuloides* (Unneberg *et al*., 2002 unpublished) was also found to have high similarity to both *PtACT47* and *PtACT49* (Appendices Figure A2.1). To ensure that the RNAi pathways targets only the genes of interest, it is vital to select a sequence region that is unique to the gene of interest and absent of conserved regions. To optimize the sequence selection process, a sequence alignment was generated (Figure 2.5). For the gene *PtACT47* a 200 bp sequence was selected which spans the coding region and the 3' UTR. The full sequence was as follows (italicized letters indicate the coding sequence, non- italicized letters indicate the 3'UTR, bold letters indicate the primer sequence used to generate the amplicon) 5'***AGGGCCAGCTACAAAGTGGGCA****AACTCATTCCAAATTTATCGCGTCTTCCTTAT AA*GTTTAATTGTTTACTTCTTTTTTTCTCCCATAAGCTAAATGGTTCCTCTGTG ATATAATGTAAGCGAGGTTAAAAGTGTGCGTGTGAAAGTGATGAGGAGTGCT GCTAAAAAGAAAAAAAGA**TAGCGACGATCGATGAGAGAAT** 3'. The primers used to generate this amplicon by PCR were as follows, underlined letters indicate restriction endonuclease sequences, *Pt*ACT47 sense fragment primers (*Pt*ACT47_Sense_*Xho*I_F - 5' GCCTCGAGAGGGCCAGCTACAAAGTGGG 3'; *Pt*ACT47_Sense_*Kpn*I_R – 5' GCGGTACCATTCTCTCATCGATCGTCGCTA 3'). *Pt*ACT47 anti-sense fragment primers (*Pt*ACT47_Antisense _*Xba*I_F – 5' GCTCTAGAAGGGCCAGCTACAAAGTGGGCA 3'; *Pt*ACT47_Antisense_*Bam*HI_R – 5' GCGGATCCATTCTCTCATCGATCGTCGCTA 3').

For gene *PtACT49* a 187 bp sequence spanning the coding sequence and 3'UTR was selected

5'***ACGACCAGACAGTTAGCTCGCA****AACTAAGTCCAAATTTATTGTATCTTCCCTATA A*GTCGATTTGCTTACTCTTTCTTTCCAGAAGCTAAAATGTTAGTCTTCGCTACA TGTGTACTAAGGTTAAAATGGTGCGAGTGAGAGTGCTGATGAAAAGACCAGA AAAA**ATTAGGGGAGGGGGGAGAACAT** 3'. The primers used to generate this amplicon by PCR were as follows, underlined letters indicate restriction endonuclease sequences, *Pt*ACT49 sense fragment primers (*Pt*ACT49_Sense_ *Xho*I_F – 5' GCCTCGAGACGACCAGACAGTTAGCTCGCA 3'; *Pt*ACT49_Sense_ *Kpn*I_R – 5' GCGGTACCATGTTCTCCCCCCTCCCCTAAT 3'). *Pt*ACT49 anti-sense fragment primers (*Pt*ACT49_Antisense_ *Xba*I_F – 5' GCTCTAGAACGACCAGACAGTTAGCTCGCA 3'; *Pt*ACT49_Antisense_ *Bam*HI_R – 5' GCGGATCCATGTTCTCCCCCCTCCCCTAAT 3').

For the 'double knock-down' (DKD) construct targeting both *PtACT47* and *PtACT49* simultaneously, a 241 bp amplicon was selected and amplified using using; DKD sense fragment primers (DK_Sense_*Xho*I_F – 5' GCCTCGAGTATGCATTGTCAATGCTCGTG 3'; DK_Sense_KpnI_R – 5' GCGGTACCAGGTATGCCCTTACCACTGTAAA 3'); antisense fragment (DK_Antisense_*Xba*I_F – 5'GCTCTAGATATGCATTGTCAATGCTCGTGAGAAA 3'; DK_Antisense_*Bam*HI_R – 5' GCGGATCCAGGTATGCCCTTACCACTGTAA 3'). It is important to note that nucleotide sequence of *PtACT47* and *PtACT49* between these two primer amplification regions is not identical, but share a 92% sequence identity. This high sequence identity suggests a high probability that the hairpin RNA produced with pKannibal would still cause significant knock-down of both genes. Sequences were amplified using PCR, conditions were 98^{o}C 3 mins, 35 repetitions of (98 ^{o}C 30 s, 58 ^{o}C 30 s, 72 ^{o}C 45 s), 72 ^{o}C 10 mins, using Phusion® high-fidelity DNA Polymerase (New England Biolabs Inc.). As described previously, the amplified fragments were cloned into pGEM®-T Easy (Promega) and sequenced to confirm the absence of PCR-generated errors. The amplicons were then excised from the pGEM®-T Easy vector by sequential digestion with appropriate restriction endonucleases, then ligated using T4 DNA ligase

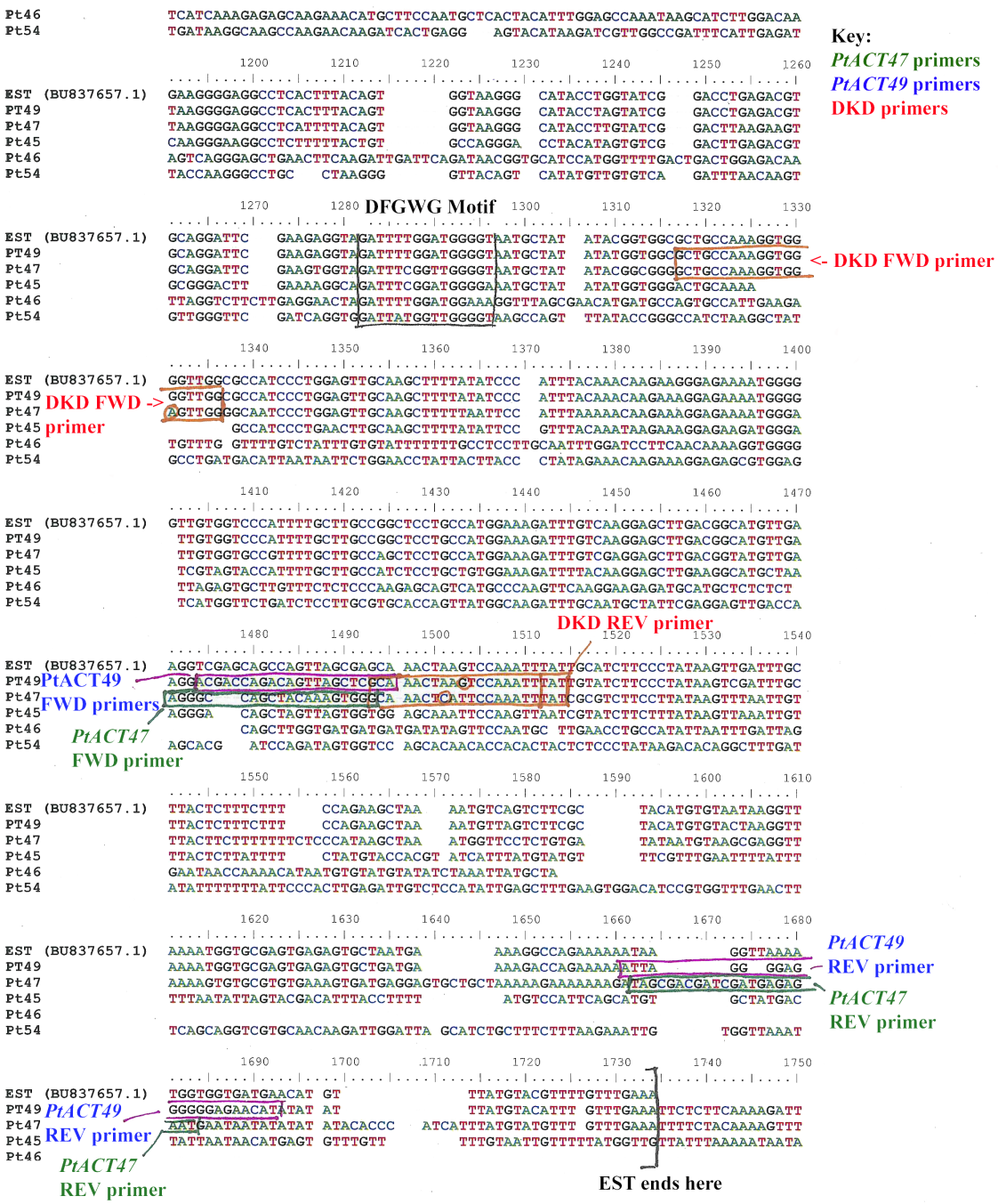

Figure 2.5. A sequence alignment for selection of gene-specific amplicons for *PtACT47*, *PtACT49* and DKD for use with the pKannibal vector.

Sequence alignment and pile up diagram generated using BioEdit software (v7.2.3) (http://*www.mbio.ncsu.edu/bioedit/bioedit.html*) (Hall, 1999). Abbreviations, FWD, sense primer location; REV, anti-sense primer location; *PtACT47*; *PtACT49*; and (DKD) double knock down of *PtACT47* and *PtACT49* combined.

(New England BioLabs Inc.) into a pKannibal vector that had previously been digested in an identical manor (Figure 2.6). Electroporation of XL1 strain *E. coli* cells, followed by selection on LB agar media plates with kanamycin (50 μg mL^{-1}) and colony PCR as described previously was performed. Successfully transformed colonies were incubated in shaking cultures for 12 hrs in liquid LB media with kanamycin (50 μg mL^{-1}) before plasmid extraction and purification using QIAprep Spin Miniprep Kit (Qiagen). The RNAi cassette was sub-cloned into the pART27 vector (Gleave, 1992) (Figure 2.7) that can be utilized by *A. tumefaciens*. The pART27 vector contains a spectinomycin resistance (Sp^R/St^R) gene is for bacterial selection. The sequence information between the left border (LB) and right border (RB) can be integrated into the plant genome by *Agrobacterium*. Included in this region is a NotI cloning site into which the pKannibal RNAi cassette was ligated and is constitutively expressed under the control of a CaMV 35 S promoter. A gene sequence that confers kanamycin resistance (Neomycin phosphotransferase II, nptII) is also present between the LB and RB that allows for kanamycin selection of positively transformed plants.

The pKannibal RNAi cassette is flanked by two *Not*I restriction endonuclease sites, however due to the size of the constructs (*PtACT47*-pKannibal, 6457 bp; *PtACT49*-pKannibal, 6431 bp; and DKD-pKannibal, 6539 bp) digestion with *Not*I alone results in two fragments of almost equal size making it difficult to separate by gel electrophoresis. For example, *NotI* digestion of *PtACT47*-pKannibal (6457 bp) results in a 3362 bp fragment containing the RNAi cassette and a 3095 bp fragment of pKannibal backbone. To mitigate this a sequential double digestion using *Not*I and *Eco*RV was performed since an *Eco*RV site in the pKannibal backbone can be exploited to split this fragment in two. For example, a *Not*I and *Eco*RV digestion of *PtACT47*-pKannibal (6457 bp) resulted in a *PtACT47*-pKannibal RNAi cassette fragment (3362 bp) and two smaller pKannibal backbone fragments of 1770 and 1339 bp that can more easily be separated by gel electrophoresis. The pKannibal RNAi cassette was excised from the gel, purified, and ligated into the *Not*I cloning site of pART27 to produce the pKannibal-pART27 binary vector.

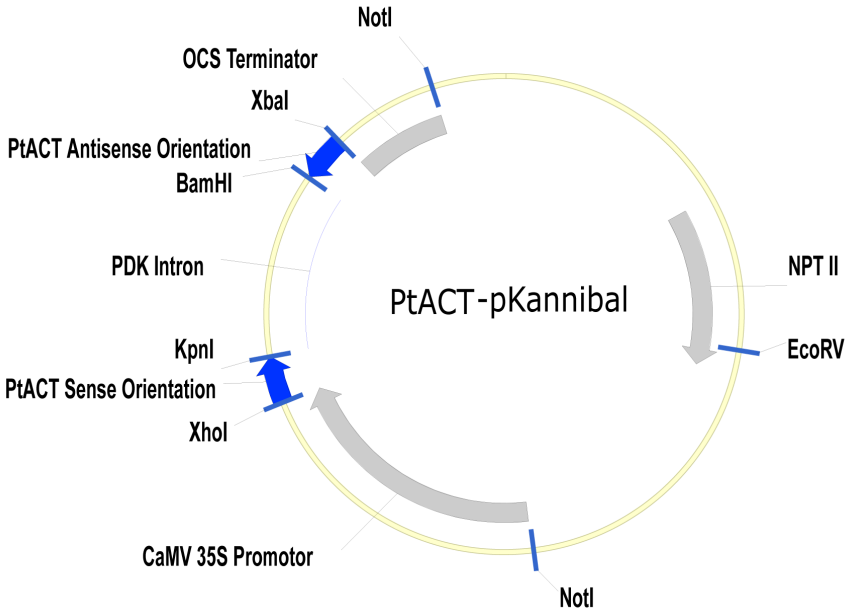

Figure 2.6. A general vector map of the predicted *Pt*ACT-pKannibal construct.

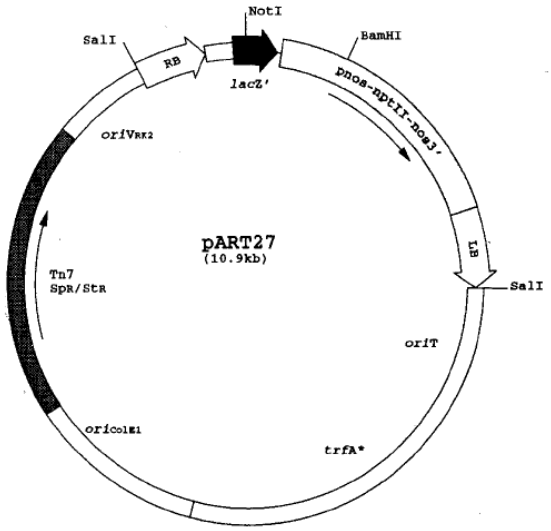

Figure 2.7. The binary vector pART27 (taken from Gleave, 1992).
The right border (RB) and left border (LB) are indicated by the arrowed boxes; the *lac Z* region (encoding the *lac* α peptide) is represented by the dark arrowed box and the chimeric *nptII* region (neomycin phosphotransferase II, kanamycin resistance, a plant selectable marker) is shaded (arrow denotes orientation of the coding region). The replication functions are indicated and the Sp^R/St^R (spectinomycin resistance) bacterial selectable marker is represented by the dark box (arrow denotes orientation of coding region).

2.16. Whole plant transformation

Electro-competent *A. tumefaciens* cells were transformed with either *PtACT47*-pKannibal-pART27, *PtACT49*-pKannibal-pART27, or DKD-pKannibal-pART27 plasmids by electroporation (as described previously) and transformed colonies were selected by incubation on LB agar media infused with gentamycin (8 μg mL^{-1}), rifampicin (50 μg mL^{-1}), and spectinomycin (100 μg mL^{-1}) antibiotics. A single successfully transformed colony was used to establish an overnight liquid shaking culture of LB with identical antibiotics at 28^{o}C, and shaking at 225 rpm. Cells were pelleted by centrifugation at 3500 rpm at room temperature for 35 mins, then re-suspended in 'induction media' consisting of Murashige-Skoog (MS) basal salts with vitamins plus 1.28 mM 2-(N-morpholino)ethanesulfonic acid (MES), 10 mM galactose, 50 μM acetosyringone to an OD_{600} = 0.5. Acetosyringone is known to increase transformation efficiency (Sheikholeslam and Weeks, 1987). The cultures were then incubated at 28^{o}C, shaking at 225 rpm for a further 30-60 min until an OD_{600} of 0.6 was reached.

In sterile conditions, whole leaves of one to three month-old 717 plants were excised and wounded with multiple fine cuts around the periphery of leaves using a scalpel, then incubated with *A. tumefaciens* culture for 1 hr at 28^{o}C at 130 rpm. Leaves were then removed and blotted on sterile filter paper to remove excess moisture, then placed (top side down) on to 'callus-inducing media 1' (CIM1) plates (0.44 % (wt/vol) MS with vitamins, 3% (wt/vol) sucrose, 0.02% (wt/vol) L-glutamine, 5 μM 6-γ-γ-[Dimethylallylamino]-purine (2iP*)*, 10 μM naphthalene acetic acid (NAA), and solidified with 3% (wt/vol) agar and 1.1% (wt/vol) Phytagel, pH to 5.7–5.8) and incubated for two days in darkness at 28^{o}C. Leaves were then moved onto CIM 2 plates (identical to CIM1 plus cefolataxine (250 μg mL^{-1}), carbenicillin (500 μg mL^{-1}), spectinomycin (100 μg mL^{-1}) and incubated in darkness at 28^{o}C for a further 21 days until callus tissue begins to form at sites of *A. tumefaciens* infiltration. Calli were then moved on to 'shoot-inducing media' (SIM) plates (0.44 % (wt/vol) MS with vitamins, 3 % (wt/vol) sucrose, 0.02 % (wt/vol) L-glutamine, cephalotaxine (250 μg mL^{-1}), carbenicillin (500 μg mL^{-1}), kanamycin (50 μg mL^{-1}), 0.2 μM thidiazuron (TDZ), and solidified with 3% (wt/vol) agar and 1.1% (wt/vol) Phytagel, pH to 5.7–5.8) and placed in light for several weeks. TDZ induces high-frequency direct shoot organogenesis (Lata *et al*., 2009). Shoots were

excised and placed in Magenta boxes with root-inducing media (RIM) (0.22 % (wt/vol) MS with vitamins, 1.5 % (wt/vol) sucrose, 0.01 % (wt/vol) L-glutamine, kanamycin (50 μg mL^{-1}), 0.5 μM indole-3-butyric acid (IBA), solidified with 3% (wt/vol) agar and 1.1% (wt/vol) Phytagel, pH to 5.7–5.8). IBA is known to stimulate root formation in plants (Ludwig-Müller *et al*., 1993). Plants were grown in light conditions with a diurnal cycle (12 hrs light, 12 hrs darkness) at 21^{o}C for 12 weeks before transfer to the greenhouse.

2.17. Screening for transgenic RNAi plants

Plants were screened at two time points, after 12 weeks of growth in RIM media, and again after an additional 8 weeks of growth in greenhouse conditions (20 weeks old total). In the first instance, only plants exhibiting root formation in kanamycin enriched RIM media were tested. Leaves were excised, frozen in liquid nitrogen, and then RNA was extracted and cDNA synthesized (as described previously). The presence of the kanamycin resistance gene in the transcriptome was indicative of a successfully transformed plant line. Presence or absence of this gene was tested by PCR using primers NPT3-AAGAAGGCGATAGAAGGCG, and NPT5-TTGGGTGGAGAGGCTATTCG, with conditions (98^{o}C 3 mins, 35 repetitions of (98 ^{o}C 30 s, 58 ^{o}C 30 s, 72 ^{o}C 45 s), 72 ^{o}C 10 mins).

Of the plant lines testing positive for the kanamycin resistance gene, the degree of RNAi-mediated gene silencing was tested using qPCR. The relative transcript abundance (RTA) of *PtACT47*, *PtACT49*, or both for DKD lines, was compared to the mean RTA from six 717 wild type plants grown in identical conditions, and harvested at the same time as transgenic lines. The four plant lines exhibiting the lowest gene expression in each case were selected for further analysis. Typically four biological replicates from each of the independent transgenic lines were selected and transferred to the greenhouse for observation of potential phenotypes and chemotypes.

After 12 weeks of additional growth in greenhouse conditions, a single leaf (LPI 5) was harvested from each biological replicate from all transgenic lines. As before, an RNA extraction, cDNA synthesis and qPCR analysis was performed again to confirm that expression of target BAHD genes were still supressed.

2.18. Condensed tannin quantification

CTs were assayed using the acid-butanol assay as described (Porter *et al*., 1986; Peters and Constabel, 2002). For each sample, four steel ball bearings were placed into a cryotube with 25-30 mg of fresh tissue. Samples were steeped in 1.5 mL of 100% MeOH and homogenized using a Precellys 24 homogenizer (Bertin technologies) at 2 x 45 s, 5500 rpm followed 10 minutes of ultra sonication at a frequency of 40 kHz generated by a VWR model 75 T ultrasonic bath (VWR). Samples were then centrifuged at 1500 rpm for 5 mins. The supernatant (1.5 mL) was removed and placed into a glass vials, than an additional 1 mL MeOH was added and samples were then vortexed. The original tissue sample was re-extracted one more time as before, and an additional 1 mL of extract was added to the glass vial, making a total extraction volume of 3.5 mL. 400 μL of this sample was mixed with 2 mL of 95% Butanol, 5% HCl and 67 μL Fe reagent in 15 mL polypropylene conical tubes. Samples were vortexed and 200 μL was removed and placed into an additional conical tube, this will be the unheated control. The original sample was incubated in a water bath at 95^{o}C for 40 mins, after which samples were allowed to cool at room temperature for 15 mins. 200 μL of heated and unheated samples were pipetted into wells of a 96 well plate and the absorbance at 550 nm recorded using Victor^{TM} X5 2030 multilabel reader (PerkinElmer, Waltham, MA, USA). Absorbance values were then compared to a standard curve made with pure *P. tremuloides* x *P. tremula* tannin standards and [CT] (mg g^{-1} fr. wt.) was estimated.

2.19. Statistical analysis

All experiments followed a completely randomized design (CRD) with treatments denoted as *k* and replicates as *n*. One-way analysis of variance (ANOVA) ($\alpha = 0.05$) and comparison of means using a student t-test were performed using SAS JMP version 7.0 (SAS institute Inc.) For qPCR analysis, the geometric mean was calculated using the following formula preset in Microsoft Excel,

$$\left(\prod_{i=1}^{n} a_i\right)^{1/n} = \sqrt[n]{a_1 a_2 \cdots a_n}.$$

Differences in relative transcript abundance (ΔC_T) was calculated using the following formula,

$\Delta C_T = C_{Tgene} - C_{Tgeomean}$

Statistical output tables for the comparison of MYB134 and wild type plants are located in Appendices A6.1 for PG content analysis and A6.2 for qPCR analysis. A similar approach was used for analysis of the wounding experiments. The statistical output for the comparison of wounded and unwounded plants is shown in Appendices A6.4 for PG content, and A6.5 for gene expression analysis.

For calculation of enzyme kinetic parameters, the Michaelis–Menten constants (K_m, μM) and maximum velocity (V_{max}, μM sec^{-1}) values were determined by nonlinear regression analysis (with 95% confidence intervals) of the substrate concentration versus reaction rate data fitted into the Michaelis-Menten equation $Y = V_{max}X[K_m + S]^{-1}$ (Michaelis and Menten, 1913), using the Michaelis-Menten nonlinear model (2P) preset function in SAS JMP IN software. See Appendices A6.3 for statistical output tables for enzyme kinetics.

For statistical analysis of transgenic plants, the genotype treatment (RNAi type) effects on PG content were analyzed using a 'linear mixed effects' (LME) function with a 'restricted maximum likelihood' (REML) method (α=0.01) using 'R' software version 3.1.2 (Free Software Foundation, Boston, MA). Typically, a separate analysis was performed for each type of tissue. The RNAi treatments tested were *PtSABT* (*PtACT47*) RNAi, *PtBEBT* (*PtACT49*) RNAi, and DKD RNAi. These were compared to empty vector RNAi controls and wild type plants. Analysis was performed for total PG content, as well as for individual PGs, salicin (1), salicortin (2), tremuloidin (3), and tremulacin (4). Tissues analyzed were young leaves, medium leaves, old leaves, stems, and roots. Typically three independent transgenic RNAi lines were used for each genotype treatment, and mean values of PG content were calculated from four replicate plants of each line. LME and REML analyses combined all three lines together for each genotype in order to detect an overall treatment effect. If significant treatment effects were detected, then a detailed comparison of individual transgenic lines was conducted by a one-way ANOVA and comparison of means using a student t-test using SAS JMP software (α=0.01). See Appendices A6.6 for full statistical output tables for transgenic analysis.

Chapter 3. Results

Some portions of text in Sections 3.1-3.3 were taken from Chedgy *et al*. (2015).

3.1. Phylogenetic analysis suggests that proteins PtACT47, PtACT49, and PtACT54 cluster with other BAHDs involved in benzenoid ester production.

Complete coding sequences were retrieved from the Phytozome database in order to carry out further studies. The *PtACT47* (Potri.013G074500) gene is localized on chromosome XIII, *PtACT49* (Potri.019G043600) on chromosome XIX, and *PtACT54* (Potri.001G448000) on chromosome I. Despite their spatial separation, the encoded proteins PtACT47 and PtACT49 share 90.6% amino acid sequence identity, while PtACT54 only shares 52.3% with PtACT47 and 52.5% with PtACT49. The characteristic BAHD motifs HXXXD and DFGWG are identical in PtACT47 and PtACT49, HTMSD (His, Thr, Met, Ser, Asp) (residue positions 166-170) and DFGWG (Asp, Phe, Gly, Trp, Gly) (381-385). PtACT54 has motif sequences that differ, they are HPMSD (His, proline Pro, Met, Ser, Asp) (165-169) and DYGWG (Asp, tyrosine Tyr, Met, Gly, Trp, Gly) (388-392). Phylogenetic analysis using full-length amino acid sequences of PtACT47, PtACT49 and PtACT54 with a selection of functionally characterized BAHDs from other plant species was carried out to determine the relationships of the new poplar proteins with the five major BAHD clades previously delineated (D'Auria, 2006).

All three proteins cluster with BAHD sub-clade V-*i*, which are involved in benzenoid ester production (Figure 3.1). It contains the enzymes that synthesize the floral volatile benzyl benzoate, including CbBEBT, the closely related NtBEBT from *Nicotiana tabacum* (D'Auria *et al*., 2002), VhBEBT from *Verbena* x *hybrida* (Togami *et al*., 2006), and PhBPBT (benzoyl-CoA:benzyl alcohol/phenylethanol benzoyltransferase) from *Petunia hybrida* (Boatright *et al*., 2004). These enzymes all have a high affinity for co-substrates benzoyl-CoA as the acyl donor and can use aromatic alcohols as the acyl acceptors. Most similar to PtACT47 and PtACT49 in the phylogeny are alcohol acyltransferases shown to utilize acetyl-CoA with alcohols for volatile ester formation. CmAAT3, an alcohol acyltransferase from *Cucumis melo*, synthesizes benzyl acetate from acetyl-CoA and benzyl alcohol but can also use butanoyl-CoA, propanoyl-CoA and

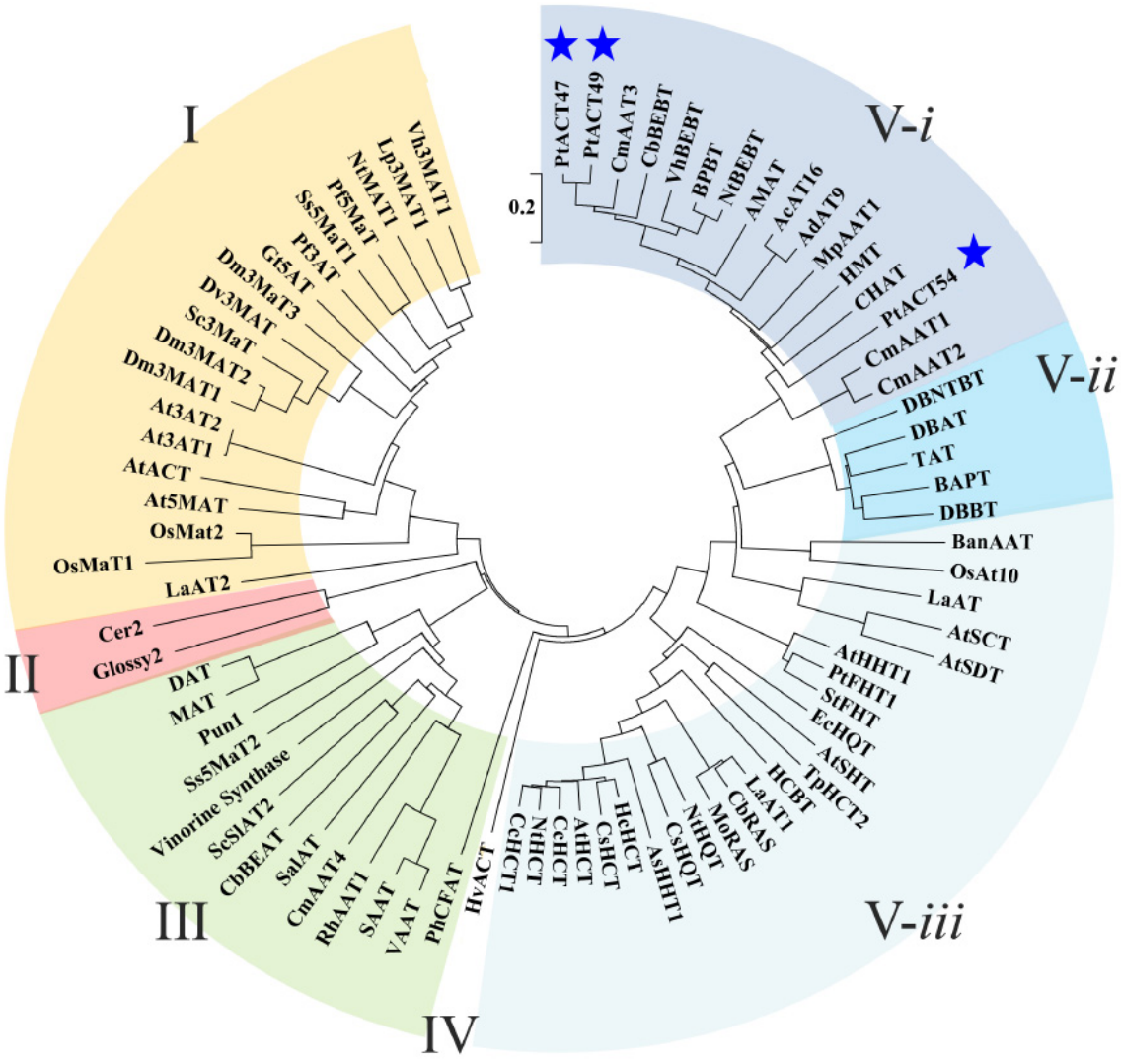

Figure 3.1. **Neighbour-joining phylogeny of functionally characterized BAHD members plus the three *P. trichocarpa* proteins of interest PtACT47, PtACT49 and PtACT54 (indicated with stars).** The 5 major clades as identified by D'Auria (2006) as having shared function are labeled, I) modification of anthocyanins; II) synthesis of long-chain epicuticular waxes; III) utilization of alcohol substrates typically with acetyl-CoA; IV) amide synthesis; V-*i*) benzenoid ester production; V-*ii*) enzymes from *Taxus* spp. involved in paclitaxel production; V-*iii*) synthesis of hydroxycinnamoyl quinate/shikimate esters. For GenBank accession numbers of proteins see section 2.4.

2-methylbutanoyl-CoA with a variety of alcohols (El-Sharkawy *et al*., 2005). MpAAT1 from *Malus pumila* uses acetyl-CoA with 2-methylbutanol to form 2-methylbutyl acetate (Souleyre *et al*., 2005). Members of this clade exhibit low substrate selectivity and are able to utilize several types of CoA thioesters and alcohols as co-substrates to yield a range of ester products. For detailed amino acid sequence analysis of BAHDs of sub-clade V-*i* see Appendices section A4.1. Appendices Table A1 shows the sequence identity index; Figure A4.1.1 shows a sequence alignment for the full coding sequences; and Figure A4.1.2 shows a sequence alignment of regions flanking the two BAHD motifs. The range of sequence identities of BAHDs belonging to sub-clade V-*i* is vast, ranging from 90.6% to 41.7%. While the characteristic BAHD motifs are relatively well conserved within this sub-clade, the regions immediately flanking these motifs by ±10 residues show some variability.

3.2. PG content and expression of *PtACT47* and *PtACT49*

In order to test if correlation exists between PG accumulation and expression of *PtACT47* and *PtACT49*, tissue from catkins, leaves, xylem, and root was harvested from wild type (*P. tremuloides* x *P. tremula*) plants and leaf tissue was harvested from MYB134 over-expressing plants (Mellway *et al*., 2009) and subjected to chemical and transcriptional analysis by qPCR. For the leaves, three different age classes were used, based on the leaf plastochron index (LPI), young leaves, LPI 1-5; medium leaves, LPI 6-10; and old leaves, LPI 11-15. A one-way analysis of variance (ANOVA) (α=0.05) and student t-test was performed to test for significant differences between control and MYB134 plants for PG content, and *PtACT47* and *PtACT49* expression.

The HPLC chromatograms of MYB134 and wild type plants were compared across different leaf ages (Figure 3.2). The total PG content was calculated as the combined total of the four most common PGs, salicin (1), salicortin (2), tremuloidin (3), and tremulacin (4) (Figure 3.3, part A). Catkins, xylem and root tissue generally contained lower PG levels than leaves. Wild type plants contained on average 2.3 times more PGs than MYB134 plants, this was significant in young and medium-aged leaves where the expression of both *PtACT47* and *PtACT49* was also significantly greater (2.4 times) in wild type compared to MYB134 plants (Figure 3.3, parts C and E). Their expression was

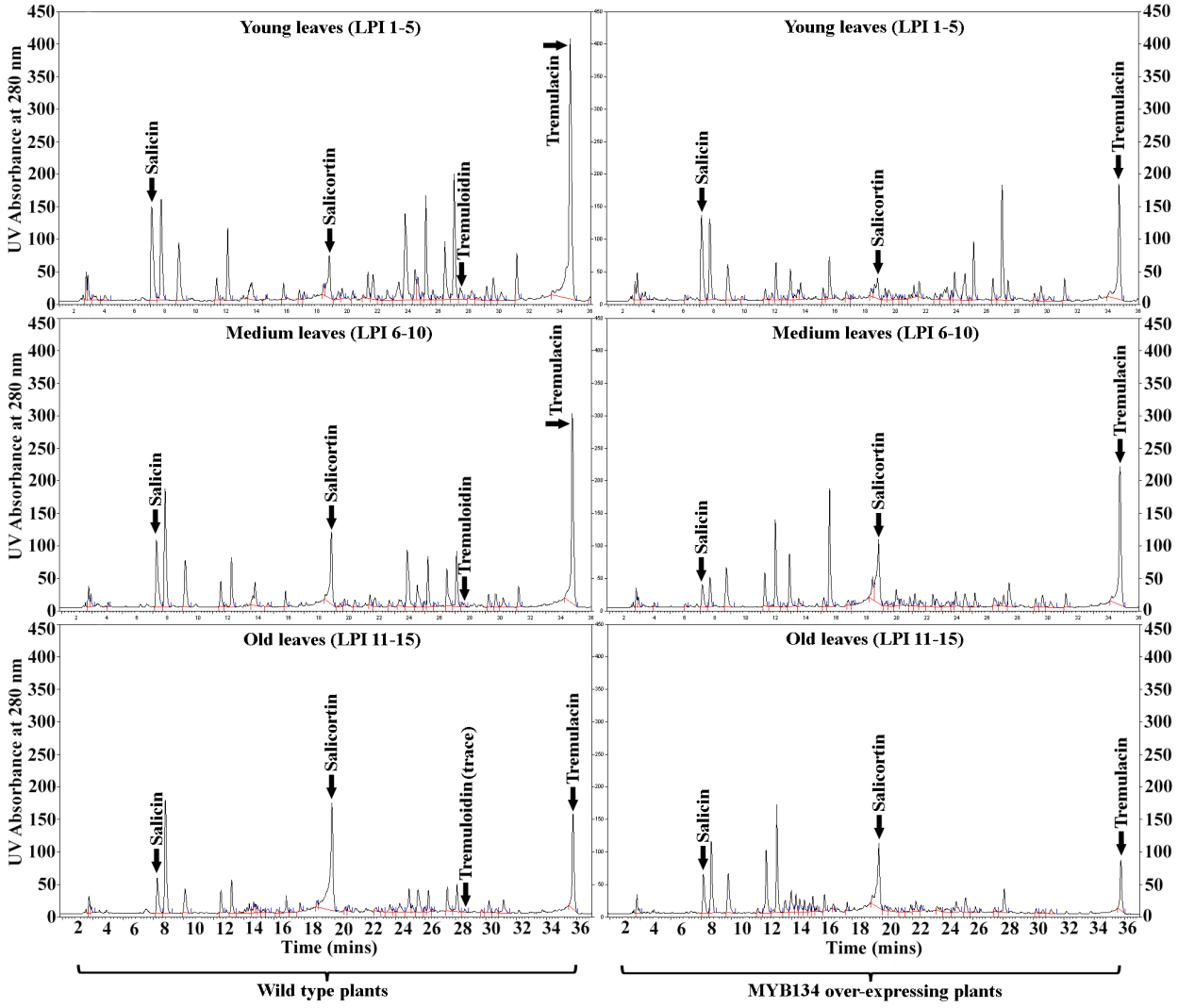

Figure 3.2. A representative comparison of RP-HPLC chromatograms (280 nm) of phenolic extracts of wild type and MYB134 over-expressing leaves of various ages.

Peaks representing salicin (1), salicortin (2), tremuloidin (3), and tremulacin (4) are labeled with arrows.

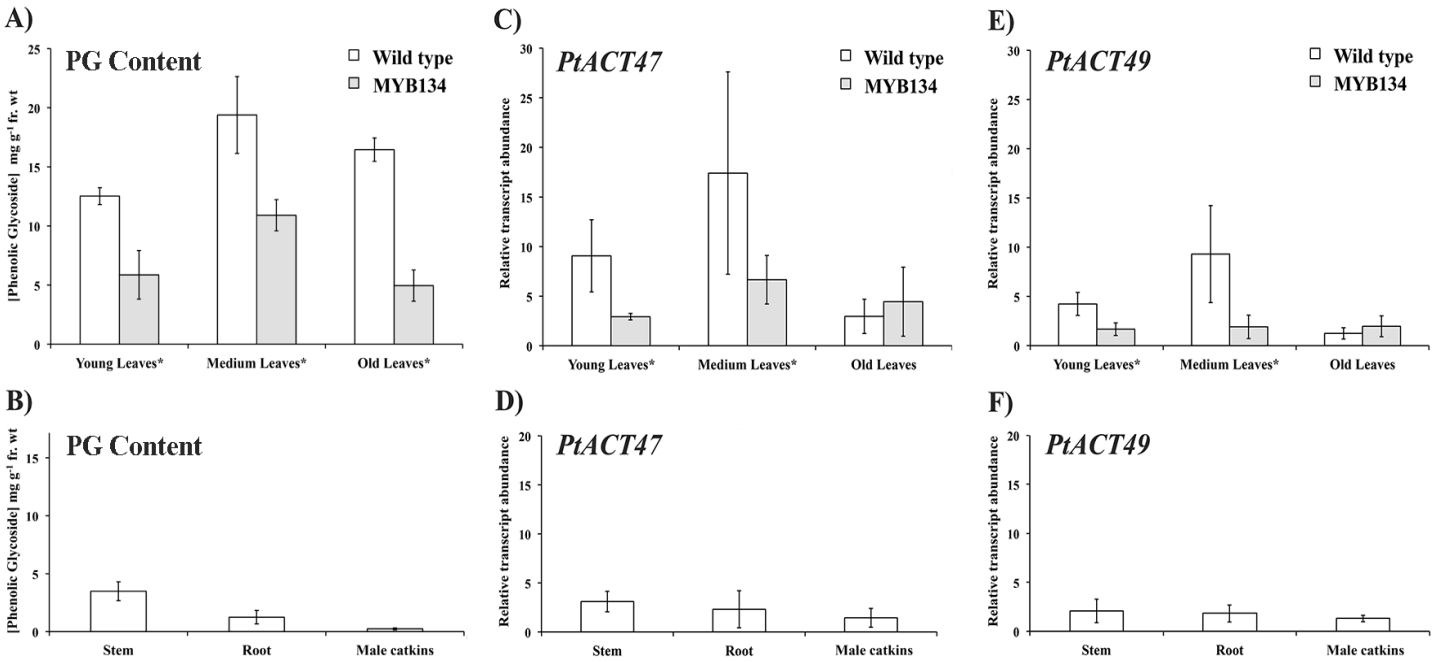

Figure 3.3. Analysis of PG content and *PtACT47* and *PtACT49* expression.

PG content was calculated as the sum of salicin (1), salicortin (2), tremuloidin (3) and tremulacin (4). Relative transcript abundance is relative to house-keeping genes *ELF4* and *UBQ10*. Top panels show comparisons of PG content and gene expression in wildtype and MYB134 overexpressor plants in leaves of three ages; asterisks indicate significant differences between wild type and MYB134 leaves using t tests ($P < 0.01$). Critical F test values were considered significant if greater than the tabular value of $F_{(1, 6)} = 5.99$ ($\alpha = 0.05$). Lower panels show PG content and transcripts in additional organs. (A) Comparison of PG content of wild-type with MYB134 plants in young, medium, and old leaves ($F_{(1, 6)} = 56.2$, 35.0, and 290.8, respectively. (B) Mean PG content in wild-type stem, root and male catkins. (C) Comparison of *PtACT47* expression in wild type and MYB134 plants in young, medium, and old leaves ($F_{(1, 6)} = 34.8$, 11.2, and 0.1, respectively). (E) Comparison of *PtACT49* expression in wild type and MYB134 plants in young, medium, and old leaves ($F_{(1, 6)} = 17.8$, 9.0, and 1.9, respectively). (D and F) *PtACT47* and *PtACT49* expression in wild-type stem, root and male catkins. Y error bars indicate standard deviations.

highest in medium-aged leaves for both plant types while old leaves exhibited relatively the low expression of both genes. In MYB134 plants, the significantly reduced *PtACT47* and *PtACT49* expression was associated with a significantly lower PG content compared with wild type plants. In contrast, *PtACT54* expression levels were low for all of the tissues tested, ranging from 2-5% of that of *PtACT47* and *PtACT49* (not shown). Interestingly, only salicin (1) and salicortin (2) were detected in the roots while all four PGs of interest were present at detectable levels in all other tissues. Analyses of individual PGs and their patterns of accumulation or decline across leaf age may offer some limited insight into potential biosynthetic pathways, or at least the order in which specific PGs are made. Salicortin (2) was the most prevalent, on average accounting for 53% in wild type plants across all leaf ages, it was significantly more abundant in wild types that contained 2.8 times more than in MYB134 plants (Figure 3.4). Salicortin (2) content increased markedly from young to old leaves. For example, wild type leaves contained 2.9 ± 0.4 mg g^{-1} fr. wt., 4.7 ± 0.7 mg g^{-1} fr. wt., and 7.5 ± 0.5 mg g^{-1} fr. wt. in young, medium and old leaves respectively. In MYB134 plants, salicortin (2) was estimated at 0.5 ± 0.3 mg g^{-1} fr. wt., 2.9 ± 0.3 mg g^{-1} fr. wt., 2.7 ± 0.4 mg g^{-1} fr. wt. in young, medium, and old leaves respectively. Interestingly, both salicin (1) and tremulacin (4) exhibited similar concentrations and pattern of abundance with leaf age, making up 21 % and 24 % of the PG content respectively. Both compounds declined in old leaves compared to young and medium leaves. While the levels of both was greater in wild type than MYB134 plants, this pattern of decline in old leaves was similar. Tremulacin (4) levels were highly variable between biological replicates such that statistically there are no significant differences between wild type and MYB134 plants in young and medium age leaves. However, wild type old leaves had significantly greater amounts of tremulacin (4) than in old MYB134 leaves.

Tremuloidin (3) was the least abundant of the four PGs measured, constituting on average 2 % of the total PGs. As was the case with salicin (1) and tremulacin (4), its levels significantly decreased with leaf age in wild types. Tremuloidin (3) was barely quantifiable in MYB134 plants, young leaves contained 4.0 ± 0.1 μg g^{-1} fr. wt. while only trace amounts were detectable in medium and old leaves.

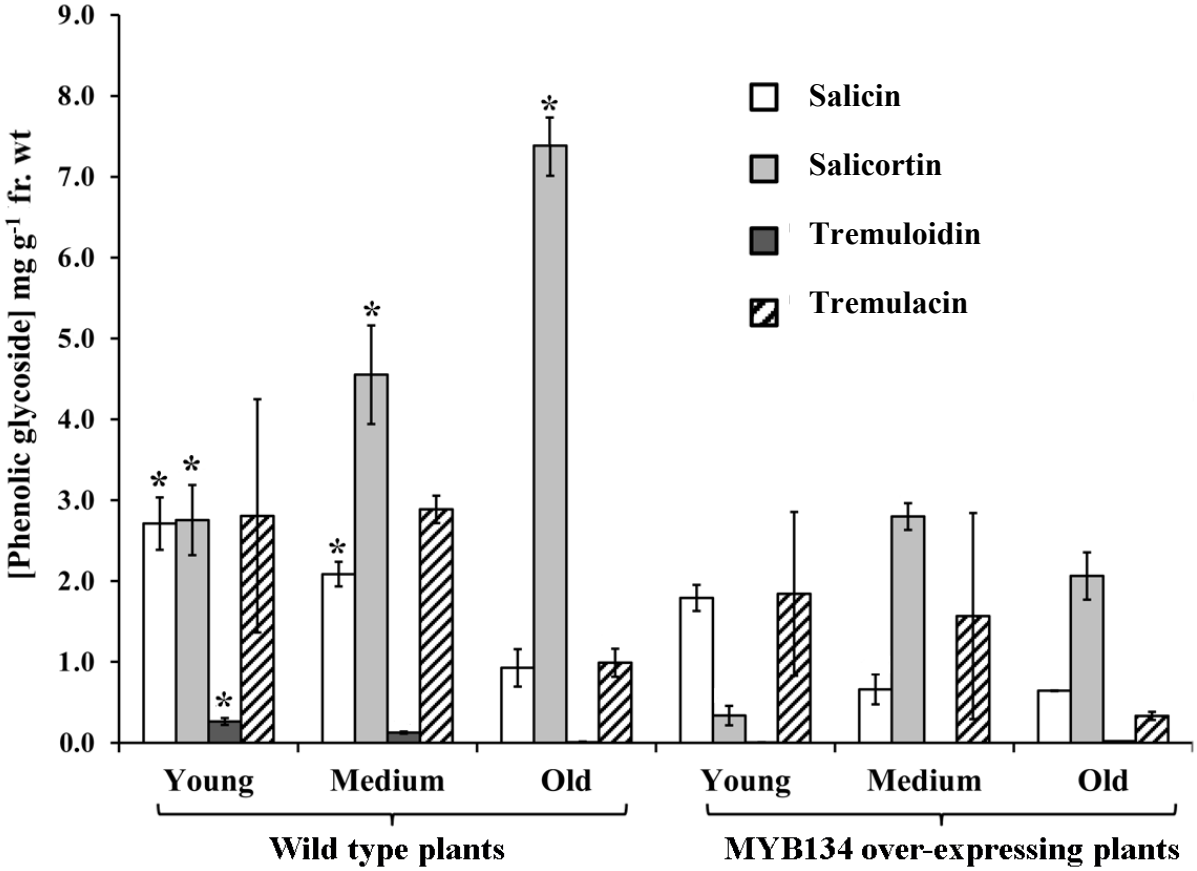

Figure 3.4. The mean estimated concentrations (mg g^{-1} fr. wt) of individual PGs in leaves of different ages in MYB134 and wild type plants.

Asterisks indicate significant differences between chemical content of wild type versus MYB134 leaves of the same age using student t-tests ($P < 0.01$). Critical F test values were considered significant if greater than the tabular value of $F_{(1, 6)} = 5.99$ ($\alpha = 0.05$). Comparing specific PG chemicals with the same leaf age class between wild type versus MYB134 over-expressing plants, for young leaves critical $F_{(1,6)}$ values are as follows for each PG, salicin, 38.9; salicortin, 173.9; tremuloidin, 6.2; tremulacin, 1.8. For medium leaves critical $F_{(1,6)}$ values are as follows for each PG, salicin, 212.3; salicortin, 46.3; tremuloidin, 25.1; tremulacin, 6.3. For old leaves critical $F_{(1,6)}$ values are as follows for each PG, salicin, 8.9; salicortin, 751.7; tremuloidin, 0.3; tremulacin, 85.7.

3.3. Enzyme activity of recombinant PtACT proteins

Full-length coding sequences for *PtACT47*, *PtACT49*, *PtACT49*-H166A and *PtACT54* were amplified from *P. trichocarpa* cDNA and cloned into His-tagged vectors for expression in *E. coli* and purification of recombinant proteins. Analysis of the gene products by SDS-PAGE revealed recombinant proteins of the expected size, 51.9 kDa for PtACT47, and 52.6 for PtACT49 (Figure 3.5). Site-directed mutagenesis was used to produce a PtACT49-H166A mutant protein as an additional control, with the HTMSD motif altered to ATMSD. This protein was also purified, and found to migrate on SDS-PAGE at the same position as recombinant PtACT49. Recombinant PtACT54 also was of the expected size at 53.6 kDa (Figure 3.5). Immuno-blotting confirmed that all of the expressed proteins contained the 6xHis-tag and were full-length proteins (Figure 3.5 for PtACT47, PtACT49, and PtACT49-H166A, Figure 3.6 for PtACT54). For the full coding sequence information of recombinant proteins see Appendices section A3.3.

Preliminary enzyme assays were carried out with benzoyl-CoA or acetyl-CoA as acyl donors with a variety of alcohol acceptor substrates to determine if the recombinant proteins were functional. Previously characterized recombinant CbBEBT (D'Auria *et al*., 2002) was used as a positive control. Assay products were analyzed by reverse-phase HPLC, and the appearance of new product peaks was monitored by UV absorbance at 260 nm and 194 nm. Products were initially identified by co-chromatography with authentic standards and UV spectra, and later verified by mass spectrometry. Both recombinant PtACT47 and PtACT49 were active across a broad pH range, typically between pH 2-12, with highest activity observed between pH 6.5-7.5 for both enzymes and half maximal activity at pH 4.5-5.5 and pH 8.5-9.0 (Figure 3.7). Recombinant PtACT54 was also observed to be active at pH 7.0.

To delineate the substrate preferences of PtACT47, PtACT49, PtACT49-H166A, and PtACT54, we tested several donor phenolic and phenylpropanoid CoAs with a series of alcohol acceptor substrates. Figure 3.8, 3.9 and 3.10 shows the HPLC chromatograms and MS data for reactions that were catalyzed by recombinant PtACT47 and PtACT49. Negative assay controls consisted of boiled recombinant proteins, which showed no activity. Both recombinant PtACT47

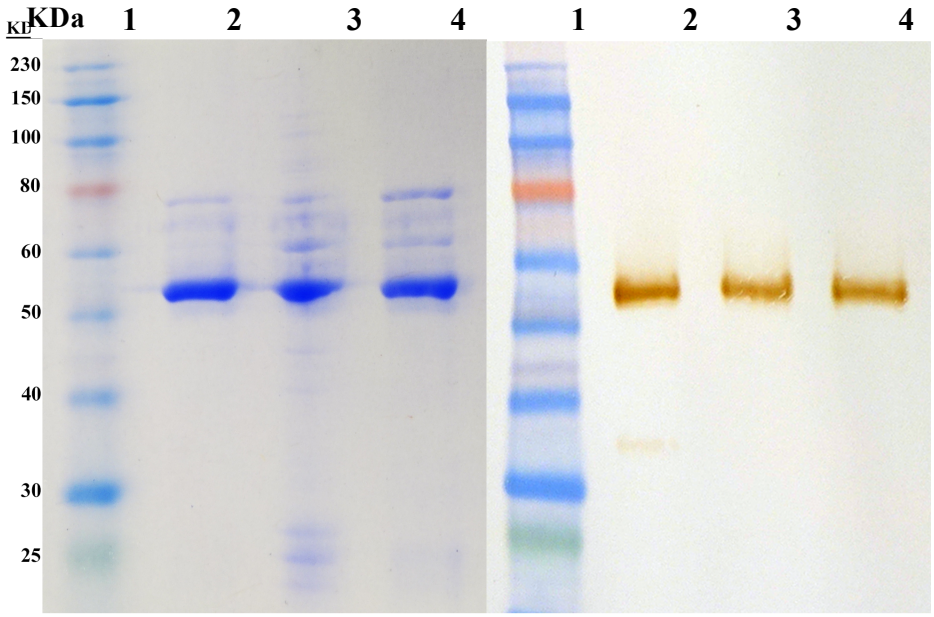

Figure 3.5. SDS–PAGE (left) and immunoblot analysis (right) of purified recombinant His-tagged fusion proteins. Lane 1, pre-stained protein molecular weight ladder; lane 2, PtACT47 (51.9 kDa); lane 3, PtACT49 (52.6 KDa); lane 4, PtACT49 H166A mutant protein (52.6 KDa).

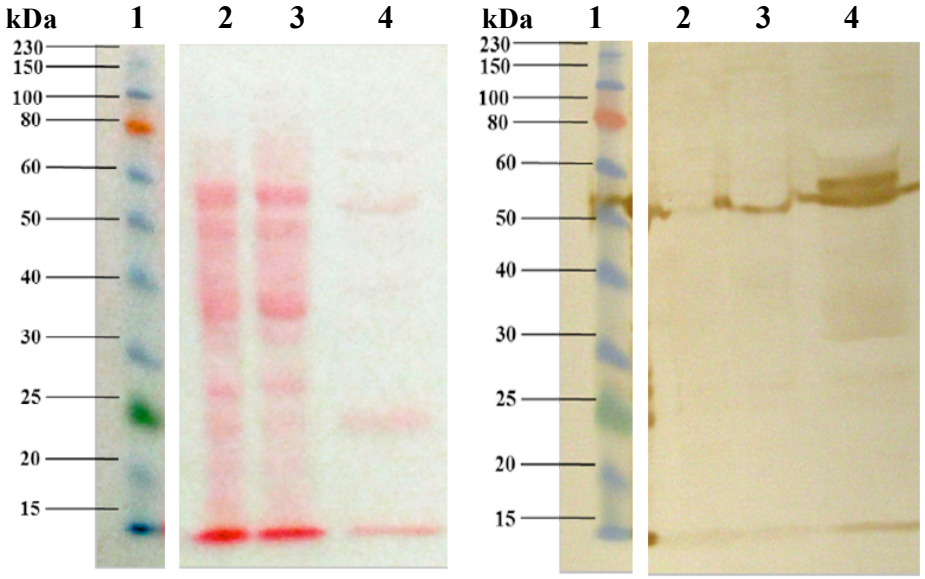

Figure 3.6. Ponceau S staining and immunoblot analysis for recombinant PtACT54 purification. Lane 1, pre-stained protein molecular weight ladder; lane 2, expressed PtACT54 insoluble fraction; lane 3, expressed PtACT54 soluble fraction, lane 4, purified PtACT54 (53.6 kDa) following elution from Ni-NTA column. To see the original gels see Appendices Figure A2.3.2.

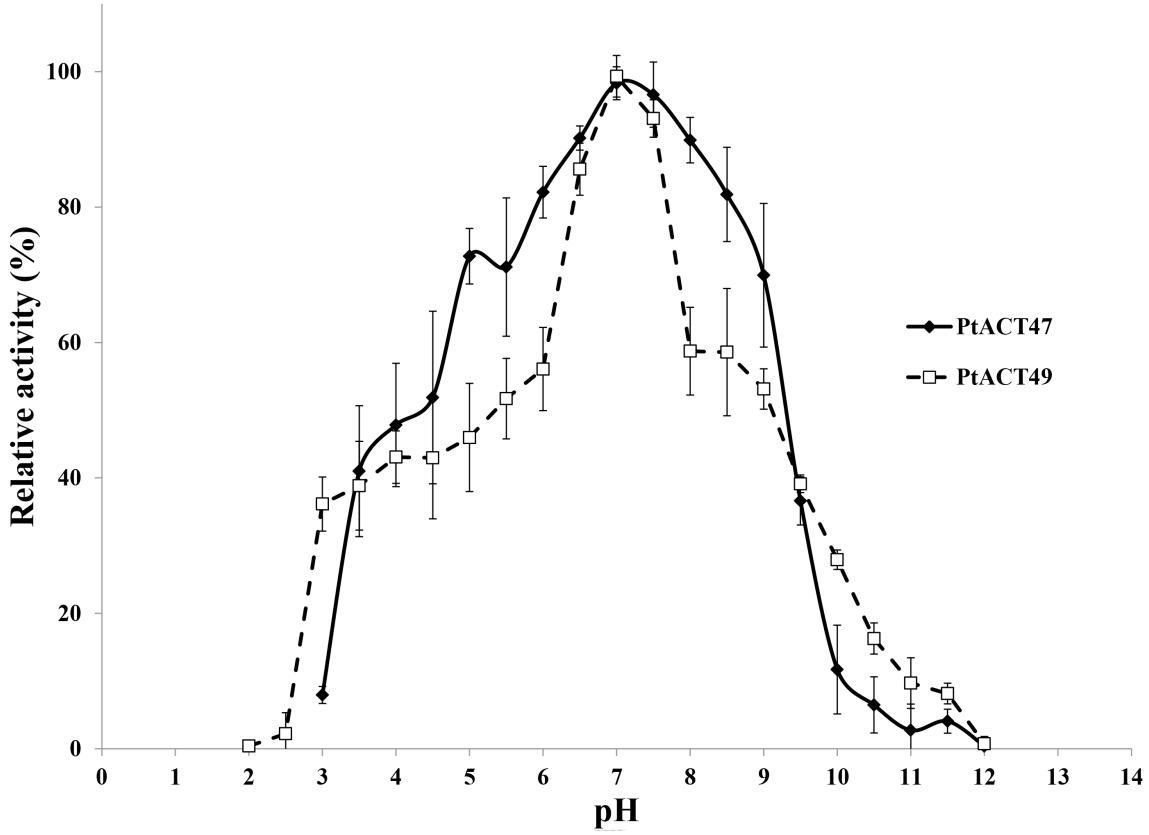

Figure 3.7. Determination of pH optima for PtACT47 and PtACT49 activity.

Relative activity was estimated by quantification of products salicyl benzoate (PtACT47) or benzyl benzoate (PtACT49). All values represent the means of three separate determinations and are reproducible to within ±10% of the mean value. Error bars represent standard deviation.

and PtACT49 preferred benzoyl-CoA as co-substrate. However, PtACT47 preferentially used salicyl alcohol whereas PtACT49 showed maximal activity with benzyl alcohol and 3-hydroxybenzyl alcohol. Other co-substrates are shown in Table 3.1. The data indicated a high affinity of PtACT47 for the substrate combination benzoyl-CoA and salicyl alcohol. Analysis by HPLC showed a marked depletion of substrate with a concomitant increase of a salicyl benzoate peak (Figure 3.8). Conversely, PtACT49 showed a high affinity for co-substrates benzoyl-CoA and benzyl alcohol, producing benzyl benzoate (Figure 3.8). Both enzymes were also able to use acetyl-CoA as a donor substrate, but only PtACT47 also could use cinnamoyl-CoA. For acceptor substrates, PtACT47 also showed reduced selectivity, utilizing several common phenylpropanoid alcohols (cinnamyl and coniferyl alcohols). PtACT47 also showed some activity with 4-hydroxybenzyl alcohol with both acetyl-CoA and benzoyl-CoA, however, the products appeared to be unstable and could not be confirmed by MS (data not shown). By contrast, PtACT49 showed significant activity only with benzyl alcohol and 3-hydroxybenzyl alcohol (Figure 3.9). The mutant PtACT49-H166A enzyme exhibited drastically diminished activity (97% loss of activity) and complete loss of function for some reactions in its native state compared to wild type PtACT49 (Figure 3.11).

Interestingly, both PtACT47 and PtACT49 showed some activity with alcohols known to be important for poplar volatiles. Both proteins utilized acetyl-CoA and benzoyl-CoA with *cis*-3-hexen-1-ol, 5-hexen-1-ol, and 1-octanol to produce volatile products *cis*-3-hexenyl-, 5-hexenyl- and 1-octyl acetates and benzoates, respectively. We could not detect these products by HPLC, but they were positively identified by GC-MS (Figure 3.10).

Recombinant PtACT54 was subjected to the same activity screening with identical substrate combinations as PtACT47 and PtACT49. It only showed activity with benzoyl-CoA and benzyl alcohol to produce benzyl benzoate (Figure 3.12). This level of catalysis was at a much lower activity level than was observed with PtACT49 with the same substrates, producing between 65-80% less product that PtACT49 in identical experimental conditions. Given the fact that many related BAHDs exhibit a wide range of activities with many combinations of co-substrates, it is unlikely that this is the only reaction catalyzed by PtACT54, more testing with other substrates is needed.

Table 3.1. Relative activity of recombinant PtACT47 and PtACT49 with a variety of substrates

	PtSABT (PtACT47)			PtBEBT (PtACT49)	
Alcohol substrates	Acetyl-CoA	Benzoyl-CoA	Cinnamoyl-CoA	Acetyl-CoA	Benzoyl-CoA
Benzyl alcohol	50.9	-	28.6	13.2	100[b]
Salicyl alcohol	43.5	100[a]	11.5	-	-
3-Hydroxybenzyl alcohol	40.9	96.8	-	12.0	112.7
Cinnamyl alcohol	-	44.5	-	-	-
Coniferyl alcohol	-	70.8	-	-	-
p-Coumaryl Alcohol	-	-	-	-	-
1-Octanol	-	Trace	-	-	Trace
cis-3-Hexen-1-ol	-	Trace	-	-	Trace
Ethanol	-	-	-	-	-
5-Hexen-1-ol	-	Trace	-	-	Trace
Linalool	-	-	-	-	-

[a] Activity of recombinant PtACT47 with salicyl alcohol and benzoyl-CoA was set at 100% which represents a rate of 11.7 μM sec^{-1}. [b] Activity with benzyl alcohol and benzoyl-CoA was set at 100% for recombinant PtACT49 which represents a rate of 9.8 μM sec^{-1}. 'Trace' indicates that a product was detectable using GC–MS but not by HPLC and could not be quantified. No activity was observed with recombinant PtACT47 using *p*-coumaroyl-CoA, or caffeoyl-CoA, and recombinant PtACT49 using cinnamoyl-CoA, *p*-coumaroyl-CoA, or caffeoyl-CoA (data not shown).

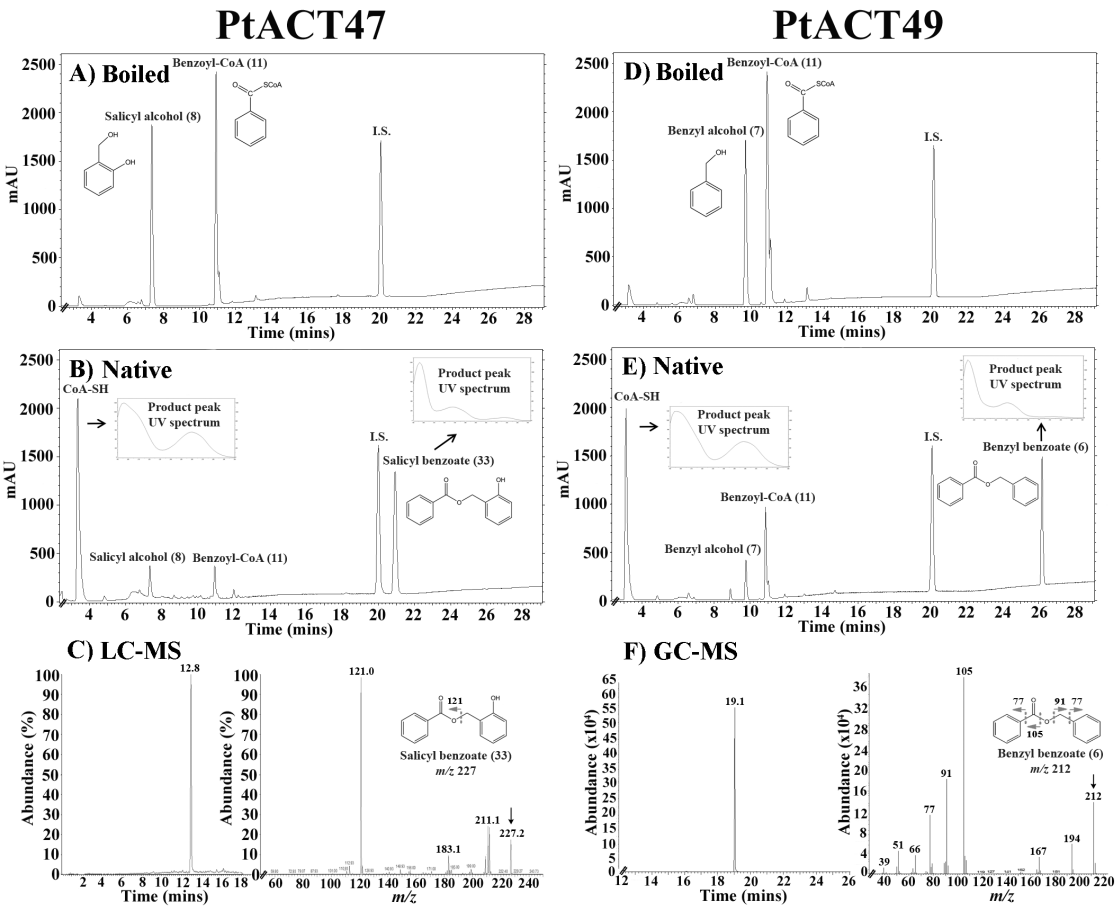

Figure 3.8. Maximum plot HPLC chromatograms (190–600 nm) and mass spectrometry data for key enzyme reactions of PtACT47 and PtACT49.

Controls represent boiled enzyme incubated with substrates, native enzyme represents active enzyme perparation. (A) boiled PtACT47 control; (B) native PtACT47; (C) confirmation of salicyl benzoate (*m/z* 227) product peak by MS using Orbitrap Fusion as described in section 2.14. Extracted ion chromatogram at m/z 227 (left) and LC–MS fragment ions (right). (D) boiled PtACT49 control; (E) native PtACT49; (F) confirmation of benzyl benzoate product (*m/z* 212) using GC–MS showing extracted ion chromatogram at *m/z* 212 (left) and MS fragment ions (right). Potential fragmentation patterns are indicated on the structure. In MS data the arrow indicates the molecular ion peak. I.S. refers to the internal standard, insets show UV spectra (190–300 nm). Spectra were identical to those of pure standards, although salicyl benzoate is not commercially available. A small CoA-SH peak is often present in boiled controls due to the instability of CoA thioesters.

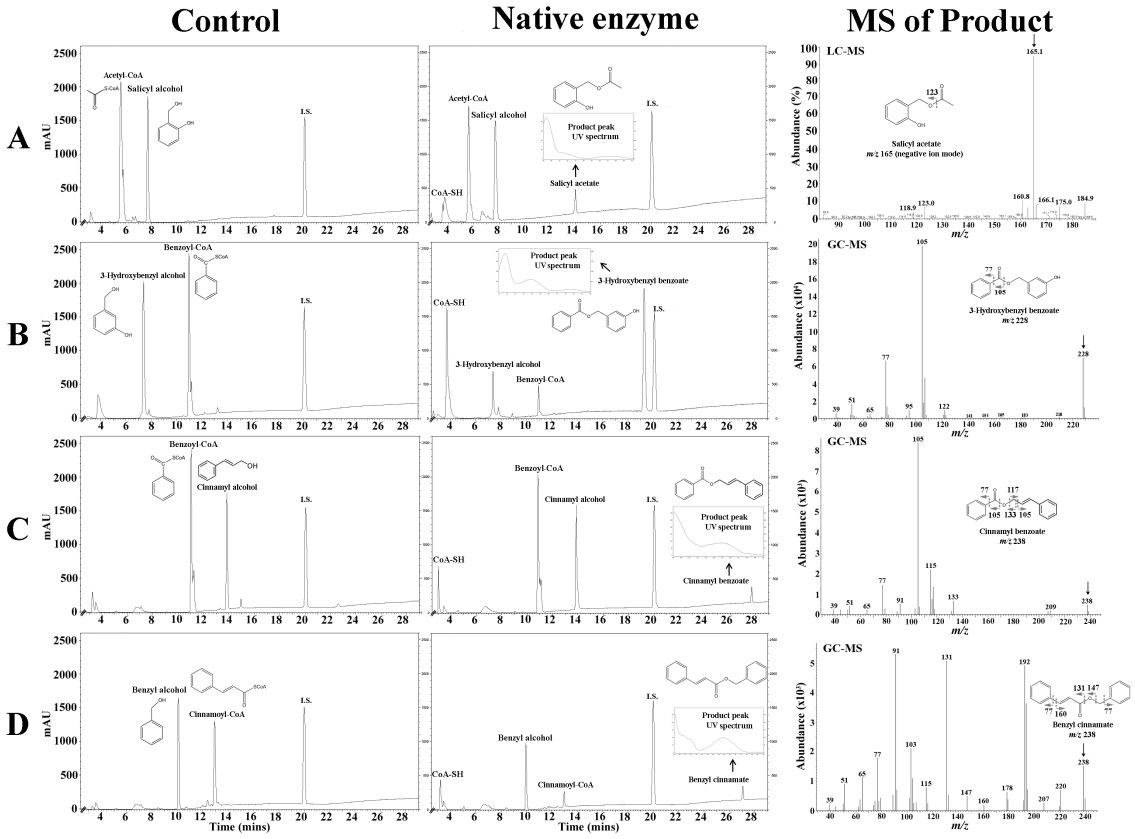

Figure 3.9. Maximum plot RP-HPLC chromatograms (190-600 nm) and mass spectrometry data of other notable reactions carried out on recombinant PtACT47 and PtACT49.

Controls represent boiled enzyme incubated with substrates, native enzyme represents active enzyme preparation. A) Acetyl-CoA + salicyl alcohol ⇆ salicyl acetate + CoA-SH, catalyzed by PtACT47 but not by PtACT49, ToF-MS in negative ion mode; B) benzoyl-CoA + 3-hydroxybenzyl alcohol ⇆ 3-hydroxybenzyl benzoate + CoA-SH, catalyzed by both PtACT47 and PtACT49, GC-MS; C) benzoyl-CoA + cinnamyl alcohol ⇆ cinnamyl benzoate + CoA-SH, catalyzed by PtACT47 only, GC-MS; D) cinnamoyl-CoA + benzyl alcohol ⇆ benzyl cinnamate + CoA-SH, catalyzed by PtACT47 only, GC-MS.

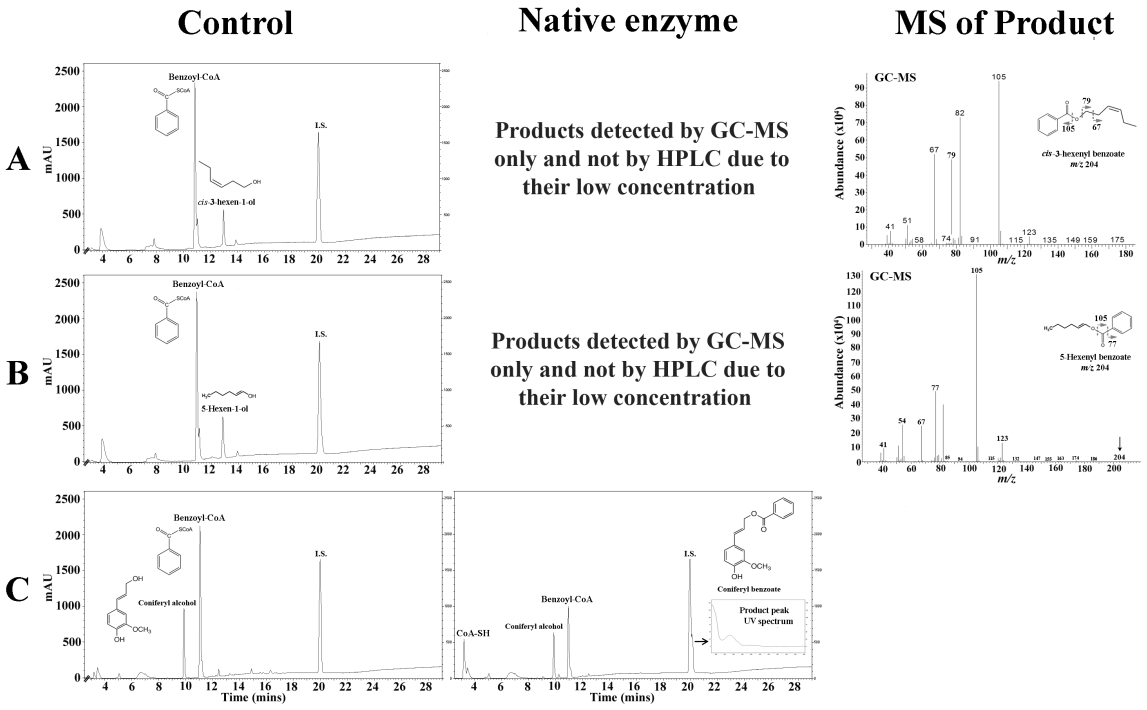

Figure 3.10. Maximum plot RP-HPLC chromatograms (190-600 nm) and mass spectrometry data of trace level and secondary enzyme reactions.

Controls represent boiled enzyme incubated with substrates, native enzyme represents active enzyme preparation. A) benzoyl-CoA + *cis*-3-hexen-1-ol ⇆ *cis*-3-hexenyl benzoate + CoA-SH, catalyzed by both PtACT47 and PtACT49. The product was not visible by RP-HPLC but was detectable by GC-MS; B) benzoyl-CoA + 5-hexen-1-ol ⇆ *5*-hexenyl benzoate + CoA-SH, catalyzed by both PtACT47 and PtACT49, product not visible by RP-HPLC but detectable by GC-MS; C) benzoyl-CoA + coniferyl alcohol ⇆ coniferyl benzoate + CoA-SH, MS data not available, product peak partially co-elutes with I.S. peak.

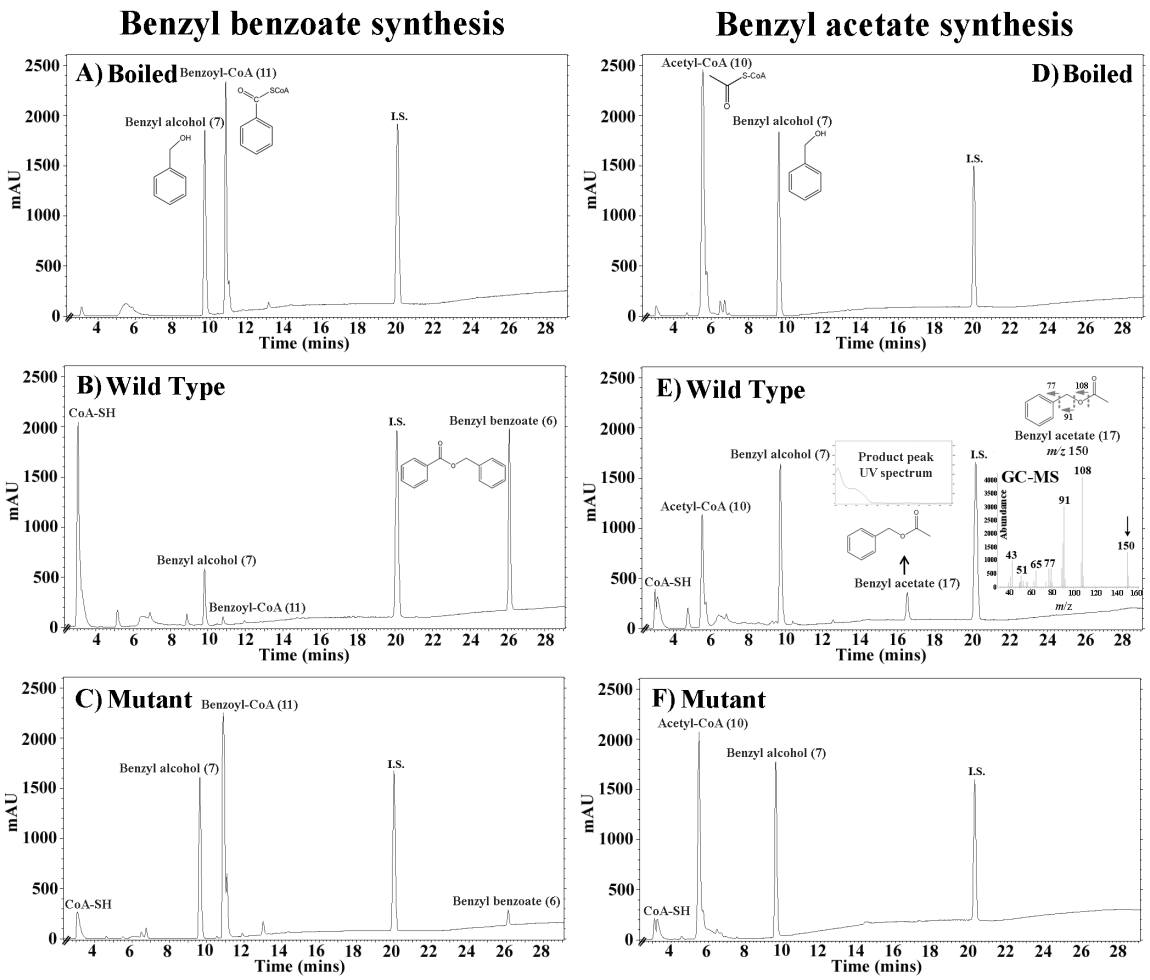

Figure 3.11. Maximum plot HPLC chromatograms (190-600 nm) to show altered activity of a PtACT49 H166A mutant protein.

Controls represent boiled enzyme incubated with substrates, wild type represents an unaltered PtACT49 in its native/active state, mutant represents PtACT49 with an altered motif. A) boiled enzyme negative control with substrates benzoyl-CoA and benzyl alcohol; B) wild type PtACT49 incubated with benzoyl-CoA and benzyl alcohol showing benzyl benzoate product; C) recombinant H166A mutant protein showing only trace benzyl benzoate product; D) boiled enzyme control with acetyl-CoA and benzyl alcohol; E) wild type PtACT49 incubated with acetyl CoA, and benzyl alcohol, yields benzyl acetate, GC-MS of the benzyl acetate product was also shown, arrow indicates the molecular ion peak; F) recombinant H166A mutant incubated with acetyl-CoA, and benzyl alcohol, showing loss of function.

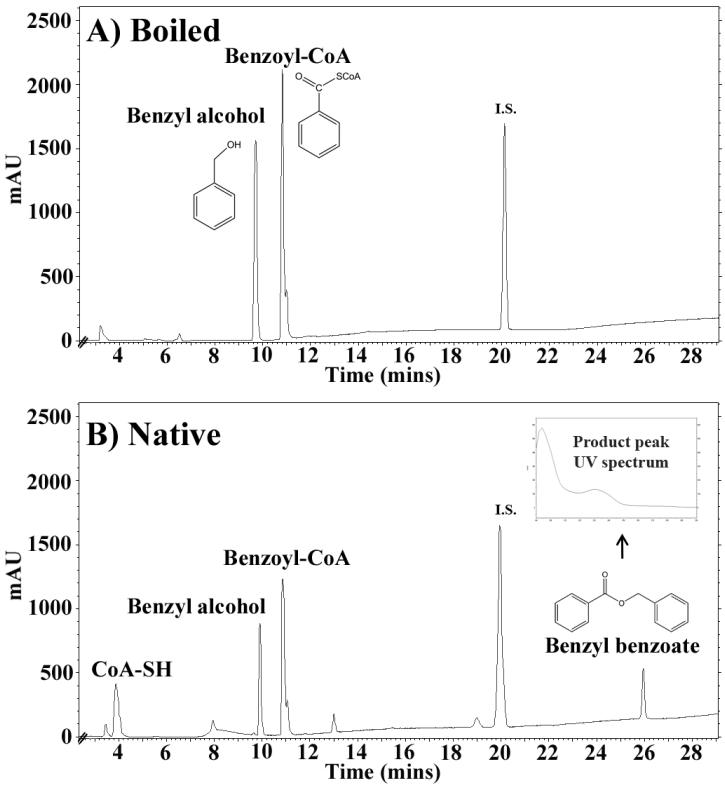

Figure 3.12. Maximum plot HPLC chromatograms (190-600 nm) to show synthesis of benzyl benzoate by recombinant PtACT54.

Controls represent boiled enzyme incubated with substrates, native enzyme represents active enzyme perparation. A) Boiled recombinant PtACT54 incubated with substrates benzyl alcohol and benzoyl-CoA; B) Native recombinant PtACT54 synthesizing benzyl benzoate from substrates benzyl alcohol and benzoyl-CoA. UV spectrum of benzyl benzoate matches the profile of pure standard. This represents the only observed activity of PtACT54 with the substrates tested in this work. I.S. is the internal standard.

Table 3.2. Kinetic parameters of recombinant PtACT47.

	K_m (μM)	K_{cat} (sec^{-1})	K_{cat}/K_m (nM^{-1} sec^{-1})
Salicyl alcohol (with benzoyl CoA)	44.23	2.06	46.56
Benzoyl CoA (with salicyl alcohol)	45.87	2.06	45.00
3-Hydroxy benzyl alcohol (with benzoyl CoA)	56.79	1.42	30.42
Benzoyl CoA (with 3-hydroxybenzyl alcohol)	62.54	2.01	32.13
Acetyl CoA (with salicyl alcohol)	246.32	0.43	1.73
Salicyl alcohol (with acetyl CoA)	338.99	0.35	1.03

[a] Kinetic parameters calculated using SAS JMP Version 7.0 (SAS Institute Inc.) with the Michaelis–Menten nonlinear model (2P) preset function. Values are arranged from lowest to highest K_m values.

Table 3.3. Kinetic parameters of recombinant PtACT49.

	K_m (μM)	K_{cat} (sec^{-1})	K_{cat}/K_m (nM^{-1} sec^{-1})
Benzoyl CoA (with benzyl alcohol)	51.78	1.72	33.24
Benzyl alcohol (with benzoyl CoA)	58.75	1.79	30.40
3-Hydroxy benzyl alcohol (with benzoyl CoA)	66.51	1.97	32.62
Benzoyl CoA (with 3-hydroxybenzyl alcohol)	63.24	2.25	35.51
Acetyl CoA (with benzyl alcohol)	364.73	0.32	0.89
Benzyl alcohol (with acetyl CoA)	395.18	0.40	1.02

[a] Kinetic parameters calculated using SAS JMP Version 7.0 (SAS Institute Inc.) with the Michaelis–Menten nonlinear model (2P) preset function. Values are arranged from lowest to highest K_m values.

We determined the kinetic parameters for these reactions, as well as several other prominent substrates, and varied both the CoA donor and the acceptor alcohols. These analyses indicate that PtACT47 has the lowest K_m and greatest turnover rates for benzoyl-CoA in combination with salicyl alcohol (Table 3.2). This enzyme clearly prefers benzyl-CoA over acetyl-CoA, and cinnamoyl-CoA, and is slightly more active with salicyl alcohol than 3-hydroxybenzyl alcohol. With benzoyl-CoA as the acyl donor and salicyl alcohol as the acyl acceptor, PtACT47 exhibits a mean Michaelis constant (K_m) of 45.1 μM, and a mean specificity constant (K_{cat}/K_m) of 45.8 nM^{-1} sec^{-1}. PtACT49 showed highest affinity for substrates benzoyl-CoA with benzyl alcohol, with a mean K_m of 55.3 μM and mean K_{cat}/K_m of 31.8 nM^{-1} sec^{-1} (Table 3.3).

3.4. The effect of wounding on PG content and expression of *PtACT47* and *PtACT49*.

Sixteen week-old hybrid '717' poplars (*P. tremula* x *P. alba*) were wounded using pliers to crush the periphery of leaves in order to mimic herbivory. Leaves were harvested at three time points, 6 hrs, 12 hrs and 24 hrs and subjected to chemical analysis by HPLC and expression analysis by qPCR. As before, leaves belonging to the three different age classes were analyzed, young (LPI 1-5), medium (LPI 6-10), and old (LPI 11-15). A one-way analysis of variance (ANOVA) ($\alpha = 0.05$) and student t-test was performed to test for significant differences between unwounded and wounded plants for PG content, and *PtACT47* and *PtACT49* expression.

The concentration of total PGs was significantly higher in wounded leaves compared to unwounded controls in young and medium age leaves (Figure 3.13). In young leaves, the total PG levels were significantly higher after 48 hrs, and in medium leaves this difference was significant at both 24 and 48 hrs post-wounding. Old leaves showed no significant differences in total PG levels. Quantification of individual PGs (Figure 3.14) showed that salicin (1) and salicortin (2) significantly increased after wounding. In young leaves, salicin (1) levels were significantly greater at 24 and 48 hrs, tremulacin (3) at 24 hrs, and salicortin (2) at 48 hrs. In medium age leaves, salicin (1) was significantly greater after 6 and 24 hrs; salicortin (2), was enhanced at 24 and 48 hrs after wounding. In old leaves, only salicortin (2) levels were significantly elevated at 6, 24 and 48 hrs compared to unwounded controls.

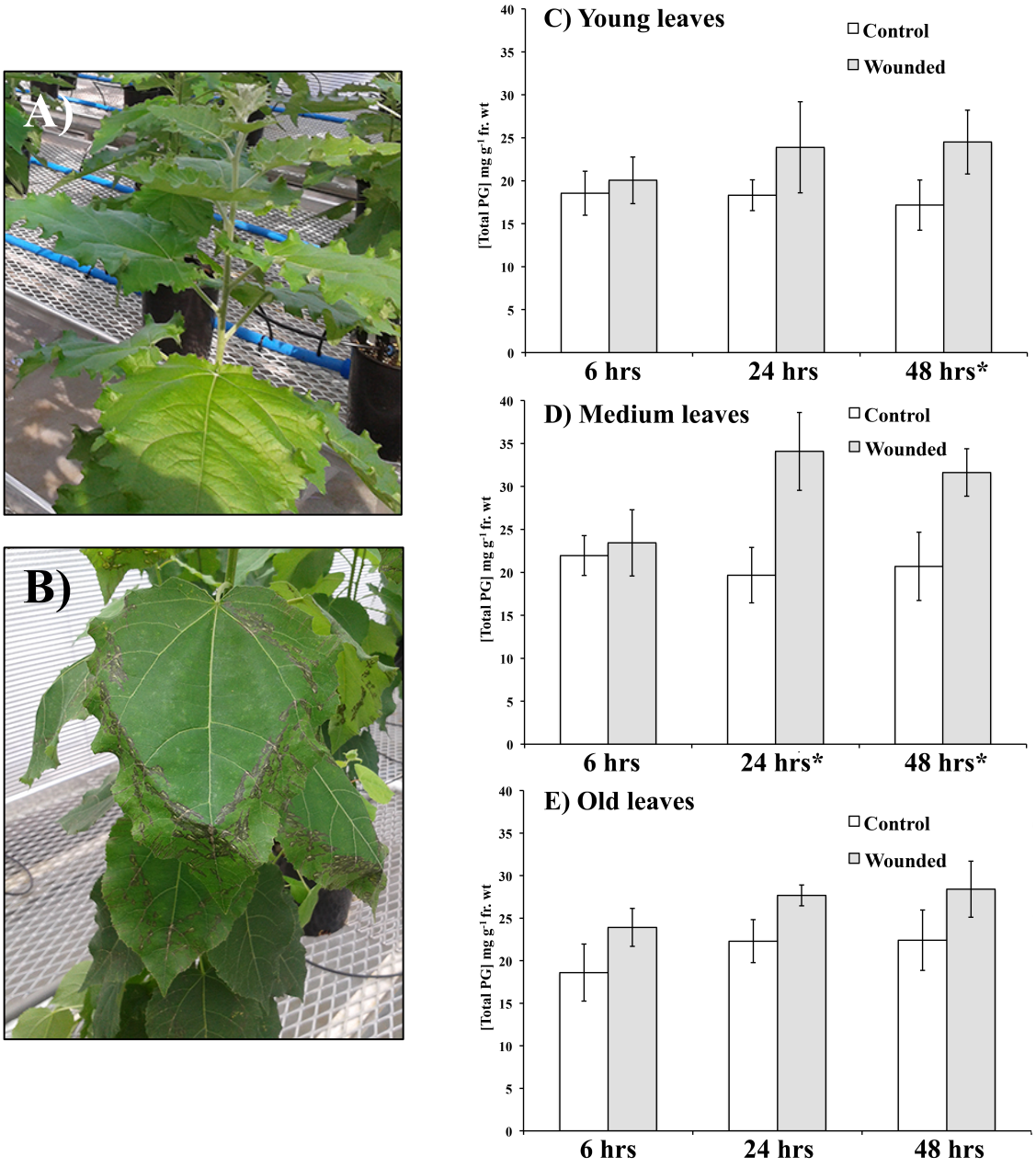

Figure 3.13. The effect of mechanical wounding on total PG content.
A, B) photographs of control (A) and wounded (B) 717 hybrid poplar leaves; C-E) total PG content in young (C), medium (D), and old (E) leaves. Mean values were calculated from four replicate plants used per treatment. Asterisks indicate significant differences between control and wounded leaves using student t-tests ($P < 0.01$). Critical *F* test values were considered significant if greater than the tabular value of $F_{(1, 6)} = 5.99$ ($\alpha = 0.05$). Comparison of total PG content of control with wounded plants in young leaves critical $F_{(1, 6)}$ values were, 6 hrs, 5.7; 24 hrs, 4.5; and 48 hrs, 21.3. Medium leaves, 6hrs, 0.8; 24 hrs, 18.4; and 48 hrs, 3.11. Old leaves, 6hrs, 0.2; 24 hrs, 0.1; 48 hrs, 0.3.

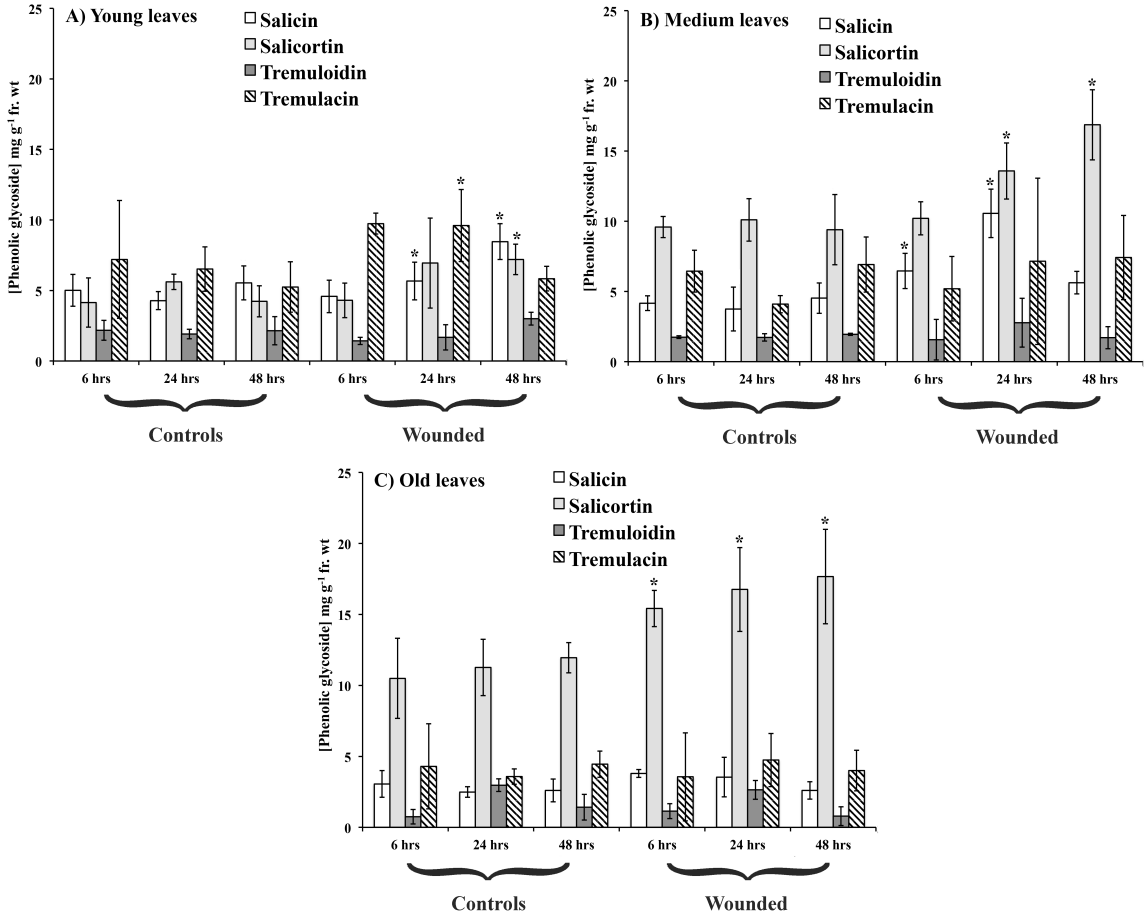

Figure 3.14. Time course concentrations of individual PGs in control and wounded plants.

Mean concentrations of specific PGs (mg g^{-1} fr. wt) in control (unwounded) and wounded plants at three time points. Asterisks indicate significant differences between chemical content of wounded versus control leaves of the same age at the same time (hrs) using student t-tests ($P < 0.01$). Y error bars indicate standard deviations (n=4). Critical *F* test values were considered significant if greater than the tabular value of $F_{(1, 6)} = 5.99$ ($\alpha = 0.05$). Comparing specific PG chemicals with the same time (hrs) between wounded versus control plants, for young leaves critical $F_{(1, 6)}$ values are as follows for each PG, salicin, 6hrs, 0.2; 24 hrs, 10.8; 48 hrs, 19.6; salicortin, 6 hrs, 4.8; 24 hrs, 1.1; 48 hrs, 23.6; tremuloidin, 6 hrs, 3.0; 24 hrs, 0.4; 48 hrs, 1.3; tremulacin, 6 hrs, 0.7; 24 hrs, 6.4; 48 hrs, 0.7. For medium leaves critical $F_{(1, 6)}$ values are as follows for each PG, salicin, 6 hrs, 6.5; 24 hrs, 82.4; 48 hrs, 0.0; salicortin, 6 hrs, 1.2; 24 hrs, 25.1; 48 hrs, 33.6; tremuloidin, 6 hrs, 2.8; 24 hrs, 2.8; 48 hrs, 3.6; tremulacin, 6 hrs, 3.4; 24 hrs, 1.6; 48 hrs, 5.4. For old leaves critical $F_{(1, 6)}$ values are as follows for each PG, salicin, 6 hrs, 0.8; 24 hrs, 4.4; 48 hrs, 0.4; salicortin, 6 hrs, 25.2; 24 hrs, 19.0; 48 hrs, 22.4; tremuloidin, 6 hrs, 1.7; 24 hrs, 0.6; 48 hrs, 1.9; tremulacin, 6 hrs, 1.4; 24 hrs, 1.6; 48 hrs, 0.4.

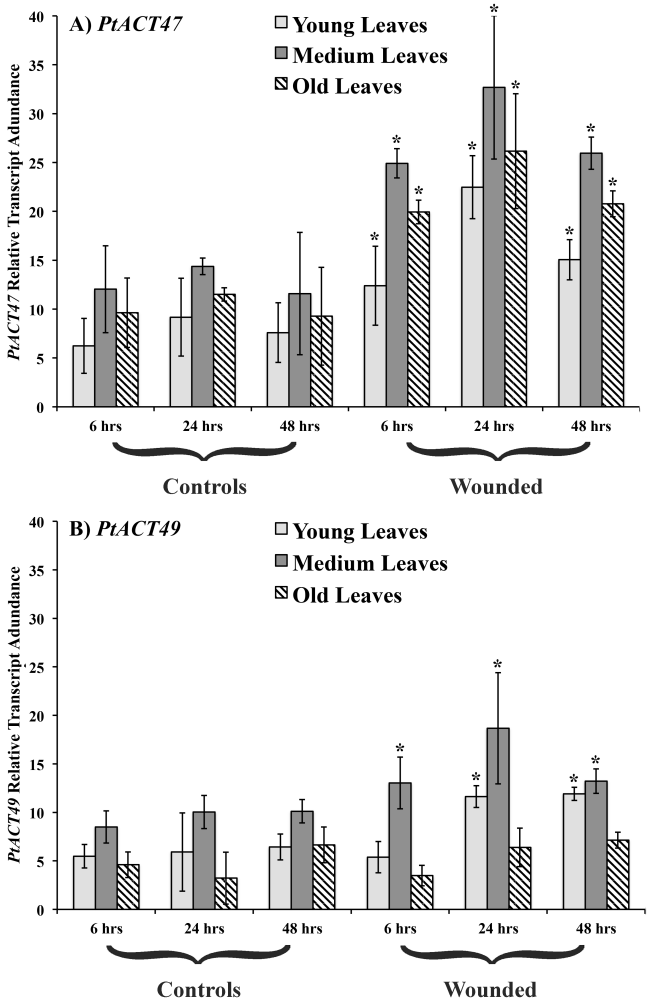

Figure 3.15. Time course of *PtACT47* and *PtACT49* expression in wounded and control plants.

A) Comparison of *PtACT47* expression in wounded and control plants in young, medium, and old leaves at 6, 12, and 24 hrs post wounding. B) Comparison of *PtACT49* expression in wounded and control plants in young, medium, and old leaves at 6, 12, and 24 hrs post wounding. Relative transcript abundance is relative to house-keeping genes *ELF4* and *UBQ10*. Y error bars indicate standard deviations (n=4). Asterisks indicate significant differences in expression in wounded versus control leaves of the same age and at the same time point (hrs) using student t-tests ($P < 0.01$). Critical *F* test values were considered significant if greater than the tabular value of $F_{(1, 6)} = 5.99$ ($\alpha = 0.05$). Comparing *PtACT47* expression levels with the same time (hrs) between wounded versus control plants, for young leaves critical $F_{(1, 6)}$ values were, 6 hrs, 8.6; 24 hrs, 48.5; 48 hrs, 29.9; medium leaves, 6 hrs, 35.9; 24 hrs, 41.6; 48 hrs, 14.4; old leaves, 6 hrs, 8.1; 24 hrs, 28.2; 48 hrs, 33.0. Comparing *PtACT49* expression levels with the same time (hrs) between wounded versus control plants, for young leaves critical $F_{(1, 6)}$ values were, 6 hrs, 4.2; 24 hrs, 14.2; 48 hrs, 34.9; medium leaves, 6 hrs, 27.1; 24 hrs, 8.1; 48 hrs, 17.4; old leaves, 6 hrs, 2.9; 24 hrs, 3.5; 48 hrs, 0.0.

Expression of both *PtACT47* and *PtACT49* (Figure 3.15) showed correspondingly greater levels in most tissues following wounding. *PtACT47* expression was significantly higher in wounded plants than in unwounded plants in all leaves at all time points, while *PtACT49* expression was only significantly greater in young leaves at 24 and 48 hrs, and in medium leaves at 6, 24, 48 hrs. No differences in *PtACT49* expression were observed in old leaves. However, an anomaly was observed in this experiment with regard to gene expression across leaf age in the '717' *P. tremula* x *P. alba* hybrid poplars. Specifically, old leaves showed slightly higher expression of *PtACT47* and *PtACT49* than that observed in the '353' *P. tremula* x *P. tremuloides* hydrid (Figure 3.3). This may be attributed to genotypic variation or possibly due to differences in greenhouse conditions, as plants harvested for data in Figure 3.3 occurred in the Fall of 2013, while the wounding experiments were conducted in May-June 2014 in Victoria, BC, Canada, temperate zone.

3.5. The effect of *PtACT47* and *PtACT49* RNAi knock-down constructs on PG content in transgenics.

In order to delineate the roles of genes *PtACT47* and *PtACT49 in planta*, 717 hybrid poplar (*P. tremula x P. alba*) tissue was subjected to *Agrobacterium*-mediated transformation with the insertion of a pKannibal cassette into its genome that is capable of generating gene-specific hairpin RNAs (hpRNAs) that stimulate the RNAi pathway resulting in suppressed gene expression (see Sections 2.15-2.17). Four different types of RNAi plant were manufactured, (a) empty vector controls in which the pKannibal cassette did not contain any gene specific sequences; (b) *PtACT47* RNAi plants in which a *PtACT47*-specific hpRNA was generated and only *PtACT47* was suppressed; (c) *PtACT49* RNAi plants in which *PtACT49* was suppressed; (d) and double knock-down (DKD) RNAi plants in which both *PtACT47* and *PtACT49* were simultaneously suppressed. For each type of RNAi plant, twelve independent lines were regenerated and gene expression was assayed by qPCR after two months growth in sterile conditions in Magenta boxes. For each RNAi plant type, the three most suppressed independent transgenic lines were selected for further experimentation. Four replicate clones of each of these selected lines were moved to the greenhouse and grown for an additional three

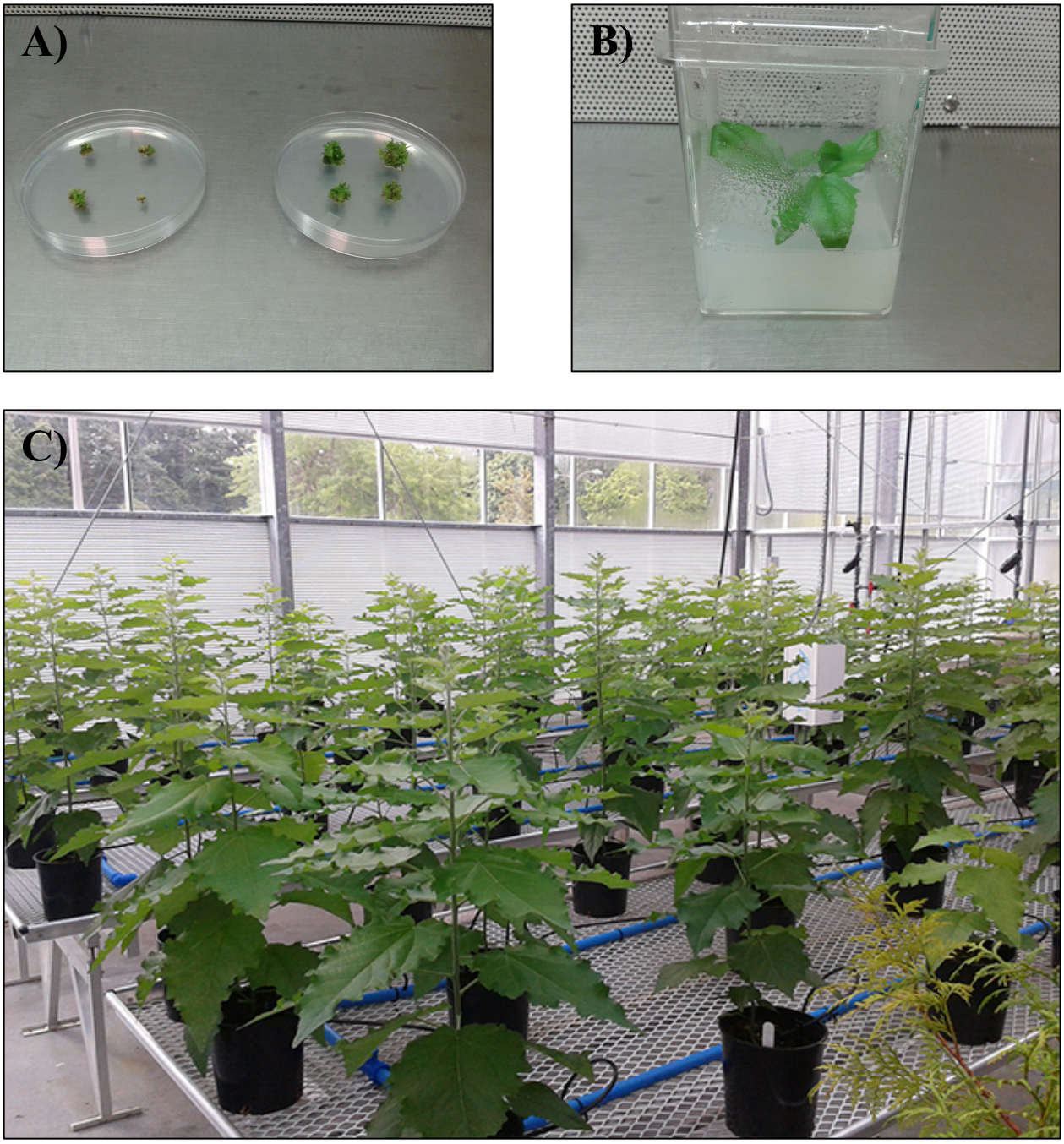

Figure 3.16. Manufacture of RNAi transgenic hybrid poplar lines.

A) pKannibal-pART27 transformed calli on tissue culture media plates containing shoot inducing hormones and kanamycin for selection; B) a propagated transformant in a Magenta boxe in agar media containing root inducing hormones and kanamycin; C) two month-old RNAi transgenic plants in the greenhouse potted in soil.

months. After one month's growth, leaves at LPI position 5 were harvested and used for qPCR analysis in order to confirm that the gene(s) of interest were still suppressed as previously observed *in vitro*. Photographs of the various stages and selection processes employed in the manufacture and growth of transgenic RNAi plants are illustrated in Figure 3.16.

Empty vector control lines 9, 11 and 6 were selected, since gene expression was very similar to wild type expression for *PtACT47* (96.9%, 107.1%, and 114.6% respectively), and for *PtACT49* (85.9%, 105.1%, and 91.1% respectively) (Figure 3.17, panels A and B). Of the twelve empty vector control lines that were regenerated in total, all had *PtACT47* and *PtACT49* expression levels very similar to that of wild type plants, within ±29%. For the *PtACT47* RNAi plants, lines 9, 2 and 4 were selected with *PtACT47* expression levels of 2.9%, 7.8%, and 27.7% respectively. Importantly, *PtACT49* expression was not affected (Figure 3.17, panel A). Of the twelve independent *PtACT47* RNAi lines produced, nine had *PtACT47* expression levels of <37.1% compared to wild type plants. For *PtACT49* RNAi plants, lines 8, 9, and 11 exhibited *PtACT49* expression levels of 2.1%, 18.0%, and 22.5% respectively, while *PtACT47* expression appeared to be unaffected (Figure 3.17, panel B). Of the twelve *PtACT49* RNAi lines made in total, eight had *PtACT49* expression levels <51.7%.

For the DKD plants, lines 2, 4 and 10 were selected in which *PtACT47* expression was reduced to 3.6%, 14.9%, and 32.7% respectively (Figure 3.17, panel A), and *PtACT49* expression of 11.0%, 36.7%, and 16.1% respectively (Figure 3.17, panel B). Of the twelve lines regenerated, *PtACT47* expression was <50.3% in seven of the lines. *PtACT49* levels were <55.7% in ten lines. In all of the RNAi lines used in this work, expression of phenylpropanoid-related genes *DFR1* (dihydroflavonol reductase 1) and *ANR1* (anthocyanidin reductase 1) remained unaffected, demonstrating that the pKannibal RNAi constructs were specific to their target genes (Figure 3.18).

Analysis of transgenic plant tissues by HPLC was carried out, and the four PGs of interest were quantified. To determine the effect of the RNAi constructs on total PG content, this was calculated based on the individual peaks (Figure 3.19). Statistical analyses showed that only *PtACT47* RNAi and DKD RNAi lines exhibited significant changes in total PG levels in at least one tissue type. Two *PtACT47* RNAi lines showed

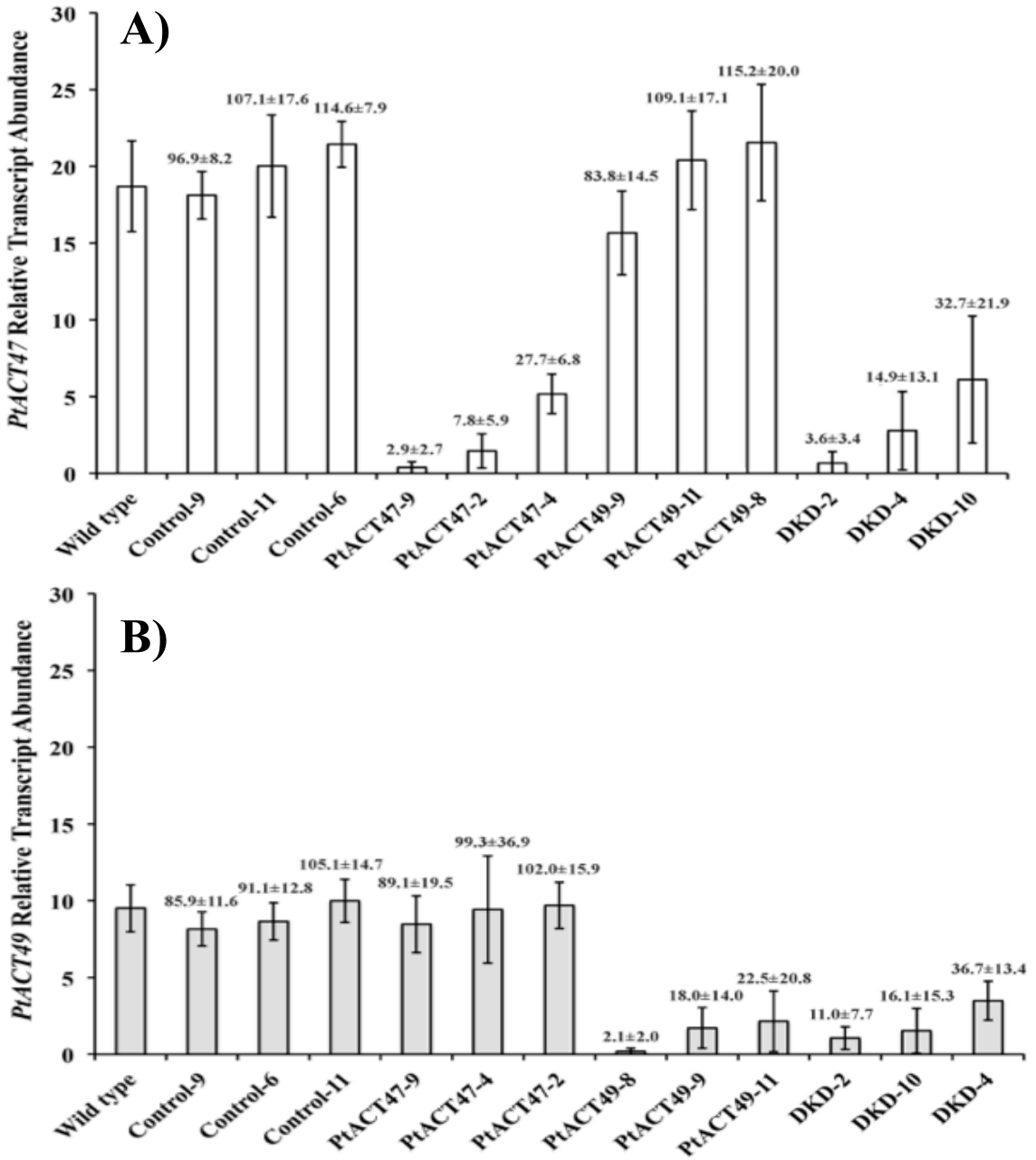

Figure 3.17. Transcriptional analysis of transgenic RNAi lines, *PtACT47* and *PtACT49* expression.

A) *PtACT47* expression; B) *PtACT49* expression. Lines are ordered from low to high expression for each type of transgenic plant for ease of reading. Relative transcript abundance is relative to house-keeping genes *ELF4* and *UBQ10*. Y error bars represent standard deviation. Mean values calculated from four replicate plants used per treatment. Numbers above bars indicate the relative expression as a percentage ± standard deviation to wild type plants. Only the best three transgenic lines of each plant type that were selected for the experiment are shown.

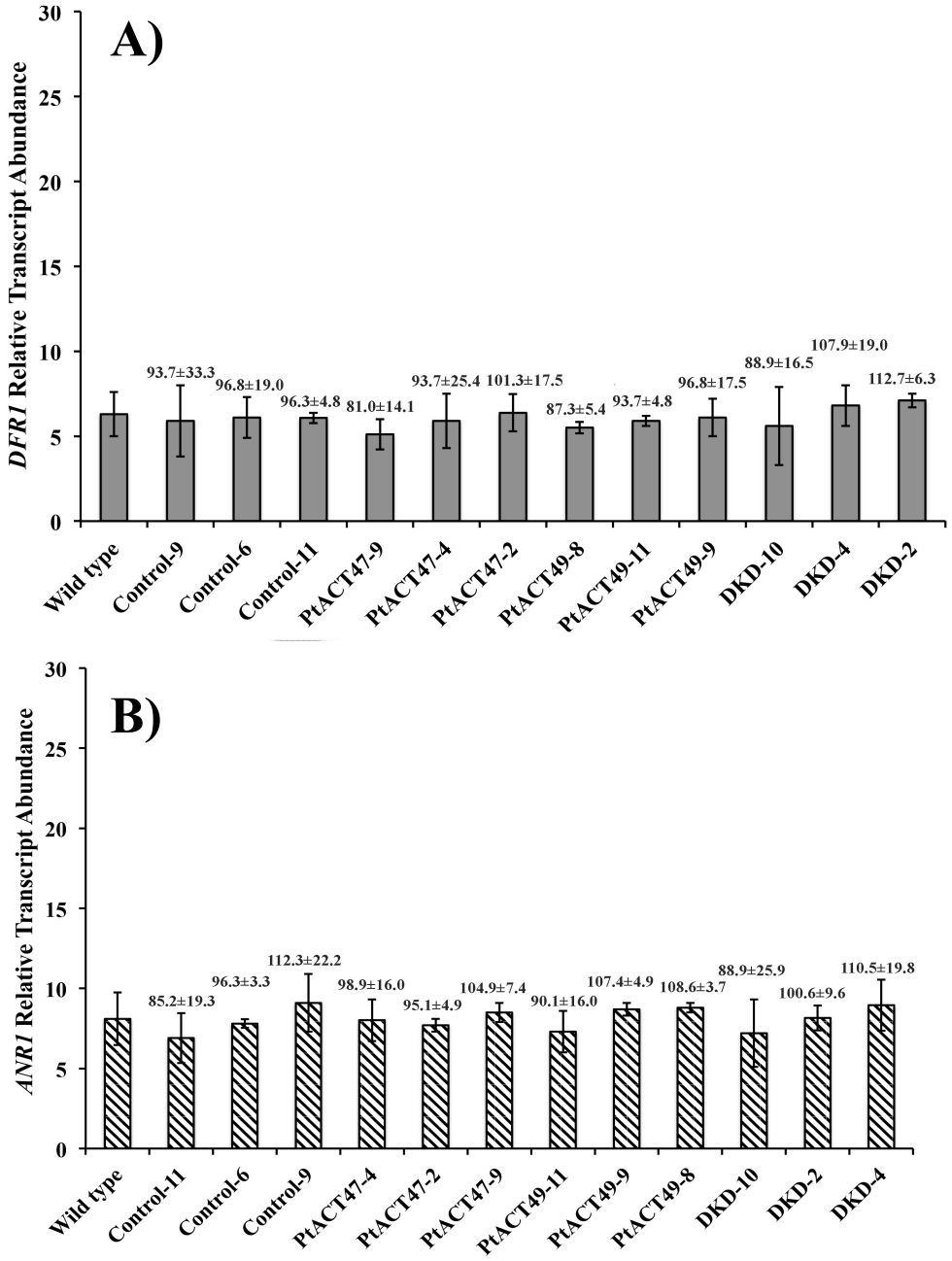

Figure 3.18. Transcriptional analysis of transgenic RNAi lines, *DFR1* and *ANR1* expression.

A) mean *DFR1* (dihydroflavonol reductase 1) expression; B) mean *ANR1* (anthocyanidin reductase 1) expression. Relative transcript abundance is relative to house-keeping genes *ELF4* and *UBQ10*. Y error bars represent standard deviation. Mean values calculated from four replicate plants used per treatment. Numbers above bars indicate the relative expression as a percentage ± standard deviation to wild type plants. Only the best three transgenic lines of each plant type that were selected for the experiment are shown.

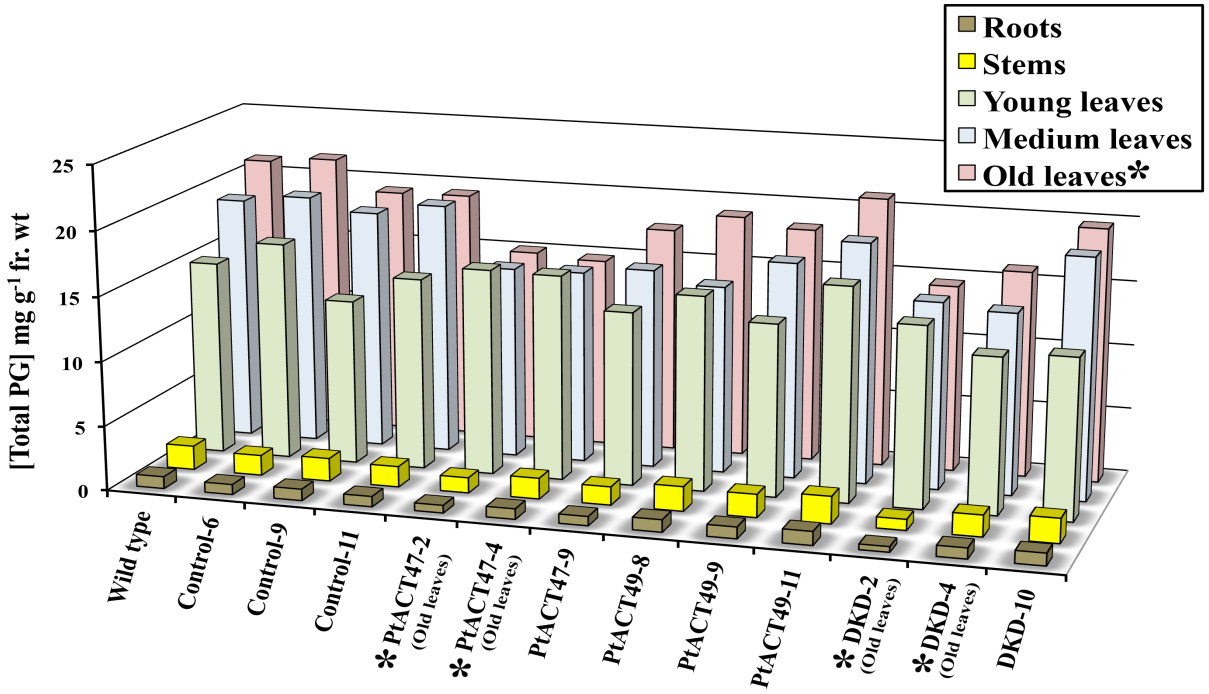

Figure 3.19. A comparison of mean [total PG] (mg g^{-1} fr. wt) of transgenic lines to controls and wild type plants in various tissues.

Mean values were calculated from four replicate plants for each transgenic line. Asterisks next to the tissue type name in the legend indicate that a significant treatment effect on [total PG] was detected following statistical analysis using a 'linear mixed effect' (LME) function with 'restricted maximum likelihood' (REML) method using 'R' software (α=0.01) for all three transgenic lines combined for each RNAi treatment (n=12, 3 lines each with 4 replicates) compared to controls and wild type plants. Asterisks next to the transgenic line name in the x-axis indicate which specific lines showed significant differences and in which tissue significant effects were observed in parenthesis following a one-way ANOVA and comparison of means using a student t-test in SAS JMP software (α=0.01) (n=4, means calculated for each line from four replicate plants). See Appendices A6.6.1 for full statistical output tables.

some significant changes, and two DKD lines showed significantly lower levels. No significant changes in total PG content was observed in any tissues in the PtACT49 RNAi lines.

Examination of individual PG levels in the same tissues (Figure 3.20 and 3.21) showed that salicin (1), tremuloidin (3), and tremulacin (4) levels were not significantly altered in RNAi plants (Figures 3.20, and 3.21). However salicortin (2) seemed to be affected in *PtACT47* and DKD lines (Figure 3.20). In *PtACT47* RNAi lines salicortin (2) was significantly lower in

medium leaves only in line 9, and in old leaves for lines 2 and 4. In DKD plants, line 4 showed significantly lower salicortin (2) in medium age leaves, while in line 2 this was the case in old leaves only (Figure 3.20). DKD line 10 showed no reduction in PGs. No significant changes were observed in PG levels in any plants in young leaves, roots and stem tissues.

To determine if any other phenolic peaks (besides salicortin (2) and those previously examined) might be altered in the RNAi lines, twenty peaks that were consistently observed on the HPLC trace were examined for major changes (Figures 3.22 and 3.23). While the identity of many of the peaks is not unambiguously known, and since standards are not available, their abundance was compared on the basis of integrated peak area normalized by sample weight (mg fr. wt). Because old leaves showed the greatest difference in salicortin (2), the peak areas of all twenty unknown peaks was analyzed in this tissue in order to detect statistically significant changes (Table 3.4). *PtACT49* RNAi showed no obvious changes in peak areas, however *PtACT47* RNAi and the DKD RNAi plants both showed significant reductions in peaks 4, 17 and 19 (grandidentatin (19)), and in addition DKD RNAi plants had a significantly reduced peak 9. However, this data did contain high levels of variability, and since it was not possible to obtain pure standards for these peaks it is difficult to estimate what these changes in peak area represent in terms of concentration changes. Different chemicals have different response factors at specific wavelengths and different lambda max values such that for some chemicals, at 280 nm, a large change in peak area does not neccessarily indicate an equally large change in concentration. Future work will require a more accurate quantification by calibration with pure chemical standards. Preparative HPLC in which individual

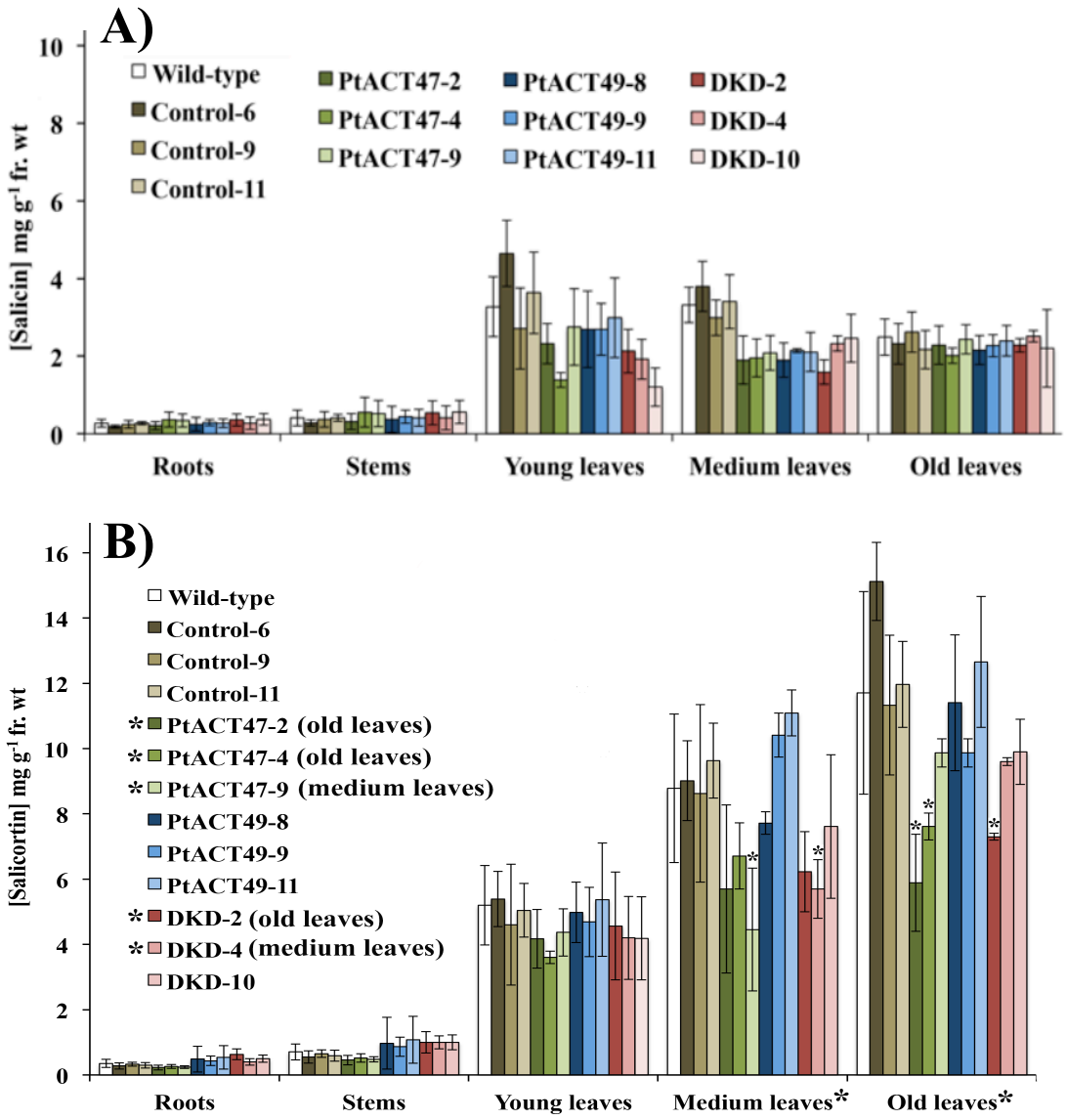

Figure 3.20. A comparison of mean [salicin] and [salicortin] concentration (mg g^{-1} fr. wt) between control plants and transgenic lines in various tissues.

A) mean [salicin(1)]; B) mean [salicortin (2)]. Y bars indicate standard deviation. Mean values were calculated from four replicate plants used per RNAi or control treatment. Asterisks next to the tissue type name in the x-axis indicate that a significant treatment effect on PG content was detected following statistical analysis using a 'linear mixed effect' (LME) function with 'restricted maximum likelihood' (REML) method using 'R' software (α=0.01). Asterisks next to the transgenic line name in the legend or above bars indicate which specific lines showed significant differences in PG level following a one-way ANOVA and comparison of means using a t-test in SAS JMP software (α=0.01). The legend also indicates in which tissue significant effects were observed in parenthesis. See Appendices A6.6.2 and A6.6.3 for full statitstical output tables.

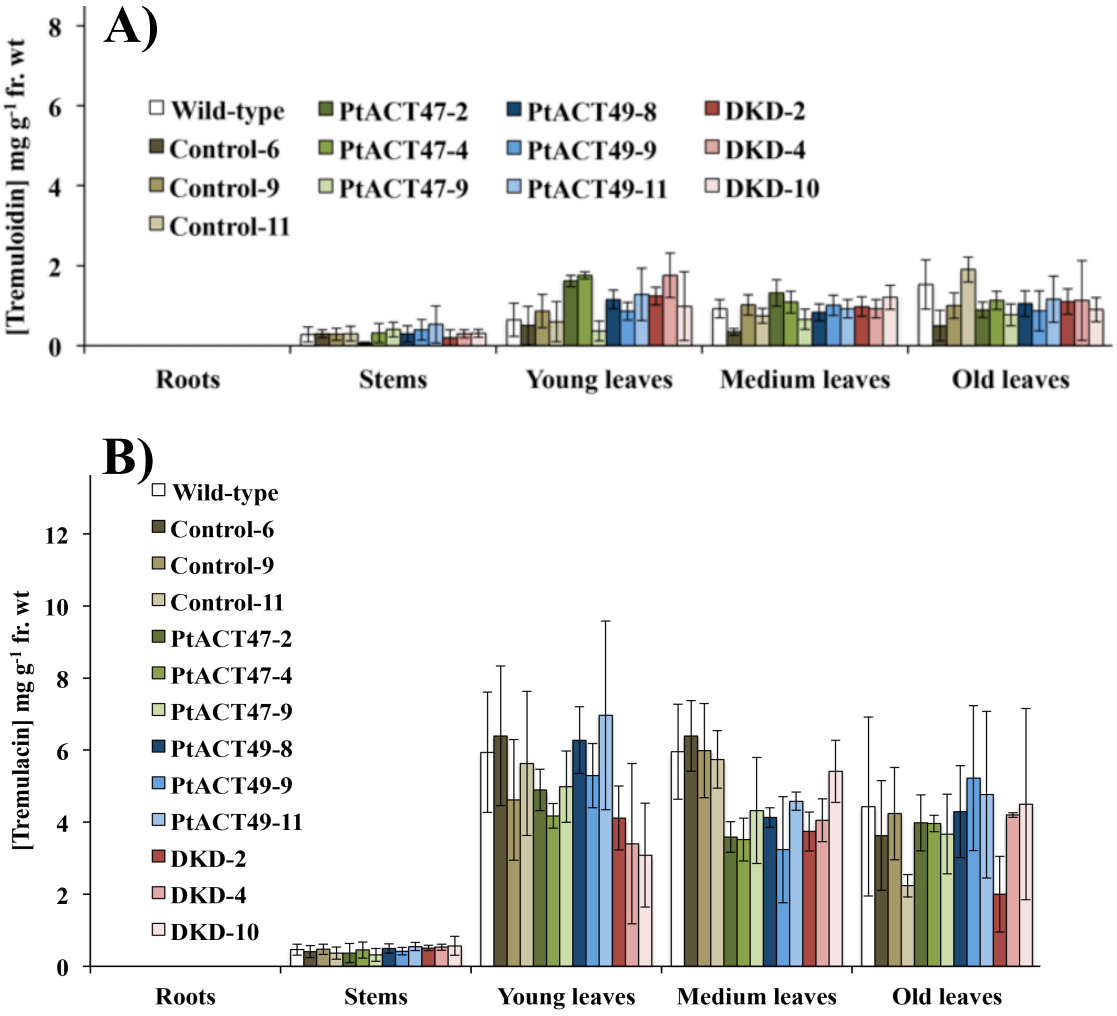

Figure 3.21. A comparison of mean [tremuloidin] and [tremulacin] concentration (mg g^{-1} fr. wt) between control plants and transgenic lines in various tissues.

A) mean [tremuloidin(3)]; B) [tremulacin(4)]. Y bars indicate standard deviation. Mean values were calculated from four replicate plants used per RNAi or control treatment. Asterisks next to the tissue type name in the x-axis indicate that a significant treatment effect on PG content was detected following statistical analysis using a 'linear mixed effect' (LME) function with 'restricted maximum likelihood' (REML) method using 'R' software (α=0.01). Asterisks next to the transgenic line name in the legend or above bars indicate which specific lines showed significant differences in PG level following a one-way ANOVA and comparsion of means using a t-test in SAS JMP software (α=0.01). The legend also indicates in which tissue significant effects were observed in parenthesis. See Apendices A6.6.2 and A6.6.3 for full statitstical output tables.

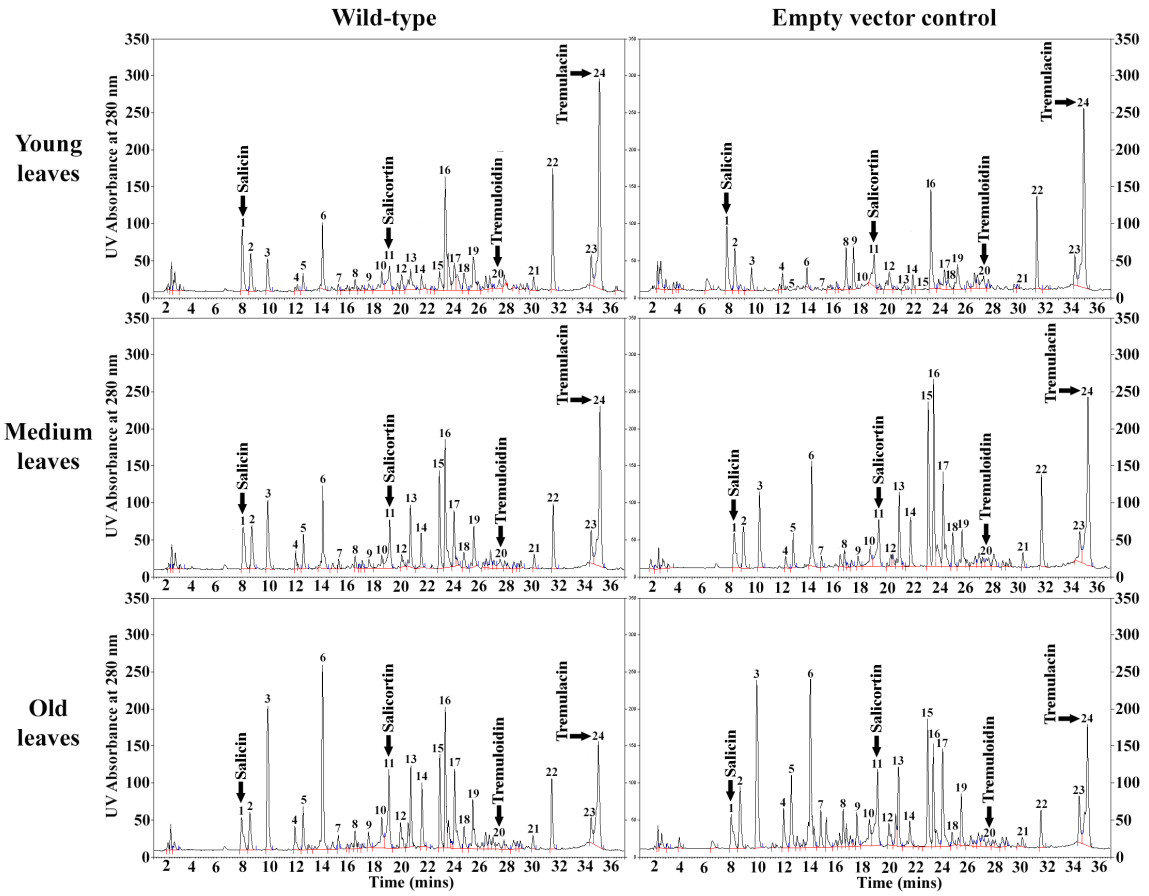

Figure 3.22. Representative RP-HPLC chromatograms (280 nm) comparing phenolic extracts of wild type and empty vector control (line 6) from different age leaves. Major peaks are numbered from 1-24. Salicin, salicortin, tremuloidin, and tremulacin are labeled with arrows.

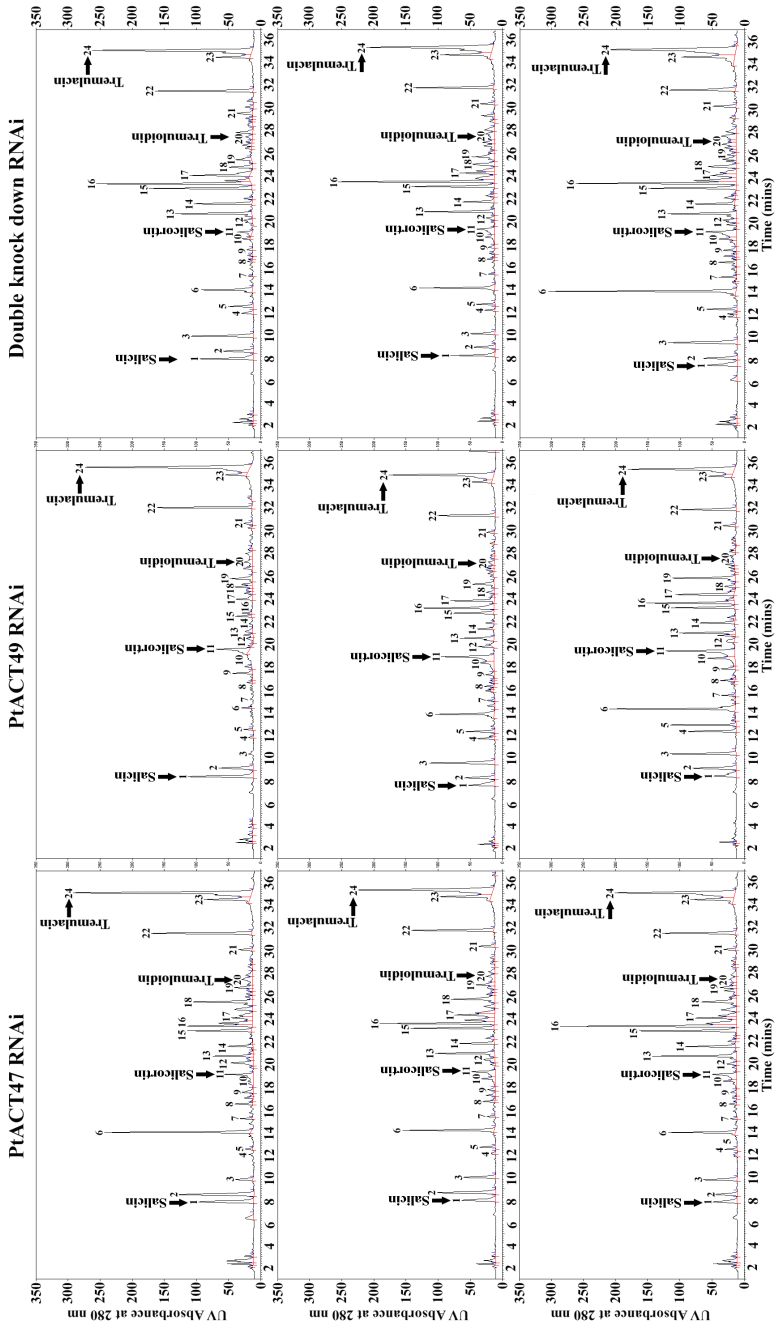

Figure 3.23 Representative RP-HPLC chromatograms (280 nm) comparing phenolic extracts of RNAi transgenic lines (*PtACT47*-2, *PtACT49*-8, DKD-2) from different age leaves.

Major peaks are numbered from 1-24. Salicin, salicortin, tremuloidin, and tremulacin are labeled with arrows.

Table 3.4. A comparison of the mean normalized intergrated peak areas from HPLC analysis of old leaf extracts.

Peak #	Name	T_R	Wild type	Empty Vector Control		*PtSABT* (*PtACT47*) RNAi		*PtBEBT* (*PtACT49*) RNAi		DKD RNAi	
			Mean peak area/mass	Peak area/mass	% of wild type	Peak area/mass	% of wild type	Peak area/mass	% of wild type	Peak area/mass	% of wild type
2	n/a	8.35	14085.9 (1318.1)	14586.2 (1311.1)	103.5 (9.3)	13666.0 (1218.5)	97.0 (8.6)	14517.7 (1323.2)	103.5 (9.4)	14234.8 (1454.4)	129.4 (10.3)
3	Chlorogenic acid-2	9.45	37805.8 (1800.4)	36144.3 (1822.5)	95.6 (4.8)	42578.7 (1705.1)	112.6 (4.5)	36103.0 (1919.8)	95.6 (5.1)	35948.1 (1859.3)	95.1 (4.9)
4*	n/a	12.01	3308.9 (195.9)	3512.1 (97.7)	106.1 (3.0)	**1885.5 (278.2)***	**56.9 (8.4)**	3402.3 (206.3)	102.8 (6.3)	**1753.6 (200.1)***	**53.0 (6.0)**
5	Catechin	12.24	9000.0 (595.3)	8645.6 (351.2)	96.1 (3.9)	8478.6 (670.1)	94.2 (7.4)	9132.9 (575.3)	101.5 (6.4)	7926.3 (492.9)	88.4 (5.4)
6	Chlorogenic acid-1	14.05	40818.7 (1302.1)	39341.1 (1348.4)	96.4 (3.3)	38949.2 (1217.1)	95.4 (3.0)	40205.1 (1117.2)	98.5 (2.7)	43232.6 (1244.6)	105.9 (3.1)
7	n/a	15.15	5106.7 (235.9)	5463.4 (276.2)	106.9 (5.4)	5358.8 (218.4)	104.9 (4.3)	5059.2 (346.0)	99.1 (6.8)	4441.8 (272.8)	86.9 (5.4)
8	n/a	16.35	5136.1 (1152.2)	5146.2 (1149.9)	100.2 (22.3)	4839.2 (1133.5)	94.2 (22.1)	4923.9 (1241.2)	95.9 (24.2)	4802.9 (1250.6)	93.5 (24.4)
9*	n/a	17.45	5591.2 (174.6)	6290.5 (182.3)	112.5 (3.4)	5404.9 (127.9)	96.6 (2.3)	5984.3 (222.6)	107.1 (3.9)	**4079.2 (317.7)***	**72.9 (5.6)**
10	n/a	18.23	11194.4 (1110.5)	10617.9 (1135.4)	94.9 (10.1)	10414.4 (957.9)	93.0 (8.6)	11017.9 (1235.4)	98.4 (11.0)	10482.8 (1178.6)	93.6 (10.5)
12	n/a	19.57	7738.2 (1082.3)	7571.4 (1160.5)	84.9 (14.9)	8333.5 (1134.6)	107.6 (14.7)	7632.4 (1360.4)	98.6 (17.6)	8605.1 (1263.9)	111.2 (16.3)
13	n/a	20.51	12644.9 (1242.9)	14838.8 (2263.6)	117.4 (17.9)	11026.3 (1378.9)	87.2 (10.9)	12006.3 (1144.0)	94.9 (90.4)	13803.3 (1690.74)	93.3 (13.4)
14	n/a	21.41	10261.6 (919.5)	9576.6 (1125.1)	93.3 (10.9)	9874.8 (997.5)	96.2 (9.7)	9643.7 (1149.9)	93.9 (11.1)	9748.9 (1025.6)	95.0 (9.9)
15	n/a	22.55	11546.1 (1576.2)	11959.1 (1779.4)	103.6 (15.4)	11940.6 (1266.6)	103.4 (10.9)	10875.3 (1528.3)	94.2 (13.2)	13332.3 (1330.25)	115.5 (11.5)
16	n/a	23.25	27829.6 (9611.9)	26732.7 (10124.2)	96.1 (36.3)	31295.8 (8327.5)	112.5 (29.9)	29352.0 (3995.2)	105.5 (14.4)	26379.7 (7142.1)	94.8 (25.7)
17*	n/a	24.00	12021.4 (813.7)	13518.2 (642.5)	112.4 (5.3)	**7587.5 (735.9)***	**63.1 (6.1)**	13422.7 (952.1)	111.7 (7.9)	**7248.7 (1038.9)***	**60.3 (8.6)**
18	n/a	24.45	4334.7 (1203.0)	4691.5 (1497.4)	108.2 (34.5)	4905.5 (1181.4)	113.1 (27.2)	4009.5 (1824.6)	92.5 (42.1)	4766.7 (1425.5)	109.9 (32.9)
19*	Grandidentatin	25.32	11361.4 (909.3)	12841.5 (892.5)	113.2 (7.9)	**6959.3 (1077.1)***	**61.2 (9.5)**	11556.3 (1304.1)	101.7 (11.5)	**6791.7 (1165.5)***	**59.7 (10.3)**
21	n/a	30.15	2804.8 (226.7)	3064.4 (153.9)	109.3 (5.5)	2967.5 (230.8)	105.8 (8.2)	3111.3 (189.4)	110.9 (6.7)	2842.3 (246.9)	101.3 (8.8)
22	n/a	31.12	11767.5 (1314.3)	11240.1 (1948.4)	95.5 (16.6)	12681.4 (1838.2)	107.7 (15.6)	11899.0 (1455.1)	101.2 (12.4)	10590.5 (1538.2)	89.9 (13.1)
23	n/a	34.25	9195.2 (619.2)	11559.3 (689.9)	125.7 (7.4)	11892.4 (580.7)	129.3 (6.3)	9467.1 (389.2)	102.9 (4.2)	9857.5 (895.4)	107.2 (9.7)

The integrated peak areas of chromatogram peaks was normalized by dividing them by the sample tissue mass (mg fr. wt). Mean values of each peak were then calculated for old leaves for each of the RNAi treatments from all three lines, each with four replicate plants (n=12). Values are also expressed as a percentage of the mean wild type peak values. Standard deviation is shown in parenthesis. Asterisks and bold text indicate a significant difference in treatments following a one-way ANOVA and comparison of means by a student t-test (see Appendices A6.6.4 for full statistical output data).

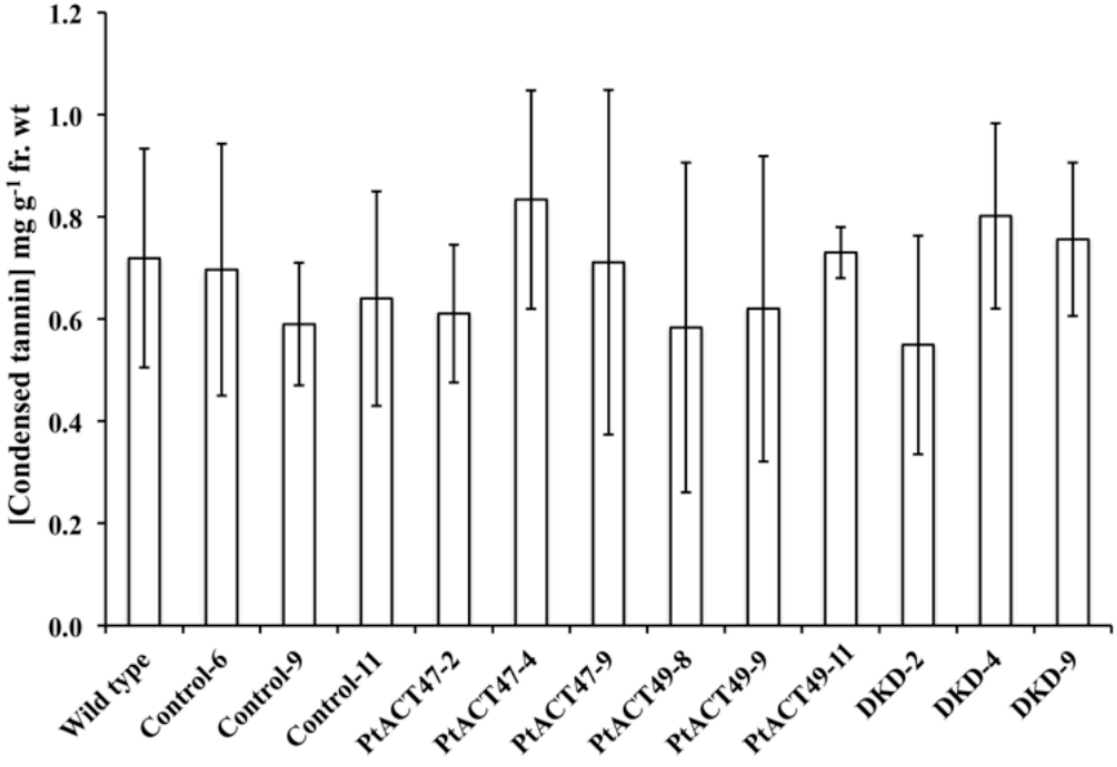

Figure 3.23. A comparison of mean CT content between RNAi transgenic plants and wild type plants.

Condensed tannins (Cts, proanthocyanidins) were quantified (mg g^{-1} fr. wt) using the acid-butanol method (see section 2.18). Mean values calculated from four replicate plants used per treatment. Y error bars indicate standard deviation.

compounds and peaks can be isolated, purified and concentrated would be a feasible approach in this case. CT levels were also measured in transgenic lines (Figure 3.24) and no significant changes were observed compared to controls.

Chapter 4. Discussion

Some portions of text in Sections 4.1; 4.2; 4.3 and 4.4 were taken from Chedgy *et al*. (2015).

The core objective of this work was to investigate the roles of putative acyltransferases *PtACT47*, *PtACT49* and *PtACT54* and their encoded proteins in *Populus spp*. These genes had been previously identified by Yu *et al*. (2009) as belonging to the BAHD family of acyltransferases due to the presence of two characteristic amino acid motifs, HXXXD and DFGWG. BAHDs are responsible for CoA-dependent acyl transfer in plants (D'Auria, 2006). In particular, *PtACT47* and *PtACT49* were of interest in light of experimental evidence from work by Mellway *et al*. (2009) that showed an indirect link between their expression levels and PG accumulation in transgenic hybrid poplar that overexpressed a MYB134 transcription factor known to affect phenylpropanoid secondary metabolites. To date, no enzymes have been characterized in the PG biosynthetic pathway. However, several radio-labeling experiments, notably by Babst *et al*. (2010); Boatright *et al*. (2004); Jarvis *et al*. (2000); and Zenk (1967) suggest that PG production may be CoA-dependent and involve benzyl benzoate as an intermediate. These observations match well with characterized BAHDs from other plant species, in particular CbBEBT from *Clarkia breweri* (D'Auria *et al*., 2002). The three main research objectives were, (a) to further characterize the correlation of PG levels and *PtACT47* and *PtACT49* expression in MYB134 and wild type plants; (b) to conduct *in vitro* functional characterization experiments on recombinant PtACT47, PtACT49 and PtACT54 proteins; and (c) to test the roles of enzymes PtACT47 and PtACT49 *in planta* by manufacturing transgenic plants with altered expression of these genes.

4.1 Phylogenetic analysis suggests that PtACT47, PtACT49 and PtACT54 are likely involved in benzenoid ester production.

Phylogenetic analysis using amino acids sequences of the three proteins of interest with a selection of other characterized BAHDs showed that they clustered with other proteins known to be involved in benzenoid ester production. All three proteins of interest cluster

to sub-clade V-*i*, associated with benzenoid ester production. PtACT47 and PtACT49 cluster very closely with each other, and further sequence analysis revealed that they share 90.6% amino acid sequence identity (Appendices Table A1). This suggests that they may have similar catalytic activity. A genome duplication is predicted to have occurred 60-65 million years ago when the *Salix* and *Populus* lineages diverged (Dode, 1905; Eckenwalder, 1996). Further to this, chromosomes XIII and XIX containing *PtACT47* and *PtACT49* respectively in the *P. trichocarpa* genome share large homologous genome blocks (Tuskan *et al*., 2006). Also adding to weight to this hypothesis that they may have similar biochemical functions is the fact that both proteins share identical BAHD motifs, HTMSD and DFGWG.

A survey of the known substrates of neighboring proteins offered insight into the potential substrates of PtACT47, PtACT49 and PtACT54. However, BAHDs are known to exhibit low substrate selectivity as even minor changes in amino acid sequence can lead to significant changes in biochemical activity. The enzymes in closest proximity to PtACT47 and PtACT49 in the phylogeny all had high affinity for benzoyl-CoA as the acyl donor and could use a variety of aromatic alcohols as the acyl acceptor. Of particular interest were CbBEBT, the closely related NtBEBT from *Nicotiana tabacum* (D'Auria *et al*., 2002), and VhBEBT from *Verbena* x *hybrida* (Togami *et al*., 2006), all of which can synthesize benzyl benzoate from co-substrates benzoyl-CoA and benzyl alcohol. This reaction would fit well into the PG pathway proposed by Babst *et al*. (2010) (Figure 1.3).

PtACT54 clustered away from PtACT47 and PtACT49 at the other pole of sub-clade V-*i*. Its closest neighbors are CHAT, a (Z)-3-hexen-1-ol-*O*-acetyltransferase involved green-leaf volatiles in *A. thaliana* (D'Auria *et al*., 2002; Hoffmann *et al*., 2003), and HMT, (-)-13alpha-hydroxymultiflorine/(+)-13alpha-hydroxylupanine *O*-tigloyltransferase involved in alkaloid synthesis in *Lupinus albus* (Okada *et al*., 2005). Interestingly, the characteristic BAHD motifs differ substantially in PtACT54 compared to those in PtACT47 and PtACT49, they are HPMSD and DYGWG.

Positioned between PtACT47 and PtACT49, and PtACT54, are several alcohol acyltransferases shown to utilize acetyl-CoA with alcohols for volatile ester formation. For example, CmAAT3, an alcohol acyltransferase from *Cucumis melo*, synthesizes benzyl acetate from acetyl-CoA and benzyl alcohol (El-Sharkawy *et al*., 2005). Despite

the wide range of catalyzing ability of the members of sub-clade V-*i*, sequence alignment analysis of the two BAHD motifs and the residues immediately flanking these motifs suggests that the motifs well conserved with only limited variation in their flanking regions (Appendices Figure A4.1.2). This evidence points toward the possibility that the HXXXD and DFGWG are important for conferring general acyltransferase catalysis, however they may work in conjunction with other residues and motifs located else where in the protein that may determine substrate specificity. This would concur with findings by El-Sharkawy *et al*. (2005) who showed that in CmAAT, alteration of residues outside of the two BAHD motifs impacted substrate specificity.

4.2 Expression of *PtACT47* and *PtACT49* generally correlated with PG content

Mellway *et al*. (2009) observed that over-expression of the MYB134 transcription factor in hybrid poplar led to significant up-regulation of genes involved in flavonoid and CT production (Figure 1.2), but also led to a simultaneous decrease in PG content. Specifically, PGs salicortin (2) and tremulacin (4) were significantly lower in MYB134 plants. Thus, these plants exhibit a metabolic shift to enhanced CT production and suppressed PG production. Further to this, Boeckler *et al*. (2014) conducted insect bioassays using the MYB134 plants on the food preference and performance of generalist tree-feeding Lepidoptera, forest tent caterpillars (*Malacosoma disstria*) and gypsy moth (*Lymantria dispar*) caterpillars. The researchers observed that both species preferred the MYB134 plants over wild type plants as a food source suggesting that the PG concentration determines food choice rather than CT content. The pupal weight of *L. dispar* was greater and showed reduced time to pupation when reared on the MYB134 over-expressing poplar compared to wild type material. Kosonen *et al*. (2012) also used the same MYB134 plants and conducted chemical analysis which confirmed the tradeoff between CT and PG production. They observed that at ambient temperatures, the concentration of tremulacin (4) was significantly lower in MYB134 than in wild type plants. The researchers also showed that at higher growth temperatures, both salicortin (2) and tremulacin (4) were significantly lower in MYB134 plants than in wild type plants.

Interestingly, in microarray analysis, Mellway *et al*. (2009) observed that the MYB134 plants also exhibited a significant decease in the expression of two BAHD-like genes *PtACT47* and *PtACT49*. In order to further characterize the observations made by Mellway *et al*. (2009) we measured the total PG content as well as the concentrations of four prevalent PGs, salicin (1), salicortin (2), tremuloidin (3), and tremulacin (4), as well as the expression of *PtACT47* and *PtACT49* in a variety of tissues in both wild type and MYB plants. Wild type plants typically contained a significantly greater total PG content than MYB134 plants and in most tissues, and this correlated with higher *PtACT* gene expression in wild types versus MYB134 plants (Figure 3.3). In addition, in wild type plants, PG levels across most tissues types generally correlated *PtACT47* and *PtACT49* gene expression levels. Medium aged leaves typically contained the greatest overall PG concentration and also exhibited the highest *PtACT47* and *PtACT49* gene expression. However, while we observed this correlation in young and medium aged leaves, this was not the case in old leaves, which exhibited high total PG content but lower gene expression. One interpretation of this data, taking a plant developmental perspective, could be that elevated expression levels of *PtACT47* and *PtACT49* in young leaves where the plant is most vulnerable to herbivory may improve plant fitness by stimulating the production of PGs that protect vulnerable tissues. Some PGs are known to persist in tissue and are not prone to rapid turnover (Warren *et al*., 2003), thus in older leaves a high level of PGs may simply be a remnant of past production.

Individual PGs followed differing patterns of accumulation or decline with leaf age (Figure 3.4). This may be indicative of their relative stability, or their order of production in the PG synthetic pathway(s). Salicortin (2) was typically the most abundant PG and exhibited a consistent pattern of increasing concentration from young to old leaves. Given that its a higher order PG in terms structural complexity, it may represent a stable end product in line with Babst *et al*. (2010) who place it downstream in their model. Salicortin (2) production would also fit well with the ‘optimal defense’ strategy as it represents a significant carbon sink, it is present in young to old leaves, and is known to confer strong anti-herbivory properties (Clausen *et al*., 1989; Ruuhola *et al*., 2001; Ruuhola *et al*., 2003*b*) that may offset its carbon allocation with enhanced plant fitness. However, other PGs such as tremulacin (4) have comparable toxicity levels to salicortin

(2), yet did not follow the same patterns of accumulation, instead peaking in young tissue and decreasing in content with leaf age.

Other PGs such as salicin (1), tremuloidin (3) were less prevalent and were greatest in abundance in young leaves before following a pattern of decline with increasing leaf age. This may suggest a lack of stability, or that they are further modified into other compounds. Salicin (1) is known to be a relatively stable compound (Sou, 2012; Zhang *et al*., 2011) and less prone to spontaneous degradation. Its decline may be due to enzymatic degradation or decoration of its structure converting it to a new compound. To this end, Babst *et al*. (2010) included a step in their proposed model that coverts salicin to salicortin with the addition of 6-HCH moiety (33).

Salicortin (2) levels were significantly lower in MYB134 plants, while the concentration of tremulacin (4), at face value, also appeared to be decreased in MYB134 plants, however this decrease was not statistically significant. Throughout the analyses, tremulacin (4) content was prone to high levels of variability compared with the other PGs measured, which potentially explain the lack of statistically significant differences. This is in contrast to Kosonen *et al*. (2012) who observed statistically lower tremulacin (4) levels in the same MYB134 line. This may be due to different experimental conditions. High variability may also be indicative of a lack of stability. Salicylates have been reported to readily hydrolyze from tremulacin (4) to salicortin (2), tremuloidin (4), salicin (1) and related compounds (Lindroth and Pajutee 1987; Warren *et al*., 2003). This could theoretically occur via the cleavage of the ester bond between the glucosyl group at C2, releasing a benzoic acid molecule, likely via an enzymatic reaction. If this were the case, it may partially explain the increase in salicortin (2) from young to old leaves and the concomitant decline of tremulacin (4).

Tremuloidin (3) was the least abundant of all the PGs quantified and was only present at trace levels in the MYB plants. It did however show a clear decline from young to old leaves. Although speculative, a degradation of tremuloidin (3) to salicin (1) could theoretically occur with release of benzoic acid by cleavage the benzoyl moiety that is ester bound to the C2 of its glucosyl group in tremuloidin (3). Although no experimental evidence exists for this conversion, such a cleavage of this C2 ester bond in both tremuloidin (3) and tremulacin (4) could be catalyzed enzymatically. In related work,

Julkunen-Titto and Sorsa (2001) showed that in drying experiments, decomposition of salicortin (2) and tremulacin (4) produced salicin (1) and tremuloidin (3), respectively.

Overall, PG quantification and gene expression analysis data suggest that *PtACT47* and *PtACT49* expression generally correlated with PG content across multiple tissue types. The exception was old leaves where gene expression was low yet PG content remained high. In MYB134 over-expressing plants, significantly lower PG content was accompanied with proportionally lower gene expression also. These observations suggest that enzymes PtACT47 and PtACT49 may directly or indirectly contribute to PG synthesis in some way.

4.3. *PtACT47* and *PtACT49* encode functional benzoyl-CoA:salicyl alcohol *O*-benzoyltransferase (PtSABT) and benzoyl-CoA:benzyl alcohol *O*-benzoyltransferase (PtBEBT) while recombinant PtACT54 shows limited BEBT-like activity.

Full-length recombinant PtACT47, PtACT49 and PtACT54 proteins were successfully heterogeneously expressed in *E. coli*, purified, and functionally characterized *in vitro* with a range of co-substrates. Recombinant PtACT47 and PtACT49 were active across a broad pH range, typically between pH 2-12, with optima between pH 6.5-7.5 for both enzymes with half maximal activity at pH 4.5-5.5 and pH 8.5-9.0 (Figure 3.7). Recombinant PtACT54 was also shown to be active at pH 7.0. This was similar to results obtained for fully characterized BAHDs that clustered close by in phylogenetic analyses such as CbBEBT which had an optimum between pH 6.5-9.0 (D'Auria *et al*., 2002), and CHAT which has a pH optima between 7.1 and 7.3, with only 89% and 45% activity remaining at a pH of 6.3 and 9.0, respectively (D'Auria *et al*., 2007).

Although PtACT47 and PtACT49 share high amino acid sequence identity, they do not appear to be functionally redundant given their contrasting ranges of co-substrate usage as shown in Table 3.1. PtACT47 exhibited the lowest substrate specificity and was able to utilize three different CoA thioesters, acetyl-CoA, benzoyl-CoA and cinnamoyl-CoA with a range of alcohols. In comparison, PtACT49 has higher substrate selectivity, only able to use acetyl-CoA and benzoyl-CoA with a limited number of alcohols. The most striking difference between them was the ability of PtACT47 to use salicyl alcohol but not benzyl alcohol, and conversely PtACT49 was able to use benzyl alcohol but was

unable to use salicyl alcohol. For example, PtACT47 could use benzoyl-CoA with salicyl alcohol to produce salicyl benzoate; and PtACT49 could use benzoyl-CoA with benzyl alcohol to produce benzyl benzoate (Figure 3.8). These might be regarded as 'niche' reactions for each of these enzymes given lack of catalytic overlap in this case. Another difference between the two enzymes was the ability of PtACT47 to use cinnamoyl compounds such as cinnamyl alcohol and cinnamoyl-CoA (Figure 3.9), products of which have roles in plant defense. For example, benzyl cinnamate produced from cinnamyl alcohol and benzoyl-CoA; and cinnamyl benzoate produced from cinnamyl alcohol and benzoyl-CoA are known to exhibit antifungal properties (Teramoto *et al*., 1994). In addition, PtACT47 was able to synthesize the volatile coniferyl benzoate using benzoyl-CoA and coniferyl alcohol (Figure 3.10), which has been shown to act as a herbivore feeding deterrent in *P. tremuloides* (Jakubas and Gullion, 1990; Jakubas and Mason, 1991).

Interestingly, there are several reactions that both PtACT47 and PtACT49 were able to catalyze, including the production of important green leaf volatiles. Both proteins were able to utilize acetyl-CoA and benzoyl-CoA with *cis*-3-hexen-1-ol, 5-hexenol, and 1-octanol to produce volatile products *cis*-3-hexenyl-, 5-hexenyl- and 1-octanyl- acetates and -benzoates respectively (Figure 3.10). Such products, including *cis*-3-hexenyl acetate can act as signaling volatiles capable of priming of chemical defenses against herbivores in hybrid poplars (Frost *et al*., 2008). However, production of these volatiles appeared to be at trace level and was detectable only by GC-MS. In addition, both PtACT47 and PtACT49 were able to use 3-hydroxybenzyl alcohol with acetyl-CoA or benzoyl-CoA.

Kinetic analysis showed that recombinant PtACT47 exhibited the greatest K_m/K_{cat} ratio (45.8 nM^{-1} s^{-1}) and lowest K_m values (45.1 μM) with benzoyl-CoA and salicyl alcohol to produce salicyl benzoate, and was named benzoyl-CoA:salicyl alcohol *O*-benzoyltransferase (PtSABT). This is first recorded example of a BAHD acyltransferase that is capable of using salicyl alcohol as a substrate. Recombinant PtACT49 showed its highest K_m/K_{cat} (31.8 nM^{-1} s^{-1}) and lowest K_m (55.3 μM) with benzoyl-CoA and benzyl alcohol, producing benzyl benzoate, and it was named benzoyl-CoA:benzyl alcohol *O*-benzoyltransferase (PtBEBT). The primary reactions of PtSABT and PtBEBT are shown in Figure 4.1. These parameters are comparable to data reported for other BEBTs using

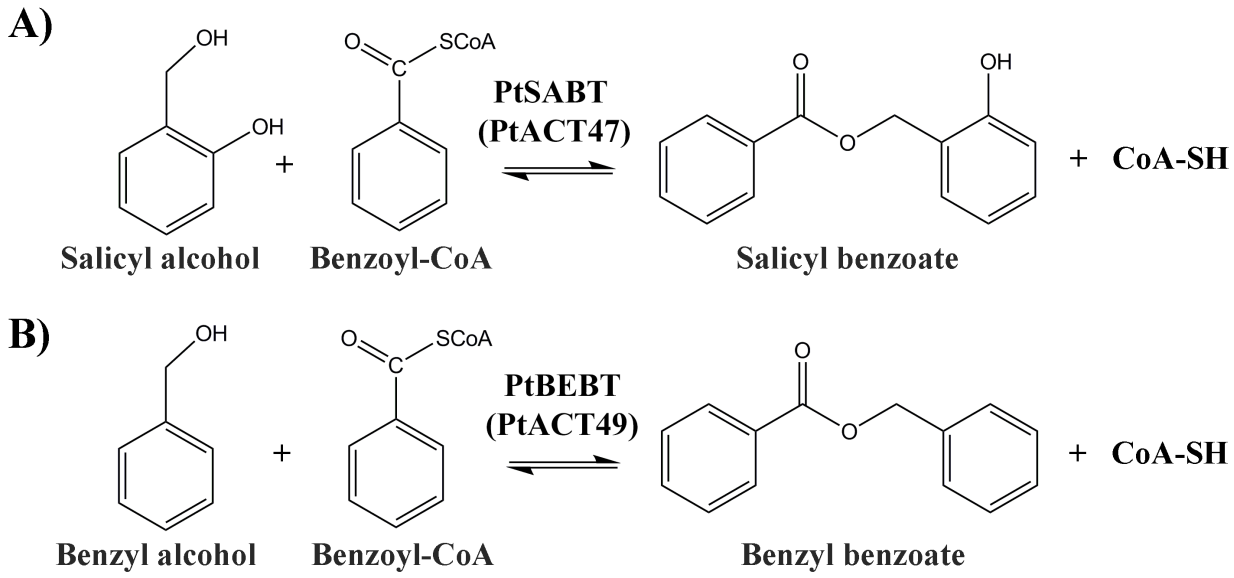

Figure 4.1 The primary reactions catalyzed by PtSABT (PtACT47) (A) and PtBEBT (PtACT49) (B).

benzoyl-CoA and benzyl alcohol. For example CbBEBT has a mean K_m 33.7 μM and K_{cat}/K_m 104.6 nM^{-1} sec^{-1} (D'Auria *et al*., 2002); and PhBPBT from Petunia can also synthesize benzyl benzoate with an apparent K_m of 999.5 μM, and a K_{cat}/K_m of 60.2 nM^{-1} sec^{-1} (Boatright *et al*., 2004).

Resembling other BEBT-like proteins such as CbBEBT (D'Auria *et al*., 2002), both PtSABT and PtBEBT showed high affinity for acetyl-CoA and benzoyl-CoA, with a preference for the latter. However, only CbBEBT and PtSABT could also use cinnamoyl-CoA, while PtBEBT could not. The position of the hydroxyl group on the alcohol substrate is important since all three enzymes showed high activity with 3-hydroxybenzyl alcohol, but only PtSABT could use salicyl alcohol (2-hydroxybenzyl alcohol). Like CbBEBT, both PtBEBT and PtSABT could not use linalool or ethanol. The ability to use alcohols such as *cis*-3-hexen-1-ol, octanol, and hexanol appears to be a common feature of BEBT-like enzymes.

The PtBEBT (PtACT49) H166A mutant with its HTMSD motif altered to ATMSD resulted in a significant reduction of activity. Production of benzyl benzoate from benzoyl-CoA and benzyl alcohol was reduced by 97%, while a complete loss of function

was observed for the synthesis of benzyl acetate from acetyl-CoA and benzyl alcohol (Figure 3.11). These data concur with observations made by Susuki *et al*. (2003) on malonyl-CoA:anthocyanin 5-*O*-glucoside-6’’’-*O*-malonyltransferase (Ss5MaT1) from *Salvia splendens.* The researchers reported a reduced relative *k*cat of 0.02% compared to an unaltered enzyme resulting from an identical replacement of His with Ala. Furthermore, Bayer *et al*. (2004) observed a complete loss of function in vinorine synthase of *Rauvolfia serpentine* when replacing either the His or Asp residues of the HXXXD motif with Ala. Based on these and other results, the histidine residue is believed to act as a general base during catalysis, deprotonating the hydroxyl group(s) of the acyl acceptor to facilitate its nucleophilic attack on the carbonyl carbon of CoA thioester, thus initiating the reaction. It seems that the HXXXD motif is likely the active or catalytic site and the DFGWG motif is a structural site. However, substrate specificity must be determined by other residues or motifs in the protein since both PtACT47 and PtACT49 share identical HTMSD catalytic motifs but exhibit very different activities.

Recombinant PtACT54 was subjected to an identical substrate regime as recombinant PtACT47 (PtSABT) and PtACT49 (PtBEBT) but only showed moderate BEBT-like activity with benzoyl-CoA and benzyl alcohol to produce benzyl benzoate (Figure 3.12), yielding between 65-80% less benzyl benzoate compared to PtBEBT in identical conditions. More research is required into its function, and given its very different HXXXD motif, this may shed light on the roles of the other amino acids within this motif.

PtSABT and PtBEBT share high amino acid sequence identity and catalyze similar yet distinct reactions. This may suggest that they are paralogs. While some functional redundancy exists between the two enzymes, each can utilize certain combinations of substrates that the other cannot. For example, PtSABT can produce salicyl benzoate but not benzyl benzoate, and vice versa for PtBEBT. Notably, PtSABT utilizes a wider range of substrates than does PtBEBT, this functional diversification may have arisen via a process known as neofunctionalization. In this process, following gene duplication likely resulting from ‘the salicinoid genome duplication event’ estimated to have occurred 60-65 million years ago (Dode, 1905; Eckenwalder, 1996) there would have been full functional redundancy between the ancestral and duplicate gene. This may have led to a

temporary lapse in the normal selection pressures placed upon the duplicate gene to produce its major product. Over time, an accumulation of mutations in the duplicate gene can lead to neofunctionalization through which it may acquire novel function(s) (Duarte *et al*., 2006). One interpretation of the data would be that PtBEBT is likely the ancestral gene given its comparatively narrow range of catalytic activities, and that its major product benzyl benzoate is an important intermediate for several benzenoid pathways including for plant volatile synthesis (Orlova *et al*., 2006; Raguso and Pichersky, 1995). Sustained selection pressure on PtBEBT to maintain its benzyl benzoate production is conceivable, while the pressure may have partially diminished for PtSABT, paving the way for new functions to evolve, and in this case, resulting in the novel ability to use salicyl alcohol and a wider range of activities in general.

4.4. Wounding stimulates PG production and expression of *PtSABT* and *PtBEBT*.

Wild type hybrid '717' poplar plants were mechanically wounded and analyzed for phenolic content and expression of *PtSABT* and *PtBEBT* at 6, 24, and 48 hrs post-wounding. Wounded plants had significantly higher levels of total PG content in young leaves at 48 hrs and medium aged leaves at both 24 and 48 hrs. Post-wounding old leaves showed no significant wound-induction in total PG concentrations (Figure 3.13). However, examination of individual PG levels (Figure 3.14) revealed that different PGs were induced at different time frames after wounding stress. Of the four PGs measured, salicin (1) and salicortin (2) levels were the most 'reactive' to wounding. Significantly higher levels of salicin (1) were only detected in young and medium leaves and only within the 6-24 hr period. Salicortin (2) showed significantly greater concentrations in wounded leaves of all ages, but this accumulation was only observed in the 24-48 hr period after wounding. An exception to this pattern was seen in old leaves where salicortin (2) levels were higher at all time points compared to controls. Also, noteworthy was a greater concentration of tremulacin (4) in young leaves at 24 hrs. It appears that the pattern of PG wound-induction is characterized by an initial accumulation of salicin (1) (possibly mixed together with tremulacin (4)) between 0-24hrs after wounding. This was followed by salicortin (2) between 24-48hrs. This pattern was most obvious in young and medium aged leaves, but will need to be confirmed.

Differences between *PtSABT* and *PtBEBT* in wound-induced expression levels were also apparent (Figure 3.15). While the expression of both genes were significantly up-regulated following wounding, *PtSABT* transcript levels were significantly enhanced in wounded plants in young, medium and old leaves at all three time points. In contrast, *PtBEBT* transcription was only up-regulated in young and medium aged leaves, between 24-48hrs in young leaves, and 6, 24, and 48 hrs in medium aged leaves. Old leaves showed no significant differences in *PtBEBT* levels.

Expression of *PtSABT* and *PtBEBT* generally correlated with PG levels, adding weight to their potential involvement in PG production. The patterns of PG accumulation may also shed light on to the PG pathway. The fact that salicortin (2) represents a more delayed response to wounding compared to salicin (1) and tremulacin (4) may be indicative of it being an end product. In contrast, salicin (1) and possibly tremulacin (4) where found to be a more immediate response to wounding, possibly being initially synthesized before undergoing subsequent modification. Alternatively, their speed of induction may be caused by the release of foliar esterases due to mechanical damage of cells. This may degrade pre-existing stores of high order PGs such as salicortin (2) and tremulacin (3) which are known to rapidly degrade into salicin (1) and other compounds such as catechol (32) and the 6-HCH moiety (33) (Clausen *et al*., 1989; Haruta *et al*., 2001; Julkunen-Tiitto and Meier, 1992; Mattes *et al*., 1987; Ruuhola *et al*., 2003*b*). However, this does not explain the increase in salicortin (2) that is observed during wounding.

The observed inducibilty of PGs also fits well with ‘optimal defense hypothesis’ (McKey, 1974; Rhoades, 1979). These data also suggest that the observed PG induction occurs locally at the site of wounding, though it is unclear if PGs levels are systemically induced at tissues in distal leaves. Further work would be of interest in this regard. Published literature on the inducibility of PGs has been mixed. Some data suggests that PG concentrations do not typically increase rapidly following herbivore damage (Osier and Lindroth, 2001, 2006; Stevens and Lindroth, 2005). Others have shown that PG content significantly increased following abiotic wounding in members of the Salicaceae (Clausen *et al*, 1989; Ruuhola *et al*., 2001*b*). Experiments by Osier and Lindroth (2001), and Stevens and Lindroth (2005) examined the total PG levels rather than quantifying

individual PG levels. Examination of individual PGs provides a more detailed data set, and shows that some PGs such as salicin (1) react quickly to wounding stress within 6 hrs. Further research in this area would be valuable, and the inclusion of transgenic plants with altered gene-expression and/or PG content in wounding experiments would be useful.

4.5. Potential roles of PtBEBT and PtSABT in PG synthesis *in planta*.

Data from the transgenic RNAi plants lines provide the first direct evidence that the BAHD acyltransferases play a role in PG synthesis in *Populus*. Plant lines with down-regulated *PtSABT* (*PtACT47*) expression resulted in a significantly decreased salicortin (2) content in medium and old leaves in some transgenic lines, despite high variability observed in the data. In contrast, PtBEBT (PtACT49) RNAi lines showed no significant changes in PG content. One interpretation of this would be that benzyl benzoate production is not involved in PG production. However, experimental evidence including radio-labeling experiments by Babst *et al*. (2010), and Zenk (1967) have consistently placed benzyl benzoate as an intermediate in salicortin (2) production. In addition, *PtBEBT* (*PtACT49*) expression generally correlated with PG levels across a wide range of tissues in hybrid poplar in this work. Alternatively, as *in vitro* functional characterization of recombinant PtACT54 showed, BEBT-like activity may be a common function among closely related BAHDs. Knocked down expression of *PtBEBT* may have been compensated for by other BEBT-like enzymes that are also able to manufacture benzyl benzoate in its absence. Further to this, within the genome of *P. trichocarpa* there are several putative BAHDs identified by Yu *et al*. (2009) that have high amino acid sequence identity to PtBEBT. Examples include *PtACT45*, Potri.013G074400, 90.2% identity to PtBEBT; *PtACT46*, Potri.013G074300, 87.0%; and *PtACT48*, Potri.019G002900, 78.1%. Two of these genes, *PtACT45* and *PtACT46*, have also been indirectly implicated in having defensive roles as their expression was up-regulated following *Melampsora* rust infection by Levée *et al*. (2009). In addition, the presence of large genome blocks of duplicated genes that were observed by Tuskan *et al*. (2006) in the *P. trichocarpa* genome suggests that potentially large numbers of gene copies may exist. For future work it may be necessary to make transgenic plants that simultaneously

knock-down the expression of this entire suite of genes, followed by their incremental restoration of expression gene by gene in order to clearly delineate their roles, if any, in PG production. In addition, co-expression studies may be useful for identifying other genes that have linked or similar expression patterns to *PtBEBT* and *PtSABT* that may also play a role. These could potentially include other classes of enzymes such as GTs and CoA-ligases.

Combining the information from already published material and drawing on the data collected in this thesis from *in vitro* functional characterization of PtSABT and PtBEBT, transgenic plants and patterns of PG accumulation *in planta* from both wild type and wounded plants, a modified model of PG production is proposed (Figure 4.2). A major difference between this model and the one presented by Babst *et al*., (2010) is the synthesis of salicyl benzoate from benzoyl-CoA and salicyl alcohol by PtSABT. The researchers' original model suggested that benzyl benzoate was potentially converted to benzyl-HCH and then to salicyl-HCH, although no enzymes have been characterized that can convert the benzyl alcohol moiety of benzyl benzoate to the 6-HCH moiety. Babst *et al*. (2010) showed via radio-labeling that atoms within the benzyl benzoate compound are incorporated into PGs such as salicortin (2). Salicortin (2) could thus be synthesized with the addition of glucose moiety to the salicyl-HCH by an as yet unknown GT. However, Babst *et al*. (2010) also showed that salicyl alcohol was not converted to salicortin (2); thus a direct route from salicyl benzoate to salicortin (2) would contradict their data.

Some interesting questions regarding PG synthesis are, how is the 6-HCH moiety (33) formed in these potential intermediates? Is it possible that it exists in a 6-HCH-CoA thioester form? If so, it would be feasible that BAHD acyltransferases (as yet unknown) are able to transfer the 6-HCH moiety (33) to acceptor molecules. Unfortunately, HCH compounds are not readily available to test as substrates. Alternatively, other as yet unidentified enzymes may be able to convert compounds such as benzyl benzoate and salicyl benzoate to benzyl-HCH and salicyl-HCH respectively.

A possible role of other PGs such as and tremuloidin (3) and tremulacin (4), in salicortin (2) synthesis is unclear. Salicortin (2) maybe a stable end product given its prevalence and pattern of accumulation from young to older leaves. Salicin (1), tremuloidin (3) and tremulacin (4) all follow a pattern of decline from young to old

tissues. Abiotic wounding of leaves resulted in an initial burst of salicin (1) and tremulacin (4), followed by a spike in salicortin (2). This may indicate that salicin (1) and tremulacin (4) are feeding salicortin (2) production in some way, and speculative routes for these conversions are illustrated in Figure 4.2. The addition of a 6-HCH moiety to salicin (1) would lead directly to salicortin (2). Addition of a benzoic acid moiety to salicin (1) could produce tremuloidin (4). An addition of a 6-HCH moiety to tremuloidin (3) would yield tremulacin (4). Cleavage of benzoic acid from tremulacin (4) would lead to salicortin (2), a hypothesis that is in line with Warren *et al*. (2003) who also speculate that salicortin (2) may be derived partially from tremulacin (4). However, no strong experimental data exists for a potential *in planta* chemical conversion between PGs. It would be interesting to conduct assays using grandidentatin (19) and purified compounds responsible for chromatogram peaks 4, 9, 17 that showed significant changes in transgenic *PtACT47* RNAi and DKD RNAi plants, which may have roles in PG synthesis. For example, it would be interesting to test recombinant PtACT47, PtACT49 and PtACT54 with the purified compounds from these peaks to observe if they can be utilized as substrates.

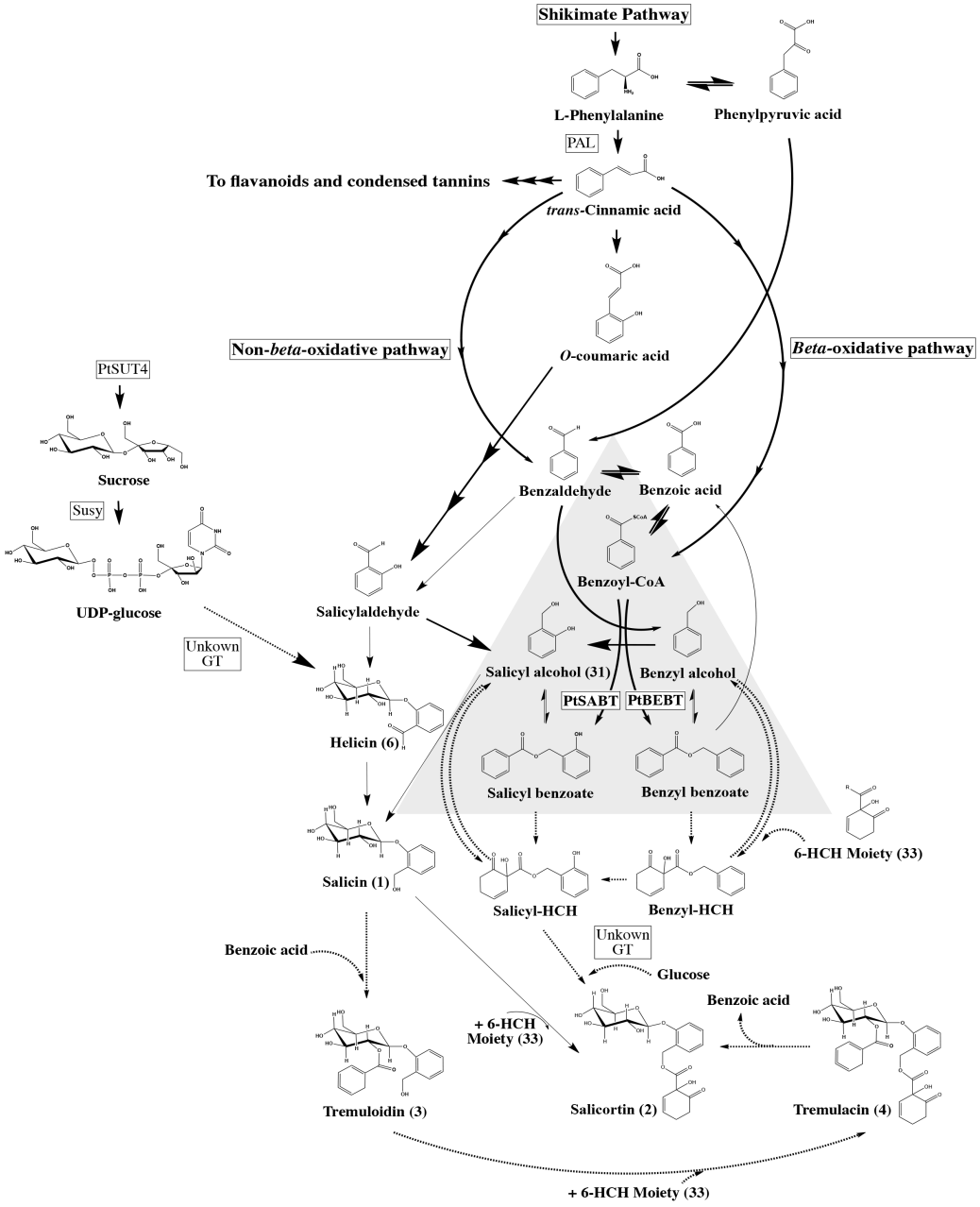

Figure 4.2. An updated model for salicinoid PG synthesis in poplar (redrawn and updated from Babst *et al*., 2010). Based on data from the functional characterization of PtSABT and PtBEBT; on patterns of accumulation in wild type and wounded plants; and data from Babst *et al*., 2010; Boatright *et al*., 2004; Jarvis *et al*., 2000; Long *et al*., 2009; Orlova *et al*., 2006; Pierpont, 1994; Payyavula *et al*., 2009; 2011; Ruuhola and Julkunen-Tiitto, 2003; Zenk, 1967. The grey shaded area indicates the regions where PtSABT and PtBEBT may act. Solid black bold arrows indicate reactions catalyzed by functionally characterized enzymes. Solid black un-bolded arrows indicate pathways proposed previously in willow, tobacco, petunia and snapdragon. Dashed black arrows indicate hypothesized pathways based in part on isotope-labeling feeding studies.

4.6. Conclusions

In this thesis, I investigated the roles of three BAHD acyltransferases in the secondary metabolism of *Populus* spp. I approached this research with a working hypothesis that two of these genes, *PtACT47* and *PtACT49*, may play a role PG synthesis based on indirect evidence that their suppressed expression led to a decrease in PG concentration in hybrid poplars with mis-regulated expression of the MYB134 tannin regulator protein (Mellway, *et al*., 2009). I conducted detailed gene expression profiling of MYB134 and wild type plants in order to further characterize this relationship. Expression of *PtACT47* and *PtACT49* generally correlated with PG concentrations in a variety of plant tissues. Further indirect evidence of a link between PG production and the expression of *PtACT47* and *PtACT49* was observed in wounding experiments. Mechanical damage of leaves to mimic herbivory resulted in an increase in PG concentration that was mirrored by a proportional response of increased *PtACT47* and *PtACT49* gene expression.

I provided evidence that the proteins encoded by *PtACT47* and *PtACT49* are involved in the production of benzenoid ester compounds that are similar to- or identical to compounds previously predicted to be important in PG synthesis by other researchers. Firstly, phylogenetic analysis based on the amino acid sequences encoded by *PtACT47*, *PtACT49* and *PtACT54* showed that they clustered with other BAHD proteins known to synthesize benzenoid esters. This gave rise to the hypothesis that *PtACT47*, *PtACT49* and *PtACT54* may have similar biochemical functions and may also produce benzenoid esters as their major products. I conducted *in vitro* functional characterisation experiments using recombinant proteins which supported this hypothesis. Recombinant PtACT47 could utilize a range of CoA thioesters and alcohols and make a wide range of acetates, benzoates and cinnamates, its primary reaction was the production of salicyl benzoate from benzoyl-CoA and salicyl alcohol and was named benzoyl-CoA:salicyl alcohol *O*-benzoyltransferase (PtSABT). This is the first reported example of a BAHD protein capable of using salicyl alcohol as a preferred substrate, this suggests new possibilities for the PG pathway that have not been previously considered. Recombinant PtACT49 had a narrower range of activities, its primary reaction was the synthesis of benzyl benzoate from benzoyl-CoA and benzyl alcohol, a compound specifically predicted as an intermediate in PG synthesis in stable isotope labeling experiments by Babst *et al*.

(2010). It was named benzoyl-CoA:benzyl alcohol *O*-benzoyltransferase (PtBEBT) accordingly. Interestingly, both PtSABT and PtBEBT could produce plant volatile esters at trace levels, although the significance of this is not yet clear. In contrast, recombinant PtACT54 was shown to encode a protein with moderate BEBT-like properties, but more work is needed to fully characterize its activity *in vitro*. It does however suggest that BEBT-like activity may be common among related BAHD acyltransferases. *PtSABT* and *PtBEBT* are candidate paralogous genes, possibly a result of gene duplication and neofunctionalization.

For future work, it would be interesting to extract, purify, and measure the amount of these enzymes *in planta,* possibly using ammonium sulfate fractionation, and ion exchange column purification. These approaches coupled with the LC-MS methods that I have already developed, may shed light on the abundance of these enzymes in various tissues, and potentially how this influences their phenolic profiles. This line of enquiry would be complemented by the use of protein-specific antibodies that offer highly sensitive detection. Furthermore, taking a transgenic approach such as using a promotor:reporter construct and fluorescence microscopy using green flourenscent protein (GFP) (Lippincott-Schwartz *et al*., 2001), may provide information about the expression patterns of the genes encoding these enzymes and provide clues as to their sub-cellular localization.

I also provide the first direct evidence that BAHD benzoyltransferases are important in PG production using transgenic RNAi hybrid poplar with suppressed gene expression. Suppression of *PtSABT* significantly affected salicortin (2) content in medium and old leaves. If corroborated, this would be the first demonstration of an enzyme in the poplar salicinoid PG pathway. Supression of *PtBEBT*, however, did not have a significant effect on PGs. This may have been due to other BEBT-like enzymes present that may have obscured a potential chemical phenotype in the *PtBEBT*-RNAi lines. Further work is required in this area with the generation of transgenic plants that have suppression of multiple BEBT-like genes in order to better delineate their functions. Co-expression studies may also lead to the discovery of more enzymes in the PG biosynthetic pathway(s).

My work opens up novel avenues to delineate the pathways leading to PG formation. For example, it suggests that salicyl benzoate should be an intermediate in this pathway, and this idea could be tested directly with radiolabeling this compound for metabolic feeding studies. Recombinant PtSABT could be used to produce this compound which could be fed to *Populus* spp. tissue *in vitro* in a similar approach to Babst *et al*. (2010). Detection of the radiolabel in various phenolic metabolites would provide further clues as to the nature of the PG pathways. Based on substrate preferences of PtSABT and PtBEBT, this work also suggests that 3-hydroxybenzyl alcohol or related compounds may be important in the PG pathway. This has not previously been suggested in the literature. The high affinity of both PtSABT and PtBEBT for 3-hydroxybenzyl alcohol thus remains an intriguing question. Both PtSABT and PtBEBT accepted 3-hydroxybenzyl alcohol, but only PtSABT used salicyl alcohol (2-hydroxybenzyl alcohol) and not benzyl alcohol, while PtBEBT could only use benzyl alcohol and not salicyl benzoate. Solving the structure of these enzymes by x-ray crystallography would allow for detailed modelling of the active sites and provide information about the molecular basis of this phenomenon.

This thesis suggests that Salicortin (2) may be a stable end product of the PG biosynthetic pathway, while salicin (1), tremuloidin (3), and tremulacin (4) may be positioned up-stream or be converted to salicortin (2). Tentative evidence for this comes from the quantification of individual PGs in wild type plants which showed that specific PGs follow contrasting patterns of accumulation or decline with respect to leaf age. PGs, salicin (1), tremuloidin (3), tremulacin (4) generally declined from young to old leaves, while salicortin (2), the most abundant of the PGs, increased in concentration with leaf age. Further evidence for this order of production was observed in wounding experiments in which salicin (1) and tremulacin (4) levels increased within 6-12hrs after damage, while increases salicortin (2) concentrations followed later at 12-14hrs post-wounding.

Populus spp. are important for the pulp and paper industry (Mahdavi *et al*., 2013) as well as a bioenergy feedstock (El Kasmioui and Ceulemans, 2012). A better understanding of the genes required for PG biosynthesis and other defense chemicals allows for enhanced selection processes or engineering of plants with heightened resistant to pathogenic attack and herbivory. Given that many of the phenolic precursors feeding

the PG pathway(s) are ubiquitous in higher plants, this may afford the opportunity to one day reconstruct the complete PG pathway in to species which otherwise would not be able to synthesize them, potentially enhancing resistance to pathogens and herbivory in food crop species. In addition, this work may be of interest to the heatlth science and pharmaceutical fields given that phenolic compounds with salicyl moieties are known to have pain relieving and blood-thinning properties, most notabably aspirin (acetylsalicylic acid) (Vlachojannis, 2011).

References

Aharoni A, Keizer LCP, Bouwmeester HJ, Sun ZK, Alvarez-Huerta M, Verhoeven HA, Blaas J, van Houwelingen A, DeVos RCH, van der Voet H (2000) Identification of the SAAT gene involved in strawberry flavor biogenesis by use of DNA microarrays. Plant Cell 12: 647-661.

Aharoni A, Verhoeven HA, Luecker J, O'Connell AP, Van Tunen AJ (2000) Fruit flavor related genes and use thereof. Patent: WO 0032789-A 30.

Allen AH (1889) Commercial organic analysis. Volume 3, issue 1. J & A Churchill publishers, London, UK.

Arnold T, Appel H, Patel V, Stocum E, Kavalier A, Schultz, J. (2004) Carbohydrate translocation determines the phenolic content of *Populus* foliage: a test of the sink-source model of plant defense. New Phytol 164: 157-164.

Babst BA, Harding SA, Tsai C-J (2010) Biosynthesis of phenolic glycosides from phenylpropanoid and benzenoid precursors in *Populus*. J Chem Ecol 36: 286-297.

Bailey JK, Schweitzer JA, Rehill BJ, Irschick DJ, Whitham TG, Lindroth RL (2007) Rapid shifts in the chemical composition of aspen forests: an introduced herbivore as an agent of natural selection. Biol Invasions 9: 715-722.

Barkley MD, Bourgeois S (1978) Repressor recognition of operator and effectors. In: Miller JH, Reznikoff WS (Eds.), The operon, Cold Spring Harbor Laboratory Press, Cold Spring Harbor, NY, USA: 177-220.

Bayer A, Ma XY, Stockigt J, (2004) Acetyltransfer in natural product biosynthesis - functional cloning and molecular analysis of vinorine synthase. Bioorg Med Chem 12: 2787-2795.

Beekwilder J, Alvarez-Huerta M, Neef E, Verstappen FWA, Bouwmeester HJ, Aharoni A (2004) Functional characterization of enzymes forming volatile esters from strawberry and banana. Plant Physiol 135: 1865-1878.

Benedec D, Oniga I, Muresan B, Mot AC, Damian G, Nistor A, Silaghi-dumitrescu R, Hanganu D, Duma M, Vlase L (2014) Contrast between water‐ and ethanol‐based antioxidant assays: aspen (*Populus tremula*) and black poplar (*Populus nigra*) extracts as a case study. J Food Quality 37(4): 259-267.

Berger A, Meinhard J, Petersen M (2006) Rosmarinic acid synthase is a new member of the superfamily of BAHD acyltransferases. Planta 224(6): 1503-1510.

Beuning L, Bowen J, Crowhurst R, Gleave A, Janssen B, McArtney S, Newcomb R, Ross G, Snowden K, Walton E, Yauk Y (2004) Plant and food research apple EST project. Unpublished, direct submission to NCBI.

Boatright J, Negre F, Chen X, Kish CM, Wood B, Peel G, Orlova I, Gang DR, Rhodes D, Dudareva N (2004) Understanding *in vivo* benzenoid metabolism in petunia petal tissue. Plant Physiol 135: 1993-2011.

Boeckler GA, Gershenzon J, Unsicker SB (2011) Phenolic glycosides of the *Salicaceae* and their role as anti-herbivore defenses. Phytochemistry 72(13): 1497-509.

Boeckler GA, Gershenzon J, Unsicker SB (2013) Gypsy moth caterpillar feeding has only a marginal impact on phenolic compounds in old-growth black poplar. J Chem Ecol 39: 1301-1312.

Boeckler GA, Towns M, Unsicker SB, Mellway RD, Yip L, Hilke I, Gershenzon J, Constabel CP (2014) Transgenic upregulation of the condensed tannin pathway in poplar leads to a dramatic shift in leaf palatability for two tree-feeding Lepidoptera. J Chem Ecol 40: 150–158.

Bradford MM (1976) Rapid and sensitive method for the quantitation of microgram quantities of protein utilizing the principle of protein-dye binding. Anal Biochem 72: 248–254.

Braig K, Otwinowski Z, Hegde R, Boisvert DC, Joachimiak A, Horwich AL, Sigler, PB (1994) The crystal structure of the bacterial chaperonin GroEL at 2.9 Å, Nature 371: 578-86.

Bridel M (1919) Application of the biochemical method to the branches and barks of various species of the genus *Populus.* J Pharm Chem 19: 429-434.

Bryant JP, Kuropat PJ (1980) Selection of winter forage by sub-arctic browsing vertebrates - the role of plant chemistry. Annu Rev Ecol Syst 11: 261–285.

Bujard H, Gentz R, Lanzer M, Stüber D, Müller M, Ibrahimi I, Häuptle MT, Dobberstein B (1987) A T5 promotor based transcription-translation system for the analysis of proteins in vivo and *in vitro*. Methods Enzymol 155: 416-433.

Bunsupa S, Okada T, Saito K, Yamazaki M (2011) An acyltransferase-like gene obtained by differential gene expression profiles of quinolizidine alkaloid-producing and non-producing cultivars of *Lupinus angustifolius*. Plant Biotechnol 28: 89-94.

Burhenne K, Kristensen BK, Rasmussen SK (2003) A new class of N-hydroxycinnamoyltransferases. Purification, cloning, and expression of a barley agmatine coumaroyltransferase (EC 23. 1. 64). J Biol Chem 278(16): 13919-13927.

Burnette WN (1981) Western blotting: electrophoretic transfer of proteins from sodium dodecyl sulfate-polyacrylamide gels to unmodified nitrocellulose and radiographic detection with antibody and radioiodinated protein A. Anal Biochem 112(2): 195-203.

Camm EL, Towers GHN (1973) Phenylalanine ammonia lyase. Phytochemistry 12: 961-973.

Charaux C, Rabate J (1942) The $CHCl_3$ complex of aspen leaves. Salicyloylpopuloside and salicylic salicoside. J Pharm Chem 2: 289-303.

Chedgy RJ, Köllner TG, Constabel CP (2015) Functional characterization of two acyltransferases from *Populus trichocarpa* capable of synthesizing benzyl benzoate and salicyl benzoate, potential intermediates in salicinoid phenolic glycoside biosynthesis. Phytochemistry (*in press*).

Chen F, Liu C-J, Tschaplinski TJ, Zhao N (2009) Genomics of secondary metabolism in *Populus*: interactions with biotic and abiotic environments. Crit Rev Plant Sci 28(5): 375-392.

Cheng A-X, Gou J-Y, Yu X-H, Yang H, Fang X, Chen X-Y, Liu C-J (2013) Characterization and ectopic expression of a *Populus* hydroxyacid hydroxycinnamoyltransferase. Mol Plant 6(6): 1889-903.

Chowdhury EMD, Choi BS, Park SU, Lim H-S, Bae H (2012) Transcriptional analysis of hydroxycinnamoyl transferase (HCT) in various tissues of *Hibiscus cannabinus* in response to abiotic stress conditions. Plant Omics 5(3): 305-313.

Clark JM (1988) Novel non-templated nucleotide addition reactions catalyzed by procaryotic and eucaryotic DNA polymerases. Nucl Acids Res 16(20): 9677-9686.

Clausen TP, Reichardt PB, Bryant JP, Sinclair ARE (1992) Chemical defense of *Populus balsamifera*: a clarification. J Chem Ecol 18(9): 1505-1510.

Clausen TP, Reichardt PB, Bryant JP, Werner RA, Post, K, Frisby K (1989) A chemical model for short-term induction in quaking aspen (*Populus tremuloides*) foliage against herbivores. J Chem Ecol 15(9): 2335-2346.

Comino C, Hehn A, Moglia A, Menin B, Bourgaud F, Lanteri S, Portis E (2009) The isolation and mapping of a novel hydroxycinnamoyltransferase in the globe artichoke chlorogenic acid pathway. BMC Plant Biol 9(30): online only.

Comino C, Lanteri S, Portis E, Acquadro A, Romani A, Hehn A, Larbat R, Bourgaud F (2007) Isolation and functional characterization of a cDNA coding a hydroxycinnamoyltransferase involved in phenylpropanoid biosynthesis in *Cynara cardunculus* L. BMC Plant Biol. 7(14): online only.

Constabel CP, Lindroth RL (2010) The impact of genomics on advances in herbivore defense and secondary metabolism in *Populus*. In: Jansson S, Bhalerao R, Groover A (Eds.), The genetics and genomics of *Populus*. Plant genetics and genomics, Springer-Verlag Inc., New York, NY, USA: 279-305.

D'Auria JC (2006) Acyltransferases in plants: a good time to be BAHD. Curr Opin Plant Biol 9: 331-340.

D'Auria JC, Reichelt M, Luck K, Svatos A, Gershenzon J (2007) Identification and characterization of the BAHD acyltransferase malonyl-CoA:anthocyanidin 5-*O*-glucoside-6″-*O*-malonyltransferase (At5MAT) in *Arabidopsis thaliana*. FEBS Lett 581(5): 872-878.

D'Auria JC, Chen F, Pichersky E (2002) Characterization of an acyltransferase capable of synthesizing benzylbenzoate and other volatile esters in flowers and damaged leaves of *Clarkia breweri*. Plant Physiol 130: 466-476.

Davies J, Jacob F (1968) Genetic mapping of the regulator and operator genes of the *lac* operon. J Mol Biol 36(3): 413-417.

Dexter R, Qualley A, Kish CM, Ma CJ, Koeduka T, Nagegowda DA, Dudareva N, Pichersky E, Clark D (2007) Characterization of a petunia acetyltransferase involved in the biosynthesis of the floral volatile isoeugenol. Plant J 49: 265-275.

Dode LA (1905) Extracts of unprecedented monograph of the genus *Populus*. Bull Soc Hist Nat Autun 18: 161-231.

Donaldson JR, Kruger EL, Lindroth RL (2006*b*) Competition- and resource-mediated tradeoffs between growth and defensive chemistry in trembling aspen (*Populus tremuloides*). New Phytol 169: 561-570.

Donaldson JR, Stevens MT, Barnhill HR, Lindroth RL (2006*a*) Age-related shifts in leaf chemistry of clonal aspen (*Populus tremuloides*). J Chem Ecol 32: 1415-1429.

Duarte JM, Cui L, Wall PK, Zhang Q, Zhang X, Leebens-Mack J, Ma H, Altman N, dePamphilis CW (2006) Expression pattern shifts following duplication indicative of subfunctionalization and neofunctionalization in regulatory genes of *Arabidopsis*. Mol Biol Evol 23(2): 469-478.

Dudareva N, D'Auria JC, Nam KH, Raguso RA, Pichersky E (1998) Acetyl-CoA:benzylalcohol acetyltransferase - an enzyme involved in floral scent production in *Clarkia breweri*. Plant J 14: 297-304.

Eckenwalder JE (1996) in biology of *Populus* and its implications for management and conservation. In: Stettler RF, Bradshaw HD Jr., Heilman PE, Hinckley TM (Eds.), Biology of *Populus* and its implications for management and conservation, NRC Research Press, Ottawa, ON, Canada: 7-32.

El Kasmioui O, Ceulemans R (2012) Financial analysis of the cultivation of poplar and willow for bioenergy. Biomass Bioenerg 43: 52-64.

El-Sharkawy I, Manríquez D, Flores FB, Regad F, Bouzayen M, Latché A, Pech J-C (2005) Functional characterization of a melon alcohol acyl-transferase gene family involved in the biosynthesis of ester volatiles. Identification of the crucial role of a threonine residue for enzyme activity. Plant Mol Biol 59: 345-362.

English S, Greenaway W, Whatley FR (1991) Analysis of phenolics of *Populus trichocarpa* bud exudate by GC-MS. Phytochemistry 30: 531-533.

Erdmann CGH (1841) Textbook of chemistry and pharmacology for doctors, physicians and thier pharmaceutists for self teaching and designed for lectures and consumption. Veit and co., Berlin, Germany.

Erickson RL, Pearl IA, Darling SF (1970) Populoside and grandidentoside from the bark of *Populus grandidentata*. Phytochemistry 9(4): 857-863.

Felton GW, Donato K, Delvecchio RJ, Duffey SS (1989) Activation of plant foliar oxidases by insect feeding reduces nutritive quality of foliage for noctuid herbivores. J Chem Ecol 15: 2667-2694.

Felton GW, Donato KK, Broadway RM, Duffey SS (1992) Impact of oxidized plant phenolics on the nutritional quality of dietary protein to a noctuid herbivore, *Spodoptera exigua*. J. Insect Physiol 38: 277-285.

Frost CJ, Mescher MC, Dervinis C, Davis JM, Carlson JE, De Moraes CM (2008) Priming defense genes and metabolites in hybrid poplar by the green leaf volatile *cis*-3-hexenyl acetate. New Phytol 180(3): 722-734.

Fujiwara H, Tanaka Y, Fukui Y, Nakao M, Ashikari T, Kusumi T (1997) Anthocyanin 5-aromatic acyltransferase from *Gentiana triflora*. Purification, characterization and its role in anthocyanin biosynthesis. Eur J Biochem 249: 45-51.

Fujiwara H, Tanaka Y, Yonekura-Sakakibara K, Fukuchi-Mizutani M, Nakao M, Fukui Y, Yamaguchi M, Ashikari T, Kusumi T (1998) cDNA cloning, gene expression and subcellular localization of anthocyanin 5-aromatic acyltransferase from *Gentiana triflora*. Plant J 16: 421-431.

Fukui Y (1954) Constituents of plants in Kyushu. I. A new glucoside isolated from *Xylosma apactis*. Yakugaku Zasshi 74: 735-737.

Gird CE, Mihele D, Siboiu D (2001) Comparative qualitative and quantitative chemical study of catkins, leaves and barks of willows. Note I. The qualitative chemical study. Farmacia 49(3): 73-77.

Gou JY, Yu XH, Liu CJ (2009) A hydroxycinnamoyltransferase responsible for synthesizing suberin aromatics in *Arabidopsis*. Proc Natl Acad Sci USA 106(44): 18855-18860.

Grienenberger E, Besseau S, Geoffroy P, Debayle D, Heintz D, Lapierre C, Pollet B, Heitz T, Legrand M (2009) A BAHD acyltransferase is expressed in the tapetum of *Arabidopsis* anthers and is involved in the synthesis of hydroxycinnamoyl spermidines. Plant J 58(2): 246-259.

Grothe T, Lenz R, Kutchan TM (2001) Molecular characterization of the salutaridinol 7-*O*-acetyltransferase involved in morphine biosynthesis in opium poppy *Papaver somniferum*. J Biol Chem 276: 30717-30723.

Hall TA (1999) BioEdit: a user-friendly biological sequence alignment editor and analysis program for Windows 95/98/NT. Nucl Acids Symp Ser 41: 95-98.

Haruta M, Pedersen JA, Constabel CP (2001) Polyphenol oxidase and herbivore defense in trembling aspen (*Populus tremuloides*): cDNA cloning, expression, and potential substrates. Physiologia Plantarum 112: 552-558.

Heiska S, Tikkanen O-P, Rousi M, Julkunen-Tiitto R (2007) Bark salicylates and condensed tannins reduce vole browsing amongst cultivated dark-leaved willows (*Salix myrsinifolia*). Chemoecology 17: 245-253.

Hemming JDC, Lindroth RL (1995) Intraspecific variation in aspen phytochemistry: effects on performance of gypsy moths and forest tent caterpillars. Oecologia 103: 79-88.

Hemming JDC, Lindroth RL (1999) Effects of light and nutrient availability on aspen: growth, phytochemistry, and insect performance. J Chem Ecol 25(7): 1687-1714.

Hemming JDC, Lindroth RL (2000) Effects of phenolic glycosides and protein on gypsy moth (Lepidoptera: Lymantriidae) and forest tent caterpillar (Lepidoptera: Lasiocampidae) performance and detoxification activities. Environ Entomol 29(6): 1108-1115.

Hoffmann L, Besseau S, Geoffroy P, Ritzenthaler C, Meyer D, Lapierre C, Pollet B, Legrand M (2004) Silencing of hydroxycinnamoycoenzyme A shikimate/quinate hydroxycinnamoyltransferase affects phenylpropanoid biosynthesis. Plant Cell 16:1446-1465.

Hoffmann L, Maury S, Martz F, Geoffroy P, Legrand M (2003) Purification, cloning, and properties of an acyltransferase controlling shikimate and quinate ester intermediates in phenylpropanoid metabolism. J Biol Chem 278(1): 95-103.

Hwang SY, Lindroth RL (1997) Clonal variation in foliar chemistry of aspen: effects on gypsy moths and forest tent caterpillars. Oecologia 111: 99-108.

Inada T, Kimata K, Aiba H (1996) Mechanism responsible for glucose-lactose diauxie in *Escherichia coli*: Challenge to the cAMP model. Genes Cells 1: 293-301.

Jaakola L, Pirttila AM, Halonen M, Hohtola A (2001) Isolation of high quality RNA from bilberry (*Vaccinium myrtillus* L.) fruit. Mol Biotech 19: 201-203.

Jakubas WJ, Gullion GW (1990) Coniferyl benzoate in quaking aspen a Ruffed Grouse feeding deterrent. J Chem Ecol 16(4): 1077-1086.

Jakubas WJ, Gullion GW, Clausen TP (1989) Ruffed grouse feeding behavior and its relationship to secondary metabolites of quaking aspen flower buds. J Chem Ecol 15(6): 1899-1917.

Jakubas WJ, Mason JR (1991) Role of avian trigeminal sensory system in detecting coniferyl benzoate, a plant allelochemical. J Chem Ecol 17(11): 2213-2221.

Jarvis AP, Schaaf O, Oldham NJ (2000) 3-Hydroxy-3-phenylpropanoic acid is an intermediate in the biosynthesis of benzoic acid and salicylic acid but benzaldehyde is not. Planta 212: 119-126.

Jones P, Vogt T (2001) Glycosyltransferases in secondary plant metabolism: tranquilizers and stimulant controllers. Planta 213(2): 164-174.

Julkunen-Tiitto R, Meier R (1992) The enzymic decomposition of salicin and its derivatives obtained from Salicaceae species. J Nat Prod 55(9): 1204-1212.

Julkunen-Tiitto R, Sorsa S (2001) Testing the effects of drying methods on Willow flavonoids, tannins, and salicylates. J Chem Ecol 27(4): 779-789.

Karban R, Baldwin IT (1997) Induced responses to herbivory. The University of Chicago Press, Chicago, IL, USA.

Kimata K, Takahashi H, Inada T, Postma P, Aiba H (1997) cAMP receptor protein-cAMP plays a crucial role in glucose-lactose diauxie by activating the major glucose transporter gene in *Escherichia coli*. Proc Natl Acad Sci USA 94: 12914-12919.

Koch K (2004) Sucrose metabolism: regulatory mechanisms and pivotal roles in sugar sensing and plant development. Curr Opin Plant Biol 7(3): 235-246.

Kolehmainen J, Julkunen-Tiitto R, Roininen H, Tahvanainen J (1995) Phenolic glucosides as feeding cues for willow-feeding leaf beetles. Entomol Experim App 74(3): 235-243.

Kosonen M, Keski-Saari S, Ruuhola T, Constabel CP, Julkunen- Tiitto R. 2012. Effects of overproduction of condensed tannins and elevated temperature on chemical and ecological traits of genetically modified hybrid aspens (*Populus tremula* × *P. tremuloides*). J Chem Ecol 38: 1235–1246.

Laemmli UK (1970) Cleavage of structural proteins during the assembly of the head of bacteriophage T4. Nature 227: 680-685.

Laflamme P, St Pierre B, De Luca V (2001) Molecular and biochemical analysis of a Madagascar periwinkle root-specific minovincinine-19-hydroxy-*O*-acetyltransferase. Plant Physiol 125: 189-198.

Landmann C, Hucherig S, Fink B, Hoffmann T, Dittlein D, Coiner HA, Schwab W (2011) Substrate promiscuity of a rosmarinic acid synthase from lavender (*Lavandula angustifolia* L.). Planta 234(2): 305-320.

Larkin MA, Blackshields G, Brown NP, Chenna R, McGettigan PA, McWilliam H, Valentin F, Wallace IM, Wilm A, Lopez R, Thompson JD, Gibson TJ, Higgins DG (2007) Clustal W and Clustal X version 2.0. Bioinformatics 23: 2947-2948.

Lepelley M, Cheminade G, Tremillon N, Simkin A, Caillet V, McCarthy J (2007) Chlorogenic acid synthesis in coffee: An analysis of CGA content and real-time RT-PCR expression of HCT, HQT, C3H1, and CCoAOMT1 genes during grain development in *C. canephora*. Plant Sci 172(5): 978-996.

Levée V, Major I, Levasseur C, Tremblay L, MacKay J, Séguin A (2009) Expression profiling and functional analysis of *Populus* WRKY23 reveals a regulatory role in defense. New Phytol 184: 48-70.

Lindroth RL, Hsai MTS, Scriber JM (1987) Seasonal patterns in the phytochemistry of three *Populus* species. Biochem Syst Ecol 15(6): 681-686.

Lindroth RL, Hwang S-Y, Osier TL (1999) Phytochemical variation in quaking aspen: effects on gypsy moth susceptibility to nuclear polyhedrosis virus. J Chem Ecol 25(6): 1331-1341.

Lindroth RL, Hwang SY (1996) Diversity, redundancy, and multiplicity in chemical defense systems of aspen. In: Romeo JT, Saunders JA, Barbosa P (Eds.), Phytochemical diversity and redundancy in ecological interactions, Plenum Press, New York, NY, USA: 25-56.

Lindroth RL, Kinney KK (1998) Consequences of enriched atmospheric CO_2 and defoliation for foliar chemistry and gypsy moth performance. J Chem Ecol 24(10): 1677-1695.

Lindroth RL, Kopper BJ, Parsons WFJ, Bockheim JG, Karnosky DF, Hendrey GR, Pregitzer KS, Isebrands JG, Sober J (2001) Consequences of elevated carbon dioxide and ozone for foliar chemical composition and dynamics in trembling aspen (*Populus tremuloides*) and paper birch (*Betula papyrifera*). Environ Pollut 115(3): 395-404.

Lindroth RL, Koss PA (1996) Preservation of *Salicaceae* leaves for phytochemical analysis: further assessment. J Chem Ecol 22(4): 765-771.

Lindroth RL, Pajutee MS (1987) Chemical analysis of phenolic glycosides: art, facts and artifacts. Oecologia 74: 144-148.

Lindroth RL, Peterson SS (1988) Effects of plant phenols on performance of southern armyworm larvae. Oecologia 75: 185-189.

Lindroth RL, Scriber JM, Hsai MTS (1988) Chemical ecology of the tiger swallow: mediation of host use by phenolic glycosides. Ecology 69(3): 814-822.

Lindroth RL, St. Clair SB (2013) Adaptations of quaking aspen (*Populus tremuloides* Michx.) for defense against herbivores. Forest Ecol Manag 299: 14-21.

Long MC, Nagegowda DA, Kaminaga Y, Ho KK, Kish CM, Schnepp J, Sherman D, Weiner H, Rhodes D, Dudareva N (2009) Involvement of snapdragon benzaldehyde dehydrogenase in benzoic acid biosynthesis. Plant J 59: 256-265.

Lippincott-Schwartz J, Snapp E, Kenworthy A (2001) Studying protein dynamics in living cells. Nat Rev Mol Cell Biol 2:444–456.

Luo J, Fuell C, Parr A, Hill L, Bailey P, Elliott K, Fairhurst SA, Martin C, Michael AJ (2009) A novel polyamine acyltransferase responsible for the accumulation of spermidine conjugates in *Arabidopsis* seed. Plant Cell 21(1): 318-333.

Ma X, Koepke J, Panjikar S, Fritzseh C, Stockigt J (2005) Crystal structure of vinorine synthase, the first representative of the BAHD superfamily. J Biol Chem 280: 13576-13583.

Mahdavi S, Kermanian H, Ramezani O, Molavi S (2013) Assessment of five successful poplar clones for kraft pulp production considering technical and economics aspects. Cell Chem technol 47: 267-275.

Major IT, Constabel CP (2006) Molecular analysis of poplar defense against herbivory: comparison of wound- and insect elicitor-induced gene expression. New Phytol 172: 617-635.

Manjasetty BA, Yu XH, Panjikar S, Taguchi G, Chance MR, Liu CJ (2012) Structural basis for modification of flavonol and naphthol glucoconjugates by *Nicotiana tabacum* malonyltransferase (NtMaT1). Planta 236(3): 781-793.

Marrs KA, Alfenito MR, Lloyd AM, Walbot V (1995) A glutathione S-transferase involved in vacuolar transfer encoded by the maize gene bronze-2. Nature 375: 397-400.

Massad TJ, Trumbore SE, Ganbat G, Reichelt M, Unsicker S, Boeckler A, Gleixner G, Gershenzon J, Ruehlow S (2014) An optimal defense strategy for phenolic glycoside production in *Populus trichocarpa* - isotope labeling demonstrates secondary metabolite production in growing leaves. New Phytologist 203: 607-619.

Mattes BR, Clausen TP, Reichardt PB (1987) Volatile constituents of balsam poplar: The phenol glycoside connection. Phytochemistry 26:1361-1366.

Mattson WJ, Hart EA, Bolney WJA (2001) Insect pests of *Populus*: coping with the inevitable. In: Isebrands JG, Dickmann DI, Eckenwalder JE, Richardson J (Eds.), Poplar culture in north America, NRC Research Press, Ottawa, ON, Canada: 219-248.

McCown BH, Lloyd G (1981) Woody Plant Medium (WPM) - a mineral nutrient formulation for microculture for woody plant species. Horticultural Sci 16: 453.

McKey D (1979) The distribution of secondary compounds within plants. In: Rosenthal GA, Janzen DH (Eds.), Herbivores, their interaction with secondary plant metabolites, Academic press, New York, NY, USA: 55-133.

Meadow ND, Fox DK, Roseman S (1990) The bacterial phosphoenolpyruvate: Glycose phosphotransferase system. Annu Rev Biochem 59: 497–542.

Meier B, Julkunen-Tiitto R, Tahvanainen J, Sticher O (1988) Comparative high-performance liquid and gas-liquid chromatographic determination of phenolic glucosides in Salicaceae species. J Chromatography 442: 175-186.

Meier B, Lehmann, D, Sticher O, Bettschart A (1987) Salicylate in medicinal plants. Screening methods (HPLC, TLC) for detection. Deutsche Apotheker Zeitung 127(46): 2401-2407.

Mellway RD, Tran LT, Prouse MB, Campbell MM, Constabel CP (2009) The wound-, pathogen-, and ultraviolet B-responsive MYB134 gene encodes an R2R3 MYB transcription factor that regulates proanthocyanidin synthesis in poplar. Plant Physiol 150: 924-941.

Michaelis L, Menten ML (1913) The kinetics of enzymes. Biochem Z 49: 333-369.

Mizuno M, Kato M, Misu C, Iinuma M, Tanaka T (1991) Chaenomeloidin: a phenolic glucoside from leaves of *Salix chaenomeloides*. J Nat Prod 54(5): 1447-1450.

Muroi A, Ishihara A, Tanaka C, Ishizuka A, Takabayashi J, Miyoshi H, Nishioka T (2009) Accumulation of hydroxycinnamic acid amides induced by pathogen infection and identification of agmatine coumaroyltransferase in *Arabidopsis thaliana*. Planta 230(3): 517-527.

Nakayama T, Suzuki H, Nishino T (2003) Anthocyanin acyltransferases: specificities, mechanism, phylogenetics, and applications. J Mol Catal B Enzym 23: 117-132.

Negruk V, Yang P, Subramanian M, McNevin JP, Lemieux B (1996) Molecular cloning and characterization of the CER2 gene of *Arabidopsis thaliana*. Plant J 9: 137-145.

Nichols-Orians CM, Clausen TP, Fritz RS, Reichardt PB, Wu J (1992) 2'-Cinnamoyl salicortin, a phenolic glycoside from *Salix sericea*. Phytochemistry 31(6): 2180-2181.

Niggeweg R, Michael AJ, Martin C (2004) Engineering plants with increased levels of the antioxidant chlorogenic acid. Nat Biotechnol, 22: 746-754.

Ohyanagi H, Tanaka T, Sakai H, Shigemoto Y, Yamaguchi K, Habara T, Fujii Y, Antonio BA, Nagamura Y, Imanishi T, Ikeo K, Itoh T, Gojobori T, Sasaki T (2006) The rice annotation project database (RAP-DB): hub for *Oryza sativa* ssp. *japonica* genome information. Nucleic Acids Res 34(database issue): D741-D744.

Okada T, Hirai MY, Suzuki H, Yamazaki M, Saito K (2005) Molecular characterization of a novel quinolizidine alkaloid *O*-tigloyltransferase: cDNA cloning, catalytic activity of recombinant protein and expression analysis in *Lupinus* plants. Plant Cell Physiol 46: 233-244.

Orlova I, Marshall-Colon A, Schnepp J, Wood B, Varbanova M, Fridman E, Blakeslee JJ, Peer WA, Murphy AS, Rhodes D, Pichersky E, Dudareva N (2006) Reduction of benzenoid synthesis in petunia flowers reveals multiple pathways to benzoic acid and enhancement in auxin transport. Plant Cell 18: 3458-3475.

Osier TL, Hwang S-Y, Lindroth RL (2000) Within- and between-year variation in early season phytochemistry of quaking aspen (*Populus tremuloides* Michx.) clones. Biochem Syst Ecol 28: 197-208.

Osier TL, Lindroth RL (2001) Effects of genotype, nutrient availability, and defoliation on aspen phytochemistry and insect performance. J. Chem. Ecol. 27, 1289-1313.

Osier TL, Lindroth RL (2004) Long-term effects of defoliation on quaking aspen in relation to genotype and nutrient availability: plant growth, phytochemistry and insect performance. Oecologia 139: 55-65.

Osier TL, Lindroth RL (2006) Genotype and environment determine allocation to and costs of resistance in quaking aspen. Oecologia 148: 293-303.

Palo RT (1984) Distribution of birch (*Betula* spp), willow (*Salix* spp), and poplar (*Populus* spp) secondary metabolites and their potential role as chemical defense against herbivores. J Chem Ecol 10: 499-520.

Payyavula R, Babst B, Nelsen M, Harding S, Tsai C-J (2009) Glycosylation-mediated phenylpropanoid partitioning in *Populus tremuloides* cell cultures. BMC Plant Biol 9: 151.

Payyavula RS, Tay KHC, Tsai C-J, Harding SA (2011) The sucrose transporter family in *Populus*: the importance of a tonoplast PtaSUT4 to biomass and carbon partitioning. Plant J 65: 757–770.

Pearl IA, Darling SF (1959) Studies on the barks of the family Salicaceae. I. Tremuloidin, a new glucoside from the bark of *Populus tremuloides*. J Org Chem 24(6): 731-735.

Pearl IA, Darling SF (1962) Studies on the barks of the family Salicaceae. VI. Grandidentatin, a new glucoside from the bark of *Populus grandidentata*. J Org Chem 27(5): 1806-1809.

Pearl IA, Darling SF (1971*a*) Barks of the family Salicaceae. XXVI. Hot water extractives of the bark and leaves of *Populus deltoides*. Can J Chem 49(1): 49-55.

Pearl IA, Darling SF (1971*b*) Studies on leaves of family Salicaceae. 16. Phenolic extractives of leaves of *Populus balsamifera* and of *P. trichocarpa*. Phytochemistry 10: 2844-2847.

Pearl IA, Darling SF (1971*c*) The structures of salicortin and tremulacin. Phytochemistry 10: 3161-3166.

Peters DJ, Constabel CP (2002) Molecular analysis of herbivore-induced condensed tannin synthesis: cloning and expression of dihydroflavonol reductase from trembling aspen (*Populus tremuloides*). Plant J 32: 701-712.

Picard S, Chenault J, Augustin S, Venot C (1994) Isolation of a new phenolic compound from leaves of *Populus deltoids*. J Nat Prod 57(6): 808-810.

Pierpont WS (1994) Salicylic acid and its derivatives in plants: medicines, metabolites and messenger molecules. Adv Bot Res 20: 163-235.

Porter LJ, Hrstich LN, Chan BG (1986) The conversion of procyanidins and prodelphinidins to cyanidin and delphinidin. Phytochemistry 25: 223-230.

Postma PW, Lengeler JW, Jacobson GR (1996) Phosphoenolpyruvate: carbohydrate phosphotransferase systems. In: Neidhardt FC, Curtiss III R, Ingraham JL, Lin ECC, Low KB, Magasanik B, Reznikoff WS, Riley M, Schaechter M, Umbarger HE (Eds.), *Escherichia coli* and *Salmonella*: cellular and molecular biology, 2nd ed., American Society for Microbiology, Washington, DC, USA: 1149–1174.

Poukens-Renwart P, Tits M, Angenot L (1993) Densitometric determination of salicin in willow stem bark. J Planar Chromatography. 6(6): 434-437.

Prudic KL, Khera S, Solyom A, Timmermann BN (2007) Isolation, identification, and quantification of potential defensive compounds in the viceroy butterfly and its larval host-plant, carolina willow. J Chem Ecol 33: 1149–1159.

Qiagen (2001) QIAexpressionist manual. Qiagen Inc., Toronto, ON, Canada.

Raguso, R.A., Pichersky, E., 1995. Floral volatiles from *Clarkia breweri* and *C. Concinna* (Onagraceae): recent evolution of floral scent and moth pollination. Plant Syst Evol 194: 55-67.

Raven PH, Evert RF, Eichhorn SE (1999) Biology of plants, 6th Ed., Freeman WH and company/Worth Publishers, New York, NY, USA.

Reichardt PB, Merken HM, Clausen TP, Wu J (1992) Phenolic glycosides from *Salix lasiandra*. J Nat Prod 55(7): 970-973.

Rhoades DF (1979) Evolution of plant chemical defense against herbivores. In: Rosenthal GA, Janzen DH (Eds.), Herbivores: their interaction with secondary plant metabolites, Academic Press, New York, NY, USA: 3-54.

Richtmyer NK, Yeakel EH (1934) Structure of populin. J Am Chem Soc 56: 2495-2497.

Ro DK, Mah N, Ellis BE, Douglas CJ (2001) Functional characterization and subcellular localization of poplar (*Populus trichocarpa* × *Populus deltoides*) cinnamate 4-hydroxylase. Plant Physiol 126(1): 317-329.

Rowell-Rahier M, Pasteels JM (1990) Phenolglucosides and interactions at three trophic levels: Salicaceae–herbivores–predators. In: Bernays EA (Ed.), Insect-plant interactions vol. 2, CRC Press, Boca Raton, FL, USA: 75-94.

Ruuhola T, Julkunen-Tiitto R, Vainiotalo P (2003*b*) *In vitro* degradation of willow salicylates. J Chem Ecol 29(5): 1083-1097.

Ruuhola T, Julkunen-Titto R (2003*a*) Trade-off between synthesis of salicylates and growth of micropropagated *Salix pentandra*. J Chem Ecol 29(7): 1565-1588.

Ruuhola T, Tikkenen O-P, Tahvanainen J (2001) Differences in host use efficiency of larvae of a generalist moth, *Operophtera brumata* on tree chemically divergent *Salix* species. J Chem Ecol 27: 1595-1615.

Ruuhola TM, Julkunen-Tiitto Kristiina (2000) Salicylates of intact *Salix myrsinifolia* plantlets do not undergo rapid metabolic turnover. Plant Physiology. 122(3): 895-905.

Ruuhola TM, Sipura M, Nousiainen O, Tahvanainen J (2001*b*) Systemic induction of salicylates in *Salix myrsinifolia* (Salisb.). Ann Bot 88: 483-497.

Saier Jr. MH, Ramseier TM, Reizer J (1996) Regulation of carbon utilization. In: Neidhardt FC (Ed.). *Escherichia coli* and *Salmonella typhimurium*: cellular and molecular biology, 2nd ed., American Society of Microbiology, Washington, DC, USA: 1325-1343.

Sambrook J, Fritschi EF, Maniatis T (1989) Molecular cloning: a laboratory manual. Cold Spring Harbor Laboratory Press, New York, NY, USA.

Sasaki T, Matsumoto T, Yamamoto K (2002) *Oryza sativa* nipponbare (GA3) genomic DNA, chromosome 2, PAC clone: P0036H07. Published Only in Database.

Schwarz E, Scherrer G, Hobom G, Kössel H (1978) Nucleotide sequence of cro, cII and part of the 0 gene in phage lambda DNA. Nature 272: 410-414.

Scriber JM, Slansky F JR (1981) The nutritional ecology of immature insects. Annu Rev Entomol 26: 183-211.

Serra O, Hohn C, Franke R, Prat S, Molinas M, Figueras M (2010) A feruloyl transferase involved in the biosynthesis of suberin and suberin-associated wax is required for maturation and sealing properties of potato periderm. Plant J 62(2): 277-290.

Shalit M, Guterman I, Volpin H, Bar E, Tamari T, Menda N, Adam Z, Zamir D, Vainstein A, Weiss D, Pichersky E, Lewinsohn E (2003) Volatile ester formation in roses. Identification of an acetyl-coenzyme A geraniol/citronellol acetyltransferase in developing rose petals. Plant Physiol 131(4): 1868-1876.

Shewale JG (1982) *β*-Glucosidase: its role in cellulase synthesis and hydrolysis of cellulose. Int J Biochem 14: 435-443.

Shirley AM, McMichael CM, Chapple C (2001) The sng2 mutant of *Arabidopsis* is defective in the gene encoding the serine carboxypeptidase-like protein sinapoylglucose:choline sinapoyltransferase. Plant J 28(1): 83-94.

Souleyre EJF, Greenwood GR, Friel EN, Karunairetnam S, Newcomb RD (2005) An alcohol acyltransferase from apple (cv. Royal Gala), *Mp*AAT1, produces esters involved in apple fruit flavor. FEBS J 272(12): 3132–3144.

St. Pierre B, De Luca V (2000) Evolution of acyltransferase genes: origin and diversification of the BAHD superfamily of acyltransferases involved in secondary metabolism. In: Romeo JT, Ibrahim R, Varin L, De Luca V (Eds.), Recent advances in phytochemistry vol, 34, evolution of metabolic pathways. Elsevier Science Ltd., Amsterdam, Netherlands: 285-315.

St. Pierre B, Laflamme P, Alarco AM, De Luca V (1998) The terminal *O*-acetyltransferase involved in vindoline biosynthesis defines a new class of proteins responsible for coenzyme A dependent acyl transfer. Plant J 14: 703-713.

Stevens MT, Lindroth RL (2005) Induced resistance in the indeterminate growth of aspen (*Populus tremuloides*). Oecologia 145: 298-306.

Stewart C Jr, Kang BC, Liu K, Mazourek M, Moore SL, Yoo EY, Kim BD, Paran I, Jahn MM (2005) The *Pun1* gene for pungency in pepper encodes a putative acyltransferase. Plant J 42: 675-688.

Strauss SY, Rudgers JS, Lau JA, Irwin RE (2002) Direct and ecological costs of resistance to herbivory. Trees 17: 278–285.

Stüber D, Matile H, Garotta G (1990) System for high-level production in *Escherichia coli* and rapid purification of recombinant proteins: application to epitope mapping, preparation of antibodies, and structure-function analysis. In: Lefkovits I, Pernis B (Eds.), Immunological methods, vol. 4, Academic Press, New York, NY, USA: 121-152.

Studier FW (2005) Protein production by auto-induction in high-density shaking cultures. Protein Express Pur 41(1): 207-234.

Sullivan M (2009) A novel red clover hydroxycinnamoyl transferase has enzymatic activities consistent with a role in phaselic acid biosynthesis. Plant Physiol 150(4): 1866-1879.

Suzuki H, Nakayama T, Nagae S, Yamaguchi M-A, Iwashita T, Fukui Y, Nishino T (2004*b*) cDNA cloning and functional characterization of flavonol 3-*O*-glucoside-6*''*-*O*-malonyltransferases from flowers of *Verbena hybrida* and *Lamium purpureum*. J Mol Catal B Enzym 28(2-3): 87-93.

Suzuki H, Nakayama T, Nishino T (2003*b*) Proposed mechanism and functional amino acid residues of malonyl-CoA:anthocyanin 5-*O*-glucoside-6''-*O*-malonyltransferase from flowers of *Salvia splendens*, a member of the versatile plant acyltransferase family. Biochemistry-US, 42: 1764-1771.

Suzuki H, Nakayama T, Yamaguchi MA, Nishino T (2004*a*) cDNA cloning and characterization of two *Dendranthema* x *Morifolium* anthocyanin malonyltransferases with different functional activities. Plant Sci 166: 89-96.

Suzuki H, Nakayama T, Yonekura-Sakakibara K, Fukui Y, Nakamura N, Nakao M, Tanaka Y, Yamaguchi M, Kusumi T, Nishino T (2001) Malonyl-CoA:anthocyanin 5-*O*-glucoside-6*'''*-*O*-malonyltransferase from scarlet sage (*Salvia splendens*) flowers - enzyme purification, gene cloning, expression, and characterization. J Biol Chem 276: 49013-49019.

Suzuki H, Nakayama T, Yonekura-Sakakibara K, Fukui Y, Nakamura N, Yamaguchi MA, Tanaka Y, Kusumi T, Nishino T (2002) cDNA cloning, heterologous expressions, and functional characterization of malonyl-coenzyme a:anthocyanidin 3-*O*-glucoside-6*''*-*O*-malonyltransferase from dahlia flowers. Plant Physiol. 130(4): 2142-2151.

Suzuki H, Sawada S, Watanabe K, Nagae S, Yamaguchi M, Nakayama T, Nishino T (2004*c*) Identification and characterization of a novel anthocyanin malonyltransferase from scarlet sage (*Salvia splendens*) flowers: an enzyme that is

phylogenetically separated from other anthocyanin acyltransferases. Plant J 38: 994-1003.

Suzuki H, Sawada S, Yonekura-Sakakibara K, Nakayama T, Yamaguchi M, Nishino T (2003*a*) Identification of a cDNA encoding malonyl-CoenzymeA:anthocyanidin 3-*O*-glucoside 6"-*O*-malonyltransferase from cineraria (*Senecia curentus*) flowers. Plant Biotechnol 20: 229-234.

Tacke E, Korfhage C, Michel D, Maddaloni M, Motto M, Lanzini S, Salamini F, Doring H-P (1995) Transposon tagging of the maize Glossy2 locus with the transposable element En/Spm. Plant J 8: 907-917.

Tahvanainen J, Helle E, Julkunen-Tiitto R, Lavola A (1985*a*) Phenolic compounds of willow bark as deterrents against feeding by mountain hare. Oecologia 65: 319–323.

Tahvanainen J, Julkunen-Tiitto R, Kettunen J (1985*b*) Phenolic glycosides govern the food selection pattern of willow feeding leaf beetles. Oecologia 67: 52–56

Tamura, K., Peterson. D., Peterson, N., Stecher, G., Nei, M., Kumar, S., 2011. MEGA5: molecular evolutionary genetics analysis using maximum likelihood, evolutionary distance, and maximum parsimony methods. Mol Biol Evol 28(10): 2731-2739.

Teramoto Y, Matsuse I, Koga T, Ueda S (1994) Characterization of a novel antimycotic agent, cinnamyl benzoate, using yeast-phase *Sporothrix schenckii*. J Microbiol Biotechnol 10: 395-400.

Thieme H (1963*a*) Isolation of a new phenol glucoside from *Salix fragilis*. Naturwissenschaften 50: 477.

Thieme H (1963*b*) The phenolic glycosides in Salicaceae. 1. General survey (detection, chemical structure, synthesis, presence). Pharmazie 18: 770-774.

Thieme H (1964*a*) The phenolic glycosides in Salicaceae. 2. Isolation and demonstration. Pharmazie 19: 471-475.

Thieme H (1964*b*) The phenolic glycosides in Salicaceae. 3. Quantitative determination. Pharmazie 19: 535-538.

Thieme H (1964*c*) Isolation of a new phenol glycoside from *Salix viminalis*. Naturwissenschaften 51(9): 217.

Thieme H (1965*a*) The phenolic glycosides in Salicaceae. 4. Review of newly isolated glycosides and new work on structural information; proof and determination of new glycosides. Pharmazie 20: 436-439.

Thieme H (1965*b*) The phenolic glycosides in Salicaceae. 5. Studies on glycoside spectra and the glycoside content of types of salix in central Germany. Pharmazie 20: 570–574.

Thieme H (1965*c*) The phenolic glycosides in Salicaceae. 6. Studies on seasonal changes in glycoside concentrations, on the dependency of glycoside content on the time of day and age of the plant organs. Pharmazie 20: 688–691.

Thieme H (1965*d*) The phenolic glycosides in Salicaceae. Planta Med 13: 431–435.

Thieme H, Benecke R (1967) Isolation of a new phenol glycoside from *Populus nigra.* Pharmazie 22(1): 59-60.

Thieme H, Richter R (1966) Isolation of a new phenol glycoside from *Populus tremula*. Pharmazie 21(4): 251.

Tilly K, Murialdo H, Georgopoulos C (1981) Identification of a second *Escherichia coli* groE gene whose product is necessary for bacteriophage morphogenesis. Proc NatI Acad Sci USA 78: 1629-1633.

Togami J, Tamura M, Ishiguro K, Hirose C, Okuhara H, Ueyama Y, Nakamura N, Yonekura-Sakakibara K, Fukuchi-Mizutani M, Suzuki K, Fukui Y, Kusumi T, Tanaka Y (2006) Molecular characterization of the flavonoid biosynthesis of *Verbena hybrida* and the functional analysis of *Verbena* and *Clitoria ternatea* F3'5'H genes in transgenic verbena. Plant Biotechnol 23: 5-11.

Tuskan GA, DiFazio S, Jansson S, Bohlmann J, Grigoriev I, Hellsten U, Putnam N, Ralph S, Rombauts S, Salamov A, Schein J, Sterck L, Aerts A, Bhalerao RR, Bhalerao RP, Blaudez D, Boerjan W, Brun A, Brunner A, Busov V, Campbell M, Carlson J, Chalot M, Chapman J, Chen G-L, Cooper D, Coutinho PM, Couturier J, Covert S, Cronk Q, Cunningham R, Davis J, Degroeve S, Déjardin A, dePamphilis C, Detter J, Dirks B, Dubchak I, Duplessis S, Ehlting J, Ellis B, Gendler K, Goodstein D, Gribskov M, Grimwood J, Groover A, Gunter L, Hamberger B, Heinze B, Helariutta Y, Henrissat B, Holligan D, Holt R, Huang W, Islam-Faridi N, Jones S, Jones-Rhoades M, Jorgensen R, Joshi C, Kangasjärvi J, Karlsson J, Kelleher C, Kirkpatrick R, Kirst M, Kohler A, Kalluri U, Larimer F, Leebens-Mack J, Leplé J-C, Locascio P, Lou Y, Lucas S, Martin F, Montanini B, Napoli C, Nelson DR, Nelson C, Nieminen K, Nilsson O, Pereda V, Peter G, Philippe R, Pilate G, Poliakov A, Razumovskaya J, Richardson P, Rinaldi C, Ritland K, Rouzé P, Ryaboy D, Schmutz J, Schrader J, Segerman B, Shin H, Siddiqui A, Sterky F, Terry A, Tsai C-J, Uberbacher E, Unneberg P, Vahala J, Wall K, Wessler S, Yang G, Yin T, Douglas C, Marra M, Sandberg G, Van de Peer Y, Rokhsar D (2006) The genome of black cottonwood, *Populus trichocarpa* (Torr. & Gray). Science 313: 1596-1604.

Unno H, Ichimaida F, Suzuki H, Takahashi S, Tanaka Y, Saito A, Nishino T, Kusunoki M, Nakayama T (2007) Structural and mutational studies of anthocyanin malonyltransferases establish the features of BAHD enzyme catalysis. J Biol Chem 282(21): 15812-15822.

Varbanova M, Porter K, Lu F, Ralph J, Hammerschmidt R, Jones AD, Day B (2011) Molecular and biochemical basis for stress-induced accumulation of free and bound *p*-coumaraldehyde in cucumber. Plant Physiol 157(3): 1056-1066.

Veljanovski V, Constabel CP (2013) Molecular cloning and biochemical characterization of two UDP-glycosyltransferases from poplar. Phytochemistry 91: 148-157.

Vlachojannis J (2011) Willow species and aspirin: different mechanism of actions. Phytother Res 25(7): 1102–1104.

Walker K, Croteau R (2000*a*) Molecular cloning of a 10-deacetylbaccatin III-10-*O*-acetyl transferase cDNA from *Taxus* and functional expression in *Escherichia coli*. PNAS 97: 583-587.

Walker K, Croteau R (2000*b*) Taxol biosynthesis: molecular cloning of a benzoyl-CoA: taxane 2-alpha-*O*-benzoyltransferase cDNA from Taxus and functional expression in *Escherichia coli*. Proc Natl Acad Sci USA 97: 13591-13596.

Walker K, Fujisaki S, Long R, Croteau R (2002*a*) Molecular cloning and heterologous expression of the C-13 phenylpropanoid side chain-CoA acyltransferase that functions in taxol biosynthesis. Proc Natl Acad Sci USA 99: 12715-12720.

Walker K, Long R, Croteau R (2002*b*) The final acylation step in Taxol biosynthesis: Cloning of the taxoid C13-side-chain N-benzoyltransferase from *Taxus*. PNAS 99: 9166-9171.

Walker K, Schoendorf A, Croteau R (2000) Molecular cloning of a taxa-4(20), 11(12)-dien-5alpha-ol-*O*-acetyl transferase cDNA from *Taxus* and functional expression in *Escherichia coli*. Arch Biochem Biophys 374: 371-380.

Wang J, Constabel CP (2003) Biochemical characterization of two differentially expressed polyphenol oxidases from hybrid poplar. Phytochemistry 64(1): 115-121.

Wang J, Constabel CP (2004*a*) Polyphenol oxidase overexpression in transgenic *Populus* enhances resistance to herbivory by forest tent caterpillar (*Malacosoma disstria*). Planta 220: 87-96.

Wang J, Constabel CP (2004*b*) Three polyphenol oxidases from hybrid poplar are differentially expressed during development and after wounding and elicitor treatment. Physiol Plantarum 122: 344–353.

Wang J, De Luca V (2005) The biosynthesis and regulation of biosynthesis of Concord grape fruit esters, including 'foxy' methylanthranilate. Plant J 44: 606-619.

Warren JM, Bassman JH, Fellman JK, Mattinson S, Eigenbrodes S (2003) Ultraviolet-B radiation alters phenolic salicylate and flavonoid composition of *Populus trichocarpa* leaves. Tree Physiol 23: 527-535.

Wegrzyn JL, Eckert AJ, Choi M, Lee JM, Stanton BJ, Sykes R, Davis MF, Tsai C-J, Neale DB (2010) Association genetics of traits controlling lignin and cellulose biosynthesis in black cottonwood (*Populus trichocarpa*, Salicaceae) secondary xylem. New Phytol 188: 515–532.

Weitzel C, Petersen M (2011) Cloning and characterisation of rosmarinic acid synthase from *Melissa officinalis* L. Phytochemistry 72(7): 572-578.

Wesley SV, Helliwell CA, Smith NA, Wang MB, Rouse DT, Liu Q, Gooding PS, Singh SP, Abbott D, Stoutjesdijk PA (2001) Construct design for efficient, effective and high-throughput gene silencing in plants. Plant J 27:581-590.

Wooley S, Walker S, Vernon J, Lindroth R (2008) Aspen decline, aspen chemistry, and elk herbivory: are they linked? Rangelands 30: 17-21.

Xia Y, Nikolau BJ, Schnable PS (1996) Cloning and that affects characterization of CER2, an *Arabidopsis* gene cuticular wax accumulation. Plant Cell 8: 1291-1304.

Xu Z, Horwich AL, Sigler PB (1997) The crystal structure of the asymmetric GroEL-GroES-(ADP)7 chaperonin complex. Nature 388: 741–750.

Yang Q, Reinhard K, Schiltz E, Matern U (1997) Characterization and heterologous expression of hydroxycinnamoyl/benzoyl-CoA:anthranilate N-hydroxycinnamoyl/benzoyltransferase from elicited cell cultures of carnation, *Dianthus caryophyllus* L. Plant Mol Biol 35:777-789.

Yang Q, Trinh HX, Imai S, Ishihara A, Zhang LQ, Nakayashiki H, Tosa Y, Mayama S (2004) Analysis of the involvement of hydroxyanthranilate hydroxycinnamoyltransferase and caffeoyl-CoA 3-*O*-methyltransferase in phytoalexin biosynthesis in oat. Mol Plant Microbe Interact 17: 81-89.

Yonekura-Sakakibara K, Tanaka Y, Fukuchi-Mizutani M, Fujiwara H, Fukui Y, Ashikari T, Murakami Y, Yamaguchi M, Kusumi T (2000) Molecular and biochemical characterization of a novel hydroxycinnamoyl-CoA:anthocyanin 3-*O*-glucoside-6”-*O*-acyltransferase from *Perilla frutescens*. Plant Cell Physiol 41: 495-502.

Young B, Wagner D, Doak P, Clausen T (2010*a*) Within-plant distribution of phenolic glycosides and extrafloral nectaries in trembling aspen (*Populus tremuloides*; Salicaceae). Am J Bot 97(4): 601-610.

Young B, Wagner D, Doak P, Clausen T (2010*b*) Induction of phenolic glycosides by quaking aspen (*Populus tremuloides*) leaves in relation to extrafloral nectaries and epidermal leaf mining. J Chem Ecol 36(4): 369-77.

Yu X-H, Gou J-Y, Liu C-J (2009) BAHD superfamily of acyl-CoA dependent acyltransferases in *Populus* and *Arabidopsis*: bioinformatics and gene expression. Plant Mol Biol 70: 421-442.

Zenk MH (1967) Pathways of salicyl alcohol and salicin formation in *Salix purpurea* L. Phytochemistry 6: 245-252.

Zhang C-P, Zheng H-Q, Liu G, Hu F-L (2011) Development and validation of HPLC method for determination of salicin in poplar buds: Application for screening of counterfeit propolis. Food Chem 127: 245-350.

Zhu J, Withers SG, Reichardt PB, Treadwell E, Clausen TP (1998) Salicortin: a repeat-attack new-mechanism-based *Agrobacterium faecalis β*-glucosidase inhibitor. Biochem J 332: 367-371

Appendices Table of Contents

List of Tables

Table of Figures

Appendix I. Additional information on phenylpropanoid synthesis in *Populus* spp.

A1.1. Phenylpropanoid synthesis in *Populus* spp.

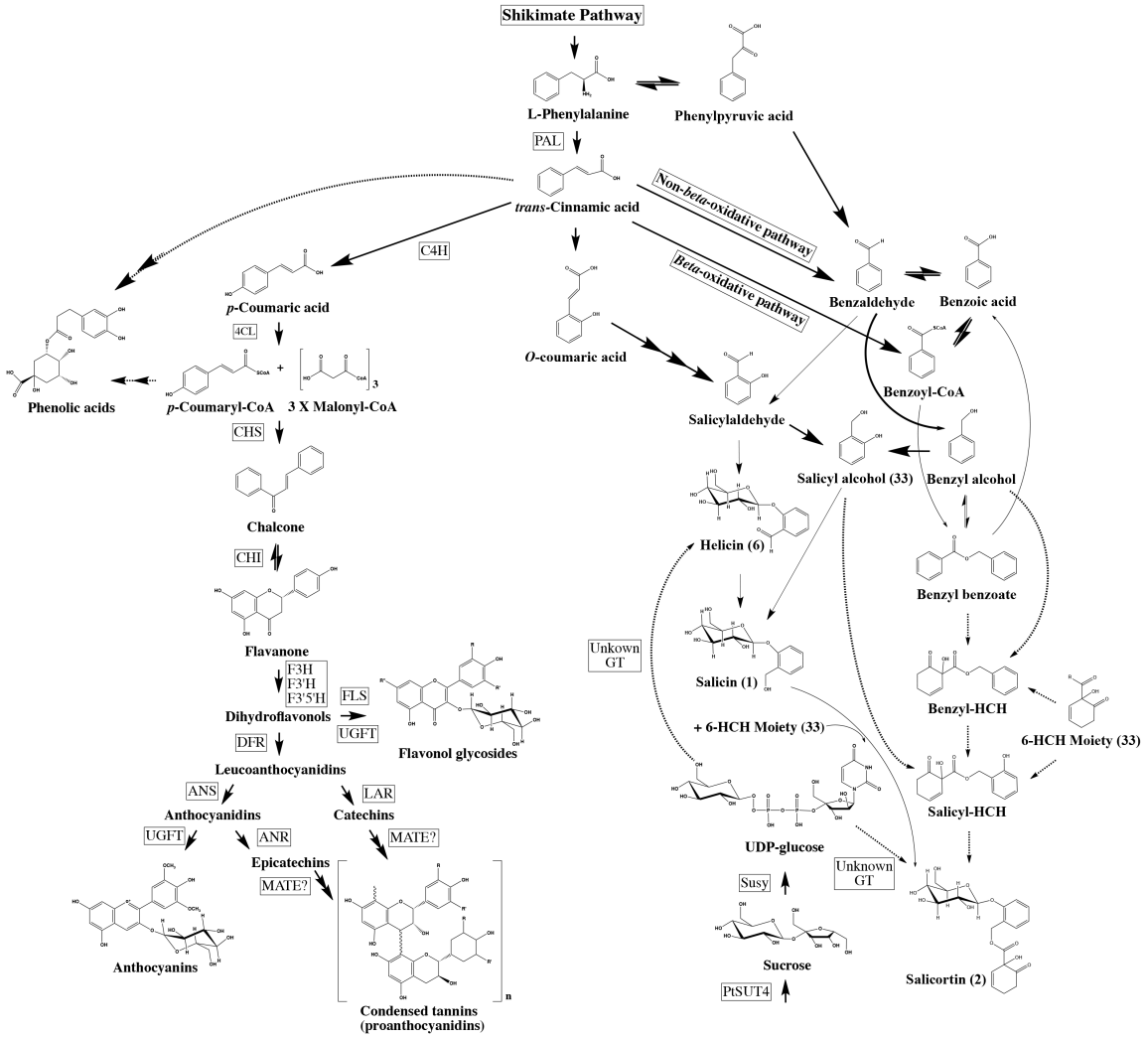

Figure A1.1.1. A complete model for phenylpronaoid synthesis in *Populus* spp. including flavonoids, phenolic acids, condensed tannins and salicinoid phenolic glycosides.

Based on data from Babst, *et al*., 2010; Boatright, *et al*., 2004; Jarvis, *et al*., 2000; Long, *et al*., 2009; Mellway, *et al*., 2009; Orlova, *et al*., 2006; Pierpont, 1994; Payyavula *et al*., 2009; 2011; Ruuhola and Julkunen-Tiitto, 2003; Zenk, 1967. Solid black bold arrows indicate reactions catalyzed by functionally characterized enzymes. Solid black un-bolded arrows indicate pathways proposed previously in willow, tobacco, petunia and snapdragon. Dashed black arrows indicate hypothesized pathways based in part on isotope-labeling feeding studies. Abbreviations, PAL, Phe ammonia-lyase; C4H, cinnamate 4-hydroxylase; 4CL, 4-coumarate CoA-ligase; CHS, chalcone synthase; CHI, chalcone isomerase; F3H, flavanone 3-hydroxylase; F3'H, flavonoid 3'-hydroxylase; F3'5'H, flavonoid 3'5'-hydroxylase; DFR, dihydroflavonol reductase; FLS, flavonol synthase; LAR, leucoanthocyanidin reductase; ANS, anthocyanidin synthase; ANR, anthocyanidin reductase; MATE, multidrug and toxic compound extrusion transporter; UFGT, UDP-Glc flavonoid glucosyltransferase.

Appendix II. Medicinal properties of PGs of the Salicaceae

A2.1. Medicinal properties of PGs.

In a wider context that extends beyond plant chemical ecology, many PGs have been shown to confer properties that have a variety of biotechnological, industrial, and pharmaceutical applications. Kwon *et al*. (2014) showed that salicortin (2) isolated from *P. euramericana* bark extract can suppress the inflammatory responses in mammalian cell systems. Using the mouse (*Mus musculus*) macrophage primary immune cell system, the researchers used the RAW 264.7 cell line known to cause Abelson Murine Leukemia virus-induced tumors. In cells that had been subjected to inflammatory stimuli such as lipopolysaccharide, salicortin (2) was observed to inhibit the induction of the inducible nitric oxide synthase (iNOS) enzyme which typically leads to nitric oxide (NO) accumulation, an inflammatory mediator compound known to contribute to the pathogenesis of a variety of human diseases. Moreover, the degree of inhibition was proportional to the dosage of salicortin (2) applied *in vitro*. These data corroborate work by Lee *et al*. (2013*a*) who observed that salicortin (2) derivatives isolated and purified from *P. davidiana* caused inhibition of NO production in identical RAW 264.7 cells. 50% maximal inhibitory concentrations (IC_{50}) values of 15 mM were reported for salicortin (2) and 50 mM for salicortin-6'-benzoate.

Debbache *et al*. (2014) examined extracts from *P. nigra* flower buds for antioxidant and anti-inflammatory properties. The researchers observed that the aqueous fraction of chloroform extract was an effective antioxidant by scavenging radicals such as diphenylpicrylhydrazil (DPPH), IC_{50}, 24.61 μg mL^{-1}; ABTS (2,2'-azino-bis(3-ethylbenzothiazoline-6-sulphonic acid), 17.09 μg mL^{-1}; nitric oxide, 9.52 μg mL^{-1}, hypochlorous acid (HOCl), 187.90 μg mL^{-1}; and hydroxyl radicals (OH^{-}), 113.79 μg mL^{-1}. The same extract exhibited anti-inflammatory properties *in vitro* by effectively inhibiting xanthine oxidase (XO), IC_{50}, 60.7 μg mL^{-1}; and lipoperoxydation, 60.7 μg mL^{-1} activity, both of which are known to trigger inflammation in mammals. Furthermore, in carrageenan-induced mice paw edema cells the same fraction (at a dosage of 200 mg kg^{-1}) significantly inhibited edema formation by 62.4%. The researchers suggest that salicylate derivative compounds may play a pivotal role in conferring these properties. Si

et al. (2009) also applied the DPPH radical-scavenging methodology to test the antioxidant properties of a range of PGs from *P. ussuriensis*. Salicortin (2) exhibited the greatest anti-oxidative capacity with an IC_{50} value of 5.92 mM, followed by isograndidentatin B (21), 6.61 mM; isograndidentatin A (20), 6.68 mM; grandidentatin (19), 6.75 mM; populoside (25), 6.76 mM; populoside A (26), 6.79 mM; and salireposide (29), 6.84 mM.

Yang *et al*. (2013) showed that components of the methanolic extract of *S. pseudo-lasiogyne*, namely salicortin (2); 2',6'-*O*-acetylsalicortin (12); 2'-*O*-acetylsalicortin (9); and 3'-*O*-acetylsalicortin (10) had strong antioxidant properties and significantly inhibited lipopolysaccharide-induced NO production in BV2 microglial cells *in vitro*. Interestingly, all of these PGs contain the 1-hydroxy-6-oxo-2-cyclohexenecarboxylate moiety (derivative of 33). Of these compounds, 2'-*O*-acetylsalicortin (9) had significant cognitive-enhancing effect on scopolamine-induced memory deficit in mice. This compound is believed to act on the brain hippocampus and cortex and reduce glutathione reductase and superoxide dismutase activity that are known to confer amnesia in mice.

Salicortin (2) extracted from willow bark of *Salix* spp. including *S. alba*, *S. daphnoides*, *S. fragilis* L. and *S. purpurea* L. reduces the expression of TNF-α induced ICAM-1, an important gene in the inflammation process in mammals (Knuth *et al*., 2011). Further to this, the researchers showed that the degradation product catechol (32), a breakdown product of salicortin (2) following ingestion by mammals, was the causal agent in effecting this decrease in expression, and mitigation of inflammation. In a follow up study by Knuth *et al*. (2013), salicortin (2) was orally administered (235.8 μM kg^{-1}) to Wistar rats (*Rattus norvegicus*) and human volunteers. In rats, following digestion, an accumulation of catechol (32) (13.0 μM) in blood serum was detected after 30 mins, and in humans a comparable level was reached after 80 mins.

Salicortin (2) has links with obesity mitigation in mammals. Lee *et al*. (2013*b*, 2013*c*) demonstrated that salicortin (2) can inhibit differentiation of adipocyte cells, also known as fat cells in mammals, excessive growth of which has links with obesity. The researchers exposed 3T3-L1 preadipocytes (cells that can differentiate in adipocytes) to the methanolic extracts of *S. pseudo-lasiogyne* twigs. This resulted in a reduced lipid accumulation in a concentration-dependent manner. Salicortin (2) and four salicortin

derivatives 2',6'-*O*-acetylsalicortin (12), 2'-*O*-acetylsalicortin (9), 3'-*O*-acetylsalicortin (10), and 6'-*O*-acetylsalicortin (11) were shown to significantly inhibit differentiation of n 3T3-L1 cells. Building on this work, Harbilas *et al*., (2013) observed that *P. balsamifera* extracts and in particular salicortin (2) could mitigate the onset of obesity and features of the metabolic syndrome in C57Bl/6 mice that were subjected to high fat diets. Whole body weights were reduced as well as hepatic triglyceride accumulation, and levels of glycemia, insulinemia, leptin, and adiponectin were improved.

Subramanian *et al*. (2006) observed that salicortin (2) has cytotoxic properties. Continuous exposure (7 days; 168 h) of salicortin (2) ([500 ng ml^{-1}]) against HCT-116 colon cancer cells was shown to result in a 10% surviving fraction of cells *in vitro*. The potential for application salicortin (2) as an anti-cancer therapy is encouraging given its pharmacokinetic profile, it rapidly disappears from the blood plasma of live mice after treatment, dropping form initial plasma concentrations of 250 μg ml^{-1} (total mouse plasma) to below 250 ng ml^{-1} after 5 minutes (Subramanian *et al*., 2006).

A2.2. References

Debbache N, Atmani D, Atmani D (2014) Chemical analysis and biological activities of *Populus nigra*, flower buds extracts as source of propolis in Algeria. Ind Crop Prod 53: 85-92.

Harbilas D, Vallerand D, Brault A, Saleem A, Arnason JT, Musallam L, Haddad PS (2013) *Populus balsamifera* extract and its active component salicortin reduce obesity and attenuate insulin resistance in a diet-induced obese Mouse model. Evid Based Complement Alternat Med 2013:172537.

Knuth S, Abdelsalam RM, Khayyal MT, Schweda F, Heilmann J, Kees MG, Mair G, Kees F, Jürgenliemk G (2013) Catechol conjugates are *in vivo* metabolites of *Salicis cortex*. Planta Med 79(16): 1489-1494.

Knuth S, Schübel H, Hellemann M, Jürgenliemk G (2011) Catechol, a bioactive degradation product of salicortin, reduces TNF-α induced ICAM-1 expression in human endothelial cells. Planta Med 77(10): 1024-1026.

Kwon D-J, Bae Y-S, Ju SM, Youn GS, Choi SY, Park J (2014) Salicortin suppresses lipopolysaccharide-stimulated inflammatory responses via blockade of NF-κB and JNK activation in RAW 264.7 macrophages. BMB Rep 47(6): 318-323.

Lee HJ, Kim JS, Kim YK, Ryu JH (2013*a*) Phenolic glycosides as inhibitors of inducible nitric oxide synthase from *Populus davidiana* in LPS-activated RAW 264.7 murine macrophages. Molecules 18(9):10484-10496.

Lee M, Lee SH, Kang J, Yang H, Jeong EJ, Kim HP, Kim YC, Sung SH (2013*b*) Salicortin-derivatives from *Salix pseudolasiogyne* twigs inhibit adipogenesis in 3T3-L1 cells via modulation of C/EBPα and SREBP1c dependent pathway. Molecules 18(9):10484-96.

Lee MA, Lee SH, Yang HJ, Park JH (2013*c*) *Salix pseudolasiogyne* extracts for preventing and treating obesity. Patent, S. Korea, Patent # KR 2013059724. Elcom Science Co., Ltd., S. Korea.

Si CL, Kim JK, Bae YS, Li SM (2009) Phenolic compounds in the leaves of *Populus ussuriensis* and their antioxidant activities. Planta Med 75(10): 1165-1167.

Subramanian B, Nakeff A, Tenney K, Crews P, Gunatilaka L, Valeriote F (2006) A new paradigm for the development of anticancer agents from natural products. J Exp Ther Oncol 5(3): 195-204.

Yang H, Lee SH, Sung SH, Kim J, Kim YC (2013) Neuroprotective compounds from *Salix pseudo-lasiogyne* twigs and their anti-amnesic effects on scopolamine-induced memory deficit in mice. Planta Med 79(1): 78-82.

Appendix III. Additional information for qPCR.

A3.1 qPCR amplicon nucleotide sequence information.

Figure A2.1.1 (below) qPCR amplicon nucleotide sequence information for *PtACT47*, *PtACT49*, and *PtACT54*.

Color coding, Primer Sequences Amplified region 3'UTR CODING SEQUENCE

PtACT47 (Potri.013G074500)

ATGGCTTCATCACCCGCTTCTCTGGTTTTCAAAGTTCACAGACGTGAGCCCGA
GCTGATCAAACCAGCGAAGCCCACCCCACATGAGTTCAAACTGTTATCTGAC
ATTGATGACCAAGAAGGGCTTCGATTCCACATTCCAGTCATACAATTCTATCG
CCACAATCCCTCAGTGCAAGGGAAAGACCCCGTCAAGGTCATCAGAGAGGC
AATTGCTAAAACGTTGGTGTTTTACTATCCATTTGCCGGTAGGCTGAGGGAAG
GGCAAAACCGCAAGCTCATGGTGGAATGCACTGGCGAGGGTATCTTGTTTAT
AGAGGCTGACGCTGATGTTACACTTGAGCAGTTTGGTGATGCACTTCAACCTC
CATTTCCTTGCCTGGAGGAGCTCATCTTTGATGTCCCTGGCTCTAGCGGGGTT
CTAAACTGCCCTCTGTTACTTATTCAGGTGACACGCCTCAAGTGTGGTGGTTT
TATCTTTGGCCTTCGCCTCAATCATACCATGAGTGATGCCTCCGGCATAGTCC
AATTCATGGCAGCGGTTGGTGAGATGGCACGCGGAGCCACTACCCCCTCCGT
CCCAGCTGTGTGGGAAAGGCATGTTCTGAATGCAAGAAACCCACCACGGGTT
ACATGCATACACCGTGAGTACGAGGAGGTAGCTGACACCAACGGTACAATTA
TTCCACTTGATGATATGGCTCATCGTTCCTTTTTCTTTGGCCCTTCAGAGATAT
CTGCTCTTCGAAAATTGATCCCGCCTCACCTTAGCCGTTGTTCCACTTTCGAA
ATATTAACAGCATGTCTTTGGAAATGTCGTACCATTGCCCTCCAACCAGATCC
TACTGAAGAGATGCGCATAATATGCATTGTCAATGCTCGTGAGAAATTTAAC
CCTCCATTACCAACTGGATACTACGGTAATGGCTTTGCTTTTCCGGTAGCAGT
GGCAACTGCCGGGGAACTCTCGGAGAAGCCATTTGGATATGCCTTGGAATTG
GTAAGAAAGGCCAAGGCTGACGTGACTGAGGAATATATGCGATCGGTAGCAT
CTTTGATGGTAACTAAGGGGAGGCCTCATTTTACAGTGGTAAGGGCATACCTT
GTATCGGACTTAAGAAGTGCAGGATTCGAAGTGGTAGATTTCGGTTGGGGTA
ATGCTATATACGGCGGGGCTGCCAAAGGTGGAGTTGGGGCAATCCCTGGAGT
TGCAAGCTTTTTAATTCCATTTAAAAACAAGAAAGGAGAAAATGGGATTGTG
GTGCCGTTTTGCTTGCCAGCTCCTGCCATGGAAAGATTTGTCGAGGAGCTTGA
CGGTATGTTGAAGGGCCAGCTACAAAGTGGGCAAACTCATTCCAAATTTATC
GCGTCTTCCTTATAA

PtACT49 (Potri.019G043600)

ATGGCATCATCACCCGCCTCTCTGTTGTTCAAAGTTCACAGACGTGAACCAGA
ACTGATCAAGCCTGCCAAGCCCACCCCACATGAGTTCAAGCTCTTATCTGAC
ATCGATGACCAAGAAGGTCTTCGATTCCACATTCCAGTCATGCAATTTTATCG
CAACAATCCCTCTATGCAAGGGAAAGACCCCGTCAAAATCATTAGGGAGGCA
CTCGCCAAGACATTAGTGTTTTACTATCCATTTGCCGGTAGACTCAGGGAAGG
GCCTAACCGCAAGCTCATGGTGGAATGTACCGGTGAGGGTATCTTGTTCATA
GAAGCTGATGCCGATGTTACACTTGAGCAATTCGGTGATGCGCTTCAACCAC
CTTTCCCCTGCTTGGAGGAGCTCCTCTTTGATGTCCCTGGCTCTAGTGGGGTG
TTGAACTGCCCTTTGTTGCTTATTCAGGTGACGCGCCTCAAGTGTGGTGGTTT
TCTGTTTGCCCTCCGCCTGAACCATACCATGAGTGATGCCGTAGGCCTAGTCC
AATTCATGGCAGCAGTGGGTGAGATGGCACGGGGAGCCAATGCGCCCTCCGT
CCCAGCTGTGTGGGAAAGACAAGTTCTCAATGCTAGTGACCCTCCACGAGTT
ACATGCACACACCGTGAGTACGAGGAGGTAGCTGACACCAAGGGTACCATTA
TTCCACTTGATGATATGGCTCATCGTTCCTTCTTCTTTGGCCCTTCAGAAATGT
CTGCTCTTCGAAAATTTGTCCCGCCTCACCTTAGCCATTGTTCTACTTTCGAAA
TTCTAACAGCATGTCTTTGGAAATGTCGTACCATTGCCCTCCAACCAGATCCT
ACCGAGGAGATGCGCATACTATGCATTGTCAATGCTCGTGAGAAATTTAACC
CTCCATTGCCAAGAGGATACTATGGTAATGGCTTTGCTTTTCCGGTAGCAGTG
GCAACTGCAGAAGAACTCTCAAAAAATCCATTTGGATACGCCTTGGAATTGG
TGAGAAAGGCTAAGGCTGACGTGACTGAGGAATACATGCGATCAGTATCATC
TTTGATGGTGATTAAGGGGAGGCCTCACTTTACAGTGGTAAGGGCATACCTA
GTATCGGACCTGAGACGTGCAGGATTCGAAGAGGTAGATTTTGGATGGGGTA
ATGCTATATATGGTGGCGCTGCCAAAGGTGGGGTTGGCGCCATCCCTGGAGT
TGCAAGCTTTTATATCCCATTTACAAACAAGAAAGGAGAAAATGGGGTTGTG
GTCCCATTTTGCTTGCCGGCTCCTGCCATGGAAAGATTTGTCAAGGAGCTTGA
CGGCATGTTGAAGGACGACCAGACAGTTAGCGCGCAAACTAAGTCCAAATTT
ATTGTATCTTCCCTATAA

PtACT54 (Potri.001G448000.1)

ATGCCAACTCCTACTTCCTTAGCATTCAATGTGCGAAGGTGCGAGCCAGAATT
GGTTGCACCAGCTAAAGCCACACCCCATGAATCCAAACCACTTTCTGATATC
GATCGCCAACTATACCTACAATTTCAATCACCACATTACAACTTTTATGCACA
CAACCCGTCCATGCAAGGGAAAGATCCTGTGAAGGTAATAAGAGAGGGAAT
TGCTCAGGCACTTGTGTATTATTATCCTTATGCCGGGAGGATTAGACAAGAGC
CAGAAAATAAGCTTGTAGTAGATTGTACAGGAGAGGGTGTCTTGTTCATTGA
AGCTGATGCTGATGGCACACTGGAGCAGTTTGGTGATCCAATTCAGCCTCCGT
TCCCTTGTGCTGAGGAACTTCTTTACAATGTCCCAGGGTCAGCAGGAATCATC
AATACCCCGTTGCTGATCATTCAGATAACACGCTTGAAGTGTGGTGGTTTTAT
ACTTGGCTTCCGTCTTAATCACCCAATGAGTGATGCCATTGGCCTAGTTCAGC
TATTGAGTGCCATAGGTGAGATCTCACGAGGTGCTCAAGCCCCTTCAATTCTA
CCTGTGTGGCAAAGAGAACTCCTTTGTGCTAGGAATCCACCTCGTGTTACTTG
CACACACAACGAATATGGCGATCATCATGATCTTGTTGTGGATCCTAGCGAG
CTCAACGTTCCTGAATTTCGGGGTAGCACTGACGGTGCAGCCCACCGTTGTTT
CATCATCGGCCCTAAAGAATTATCCAACATTCGTAAATGGATTCCTCCTCATT
TACACCCATGTTCCAAGTTTGAAATAATAACCGCATGCTTATGGAGATGCCAT
GCCATAGCATCTCAAGCAAACCCTAATGAGGAGATGCGCATTTGTATGCTCG
TCAATGCACGTTCCAAATTCAACCCTCCGTTACCAAAGGGTTATTATGGTAAC
GTGCTGGCATTGCCAGCAGCTATAACCAGTGCTAGGAAGCTTTGTTTGAACTC
ATTAGGGTATGCTCTGGAGCTGATAAGGCAAGCCAAGAACAAGATCACTGAG
GAGTACATAAGATCGTTGGCCGATTTCATTGAGATTACCAAGGGCCTGCCTA
AGGGGTTACAGTCATATGTTGTGTCAGATTTAACAAGTGTTGGGTTCGATCAG
GTGGATTATGGTTGGGGTAAGCCAGTTTATACCGGGCCATCTAAGGCTATGC
CTGATGACATTAATAATTCTGGAACCTATTACTTACCCTATAGAAACAAGAA
AGGAGAGCGTGGAGTCATGGTTCTGATCTCCTTGCGTGCACCAGTTATGGCA
AGATTTGCAATGCTATTCGAGGAGTTGACCAAGCACGATCCAGATAGTGGTC
CAGCACAACACCACACTACTCTCCCTATAAGACACAGGCTTTGATATATTTTT
TTATTCCCACTTGAGATTGTCTCCATATTGAGCTTTGAAGTGGACATCCGTGG
TTTGAACTTTCAGCAGGTCGTGCAACAAGATTGGATTAGCATCTGCTTTCTTT
AAGAAATTGTGGTTAAATAAATACTGACAAGTCTTATCCCTTCCTTATCCCTT
TCTGGTGTTAGATATATGGTTGATCGAAGAGGGATTACTTGTCATGAAAGTA
AGTCAACAGAGTGAATGTGTCTTCTGTAGGGTTTCCAATTGCTTATAAATTAC
ATGTATAAAGTCTTATCAGTGTTCTATAATTTTCTTTAAATTTGTTATCATGGT
ATCATCATCTTCGTTGTTTCTTCCCATCAATTGTTTTTTAATTGGGGTCAATAA
TGGTTGTTTCTTTCTTTCTTTCTTTCTTTTTTCTCC

A3.2. qPCR amplification efficiency curves.

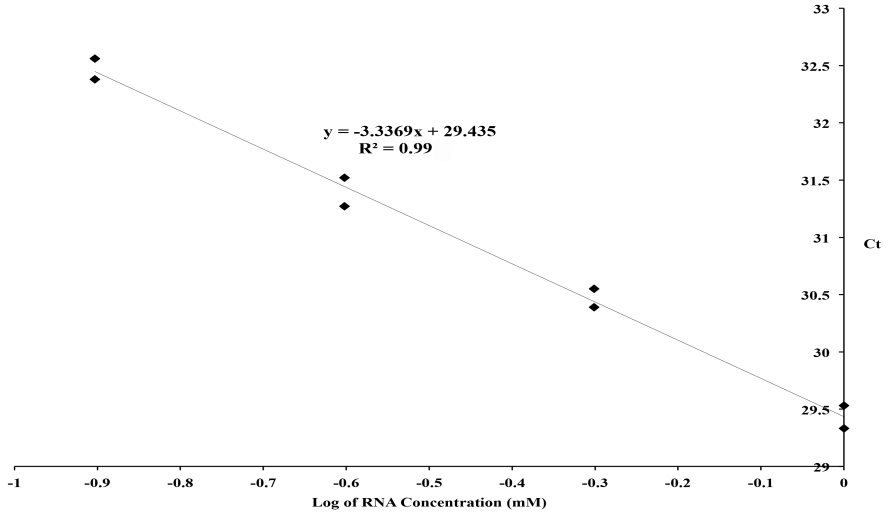

Figure A3.2.1 qPCR primers amplification efficiency curve for *PtACT47* at 60°C. An equation gradient of -3.3369 indicates 99.4% amplification efficiency.

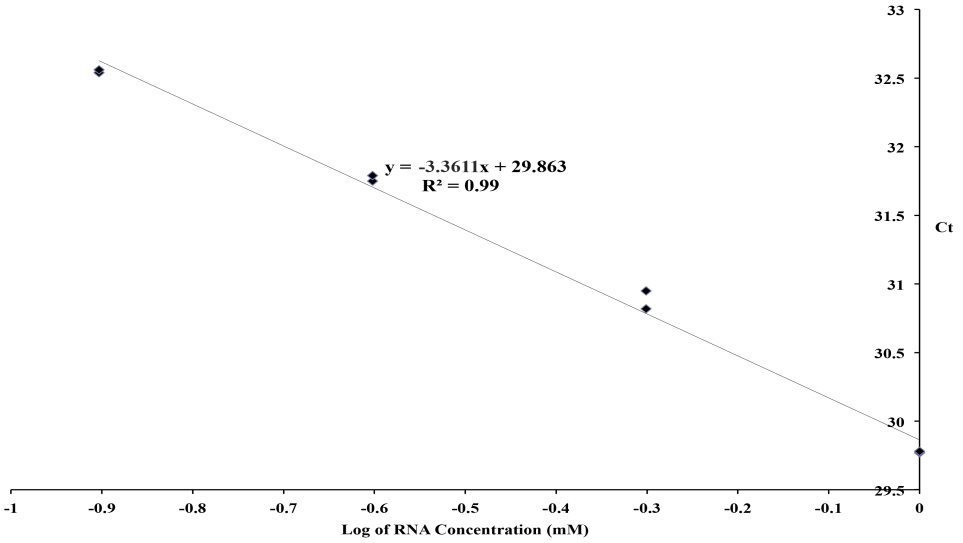

Figure A3.2.2 qPCR primers amplification efficiency curve for *PtACT49* at 59°C. An equation gradient of -3.3611 indicates 98.4% amplification efficiency.

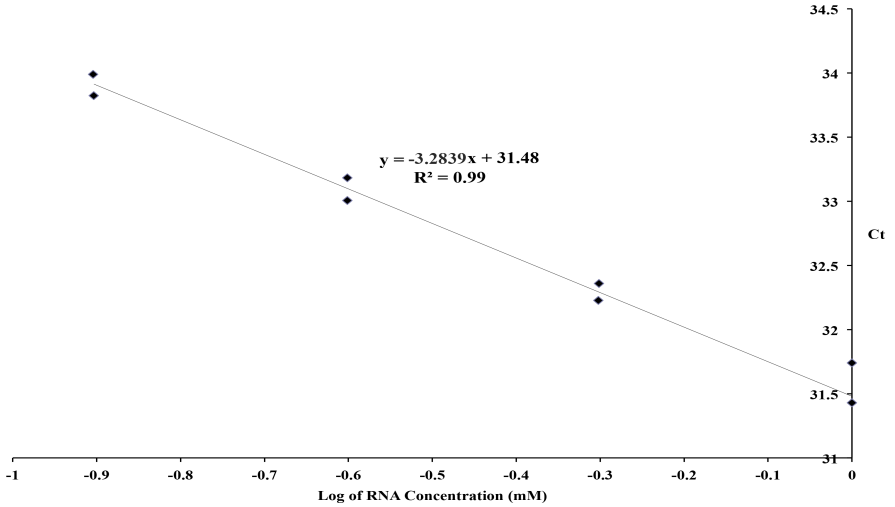

Figure A3.2.3 qPCR primers amplification efficiency curve for *PtACT54* at 60^{o}C. An equation gradient of -3.2839 indicates 101.6% amplification efficiency.

A3.3 Consolidation reports (thermal profiles, amplification plots, and dissociation curves) for qPCR of *PtACT47*, *PtACT49* and *PtACT54* (below).

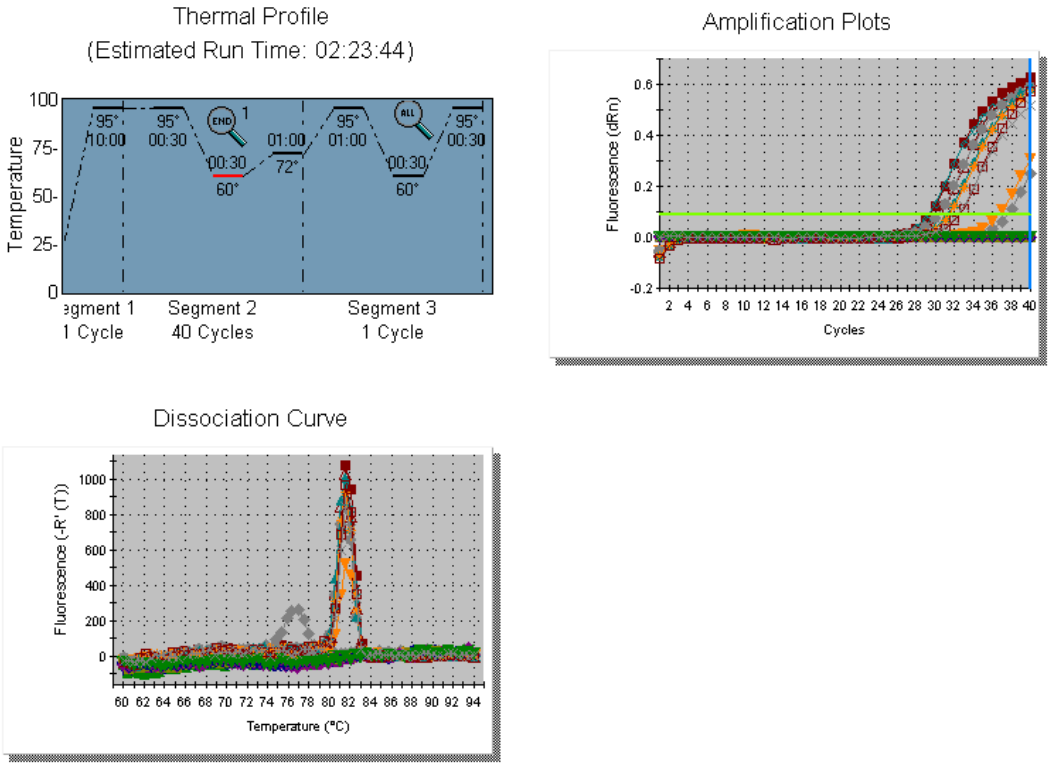

Figure A3.3.1 Consolidation report for qPCR amplification of *PtACT47*.

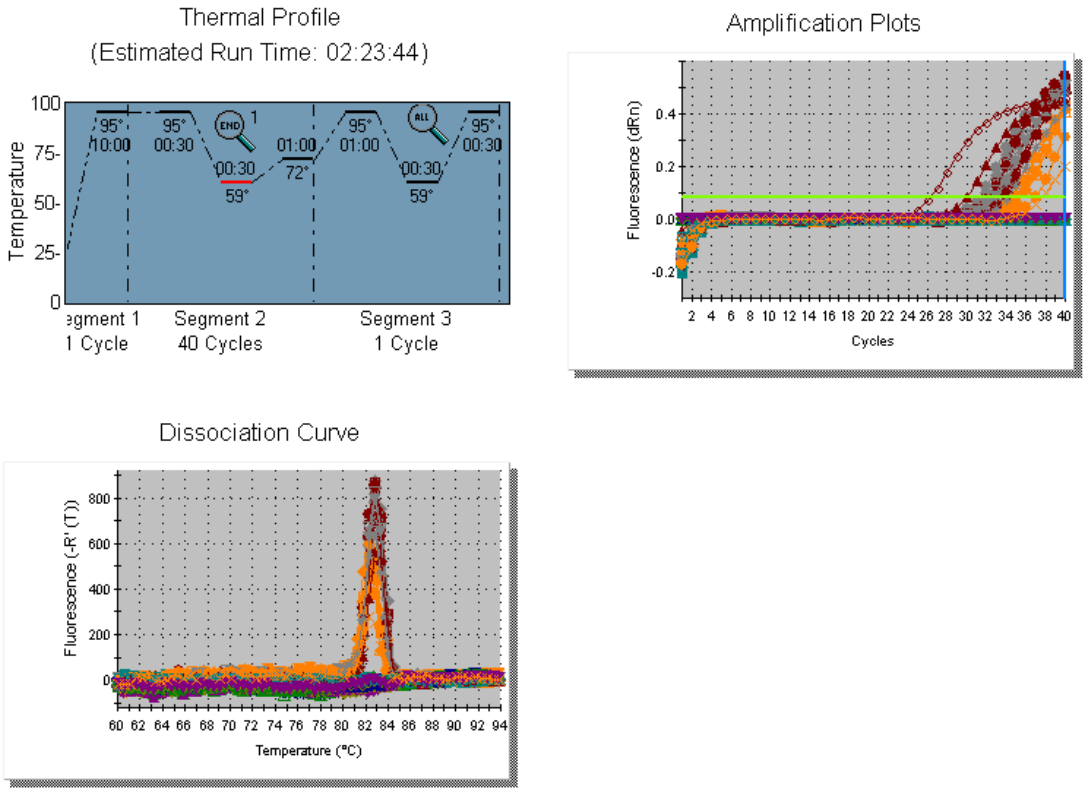

Figure A3.3.2 Consolidation report for qPCR amplification of *PtACT49*.

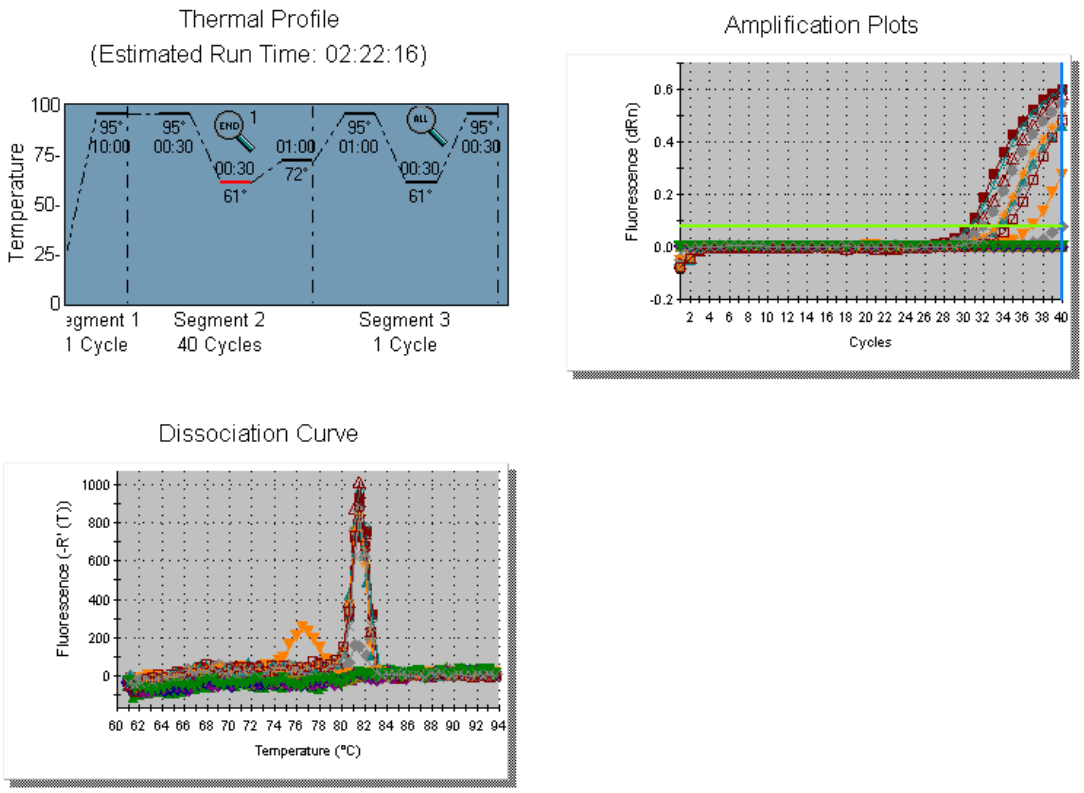

Figure A3.3.2 Consolidation report for qPCR amplification of *PtACT54*.

Appendix IV. Additional information for cloning and heterologous overexpression of recombinant proteins.

A4.1. The *lac* operon

Vectors such as pGEM®-T Easy and recombinant protein expression vectors utilize the *lac* operon present in *Escherichia coli* (Davies and Jacob, 1968). It regulates transport and metabolism of lactose and consists of the *lacUV5* promoter, the *lac* operator, and three adjacent structural genes, *lacZ* encoding *β*-galactosidase, a cytosolic enzyme that cleaves the disaccharide lactose into D-glucose and D-galactose; *lacY* encoding *β*-galactoside permease (lactose permease), a membrane-bound transport protein that pumps lactose into the cell (Grossman, *et al*., 1998); *lacA* encoding thiogalactoside transacetylase (galactoside *O*-acetyltransferase) responsible for the transfer of an acetyl group from acetyl-CoA to *β*-galactosides; and the *lac* terminator. A fourth structural gene, *lacI*, is spatially separated on the bacteria's plasmid genome and encodes the lactose repressor molecule which can bind to the *lac* operator sequence and prevent expression of the *lacZ*, *lacY*, *lacA*, under specific conditions (Figure A1.1)

When lactose is the predominant carbohydrate in the cell's environment, a lactose metabolite called allolactose, a combination of glucose and galactose, binds to the lac repressor, causing a change in its shape rendering it unable to bind to the lac operator. RNA polymerase then binds to *lacUV5* promoter immediately upstream of the structural genes. Binding of RNA polymerase is aided by the cAMP-bound catabolite activator protein (CAP, also known as the cAMP receptor protein). The three adjacent structural genes are then co-transcribed into a single polycistronic mRNA molecule, the *lacZYA* mRNA, and then translated into enzymatically active proteins. *β*-galactoside permease transports lactose into the cell which is then cleaved into D-glucose and D-galactose by *β*-galactosidase and utilized as an energy source for the cell. This system can be exploited for controlled expression of recombinant proteins by the insertion of addition gene coding sequences into the *lac* operon. Expression can be triggered by the addition of IPTG (isopropyl *β*-D-1-thiogalactopyranoside), a structural analog of allolactose, which binds to the lac repressor, altering its shape and preventing from binding to the lac operator sequence, thus allowing RNA polymerase to bind to the *lacUV5* promoter.

A) Repression of the *lac* operon

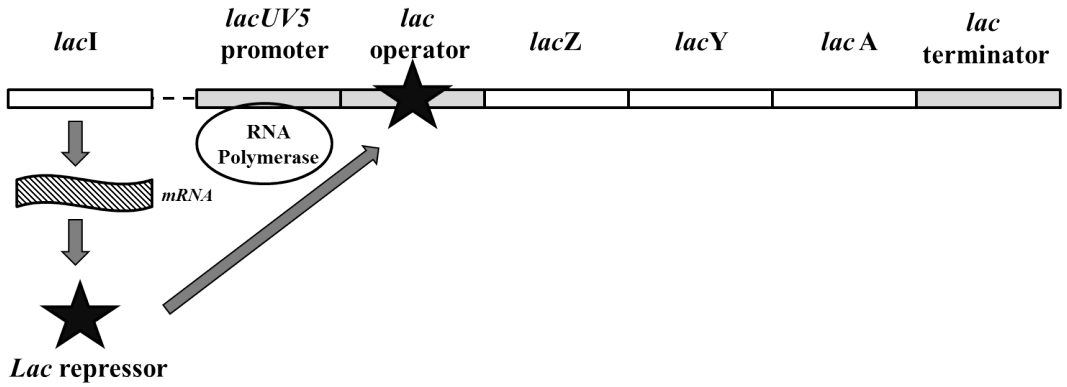

B) Expression of the *lac* operon

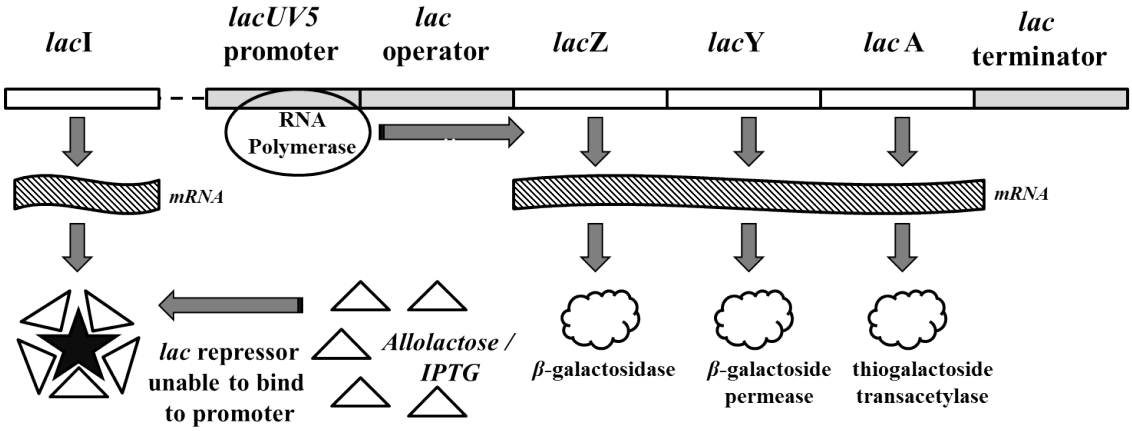

Figure A4.1.1 The *lac* operon.
A) Repression of the *lac* operon. The lactose repressor molecule is encoded by *lac*I binds to the *lac* operator sequence and prevents RNA polymerase from binding and preventing the expression of the *lacZ*, *lacY*, and *lacA*. **B**) Expression of the *lac* operon. The presence of allolactose or IPTG molecules bind to the *lac* repressor causing it to change shape and rendering it unable to bind to the *lac* operator. RNA polymerase is free to bind to the *lac*UV5 promoter and transcription of the *lacZ*, *lacY*, and *lacA*.

When lactose is absent in the cell's environment, allolactose is also absent and thus unable to bind to- and alter the shape of the *lac* repressor, thus the lac repressor binds tightly to the *lac* operator and prevent RNA polymerase from binding to the *lacUV5* promoter, preventing the transcription of *lacZYA*. An additional level of control occurs when glucose is present. In this case, a mechanism known as 'carbon catabolite repression' is initiated. In this case, a form of Enzyme II A (EIIA) specifically responsible for glucose transport and part of the phosphotransferase system, exists in its unphosphorylated form which leads to repression of *lacY* and production of *β*-galactoside permease, thought to be the only means of lactose uptake in wild type cells (Inada, *et al*., 1996; Kimata, *et al*., 1997; Meadow, *et al*., 1990; Postma, *et al*., 1996; Saier, *et al*., 1996). This dual control mechanism causes the sequential utilization of glucose and lactose in two distinct growth phases, known as 'diauxie'.

A4.2. Blue/white screening using XLI-Blue *E. coli* cells

The pGEM®-T Easy vector can be used in conjunction with XLI-Blue *E. coli* electro-competent cells to facilitate blue/white screening of successfully transformed bacterial colonies. Under normal conditions the *lacZ* gene in the *lac* operon hydrolyses lactose into $_{D}$-glucose, $_{D}$-galactose and H_2O**,** however, it can also utilize the chromogenic substrate X-gal (5-bromo-4-chloro-indolyl-*β*-$_{D}$-galactopyranoside) (Horwitz, *et al.,* 1964), an analog of lactose, to produce 5,5'-dibromo-4,4'-dichloro-indigo, an intensely blue product which is insoluble (Figure A1.2). The pGEM®-T Easy vector carries a short segment of *E. coli* DNA containing the regulatory sequences and the coding information for the first 146 amino acids of the *β*-galactosidase gene. The host *E. coli* strain XL1-Blue expresses the carboxyl-terminal portion of *β*-galactosidase. Neither the host or the vector fragments of *β*-galactosidase are themselves active, however, they can associate to form an enzymatically active protein, this is called α-complementation (Ullmann, *et al*., 1967). The resulting *lac*$^{+}$ bacteria form blue colonies in the presence of chromogenic X-gal (Horwitz *et al*., 1964; Davies and Jacob, 1968). Insertion of a fragment of foreign DNA into the poly-cloning site of pGEM®-T Easy most commonly results in the production of an amino-terminal fragment of *β*-galactosidase that is no longer capable of α-complementation, as a result the colonies are white.

A)

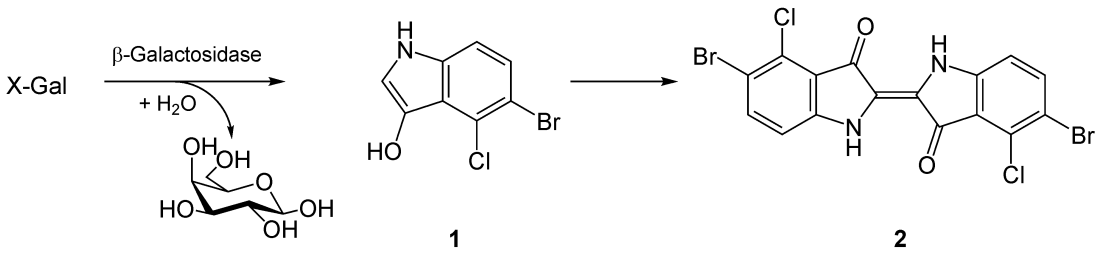

B)

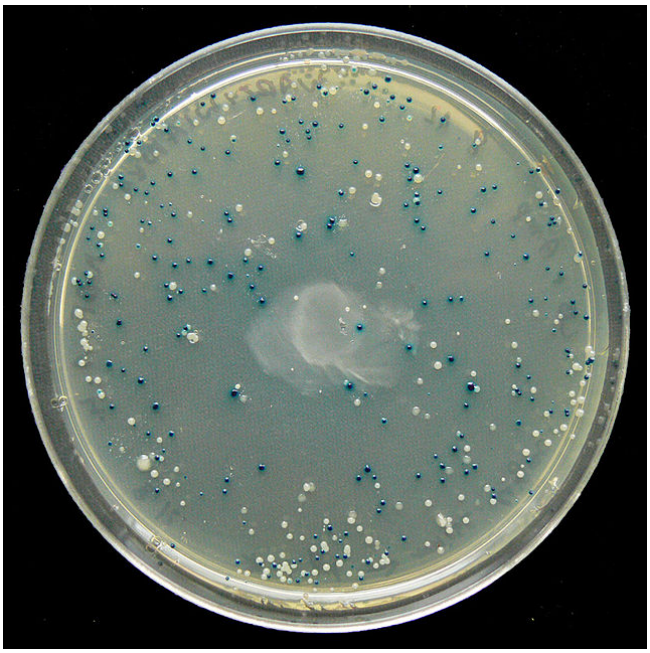

Figure A4.2.1 Synthesis of 5,5'-dibromo-4,4'-dichloro-indigo for blue/white screening.

A) X-gal is an hydrolyzed β-galactosidase enzyme by cleavage of the *β*-glycosidic bond in D-lactose yielding galactose and (**1**) 5-bromo-4-chloro-3-hydroxyindole. This spontaneously dimerizes and is oxidized into (**2**) 5,5'-dibromo-4,4'-dichloro-indigo, an intensely blue product which is insoluble. **B**) an example of blue and white XLI-Blue *E. coli* cells on an LB plate with 100 μg ml^{-1} carbenicillin.

A4.3. References

Davies J, Jacob F (1968) Genetic mapping of the regulator and operator genes of the *lac* operon. J Mol Biol 36(3): 413-417.

Horwitz JP, Chua J, Curby RJ, Tomson AJ, Da Rooge MA, Fisher BE, Mauricio J, Klundt I (1964) Substrates for cytochemical demonstration of enzyme activity. I. Substituted 3-indolyl β-$_D$-glycopyranosides. J Med Chem 7(4): 574-575.

Inada T, Kimata K, Aiba H (1996) Mechanism responsible for glucose-lactose diauxie in *Escherichia coli*: Challenge to the cAMP model. Genes Cells 1: 293-301.

Kimata K, Takahashi H, Inada T, Postma P, Aiba H (1997) cAMP receptor protein-cAMP plays a crucial role in glucose-lactose diauxie by activating the major glucose transporter gene in Escherichia coli. Proc Natl Acad Sci USA 94: 12914-12919.

Meadow ND, Fox DK, Roseman S (1990) The bacterial phosphoenolpyruvate: Glycose phosphotransferase system. Annu Rev Biochem 59: 497–542.

Postma PW, Lengeler JW, Jacobson GR (1996) Phosphoenolpyruvate: carbohydrate phosphotransferase systems. In: Neidhardt FC, Curtiss III R, Ingraham JL, Lin ECC, Low KB, Magasanik B, Reznikoff WS, Riley M, Schaechter M, Umbarger HE (Eds.), *Escherichia coli* and *Salmonella*: cellular and molecular biology, 2nd ed., American Society for Microbiology, Washington, DC, USA: 1149–1174.

Saier Jr. MH, Ramseier TM, Reizer J (1996) Regulation of carbon utilization. In: Neidhardt FC (Ed.). *Escherichia coli* and *Salmonella typhimurium*: cellular and molecular biology, 2nd ed., American Society of Microbiology, Washington, DC, USA: 1325-1343.

A4.4. Recombinant protein sequence information.

Figure A4.4.1 (Below) The translated amino acid sequences of recombinant proteins, their theoretical isoelectric points (pI) and molecular weights (kDa).

Color coding, HXXXD active site, DFGWG structural site, 6 x His N-terminus tag, Amino acids not usually present in wild type protein.

Recombinant PtACT47 (PtSABT) overexpressed using vector pQE-30.

Theoretical pI, 7.7.

Molecular weight (kDa), 51.9.

MRGSHHHHHHGSMASSPASLVFKVHRREPELIKPAKPTPHEFKLLSDIDDQEGLR
FHIPVIQFYRHNPSVQGKDPVKVIREAIAKTLVFYYPFAGRLREGQNRKLMVECT
GEGILFIEADADVTLEQFGDALQPPFPCLEELIFDVPGSSGVLNCPLLLIQVTRLKC
GGFIFGLRLNHTMSDASGIVQFMAAVGEMARGATTPSVPAVWERHVLNARNPP
RVTCIHREYEEVADTNGTIIPLDDMAHRSFFFGPSEISALRKLIPPHLSRCSTFEILT
ACLWKCRTIALQPDPTEEMRIICIVNAREKFNPPLPTGYYGNGFAFPVAVATAGE
LSEKPFGYALELVRKAKADVTEEYMRSVASLMVTKGRPHFTVVRAYLVSDLRS
AGFEVVDFGWGNAIYGGAAKGGVGAIPGVASFLIPFKNKKGENGIVVPFCLPAP
AMERFVEELDGMLKGQLQSGQTHSKFIASSL

Recombinant PtACT49 (PtBEBT) overexpressed using vector pQE-31.

Theoretical pI, 7.2.

Molecular weight (kDa), 52.6.

MRGSHHHHHHTDPTIMASSPASLLFKVHRREPELIKPAKPTPHEFKLLSDIDDQEG
LRFHIPVMQFYRNNPSMQGKDPVKIIREALAKTLVFYYPFAGRLREGPNRKLMV
ECTGEGILFIEADADVTLEQFGDALQPPFPCLEELLFDVPGSSGVLNCPLLLIQVTR
LKCGGFLFALRLNHTMSDAVGLVQFMAAVGEMARGANAPSVPAVWERQVLNA
SDPPRVTCTHREYEEVADTKGTIIPLDDMAHRSFFFGPSEMSALRKFVPPHLSHCS
TFEILTACLWKCRTIALQPDPTEEMRILCIVNAREKFNPPLPRGYYGNGFAFPVAV
ATAGELSKNPFGYALELVRKAKADVTEEYMRSVSSLMVIKGRPHFTVVRAYLVS

DLRRAGFEEVDFGWGNAIYGGAAKGGVGAIPGVASFYIPFTNKKGENGVVVPFC
LPAPAMERFVKELDGMLKDDQTVSSQTKSKFIVSSL

Recombinant PtACT49 (PtBEBT)-H166A overexpressed using vector pQE-30.

Theoretical pI, 7.6.

Molecular weight (kDa), 52.2.

MRGSHHHHHHGSMASSPASLLFKVHRREPELIKPAKPTPHEFKLLSDIDDQEGLR
FHIPVMQFYRNNPSMQGKDPVKIIREALAKTLVFYYPFAGRLREGPNRKLMVEC
TGEGILFIEADADVTLEQFGDALQPPFPCLEELLFDVPGSSGVLNCPLLLIQVTRLK
CGGFLFALRLNATMSDAVGLVQFMAAVGEMARGANAPSVPAVWERQVLNASD
PPRVTCTHREYEEVADTKGTIIPLDDMAHRSFFFGPSEMSALRKFVPPHLSHCSTF
EILTACLWKCRTIALQPDPTEEMRILCIVNAREKFNPPLPRGYYGNGFAFPVAVAT
AGELSKNPFGYALELVRKAKADVTEEYMRSVSSLMVIKGRPHFTVVRAYLVSDL
RRAGFEEVDFGWGNAIYGGAAKGGVGAIPGVASFYIPFTNKKGENGVVVPFCLP
APAMERFVKELDGMLKDDQTVSSQTKSKFIVSSL

Recombinant PtACT54 overexpressed using vector pQE-30.

Theoretical pI, 8.0.

Molecular weight (kDa), 53.6.

MRGSHHHHHHGSMPTPTSLAFNVRRCEPELVAPAKATPHESKPLSDIDRQLYLQ
FQSPHYNFYAHNPSMQGKDPVKVIREGIAQALVYYYPYAGRIRQEPENKLVVDC
TGEGVLFIEADADGTLEQFGDPIQPPFPCAEELLYNVPGSAGIINTPLLIIQITRLKC
GGFILGFRLNHPMSDAIGLVQLLSAIGEISRGAQAPSILPVWQRELLCARNPPRVT
CTHNEYGDHHDLVVDPSELNVPEFRGSTDGAAHRCFIIGPKELSNIRKWIPPHLHP
CSKFEIITACLWRCHAIASQANPNEEMRICMLVNARSKFNPPLPKGYYGNVLALP
AAITSARKLCLNSLGYALELIRQAKNKITEEYIRSLADFIEITKGLPKGLQSYVVSD
LTSVGFDQVDYGWGKPVYTGPSKAMPDDINNSGTYYLPYRNKKGERGVMVLIS
LRAPVMARFAMLFEELTKHDPDSGPAQHHTTLPIRHRL

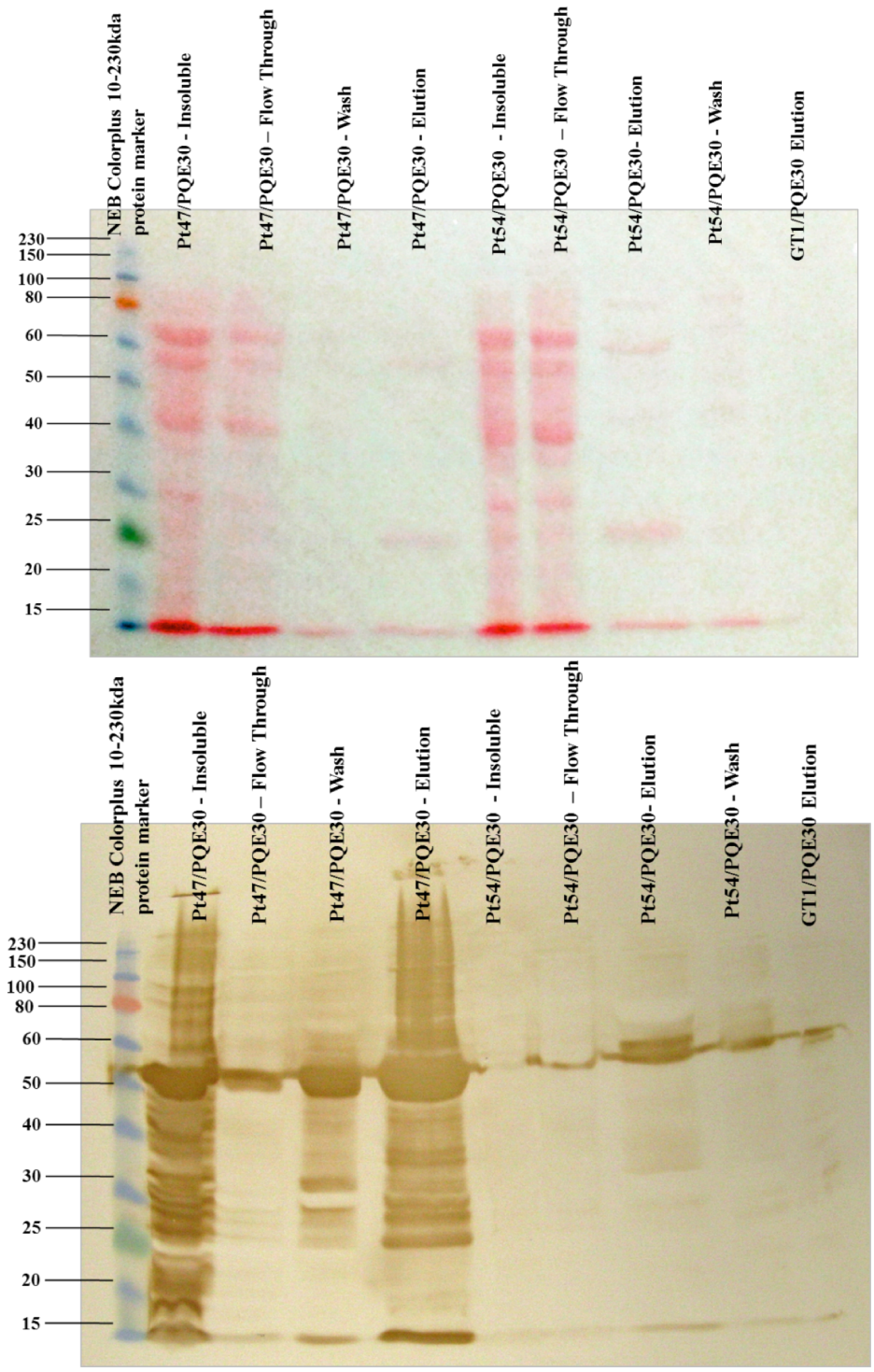

Figure A4.4.2. The original ponceau S staining and immunoblot gel showing expressed and purified recombinant PtACT54 from which Figure 3.6 was made.

Appendix V. Amino acid sequence comparison of BAHDs of clade V-*i*.

A5.1.1. Sequence identity analysis.

Amino acid sequence identity matrix for subclade V-*i*

Seq->	PtACT47	PtACT49	CmAAT3	CbBEBT	VhBEBT	BPBT	NtBEBT	AMAT	AcAT16	AdAT9	MpAAT1	HMT	CHAT	PtACT54	CmAAT1	CmAAT2
PtACT47	ID	0.906	0.766	0.688	0.703	0.731	0.733	0.556	0.548	0.546	0.521	0.535	0.538	0.523	0.516	0.53
PtACT49	0.906	ID	0.764	0.666	0.716	0.75	0.746	0.557	0.55	0.546	0.532	0.545	0.533	0.525	0.516	0.525
CmAAT3	0.766	0.764	ID	0.684	0.705	0.768	0.762	0.559	0.539	0.541	0.521	0.524	0.521	0.518	0.573	0.588
CbBEBT	0.688	0.666	0.684	ID	0.642	0.684	0.667	0.545	0.506	0.5	0.525	0.515	0.51	0.507	0.51	0.508
VhBEBT	0.703	0.716	0.705	0.642	ID	0.73	0.73	0.555	0.548	0.535	0.518	0.527	0.515	0.504	0.485	0.501
BPBT	0.731	0.75	0.768	0.684	0.73	ID	0.906	0.587	0.551	0.545	0.544	0.538	0.526	0.522	0.517	0.54
NtBEBT	0.733	0.746	0.762	0.667	0.73	0.906	ID	0.568	0.549	0.545	0.542	0.531	0.522	0.509	0.523	0.549
AMAT	0.556	0.557	0.559	0.545	0.555	0.587	0.568	ID	0.586	0.584	0.55	0.489	0.484	0.454	0.469	0.47
AcAT16	0.548	0.55	0.539	0.506	0.548	0.551	0.549	0.586	ID	0.903	0.549	0.461	0.449	0.447	0.431	0.437
AdAT9	0.546	0.546	0.541	0.5	0.535	0.545	0.545	0.584	0.903	ID	0.54	0.458	0.449	0.434	0.429	0.432
MpAAT1	0.521	0.532	0.521	0.525	0.518	0.544	0.542	0.55	0.549	0.54	ID	0.47	0.45	0.464	0.442	0.45
HMT	0.535	0.545	0.524	0.515	0.527	0.538	0.531	0.489	0.461	0.458	0.47	ID	0.455	0.486	0.453	0.447
CHAT	0.538	0.533	0.521	0.51	0.515	0.526	0.522	0.484	0.449	0.449	0.45	0.455	ID	0.418	0.425	0.417
PtACT54	0.523	0.525	0.518	0.507	0.504	0.522	0.509	0.454	0.447	0.434	0.464	0.486	0.418	ID	0.426	0.435
CmAAT1	0.516	0.516	0.573	0.51	0.485	0.517	0.523	0.469	0.431	0.429	0.442	0.453	0.425	0.426	ID	0.841
CmAAT2	0.53	0.525	0.588	0.508	0.501	0.54	0.549	0.47	0.437	0.432	0.45	0.447	0.417	0.435	0.841	ID

A5.1. Amino acid sequence analysis of BAHDs of clade V-*i*.

A5.1.2. Amino acid sequence alignment of BAHDs of clade V-*i*.

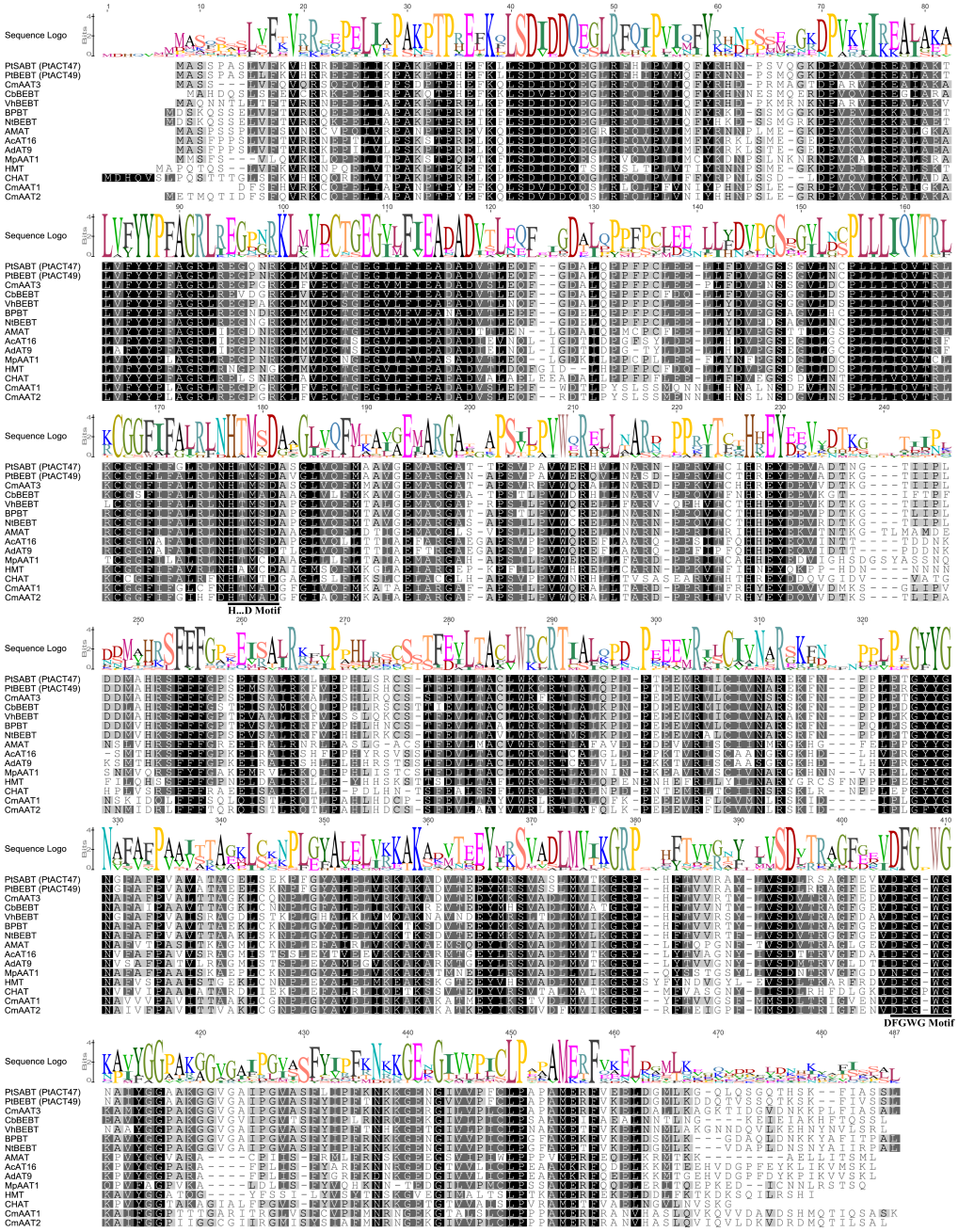

Figure A5.1.1 A comparison of the deduced amino acid sequences of BAHD members of clade V-*i*, plus *P. trichocarpa* genes PtACT47 and PtACT49. Legend, A 100% similar, A 80-100% similar, A 60-80% similar, A less than 60% similar. Alignment and sequence logo analysis were performed using Geneious® software, build 7.0.6 (Biomatters Ltd.; http://www.geneious.com).

A5.1.3. Amino acid sequence alignment of regions flanking the two BAHD motifs of BAHDs of clade V-*i*.

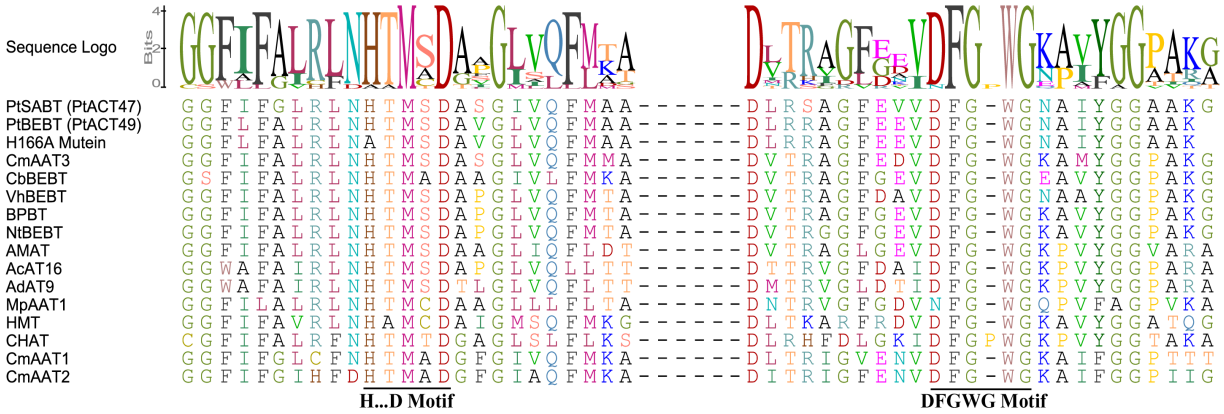

Figure A5.1.2. A comparison of the two BAHD conserved motifs H...D and DFGWG with ± ten flanking residues of clade V-*i*.

P. trichocarpa genes *PtSABT* (*PtACT47*) and *PtBEBT* (*PtACT49*) and the *PtBEBT* (*PtACT49*) H166A mutein sequences. Sequence alignment and sequence logo analysis were performed using Geneious® software, build 7.0.6 (Biomatters Ltd.; http://www.geneious.com).

Appendix VI. Statistical output tables.

A6.1. PG content of wild type versus MYB134 plants

Total PGs, Young leaves

t Test
WT-MYB

Difference	45.6000	t Ratio	8.213133
Std Err Dif	5.5521	DF	6
Upper CL Dif	59.1855	Prob > |t|	0.0002
Lower CL Dif	32.0145	Prob > t	<.0001
Confidence	0.95	Prob < t	0.9999

Analysis of Variance

Source	DF	Sum of Squares	Mean Square	F Ratio
Plant Type	1	4158.7200	4158.72	56.1555
Error	6	369.9076	61.65	
C. Total	7	4528.6276		

Total PGs, Medium leaves

t Test WT-MYB

Difference	45.2650	t Ratio	7.733197
Std Err Dif	5.8533	DF	6
Upper CL Dif	59.5876	Prob > |t|	0.0002
Lower CL Dif	30.9424	Prob > t	0.0001
Confidence	0.95	Prob < t	0.9999

Analysis of Variance

Source	DF	Sum of Squares	Mean Square	F Ratio
Plant Type	1	4097.8405	4097.84	35.0023
Error	6	411.1385	68.52	
C. Total	7	4508.9790		

Total PGs, Old Leaves

t Test WT-MYB

Difference	62.5000	t Ratio	52.93665
Std Err Dif	1.1807	DF	6
Upper CL Dif	65.3890	Prob > |t|	<.0001
Lower CL Dif	59.6110	Prob > t	<.0001
Confidence	0.95	Prob < t	1.0000

Analysis of Variance

Source	DF	Sum of Squares	Mean Square	F Ratio
Plant Type	1	7812.5000	7812.50	290.788
Error	6	16.7274	2.79	
C. Total	7	7829.2274		

Salicin, young leaves

t Test
WT-MYB

Difference	9.1900	t Ratio	6.244336
Std Err Dif	1.4717	DF	6
Upper CL Dif	12.7912	Prob > |t|	0.0008
Lower CL Dif	5.5888	Prob > t	0.0004
Confidence	0.95	Prob < t	0.9996

Analysis of Variance

Source	DF	Sum of Squares	Mean Square	F Ratio
Plant Type	1	168.91220	168.912	38.9917
Error	6	25.99200	4.332	
C. Total	7	194.90420		

Salicortin, young leaves

t Test WT-MYB

Difference	24.1800	t Ratio	13.18728
Std Err Dif	1.8336	DF	6
Upper CL Dif	28.6666	Prob > |t|	<.0001
Lower CL Dif	19.6934	Prob > t	<.0001
Confidence	0.95	Prob < t	1.0000

Analysis of Variance

Source	DF	Sum of Squares	Mean Square	F Ratio
Plant Type	1	1169.3448	1169.34	173.9044

Source	DF	Sum of Squares	Mean Square	F Ratio
Error	6	40.3444	6.72	
C. Total	7	1209.6892		

Tremuloidin, young leaves

t Test WT-MYB

Difference	2.61500	t Ratio	2.495148
Std Err Dif	1.04803	DF	6
Upper CL Dif	5.17945	Prob > |t|	0.0468
Lower CL Dif	0.05055	Prob > t	0.0234
Confidence	0.95	Prob < t	0.9766

Analysis of Variance

Source	DF	Sum of Squares	Mean Square	F Ratio
Plant Type	1	13.676450	13.6765	6.2258
Error	6	13.180500	2.1968	
C. Total	7	26.856950		

Tremulacin, young leaves

t Test WT-MYB

Difference	9.615	t Ratio	1.33603
Std Err Dif	7.197	DF	6
Upper CL Dif	27.225	Prob > |t|	0.2300
Lower CL Dif	-7.995	Prob > t	0.1150
Confidence	0.95	Prob < t	0.8850

Analysis of Variance

Source	DF	Sum of Squares	Mean Square	F Ratio
Plant Type	1	184.89645	184.896	1.7850
Error	6	621.50890	103.585	
C. Total	7	806.40535		

Salicin, medium leaves

t Test WT-MYB

Difference	14.2550	t Ratio	14.5699
Std Err Dif	0.9784	DF	6
Upper CL Dif	16.6490	Prob > |t|	<.0001
Lower CL Dif	11.8610	Prob > t	<.0001
Confidence	0.95	Prob < t	1.0000

Analysis of Variance

Source	DF	Sum of Squares	Mean Square	F Ratio
Plant Type	1	406.41005	406.410	212.2818
Error	6	11.48690	1.914	
C. Total	7	417.89695		

Salicortin, medium leaves

t Test WT-MYB

Difference	17.5450	t Ratio	6.806504
Std Err Dif	2.5777	DF	6
Upper CL Dif	23.8524	Prob > |t|	0.0005
Lower CL Dif	11.2376	Prob > t	0.0002
Confidence	0.95	Prob < t	0.9998

Analysis of Variance

Source	DF	Sum of Squares	Mean Square	F Ratio
Plant Type	1	615.65405	615.654	46.3285
Error	6	79.73330	13.289	
C. Total	7	695.38735		

Tremulacin, medium leaves

t Test WT-MYB

Difference	9.615	t Ratio	1.33603
Std Err Dif	7.197	DF	6
Upper CL Dif	27.225	Prob > |t|	0.2300
Lower CL Dif	-7.995	Prob > t	0.1150
Confidence	0.95	Prob < t	0.8850

Analysis of Variance

Source	DF	Sum of Squares	Mean Square	F Ratio
Plant Type	1	184.89645	184.896	6.2850
Error	6	621.50890	103.585	
C. Total	7	806.40535		

Tremuloidin, medium leaves

t Test WT-MYB

Difference	0.260000	t Ratio	5.003702
Std Err Dif	0.051962	DF	6
Upper CL Dif	0.387145	Prob > |t|	0.0024
Lower CL Dif	0.132855	Prob > t	0.0012
Confidence	0.95	Prob < t	0.9988

Analysis of Variance

Source	DF	Sum of Squares	Mean Square	F Ratio
Plant Type	1	0.13520000	0.135200	25.0370
Error	6	0.03240000	0.005400	
C. Total	7	0.16760000		

Salicin, old leaves

t Test WT-MYB

Difference	2.82500	t Ratio	2.983217
Std Err Dif	0.94696	DF	6
Upper CL Dif	5.14214	Prob > |t|	0.0245
Lower CL Dif	0.50786	Prob > t	0.0123
Confidence	0.95	Prob < t	0.9877

Analysis of Variance

Source	DF	Sum of Squares	Mean Square	F Ratio
Plant Type	1	15.961250	15.9612	8.8996
Error	6	10.760900	1.7935	
C. Total	7	26.722150		

Salicortin, old leaves

t Test WT-MYB

Difference	53.2300	t Ratio	27.418
Std Err Dif	1.9414	DF	6
Upper CL Dif	57.9805	Prob > |t|	<.0001
Lower CL Dif	48.4795	Prob > t	<.0001
Confidence	0.95	Prob < t	1.0000

Analysis of Variance

Source	DF	Sum of Squares	Mean Square	F Ratio
Plant Type	1	5666.8658	5666.87	751.7465
Error	6	45.2296	7.54	
C. Total	7	5712.0954		

Tremuloidin, old leaves

t Test WT-MYB

Difference	-0.03500	t Ratio	-0.50828
Std Err Dif	0.06886	DF	6
Upper CL Dif	0.13349	Prob > |t|	0.6294
Lower CL Dif	-0.20349	Prob > t	0.6853
Confidence	0.95	Prob < t	0.3147

Analysis of Variance

Source	DF	Sum of Squares	Mean Square	F Ratio
Plant Type	1	0.00245000	0.002450	0.2583
Error	6	0.05690000	0.009483	
C. Total	7	0.05935000		

Tremulacin, old leaves

t Test WT-MYB

Difference	6.57500	t Ratio	9.258038
Std Err Dif	0.71019	DF	6
Upper CL Dif	8.31278	Prob > |t|	<.0001
Lower CL Dif	4.83722	Prob > t	<.0001
Confidence	0.95	Prob < t	1.0000

Analysis of Variance

Source	DF	Sum of Squares	Mean Square	F Ratio
Plant Type	1	86.461250	86.4613	85.7113
Error	6	6.052500	1.0087	
C. Total	7	92.513750		

A6.2. *PtACT47* and *PtACT49* gene expression in wild type and MYB134 plants

PtACT47, young leaves

t Test WT-MYB

Difference	6.09250	t Ratio	5.901142
Std Err Dif	1.03243	DF	6
Upper CL Dif	8.61876	Prob > |t|	0.0011
Lower CL Dif	3.56624	Prob > t	0.0005
Confidence	0.95	Prob < t	0.9995

Analysis of Variance

Source	DF	Sum of Squares	Mean Square	F Ratio
Plant Type	1	74.237113	74.2371	34.8235
Error	6	12.790875	2.1318	
C. Total	7	87.027988		

PtACT49, young leaves

t Test WT-MYB

Difference	2.56668	t Ratio	4.223065
Std Err Dif	0.60778	DF	6
Upper CL Dif	4.05385	Prob > |t|	0.0055
Lower CL Dif	1.07950	Prob > t	0.0028
Confidence	0.95	Prob < t	0.9972

Analysis of Variance

Source	DF	Sum of Squares	Mean Square	F Ratio
Plant Type	1	13.175680	13.1757	17.8343
Error	6	4.432703	0.7388	
C. Total	7	17.608383		

PtACT47, Medium leaves

t Test WT-MYB

Difference	12.9575	t Ratio	3.351676
Std Err Dif	3.8660	DF	6
Upper CL Dif	22.4172	Prob > |t|	0.0154
Lower CL Dif	3.4978	Prob > t	0.0077
Confidence	0.95	Prob < t	0.9923

Analysis of Variance

Source	DF	Sum of Squares	Mean Square	F Ratio
Plant Type	1	335.79361	335.794	11.2337
Error	6	179.34928	29.892	
C. Total	7	515.14289		

PtACT49, medium leaves

t Test WT-MYB

Difference	7.3953	t Ratio	2.998612
Std Err Dif	2.4662	DF	6
Upper CL Dif	13.4300	Prob > |t|	0.0241
Lower CL Dif	1.3606	Prob > t	0.0120
Confidence	0.95	Prob < t	0.9880

Analysis of Variance

Source	DF	Sum of Squares	Mean Square	F Ratio
Plant Type	1	109.38115	109.381	8.9917
Error	6	72.98829	12.165	
C. Total	7	182.36944		

PtACT47, old Leaves

t Test WT-MYB

Difference	-0.3485	t Ratio	-0.33873
Std Err Dif	1.0288	DF	6
Upper CL Dif	2.1690	Prob > |t|	0.7464
Lower CL Dif	-2.8660	Prob > t	0.6268
Confidence	0.95	Prob < t	0.3732

Analysis of Variance

Source	DF	Sum of Squares	Mean Square	F Ratio
Plant type	1	0.242905	0.24290	0.1147
Error	6	12.702087	2.11701	
C. Total	7	12.944992		

PtACT49, old leaves

t Test WT-MYB

Difference	-0.7242	t Ratio	-1.36268
Std Err Dif	0.5315	DF	6
Upper CL Dif	0.5762	Prob > |t|	0.2219
Lower CL Dif	-2.0246	Prob > t	0.8890
Confidence	0.95	Prob < t	0.1110

Analysis of Variance

Source	DF	Sum of Squares	Mean Square	F Ratio
Plant type	1	1.0489488	1.04895	1.8569
Error	6	3.3893577	0.56489	
C. Total	7	4.4383065		

A6.3. Recombinant enzyme activity analysis.

Kinetic parameters calculated using SAS JMP Version 7.0 (SAS institute Inc.) with the Michaelis-Menten nonlinear model (2P) preset function.

PtACT49 (PtBEBT), benzyl alcohol (with benzyl-CoA in excess)

Nonlinear Fit

Response: Benzyl alcohol Mean Vo (µM sec-1), Predictor: Michaelis Menten Model (2P)

Criterion	Current	Stop Limit
Iteration	9	60
Obj Change	1.0015754e-9	1e-15
Relative Gradient	0.0000418211	0.000001
Gradient	7.8894657e-7	0.000001

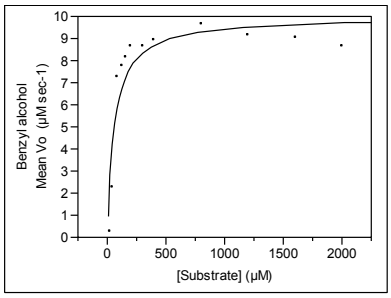

Parameter	Current Value
theta1	9.9855407979
theta2	58.749431543

SSE
15.320288774N
12
Edit Alpha
0.050Convergence Criterion
0.00001Goal SSE for CL

Solution

SSE	DFE	MSE	RMSE
15.320288774	10	1.5320289	1.2377515

Parameter	Estimate	ApproxStdErr
Vmax	9.9855407979	0.66639747
Km	58.749431543	18.9407222

PtACT49 (PtBEBT), benzyl-CoA (with benzyl alcohol in excess)

Nonlinear Fit

Response: Benzyl CoA Mean Vo (µM sec-1), Predictor: Michaelis Menten Model (2P)

Criterion	Current	Stop Limit
Iteration	11	60
Obj Change	2.83397e-10	1e-15
Relative Gradient	0.0000203015	0.000001
Gradient	4.1370548e-7	0.000001

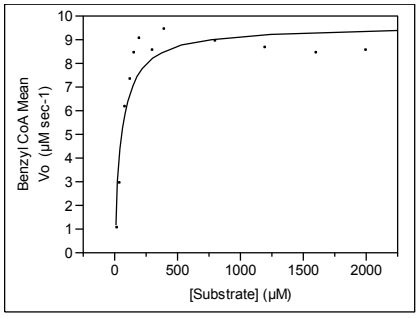

Parameter	Current Value
theta1	9.6242046398
theta2	51.781197487

SSE
10.910013795N
12
Edit Alpha
0.050Convergence Criterion
0.00001Goal SSE for CL

Solution

SSE	DFE	MSE	RMSE
10.910013795	10	1.0910014	1.0445101

Parameter	Estimate	ApproxStdErr
Vmax	9.6242046398	0.54475781

Parameter	Estimate	ApproxStdErr
Km	51.781197487	14.7965868

PtACT49 (PtBEBT), 3-hydroxybenzyl alcohol (with benzyl-CoA in excess)

Nonlinear Fit

Response: 3-Hydroxybenzyl alcohol Mean Vo (µM sec-1), Predictor: Michaelis Menten Model (2P)

Criterion	Current	Stop Limit
Iteration	12	60
Obj Change	1.2141545e-9	1e-15
Relative Gradient	0.0000518928	0.000001
Gradient	9.6991431e-7	0.000001

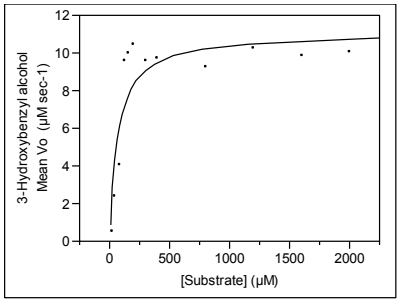

Parameter	Current Value
theta1	11.08909859
theta2	66.510808774

SSE
28.825977915N
12

Edit Alpha
0.050Convergence Criterion
0.00001Goal SSE for CL

Solution

SSE	DFE	MSE	RMSE
28.825977915	10	2.8825978	1.6978215

Parameter	Estimate	ApproxStdErr
theta1	11.08909859	0.94425023
theta2	66.510808774	26.2222587

PtACT49 (PtBEBT), benzoyl-CoA (with 3-hydroxybenzyl alcohol in excess)

Nonlinear Fit

Response: Benzyl CoA Mean Vo (µM sec-1), Predictor: Michaelis Menten Model (2P)

Criterion	Current	Stop Limit
Iteration	12	60
Obj Change	5.091944e-10	1e-15
Relative Gradient	0.0000318292	0.000001
Gradient	7.0585697e-7	0.000001

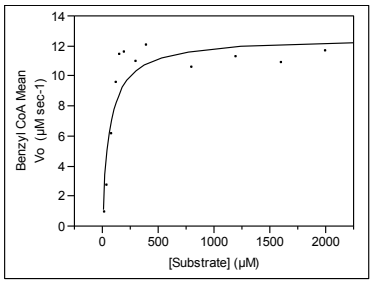

Parameter	Current Value
theta1	12.558051063
theta2	63.240267357

SSE
27.062177256N
12
Edit Alpha
0.050Convergence Criterion
0.00001Goal SSE for CL

Solution

SSE	DFE	MSE	RMSE
27.062177256	10	2.7062177	1.6450586

Parameter	Estimate	ApproxStdErr
Vmax	12.558051063	0.90278648
Km	63.240267357	21.4139377

PtACT49 (PtBEBT), benzyl alcohol (with acetyl-CoA in excess)

Nonlinear Fit

Response: Benzyl Alcohol Mean Vo (µM sec-1), Predictor: Michaelis Menten Model (2P)

Criterion	Current	Stop Limit
Iteration	6	60
Obj Change	6.7818807e-7	1e-15
Relative Gradient	0.0004484128	0.000001
Gradient	7.2908544e-7	0.000001

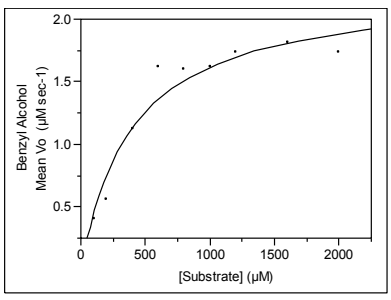

Parameter	Current Value
theta1	2.2580685284
theta2	395.18216786

SSE
0.1401886501N
9
Edit Alpha
0.050Convergence Criterion
0.00001Goal SSE for CL

Solution

SSE	DFE	MSE	RMSE
0.1401886501	7	0.020027	0.1415166

Parameter	Estimate	ApproxStdErr
Vmax	2.2580685284	0.18379031
Km	395.18216786	101.591458

PtACT49 (PtBEBT), acetyl-CoA (with benzyl alcohol in excess)

Nonlinear Fit
Response: Acetyl CoA Mean Vo (µM sec-1), Predictor: Michaelis Menten Model (2P)

Criterion	Current	Stop Limit
Iteration	6	60
Obj Change	6.6794663e-7	1e-15
Relative Gradient	0.0003426322	0.000001
Gradient	7.5785392e-7	0.000001

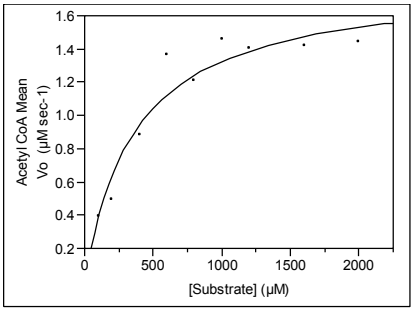

Parameter	Current Value
theta1	1.8096428042
theta2	364.73371286

SSE
0.1118170268N
9
Edit Alpha
0.050Convergence Criterion
0.00001Goal SSE for CL

Solution

SSE	DFE	MSE	RMSE
0.1118170268	7	0.0159739	0.1263877

Parameter	Estimate	ApproxStdErr
Vmax	1.8096428042	0.15493655
Km	364.73371286	102.29706

PtACT47 (PtSABT), salicyl alcohol (benzyl-CoA in excess)

Nonlinear Fit
Response: Salicylic alcohol Mean Vo (µM sec-1), Predictor: Michaelis Menten Model (2P)

Criterion	Current	Stop Limit
Iteration	14	60
Obj Change	2.292069e-10	1e-15
Relative Gradient	0.000024124	0.000001
Gradient	7.0661871e-7	0.000001

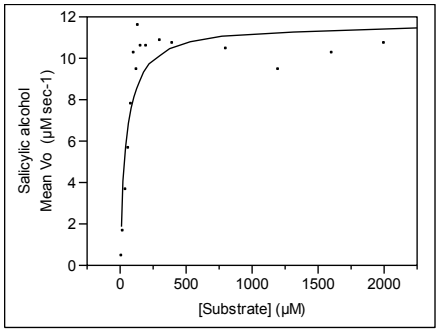

Parameter	Current Value
Vmax	11.671694756
Km	44.234433405

SSE
33.287853333N
16
Edit Alpha
0.050Convergence Criterion
0.00001Goal SSE for CL

Solution

SSE	DFE	MSE	RMSE
33.287853333	14	2.3777038	1.5419805

Parameter	Estimate	ApproxStdErr
Vmax	11.671694756	0.75298418
Km	44.234433405	13.1607478

PtACT47 (PtSABT), benzyl-CoA (with salicyl alcohol in excess)

Nonlinear Fit
Response: Benzyl CoA Mean Vo (µM sec-1), Predictor: Michaelis Menten Model (2P)

Criterion	Current	Stop Limit
Iteration	12	60
Obj Change	4.486376e-10	1e-15
Relative Gradient	0.0000246042	0.000001
Gradient	6.9975903e-7	0.000001

Parameter	Current Value
Vmax	11.697959954
Km	45.868418928

SSE
19.664869701N
16
Edit Alpha
0.050Convergence Criterion
0.00001Goal SSE for CL

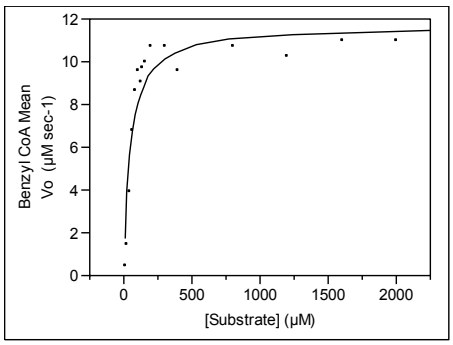

Solution

SSE	DFE	MSE	RMSE
19.664869701	14	1.4046336	1.1851724

Parameter	Estimate	ApproxStdErr
Vmax	11.697959954	0.58392796
Km	45.868418928	10.4178823

PtACT47 (PtSABT), salicyl alcohol (with acetyl-CoA in excess)

Nonlinear Fit
Response: Salicylic alcohol Mean Vo (µM sec-1), Predictor: Michaelis Menten Model (2P)

Criterion	Current	Stop Limit
Iteration	6	60
Obj Change	9.8205701e-7	1e-15
Relative Gradient	0.0001164449	0.000001
Gradient	6.5461708e-7	0.000001

Parameter	Current Value
Vmax	1.9712157755
Km	338.98814611

SSE
0.189612309N
14
Edit Alpha
0.050Convergence Criterion
0.00001Goal SSE for CL

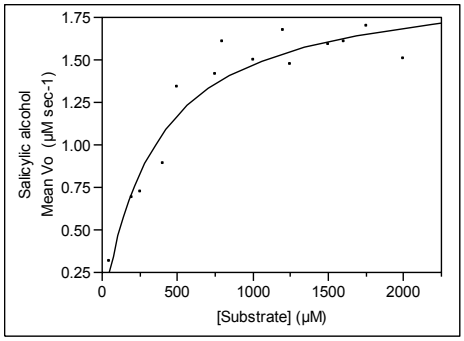

Solution

SSE	DFE	MSE	RMSE
0.189612309	12	0.015801	0.1257021

Parameter	Estimate	ApproxStdErr
Vmax	1.9712157755	0.11630534
Km	338.98814611	71.7160828

PtACT47 (PtSABT), acetyl-CoA (with salicyl alcohol in excess)

Nonlinear Fit
Response: Acetyl CoA Mean Vo (µM sec-1), Predictor: Michaelis Menten Model (2P)

Criterion	Current	Stop Limit
Iteration	7	60
Obj Change	4.7862746e-8	1e-15
Relative Gradient	0.0000807005	0.000001
Gradient	8.2078972e-8	0.000001

Parameter	Current Value
Vmax	2.41152165
Km	246.32281317

SSE
0.4836570479N

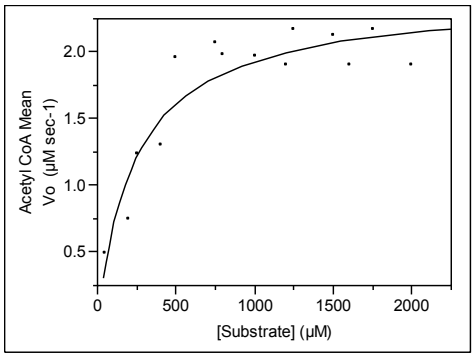

14
Edit Alpha
0.050Convergence Criterion
0.00001Goal SSE for CL
Solution

SSE	DFE	MSE	RMSE
0.4836570479	12	0.0403048	0.2007604

Parameter	Estimate	ApproxStdErr
Vmax	2.41152165	0.15247331
Km	246.32281317	65.3805494

PtACT47 (PtSABT), 3-hydroxybenzyl alcohol (with benzyl-CoA in excess)

Nonlinear Fit
Response: 3 Hydroxybenzyl alcohol Mean Vo (µM sec-1), Predictor: Michaelis Menten Model (2P)

Criterion	Current	Stop Limit
Iteration	11	60
Obj Change	1.1917051e-9	1e-15
Relative Gradient	0.0000490194	0.000001
Gradient	7.7261536e-7	0.000001

Parameter	Current Value
theta1	8.0903433575
theta2	56.796621781

SSE
10.77058015N
12
Edit Alpha
0.050Convergence Criterion
0.00001Goal SSE for CL
Solution

SSE	DFE	MSE	RMSE
10.77058015	10	1.077058	1.0378141

Parameter	Estimate	ApproxStdErr
theta1	8.0903433575	0.55394902
theta2	56.796621781	19.0082049

PtACT47 (PtSABT), benzyl-CoA (3-hydroxybenzyl alcohol in excess)

Nonlinear Fit
Response: Benzyl CoA Mean Vo (µM sec-1), Predictor: Michaelis Menten Model (2P)

Criterion	Current	Stop Limit
Iteration	11	60
Obj Change	1.2045208e-9	1e-15
Relative Gradient	0.0000469561	0.000001
Gradient	9.540174e-7	0.000001

Parameter	Current Value
Vmax	11.387351372
Km	62.537621124

SSE
18.99824492N
12
Edit Alpha
0.050Convergence Criterion
0.00001Goal SSE for CL
Solution

SSE	DFE	MSE	RMSE
18.99824492	10	1.8998245	1.3783412

Parameter	Estimate	ApproxStdErr
Vmax	11.387351372	0.75420431
Km	62.537621124	19.5842522

A6.4. Analysis of PG content in wounding experiments.

Total PGs, young leaves, 6 hrs

Analysis of Variance

Source	DF	Sum of Squares	Mean Square	F Ratio
Plant	1	113.18934	113.189	5.7430
Error	6	100.71691	16.786	
C. Total	7	213.90625		

t Test

Difference	7.523	t Ratio	2.596732
Std Err Dif	2.897	DF	4.002083
Upper CL Dif	15.565	Prob > |t|	0.0602
Lower CL Dif	-0.519	Prob > t	0.0301
Confidence	0.95	Prob < t	0.9699

Total PGs, young leaves, 24 hrs

Analysis of Variance

Source	DF	Sum of Squares	Mean Square	F Ratio
Plant	1	43.22044	43.2204	4.5035
Error	6	57.58299	9.5972	
C. Total	7	100.80343		

t Test

Difference	4.649	t Ratio	2.122136
Std Err Dif	2.191	DF	3.133331
Upper CL Dif	11.455	Prob > |t|	0.1201
Lower CL Dif	-2.158	Prob > t	0.0600
Confidence	0.95	Prob < t	0.9400

Total PGs, young leaves, 48 hrs

Analysis of Variance

Source	DF	Sum of Squares	Mean Square	F Ratio
Plant	1	255.76849	255.768	21.2487
Error	6	72.22138	12.037	
C. Total	7	327.98987		

t Test

Difference	11.3086	t Ratio	4.609632
Std Err Dif	2.4533	DF	6
Upper CL Dif	17.3115	Prob > |t|	0.0037
Lower CL Dif	5.3057	Prob > t	0.0018
Confidence	0.95	Prob < t	0.9982

Total PGs, medium leaves, 6 hrs

Analysis of Variance

Source	DF	Sum of Squares	Mean Square	F Ratio
Plant	1	5.606441	5.60644	0.8309
Error	6	40.483913	6.74732	
C. Total	7	46.090354		

t Test

Difference	1.6743	t Ratio	0.911545
Std Err Dif	1.8368	DF	6
Upper CL Dif	6.1687	Prob > |t|	0.3972
Lower CL Dif	-2.8201	Prob > t	0.1986
Confidence	0.95	Prob < t	0.8014

Total PGs, medium leaves, 24 hrs

Analysis of Variance

Source	DF	Sum of Squares	Mean Square	F Ratio
Plant	1	450.66604	450.666	18.4341
Error	6	146.68430	24.447	
C. Total	7	597.35034		

t Test

Difference	15.0111	t Ratio	4.293498
Std Err Dif	3.4962	DF	6
Upper CL Dif	23.5661	Prob > |t|	0.0051
Lower CL Dif	6.4561	Prob > t	0.0026
Confidence	0.95	Prob < t	0.9974

Total PGs, medium leaves, 48 hrs

Analysis of Variance

Source	DF	Sum of Squares	Mean Square	F Ratio
Plant	1	73.91982	73.9198	3.1135
Error	6	142.45033	23.7417	
C. Total	7	216.37015		

t Test

Difference	6.079	t Ratio	1.764511
Std Err Dif	3.445	DF	6
Upper CL Dif	14.510	Prob > |t|	0.1281
Lower CL Dif	-2.351	Prob > t	0.0640
Confidence	0.95	Prob < t	0.9360

Total PGs, old leaves, 6 hrs

Analysis of Variance

Source	DF	Sum of Squares	Mean Square	F Ratio
Plant	1	1.10358	1.1036	0.0215
Error	6	308.40241	51.4004	
C. Total	7	309.50599		

t Test

Difference	-0.743	t Ratio	-0.14653
Std Err Dif	5.070	DF	6
Upper CL Dif	11.662	Prob > |t|	0.8883
Lower CL Dif	-13.148	Prob > t	0.5558
Confidence	0.95	Prob < t	0.4442

Total PGs, old leaves, 24 hrs

Analysis of Variance

Source	DF	Sum of Squares	Mean Square	F Ratio
Plant	1	2.35377	2.3538	0.1327
Error	6	106.45561	17.7426	
C. Total	7	108.80938		

t Test

Difference	1.0848	t Ratio	0.364228
Std Err Dif	2.9785	DF	6
Upper CL Dif	8.3729	Prob > |t|	0.7282
Lower CL Dif	-6.2032	Prob > t	0.3641
Confidence	0.95	Prob < t	0.6359

Total PGs, old leaves, 48 hrs

Analysis of Variance

Source	DF	Sum of Squares	Mean Square	F Ratio
Plant	1	3.848478	3.8485	0.2844
Error	6	81.205198	13.5342	
C. Total	7	85.053676		

t Test

Difference	1.3872	t Ratio	0.533247
Std Err Dif	2.6014	DF	6
Upper CL Dif	7.7525	Prob > |t|	0.6130
Lower CL Dif	-4.9781	Prob > t	0.3065
Confidence	0.95	Prob < t	0.6935

Salicin, young leaves, 6 hrs

t Test

Difference	-0.2884	t Ratio	-0.43739
Std Err Dif	0.6594	DF	6
Upper CL Dif	1.3251	Prob > |t|	0.6771
Lower CL Dif	-1.9019	Prob > t	0.6614
Confidence	0.95	Prob < t	0.3386

Analysis of Variance

Source	DF	Sum of Squares	Mean Square	F Ratio
Plant	1	0.1663653	0.166365	0.1913
Error	6	5.2177199	0.869620	
C. Total	7	5.3840852		

Salicin, young leaves, 24 hrs

t Test

Difference	0.89432	t Ratio	3.285107
Std Err Dif	0.27223	DF	6
Upper CL Dif	1.56045	Prob > |t|	0.0167

Lower CL Dif	0.22818	Prob > t	0.0084
Confidence	0.95	Prob < t	0.9916

Analysis of Variance

Source	DF	Sum of Squares	Mean Square	F Ratio
Plant	1	1.5996003	1.59960	10.7919
Error	6	0.8893315	0.14822	
C. Total	7	2.4889318		

Salicin, young leaves, 48 hrs

t Test

Difference	3.04642	t Ratio	4.431782
Std Err Dif	0.68740	DF	6
Upper CL Dif	4.72844	Prob > |t|	0.0044
Lower CL Dif	1.36441	Prob > t	0.0022
Confidence	0.95	Prob < t	0.9978

Analysis of Variance

Source	DF	Sum of Squares	Mean Square	F Ratio
Plant	1	18.561374	18.5614	19.6407
Error	6	5.670280	0.9450	
C. Total	7	24.231654		

Salicin, medium leaves, 6 hrs

t Test

Difference	1.31919	t Ratio	2.558898
Std Err Dif	0.51553	DF	6
Upper CL Dif	2.58065	Prob > |t|	0.0430
Lower CL Dif	0.05773	Prob > t	0.0215
Confidence	0.95	Prob < t	0.9785

Analysis of Variance

Source	DF	Sum of Squares	Mean Square	F Ratio
Plant	1	3.4805324	3.48053	6.5480
Error	6	3.1892684	0.53154	
C. Total	7	6.6698008		

Salicin, medium leaves, 24 hrs

t Test

Difference	2.77246	t Ratio	9.078341
Std Err Dif	0.30539	DF	6
Upper CL Dif	3.51973	Prob > |t|	0.0001
Lower CL Dif	2.02519	Prob > t	<.0001
Confidence	0.95	Prob < t	0.9999

Analysis of Variance

Source	DF	Sum of Squares	Mean Square	F Ratio
Plant	1	15.373078	15.3731	82.4163
Error	6	1.119178	0.1865	
C. Total	7	16.492256		

Salicin, medium leaves, 48 hrs

t Test

Difference	-0.0296	t Ratio	-0.06658
Std Err Dif	0.4441	DF	6
Upper CL Dif	1.0570	Prob > |t|	0.9491
Lower CL Dif	-1.1161	Prob > t	0.5255
Confidence	0.95	Prob < t	0.4745

Analysis of Variance

Source	DF	Sum of Squares	Mean Square	F Ratio
Plant	1	0.0017483	0.001748	0.0044
Error	6	2.3662692	0.394378	
C. Total	7	2.3680175		

Salicin, old leaves, 6hrs

t Test

Difference	-1.2721	t Ratio	-0.9124
Std Err Dif	1.3942	DF	6
Upper CL Dif	2.1395	Prob > |t|	0.3967
Lower CL Dif	-4.6836	Prob > t	0.8016
Confidence	0.95	Prob < t	0.1984

Analysis of Variance

Source	DF	Sum of Squares	Mean Square	F Ratio
Plant	1	3.236382	3.23638	0.8325

Source	DF	Sum of Squares	Mean Square	F Ratio
Error	6	23.326197	3.88770	
C. Total	7	26.562578		

Salicin, old leaves, 24 hrs

t Test

Difference	1.1992	t Ratio	2.093157
Std Err Dif	0.5729	DF	6
Upper CL Dif	2.6010	Prob > |t|	0.0812
Lower CL Dif	-0.2027	Prob > t	0.0406
Confidence	0.95	Prob < t	0.9594

Analysis of Variance

Source	DF	Sum of Squares	Mean Square	F Ratio
Plant	1	2.8760488	2.87605	4.3813
Error	6	3.9386176	0.65644	
C. Total	7	6.8146665		

Salicin, old leaves, 48 hrs

t Test

Difference	0.2675	t Ratio	0.648086
Std Err Dif	0.4128	DF	6
Upper CL Dif	1.2776	Prob > |t|	0.5409
Lower CL Dif	-0.7426	Prob > t	0.2705
Confidence	0.95	Prob < t	0.7295

Analysis of Variance

Source	DF	Sum of Squares	Mean Square	F Ratio
Plant	1	0.1431505	0.143151	0.4200
Error	6	2.0449322	0.340822	
C. Total	7	2.1880827		

Salicortin, young leaves, 6 hrs

t Test

Difference	7.00850	t Ratio	8.046874
Std Err Dif	0.87096	DF	6
Upper CL Dif	9.13966	Prob > |t|	0.0002
Lower CL Dif	4.87734	Prob > t	<.0001
Confidence	0.95	Prob < t	0.9999

Analysis of Variance

Source	DF	Sum of Squares	Mean Square	F Ratio
Plant	1	98.23810	98.2381	4.7522
Error	6	9.10284	1.5171	
C. Total	7	107.34094		

Salicortin, young leaves, 24 hrs

t Test

Difference	1.3338	t Ratio	1.010158
Std Err Dif	1.3204	DF	6
Upper CL Dif	4.5647	Prob > |t|	0.3514
Lower CL Dif	-1.8971	Prob > t	0.1757
Confidence	0.95	Prob < t	0.8243

Analysis of Variance

Source	DF	Sum of Squares	Mean Square	F Ratio
Plant	1	3.558119	3.55812	1.0204
Error	6	20.921495	3.48692	
C. Total	7	24.479614		

Salicortin, young leaves, 48 hrs

t Test

Difference	3.03476	t Ratio	4.858004
Std Err Dif	0.62469	DF	6
Upper CL Dif	4.56332	Prob > |t|	0.0028
Lower CL Dif	1.50619	Prob > t	0.0014
Confidence	0.95	Prob < t	0.9986

Analysis of Variance

Source	DF	Sum of Squares	Mean Square	F Ratio
Plant	1	18.419509	18.4195	23.6002
Error	6	4.682887	0.7805	
C. Total	7	23.102396		

Salicortin, medium leaves, 6 hrs

t Test

Difference	0.6201	t Ratio	1.085577
Std Err Dif	0.5712	DF	6
Upper CL Dif	2.0177	Prob > |t|	0.3193
Lower CL Dif	-0.7776	Prob > t	0.1597
Confidence	0.95	Prob < t	0.8403

Analysis of Variance

Source	DF	Sum of Squares	Mean Square	F Ratio
Plant	1	0.7689543	0.768954	1.1785
Error	6	3.9149899	0.652498	
C. Total	7	4.6839442		

Salicortin, medium, 24 hrs

t Test

Difference	7.4051	t Ratio	5.010043
Std Err Dif	1.4780	DF	6
Upper CL Dif	11.0217	Prob > |t|	0.0024
Lower CL Dif	3.7884	Prob > t	0.0012
Confidence	0.95	Prob < t	0.9988

Analysis of Variance

Source	DF	Sum of Squares	Mean Square	F Ratio
Plant	1	109.66970	109.670	25.1005
Error	6	26.21531	4.369	
C. Total	7	135.88501		

Salicortin, medium leaves, 48 hrs

t Test

Difference	4.550	t Ratio	1.89512
Std Err Dif	2.401	DF	6
Upper CL Dif	10.425	Prob > |t|	0.1069
Lower CL Dif	-1.325	Prob > t	0.0534
Confidence	0.95	Prob < t	0.9466

Analysis of Variance

Source	DF	Sum of Squares	Mean Square	F Ratio
Plant	1	41.40598	41.4060	33.5915
Error	6	69.17369	11.5289	
C. Total	7	110.57967		

Salicortin, old leaves, 6 hrs

t Test

Difference	2.8944	t Ratio	2.287788
Std Err Dif	1.2652	DF	6
Upper CL Dif	5.9901	Prob > |t|	0.0621
Lower CL Dif	-0.2013	Prob > t	0.0311
Confidence	0.95	Prob < t	0.9689

Analysis of Variance

Source	DF	Sum of Squares	Mean Square	F Ratio
Plant	1	16.755273	16.7553	25.2340
Error	6	19.207523	3.2013	
C. Total	7	35.962796		

Salicortin, old leaves, 24 hrs

t Test

Difference	-0.0735	t Ratio	-0.06041
Std Err Dif	1.2160	DF	6
Upper CL Dif	2.9020	Prob > |t|	0.9538
Lower CL Dif	-3.0489	Prob > t	0.5231
Confidence	0.95	Prob < t	0.4769

Analysis of Variance

Source	DF	Sum of Squares	Mean Square	F Ratio
Plant	1	0.010794	0.01079	19.0036
Error	6	17.744144	2.95736	
C. Total	7	17.754938		

Salicortin, old leaves, 48 hrs

t Test

Difference	2.1876	t Ratio	1.53339
Std Err Dif	1.4266	DF	6

Upper CL Dif	5.6784	Prob > |t|	0.1761
Lower CL Dif	-1.3033	Prob > t	0.0880
Confidence	0.95	Prob < t	0.9120

Analysis of Variance

Source	DF	Sum of Squares	Mean Square	F Ratio
Plant	1	9.570902	9.57090	22.3513
Error	6	24.422993	4.07050	
C. Total	7	33.993895		

Tremuloidin, young leaves, 6 hrs

t Test

Difference	-0.7521	t Ratio	-2.45084
Std Err Dif	0.3069	DF	6
Upper CL Dif	-0.0012	Prob > |t|	0.0497
Lower CL Dif	-1.5029	Prob > t	0.9751
Confidence	0.95	Prob < t	0.0249

Analysis of Variance

Source	DF	Sum of Squares	Mean Square	F Ratio
Plant	1	1.1312188	1.13122	3.0066
Error	6	1.1299690	0.18833	
C. Total	7	2.2611878		

Tremuloidin, young leaves, 24 hrs

t Test

Difference	-0.2336	t Ratio	-0.59739
Std Err Dif	0.3910	DF	6
Upper CL Dif	0.7232	Prob > |t|	0.5721
Lower CL Dif	-1.1904	Prob > t	0.7140
Confidence	0.95	Prob < t	0.2860

Analysis of Variance

Source	DF	Sum of Squares	Mean Square	F Ratio
Plant	1	0.1091409	0.109141	0.3569
Error	6	1.8349429	0.305824	
C. Total	7	1.9440839		

Tremuloidin, young leaves, 48 hrs

t Test

Difference	1.6487	t Ratio	1.133393
Std Err Dif	1.4547	DF	6
Upper CL Dif	5.2081	Prob > |t|	0.3003
Lower CL Dif	-1.9107	Prob > t	0.1501
Confidence	0.95	Prob < t	0.8499

Analysis of Variance

Source	DF	Sum of Squares	Mean Square	F Ratio
Plant	1	5.436468	5.43647	1.2846
Error	6	25.392587	4.23210	
C. Total	7	30.829055		

Tremuloidin, medium leaves, 6 hrs

t Test

Difference	0.9850	t Ratio	1.664946
Std Err Dif	0.5916	DF	6
Upper CL Dif	2.4326	Prob > |t|	0.1470
Lower CL Dif	-0.4626	Prob > t	0.0735
Confidence	0.95	Prob < t	0.9265

Analysis of Variance

Source	DF	Sum of Squares	Mean Square	F Ratio
Plant	1	1.9403433	1.94034	2.7720
Error	6	4.1998104	0.69997	
C. Total	7	6.1401537		

Tremuloidin, medium leaves, 24hrs

t Test

Difference	0.9914	t Ratio	1.679781
Std Err Dif	0.5902	DF	6
Upper CL Dif	2.4357	Prob > |t|	0.1440
Lower CL Dif	-0.4528	Prob > t	0.0720
Confidence	0.95	Prob < t	0.9280

Analysis of Variance

Source	DF	Sum of Squares	Mean Square	F Ratio

Source	DF	Sum of Squares	Mean Square	F Ratio
Plant	1	1.9659036	1.96590	2.8217
Error	6	4.1803074	0.69672	
C. Total	7	6.1462109		

Tremuloidin, medium leaves, 48 hrs

t Test

Difference	0.7908	t Ratio	1.904214
Std Err Dif	0.4153	DF	6
Upper CL Dif	1.8071	Prob > |t|	0.1056
Lower CL Dif	-0.2254	Prob > t	0.0528
Confidence	0.95	Prob < t	0.9472

Analysis of Variance

Source	DF	Sum of Squares	Mean Square	F Ratio
Plant	1	1.2508640	1.25086	3.6260
Error	6	2.0698062	0.34497	
C. Total	7	3.3206702		

Tremuloidin, old leaves, 6 hrs

t Test

Difference	0.3851	t Ratio	1.287296
Std Err Dif	0.2992	DF	6
Upper CL Dif	1.1172	Prob > |t|	0.2454
Lower CL Dif	-0.3469	Prob > t	0.1227
Confidence	0.95	Prob < t	0.8773

Analysis of Variance

Source	DF	Sum of Squares	Mean Square	F Ratio
Plant	1	0.2966332	0.296633	1.6571
Error	6	1.0740251	0.179004	
C. Total	7	1.3706582		

Tremuloidin, old leaves, 24 hrs

t Test

Difference	-0.3286	t Ratio	-0.77312
Std Err Dif	0.4251	DF	6
Upper CL Dif	0.7115	Prob > |t|	0.4688
Lower CL Dif	-1.3688	Prob > t	0.7656
Confidence	0.95	Prob < t	0.2344

Analysis of Variance

Source	DF	Sum of Squares	Mean Square	F Ratio
Plant	1	0.2160001	0.216000	0.5977
Error	6	2.1682562	0.361376	
C. Total	7	2.3842563		

Tremuloidin, old leaves, 48 hrs

t Test

Difference	-0.6236	t Ratio	-1.36033
Std Err Dif	0.4584	DF	6
Upper CL Dif	0.4981	Prob > |t|	0.2226
Lower CL Dif	-1.7453	Prob > t	0.8887
Confidence	0.95	Prob < t	0.1113

Analysis of Variance

Source	DF	Sum of Squares	Mean Square	F Ratio
Plant	1	0.7777133	0.777713	1.8505
Error	6	2.5216349	0.420272	
C. Total	7	3.2993481		

Tremulacin, young leaves, 6 hrs

t Test

Difference	1.5549	t Ratio	0.838303
Std Err Dif	1.8549	DF	6
Upper CL Dif	6.0936	Prob > |t|	0.4340
Lower CL Dif	-2.9837	Prob > t	0.2170
Confidence	0.95	Prob < t	0.7830

Analysis of Variance

Source	DF	Sum of Squares	Mean Square	F Ratio
Plant	1	4.835606	4.83561	0.7028
Error	6	41.285718	6.88095	
C. Total	7	46.121323		

Tremulacin, young leaves, 24 hrs

t Test

Difference	3.08547	t Ratio	2.520634
Std Err Dif	1.22408	DF	6
Upper CL Dif	6.08070	Prob > |t|	0.0452
Lower CL Dif	0.09024	Prob > t	0.0226
Confidence	0.95	Prob < t	0.9774

Analysis of Variance

Source	DF	Sum of Squares	Mean Square	F Ratio
Plant	1	19.040258	19.0403	6.3536
Error	6	17.980608	2.9968	
C. Total	7	37.020866		

Tremulacin, young leaves, 48 hrs

t Test

Difference	0.6156	t Ratio	0.842154
Std Err Dif	0.7310	DF	6
Upper CL Dif	2.4044	Prob > |t|	0.4320
Lower CL Dif	-1.1731	Prob > t	0.2160
Confidence	0.95	Prob < t	0.7840

Analysis of Variance

Source	DF	Sum of Squares	Mean Square	F Ratio
Plant	1	0.7580204	0.75802	0.7092
Error	6	6.4128216	1.06880	
C. Total	7	7.1708420		

Tremulacin, medium leaves, 6 hrs

t Test

Wounded-Control

Difference	-1.1249	t Ratio	-1.84003
Std Err Dif	0.6114	DF	6
Upper CL Dif	0.3710	Prob > |t|	0.1154
Lower CL Dif	-2.6208	Prob > t	0.9423
Confidence	0.95	Prob < t	0.0577

Analysis of Variance

Source	DF	Sum of Squares	Mean Square	F Ratio
Plant	1	2.5308508	2.53085	3.3857
Error	6	4.4850743	0.74751	
C. Total	7	7.0159251		

Tremulacin, medium leaves, 24 hrs

t Test

Difference	3.0570	t Ratio	1.263573
Std Err Dif	2.4194	DF	6
Upper CL Dif	8.9770	Prob > |t|	0.2533
Lower CL Dif	-2.8629	Prob > t	0.1266
Confidence	0.95	Prob < t	0.8734

Analysis of Variance

Source	DF	Sum of Squares	Mean Square	F Ratio
Plant	1	18.690903	18.6909	1.5966
Error	6	70.239435	11.7066	
C. Total	7	88.930338		

Tremulacin, medium leaves, 48 hrs

t Test

Difference	2.16886	t Ratio	2.901697
Std Err Dif	0.74745	DF	6
Upper CL Dif	3.99780	Prob > |t|	0.0273
Lower CL Dif	0.33993	Prob > t	0.0136
Confidence	0.95	Prob < t	0.9864

Analysis of Variance

Source	DF	Sum of Squares	Mean Square	F Ratio
Plant	1	9.407939	9.40794	5.4198
Error	6	6.704119	1.11735	
C. Total	7	16.112059		

Tremulacin, old leaves, 6 hrs

t Test

Difference	-2.7503	t Ratio	-1.16788
Std Err Dif	2.3549	DF	6

Upper CL Dif	3.0120	Prob > |t|	0.2872
Lower CL Dif	-8.5126	Prob > t	0.8564
Confidence	0.95	Prob < t	0.1436

Analysis of Variance

Source	DF	Sum of Squares	Mean Square	F Ratio
Plant	1	15.128051	15.1281	1.3640
Error	6	66.548077	11.0913	
C. Total	7	81.676128		

Tremulacin, old leaves, 24 hrs

t Test

Difference	0.9736	t Ratio	1.263803
Std Err Dif	0.7704	DF	6
Upper CL Dif	2.8587	Prob > |t|	0.2532
Lower CL Dif	-0.9115	Prob > t	0.1266
Confidence	0.95	Prob < t	0.8734

Analysis of Variance

Source	DF	Sum of Squares	Mean Square	F Ratio
Plant	1	1.8959255	1.89593	1.5972
Error	6	7.1221980	1.18703	
C. Total	7	9.0181235		

Tremulacin, old leaves, 48 hrs

t Test

Difference	-0.4443	t Ratio	-0.6392
Std Err Dif	0.6952	DF	6
Upper CL Dif	1.2567	Prob > |t|	0.5463
Lower CL Dif	-2.1454	Prob > t	0.7268
Confidence	0.95	Prob < t	0.2732

Analysis of Variance

Source	DF	Sum of Squares	Mean Square	F Ratio
Plant	1	0.3948934	0.394893	0.4086
Error	6	5.7990277	0.966505	
C. Total	7	6.1939211		

A6.5. Analysis of *PtACT47* and *PtACT49* expression in wounding experiments.

PtACT47, young tissues, 6 hrs

t Test

Difference	5.46865	t Ratio	2.940093
Std Err Dif	1.86002	DF	7
Upper CL Dif	9.86691	Prob > |t|	0.0217
Lower CL Dif	1.07039	Prob > t	0.0109
Confidence	0.95	Prob < t	0.9891

Analysis of Variance

Source	DF	Sum of Squares	Mean Square	F Ratio
Plant	1	66.45798	66.4580	8.6441
Error	7	53.81745	7.6882	
C. Total	8	120.27542		

PtACT47, young leaves, 24 hrs

t Test

Difference	13.7932	t Ratio	6.964346
Std Err Dif	1.9805	DF	7
Upper CL Dif	18.4764	Prob > |t|	0.0002
Lower CL Dif	9.1099	Prob > t	0.0001
Confidence	0.95	Prob < t	0.9999

Analysis of Variance

Source	DF	Sum of Squares	Mean Square	F Ratio
Plant	1	422.78193	422.782	48.5021
Error	7	61.01741	8.717	
C. Total	8	483.79934		

PtACT47, young leaves, 48 hrs

t Test

Difference	7.8844	t Ratio	5.468172
Std Err Dif	1.4419	DF	7
Upper CL Dif	11.2939	Prob > |t|	0.0009
Lower CL Dif	4.4749	Prob > t	0.0005

Confidence	0.95	Prob < t	0.9995

Analysis of Variance

Source	DF	Sum of Squares	Mean Square	F Ratio
Plant	1	138.14176	138.142	29.9009
Error	7	32.33990	4.620	
C. Total	8	170.48166		

PtACT47, medium, 6 hrs

t Test

Difference	7.04042	t Ratio	5.989802
Std Err Dif	1.17540	DF	7
Upper CL Dif	9.81980	Prob > |t|	0.0005
Lower CL Dif	4.26104	Prob > t	0.0003
Confidence	0.95	Prob < t	0.9997

Analysis of Variance

Source	DF	Sum of Squares	Mean Square	F Ratio
Plant	1	110.15001	110.150	35.8777
Error	7	21.49105	3.070	
C. Total	8	131.64106		

PtACT47, medium leaves, 24 hrs

t Test

Difference	14.6972	t Ratio	6.44782
Std Err Dif	2.2794	DF	7
Upper CL Dif	20.0871	Prob > |t|	0.0004
Lower CL Dif	9.3072	Prob > t	0.0002
Confidence	0.95	Prob < t	0.9998

Analysis of Variance

Source	DF	Sum of Squares	Mean Square	F Ratio
Plant	1	480.01452	480.015	41.5744
Error	7	80.82143	11.546	
C. Total	8	560.83595		

PtACT47, medium leaves, 48 hrs

t Test

Difference	-1.0405	t Ratio	-0.65773
Std Err Dif	1.5820	DF	7
Upper CL Dif	2.7003	Prob > |t|	0.5317
Lower CL Dif	-4.7813	Prob > t	0.7341
Confidence	0.95	Prob < t	0.2659

Analysis of Variance

Source	DF	Sum of Squares	Mean Square	F Ratio
Plant	1	2.405935	2.40593	14.4326
Error	7	38.930669	5.56152	
C. Total	8	41.336604		

PtACT47, old leaves, 6 hrs

t Test

Difference	4.12192	t Ratio	2.839875
Std Err Dif	1.45144	DF	7
Upper CL Dif	7.55404	Prob > |t|	0.0250
Lower CL Dif	0.68980	Prob > t	0.0125
Confidence	0.95	Prob < t	0.9875

Analysis of Variance

Source	DF	Sum of Squares	Mean Square	F Ratio
Plant	1	37.756091	37.7561	8.0649
Error	7	32.770771	4.6815	
C. Total	8	70.526862		

PtACT47, old leaves, 24 hrs

t Test

Difference	9.0938	t Ratio	5.312868
Std Err Dif	1.7117	DF	7
Upper CL Dif	13.1413	Prob > |t|	0.0011
Lower CL Dif	5.0464	Prob > t	0.0006
Confidence	0.95	Prob < t	0.9994

Analysis of Variance

Source	DF	Sum of Squares	Mean Square	F Ratio
Plant	1	183.77337	183.773	28.2266
Error	7	45.57457	6.511	

Source	DF	Sum of Squares	Mean Square	F Ratio
C. Total	8	229.34794		

PtACT47, old leaves, 48 hrs

t Test

Difference	5.44762	t Ratio	5.743564
Std Err Dif	0.94847	DF	7
Upper CL Dif	7.69040	Prob > |t|	0.0007
Lower CL Dif	3.20484	Prob > t	0.0004
Confidence	0.95	Prob < t	0.9996

Analysis of Variance

Source	DF	Sum of Squares	Mean Square	F Ratio
Plant	1	65.947911	65.9479	32.9885
Error	7	13.993815	1.9991	
C. Total	8	79.941726		

PtACT49, young leaves, 6 hrs

t Test

Difference	-0.05975	t Ratio	-0.4424
Std Err Dif	0.13505	DF	7
Upper CL Dif	0.25961	Prob > |t|	0.6715
Lower CL Dif	-0.37910	Prob > t	0.6642
Confidence	0.95	Prob < t	0.3358

Analysis of Variance

Source	DF	Sum of Squares	Mean Square	F Ratio
Plant	1	0.00793297	0.007933	4.1957
Error	7	0.28372978	0.040533	
C. Total	8	0.29166274		

PtACT49, young leaves, 24 hrs

t Test

Difference	1.11226	t Ratio	3.774067
Std Err Dif	0.29471	DF	7
Upper CL Dif	1.80915	Prob > |t|	0.0069
Lower CL Dif	0.41538	Prob > t	0.0035
Confidence	0.95	Prob < t	0.9965

Analysis of Variance

Source	DF	Sum of Squares	Mean Square	F Ratio
Plant	1	2.7491781	2.74918	14.2436
Error	7	1.3510818	0.19301	
C. Total	8	4.1002599		

PtACT49, young leaves, 24 hrs

t Test

Difference	1.11226	t Ratio	3.774067
Std Err Dif	0.29471	DF	7
Upper CL Dif	1.80915	Prob > |t|	0.0069
Lower CL Dif	0.41538	Prob > t	0.0035
Confidence	0.95	Prob < t	0.9965

Analysis of Variance

Source	DF	Sum of Squares	Mean Square	F Ratio
Plant	1	2.7491781	2.74918	14.2436
Error	7	1.3510818	0.19301	
C. Total	8	4.1002599		

PtACT49, young leaves, 48 hrs

t Test

Difference	0.579334	t Ratio	5.906351
Std Err Dif	0.098087	DF	7
Upper CL Dif	0.811272	Prob > |t|	0.0006
Lower CL Dif	0.347396	Prob > t	0.0003
Confidence	0.95	Prob < t	0.9997

Analysis of Variance

Source	DF	Sum of Squares	Mean Square	F Ratio
Plant	1	0.74584054	0.745841	34.8850
Error	7	0.14965993	0.021380	
C. Total	8	0.89550047		

PtACT49, medium leaves, 6 hrs

t Test

Difference	0.645521	t Ratio	5.210481
Std Err Dif	0.123889	DF	7
Upper CL Dif	0.938472	Prob > |t|	0.0012
Lower CL Dif	0.352570	Prob > t	0.0006
Confidence	0.95	Prob < t	0.9994

Analysis of Variance

Source	DF	Sum of Squares	Mean Square	F Ratio
Plant	1	0.9259949	0.925995	27.1491
Error	7	0.2387542	0.034108	
C. Total	8	1.1647491		

PtACT49, medium, 24 hrs

t Test

Difference	0.65075	t Ratio	2.851562
Std Err Dif	0.22821	DF	7
Upper CL Dif	1.19038	Prob > |t|	0.0246
Lower CL Dif	0.11112	Prob > t	0.0123
Confidence	0.95	Prob < t	0.9877

Analysis of Variance

Source	DF	Sum of Squares	Mean Square	F Ratio
Plant	1	0.9410557	0.941056	8.1314
Error	7	0.8101167	0.115731	
C. Total	8	1.7511724		

PtACT49, medium leaves, 48 hrs

t Test

Difference	0.297930	t Ratio	4.176281
Std Err Dif	0.071339	DF	7
Upper CL Dif	0.466619	Prob > |t|	0.0042
Lower CL Dif	0.129241	Prob > t	0.0021
Confidence	0.95	Prob < t	0.9979

Analysis of Variance

Source	DF	Sum of Squares	Mean Square	F Ratio
Plant	1	0.19724967	0.197250	17.4413
Error	7	0.07916529	0.011309	
C. Total	8	0.27641496		

PtACT49, old leaves, 6 hrs

t Test

Difference	-0.18349	t Ratio	-1.72838
Std Err Dif	0.10616	DF	7
Upper CL Dif	0.06754	Prob > |t|	0.1276
Lower CL Dif	-0.43452	Prob > t	0.9362
Confidence	0.95	Prob < t	0.0638

Analysis of Variance

Source	DF	Sum of Squares	Mean Square	F Ratio
Plant	1	0.07481798	0.074818	2.9873
Error	7	0.17531742	0.025045	
C. Total	8	0.25013540		

PtACT49, old leaves, 24 hrs

t Test

Difference	0.4474	t Ratio	1.881904
Std Err Dif	0.2377	DF	7
Upper CL Dif	1.0095	Prob > |t|	0.1019
Lower CL Dif	-0.1148	Prob > t	0.0509
Confidence	0.95	Prob < t	0.9491

Analysis of Variance

Source	DF	Sum of Squares	Mean Square	F Ratio
Plant	1	0.4447657	0.444766	3.5416
Error	7	0.8790919	0.125585	
C. Total	8	1.3238576		

PtACT49, old leaves, 48 hrs

t Test

Difference	0.01848	t Ratio	0.126317
Std Err Dif	0.14633	DF	7
Upper CL Dif	0.36451	Prob > |t|	0.9030
Lower CL Dif	-0.32754	Prob > t	0.4515

Confidence		0.95 Prob < t	0.5485	
Analysis of Variance				
Source	**DF**	**Sum of Squares**	**Mean Square**	**F Ratio**
Plant	1	0.00075928	0.000759	0.0160
Error	7	0.33309988	0.047586	
C. Total	8	0.33385916		

A6.6. Statistical analysis of transgenic RNAi plants.

A6.6.1. [Total PG] (mg g^{-1} fr wt) versus RNAi treatment type calculated for each tissue type.

Analysis of [total PG] (mg g fr. wt-1) versus RNAi treatment type in various tissues using a Linear Mixed Effect (LME) function with a Restricted Maximum Likelihood (REML) method. This can test if each RNAi treatment had a significant effect on PG content for all three independent lines combined. A one-way ANOVA is also included to test if RNAi treatments have a significant effect overall. P values <0.01 are considered significant.

Young leaves

Total PGs

	Value	Std.Error	DF	t-value	p-value	Significant? (α=0.01)
(Intercept)	75.318	4.786	47	15.736	0.000	-
PtBEBT (*PtACT49*) RNAi	-0.168	6.769	8	-0.025	0.981	No
Empty Vector Control	-0.907	6.769	8	-0.134	0.897	No
DKD RNAi	-10.588	6.769	8	-1.564	0.156	No
PtSABT (*PtACT47*) RNAi	-11.325	7.285	8	-1.555	0.159	No

One way ANOVA:

	numDF	denDF	F-value	p-value	Significant? (α=0.01)
(Intercept)	1	47	1049.144	<.0001	-
RNAi Treatment	4	8	1.354	0.331	No

Medium leaves

Total PGs

	Value	Std.Error	DF	t-value	p-value	Significant? (α=0.01)
(Intercept)	94.892	5.423	47	17.498	0.000	
PtBEBT (*PtACT49*) RNAi	-11.421	7.669	8	-1.489	0.175	No
Empty Vector Control	1.284	7.669	8	0.167	0.871	No
DKD RNAi	-42.257	7.669	8	-5.510	0.060	No
PtSABT (*PtACT47*) RNAi	-32.727	7.669	8	-4.267	0.027	No

One way ANOVA:

	numDF	denDF	F-value	p-value	Significant? (α=0.01)
(Intercept)	1	47	1030.848	<.0001	-
RNAi Treatment	4	8	13.088	0.040	No

Old leaves

Total PGs

	Value	Std.Error	DF	t-value	p-value	Significant? (α=0.01)
(Intercept)	105.807	4.065	47	26.027	0.000	-
PtBEBT (*PtACT49*) RNAi	-8.943	5.749	8	-1.555	0.158	No
Empty Vector Control	-5.730	5.749	8	-0.997	0.348	No
DKD RNAi	-35.403	5.749	8	-6.158	0.000	Yes
PtSABT (*PtACT47*) RNAi	-40.313	5.749	8	-7.012	0.000	Yes

One way ANOVA:

	numDF	denDF	F-value	p-value	Significant? (α=0.01)
(Intercept)	1	47	2328.581	<.0001	-
RNAi Treatment	4	8	20.533	0.000	Yes

Stems

Total PGs

	Value	Std.Error	DF	t-value	p-value	Significant? (α=0.01)
(Intercept)	9.276	2.578	47	3.598	0.001	-
PtBEBT (*PtACT49*) RNAi	0.402	3.654	8	0.110	0.915	No
Empty Vector Control	-1.038	3.646	8	-0.285	0.783	No
DKD RNAi	1.924	3.646	8	0.528	0.612	No
PtSABT (*PtACT47*) RNAi	-2.245	4.128	8	-0.544	0.601	No

One way ANOVA:

	numDF	denDF	F-value	p-value	Significant? (α=0.01)
(Intercept)	1	47	59.520	<.0001	-
RNAi Treatment	4	8	0.307	0.866	No

Roots

Total PGs

	Value	Std.Error	DF	t-value	p-value	Significant? (α=0.01)
(Intercept)	10.203	2.836	47	3.957	0.001	-
PtBEBT (*PtACT49*) RNAi	0.443	4.020	8	0.121	1.007	No
Empty Vector Control	-1.141	4.011	8	-0.313	0.862	No
DKD RNAi	2.117	4.011	8	0.580	0.673	No
PtSABT (*PtACT47*) RNAi	-2.470	4.541	8	-0.598	0.662	No

One way ANOVA:

	numDF	denDF	F-value	p-value	Significant? (α=0.01)
(Intercept)	1	47	65.472	<.0001	-
RNAi Treatm	4	8	0.338	0.952	No

[Total PGs] by RNAi line in old leaves

Analysis of indivual lines was achieved using SAS JMP software for a one-way ANOVA and comparison of means using a student t test of the concentration of [Total PGs] (mg g fr. wt) versus independent line in old leaves where a significant treatment effect was previously detected using a Linear Mixed Effect (LME) function with a Restricted Maximum Likelihood (REML) method with R software.

Analysis of Variance

Source	DF	Sum of Squares	Mean Square	F Ratio	Prob > F
Line	14	748.0089	53.4292	7.0736	<.0001
Error	45	339.8984	7.5533		
C. Total	59	1087.9073			

Means Comparisons
Comparisons for each pair using Student's t

Level		Mean
Wild type_3	A	21.900000
Empty Vector Control_6	A	21.570000
PtBEBT (PtACT49) RNAi_11	A	20.982500

Level						Mean
Wild type_1	A	B				20.960000
Wild type_2	A	B				20.622500
Empty Vector Control_11	A	B				19.282500
Empty Vector Control_9	A	B				19.195000
PtBEBT (PtACT49) RNAi_8	A	B				18.905000
PtBEBT (PtACT49) RNAi_9	A	B	C			18.230000
DKD RNAi_10		B	C			16.700000
PtSABT (PtACT47) RNAi_9		B	C	D		16.725000
DKD RNAi_4			C	D	E	15.247500
PtSABT (PtACT47) RNAi_2				D	E	13.010000
PtSABT (PtACT47) RNAi_4					E	12.532500
DKD RNAi_2					E	11.525000

Levels not connected by same letter are significantly different.

Conclusion, *PtSABT* (*PtACT47*) RNAi line 2 and 4, and DKD RNAi 2 and 4 have significantly lower [total PGs] compared to empty vector controls and wild types.

A6.6.2. [Individual PGs] (mg g^{-1} fr wt) versus RNAi treatment type calculated for each tissue type.

Analysis of [Individual PG] (mg g fr. wt-1) versus RNAi treatment type in various tissues using a Linear Mixed Effect (LME) function with a Restricted Maximum Likelihood (REML) method. This can test if each RNAi treatment had a significant effect on PG content for all three independent lines combined. A one-way ANOVA is also included to test if RNAi treatments have a significant effect overall. P values <0.01 are considered significant.

Young leaves

Salicin

	Value	Std.Error	DF	t-value	p-value	Significant? (α=0.01)
(Intercept)	16.358	2.042	47	8.009	0.000	-
PtBEBT (*PtACT49*) RNAi	-2.405	2.888	8	-0.833	0.429	No
Empty Vector Control	1.968	2.888	8	0.681	0.515	No
DKD RNAi	-4.214	2.888	8	-1.459	0.183	No
PtSABT (*PtACT47*) RNAi	-5.600	2.888	8	-1.939	0.089	No

One way ANOVA:

	numDF	denDF	F-value	p-value	Significant? (α=0.01)
(Intercept)	1	47	245.377	<.0001	-
RNAi Treatment	4	8	2.263	0.151	No

Salicortin

	Value	Std.Error	DF	t-value	p-value	Significant? (α=0.01)
(Intercept)	26.007	1.713	47	15.185	0.000	-
PtBEBT (*PtACT49*) RNAi	-0.933	2.422	8	-0.385	0.710	No
Empty Vector Control	-0.939	2.422	8	-0.388	0.708	No
DKD RNAi	-7.313	2.422	8	-3.019	0.017	No
PtSABT (*PtACT47*) RNAi	-5.776	2.422	8	-2.385	0.044	No

One way ANOVA:

	numDF	denDF	F-value	p-value	Significant? (α=0.01)
(Intercept)	1	47	902.910	<.0001	-
RNAi Treatment	4	8	3.735	0.053	No

Tremuloidin

	Value	Std.Error	DF	t-value	p-value	Significant? (α=0.01)
(Intercept)	3.252	1.334	47	2.438	0.019	-
PtBEBT (*PtACT49*) RNAi	1.989	1.886	8	1.054	0.323	No
Empty Vector Control	0.025	1.886	8	0.013	0.990	No
DKD RNAi	4.263	1.886	8	2.260	0.054	No
PtSABT (*PtACT47*) RNAi	6.325	1.886	8	3.353	0.011	No

One way ANOVA:

	numDF	denDF	F-value	p-value	Significant? (α=0.01)
(Intercept)	1	47	93.620	<.0001	-
RNAi Treatment	4	8	4.267	0.039	No

Tremulacin

	Value	Std.Error	DF	t-value	p-value	Significant? (α=0.01)
(Intercept)	29.702	2.224	47	13.355	0.000	-
PtBEBT (*PtACT49*) RNAi	1.185	3.145	8	0.377	0.716	No
Empty Vector Control	-1.961	3.145	8	-0.623	0.550	No
DKD RNAi	-3.324	3.145	8	-1.057	0.321	No
PtSABT (*PtACT47*) RNAi	-6.276	3.145	8	-1.995	0.081	No

One way ANOVA:

	numDF	denDF	F-value	p-value	Significant? (α=0.01)
(Intercept)	1	47	771.491	<.0001	-
RNAi Treatment	4	8	1.726	0.237	No

Medium leaves

Salicin

	Value	Std.Error	DF	t-value	p-value	Significant? (α=0.01)
(Intercept)	16.593	1.489	47	11.144	0.000	-
PtBEBT (*PtACT49*) RNAi	-6.349	2.106	8	-3.015	0.017	No
Empty Vector Control	0.398	2.106	8	0.189	0.855	No
DKD RNAi	-7.833	2.106	8	-3.720	0.059	No
PtSABT (*PtACT47*) RNAi	-6.698	2.106	8	-3.181	0.013	No

One way ANOVA:

	numDF	denDF	F-value	p-value	Significant? (α=0.01)
(Intercept)	1	47	352.224	<.0001	-
RNAi Treatment	4	8	7.080	0.097	No

Salicortin

	Value	Std.Error	DF	t-value	p-value	Significant? (α=0.01)
(Intercept)	43.917	3.897	47	11.270	0.000	-
PtBEBT (*PtACT49*) RNAi	4.790	5.511	8	0.869	0.410	No
Empty Vector Control	1.544	5.511	8	0.280	0.786	No
DKD RNAi	-22.344	5.511	8	-4.055	0.004	Yes
PtSABT (*PtACT47*) RNAi	-15.811	5.511	8	-2.869	0.002	Yes

One way ANOVA:

	numDF	denDF	F-value	p-value	Significant? (α=0.01)
(Intercept)	1	47	464.378	<.0001	-
RNAi Treatment	4	8	9.419	0.004	Yes

Tremuloidin

	Value	Std.Error	DF	t-value	p-value	Significant? (α=0.01)
(Intercept)	4.621	0.967	47	4.7779	0.0000	-
PtBEBT (*PtACT49*) RNAi	-0.008	1.368	8	-0.0055	0.9958	No
Empty Vector Control	-1.101	1.368	8	-0.8049	0.4442	No
DKD RNAi	0.014	1.368	8	0.0104	0.9920	No
PtSABT (*PtACT47*) RNAi	0.494	1.466	8	0.3371	0.7447	No

One way ANOVA:

	numDF	denDF	F-value	p-value	Significant? (α=0.01)
(Intercept)	1	47	101.963	<.0001	-
RNAi Treatment	4	8	0.346	0.840	No

Tremulacin

	Value	Std.Error	DF	t-value	p-value	Significant? (α=0.01)
(Intercept)	29.763	2.107	47	14.125	0.000	-
PtBEBT (*PtACT49*) RNAi	-9.855	2.980	8	-3.307	0.021	No
Empty Vector Control	0.441	2.980	8	0.148	0.886	No
DKD RNAi	-12.098	2.980	8	-4.060	0.036	No
PtSABT (*PtACT47*) RNAi	-10.715	3.055	8	-3.507	0.080	No

One way ANOVA:

	numDF	denDF	F-value	p-value	Significant? (α=0.01)
(Intercept)	1	47	605.135	<.0001	-
RNAi Treatment	4	8	8.392	0.058	No

Old leaves

Salicin

	Value	Std.Error	DF	t-value	p-value	Significant? (α=0.01)
(Intercept)	12.463	1.366	47	9.127	0.000	-
PtBEBT (*PtACT49*) RNAi	-1.088	1.931	8	-0.564	0.589	No
Empty Vector Control	-0.618	1.931	8	-0.320	0.757	No
DKD RNAi	-1.838	1.931	8	-0.952	0.369	No
PtSABT (*PtACT47*) RNAi	-1.240	1.931	8	-0.642	0.539	No

One way ANOVA:

	numDF	denDF	F-value	p-value	Significant? (α=0.01)
(Intercept)	1	47	355.012	<.0001	-
RNAi Treatment	4	8	0.255	0.898	No

Salicortin

	Value	Std.Error	DF	t-value	p-value	Significant? (α=0.01)
(Intercept)	58.525	4.451	47	13.147	0.000	-
PtBEBT (*PtACT49*) RNAi	-1.971	6.295	8	-0.313	0.762	No
Empty Vector Control	5.513	6.295	8	0.876	0.407	No
DKD RNAi	-25.966	6.295	8	-4.125	0.003	Yes
PtSABT (*PtACT47*) RNAi	-28.277	7.827	8	-3.613	0.007	Yes

One way ANOVA:

	numDF	denDF	F-value	p-value	Significant? (α=0.01)
(Intercept)	1	47	576.291	<.0001	-
RNAi Treatment	4	8	10.122	0.003	Yes

Tremuloidin

	Value	Std.Error	DF	t-value	p-value	Significant? (α=0.01)
(Intercept)	12.655	3.681	47	3.438	0.001	-
PtBEBT (*PtACT49*) RNAi	-7.514	5.205	8	-1.444	0.187	No
Empty Vector Control	-5.305	5.205	8	-1.019	0.338	No
DKD RNAi	-7.453	5.205	8	-1.432	0.190	No
PtSABT (*PtACT47*) RNAi	-7.990	6.110	8	-1.308	0.227	No

One way ANOVA:

	numDF	denDF	F-value	p-value	Significant? (α=0.01)
(Intercept)	1	47	17.598	0.000	-
RNAi Treatment	4	8	0.769	0.575	No

Tremulacin

	Value	Std.Error	DF	t-value	p-value	Significant? (α=0.01)
(Intercept)	22.163	2.358	47	9.400	0.000	-
PtBEBT (*PtACT49*) RNAi	1.631	3.334	8	0.489	0.638	No
Empty Vector Control	-5.318	3.334	8	-1.595	0.149	No
DKD RNAi	-0.151	3.334	8	-0.045	0.965	No
PtSABT (*PtACT47*) RNAi	-2.806	3.334	8	-0.841	0.425	No

One way ANOVA:

	numDF	denDF	F-value	p-value	Significant? (α=0.01)
(Intercept)	1	47	390.398	<.0001	-
RNAi Treatment	4	8	1.350	0.332	No

Stems

Salicin

	Value	Std.Error	DF	t-value	p-value	Significant? (α=0.01)
(Intercept)	2.048	0.753	47	2.719	0.009	-
PtBEBT (*PtACT49*) RNAi	-0.013	1.067	8	-0.012	0.990	No
Empty Vector Control	-0.283	1.065	8	-0.266	0.797	No
DKD RNAi	1.281	1.065	8	1.203	0.264	No
PtSABT (*PtACT47*) RNAi	0.273	1.156	8	0.236	0.820	No

One way ANOVA:

	numDF	denDF	F-value	p-value	Significant? (α=0.01)
(Intercept)	1	47	44.053	<.0001	-
RNAi Treatment	4	8	0.652	0.642	No

Salicortin

	Value	Std.Error	DF	t-value	p-value	Significant? (α=0.01)
(Intercept)	3.531	0.680	47	5.195	0.000	-
PtBEBT (*PtACT49*) RNAi	1.334	0.963	8	1.385	0.203	No
Empty Vector Control	-0.540	0.961	8	-0.562	0.590	No
DKD RNAi	-0.166	0.961	8	-0.173	0.867	No
PtSABT (*PtACT47*) RNAi	-1.117	1.067	8	-1.046	0.326	No

One way ANOVA:

	numDF	denDF	F-value	p-value	Significant? (α=0.01)
(Intercept)	1	47	123.991	<.0001	-
RNAi Treatment	4	8	1.587	0.268	No

Tremuloidin

	Value	Std.Error	DF	t-value	p-value	Significant? (α=0.01)
(Intercept)	1.393	0.348	47	4.007	0.000	
PtBEBT (*PtACT49*) RNAi	-1.051	0.493	8	-2.132	0.066	No
Empty Vector Control	0.016	0.492	8	0.032	0.975	No
DKD RNAi	0.023	0.492	8	0.046	0.965	No
PtSABT (*PtACT47*) RNAi	-0.983	0.629	8	-1.563	0.157	No

One way ANOVA:

	numDF	denDF	F-value	p-value	Significant? (α=0.01)
(Intercept)	1	47	41.91552	<.0001	-
RNAi Treatment	4	8	2.18101	0.1616	No

Tremulacin

	Value	Std.Error	DF	t-value	p-value	Significant? (α=0.01)
(Intercept)	2.307	1.115	47	2.068	0.044	-
PtBEBT (*PtACT49*) RNAi	0.135	1.580	8	0.085	0.934	No
Empty Vector Control	-0.235	1.577	8	-0.149	0.885	No
DKD RNAi	0.784	1.577	8	0.497	0.633	No
PtSABT (*PtACT47*) RNAi	-0.418	1.736	8	-0.241	0.816	No

One way ANOVA:

	numDF	denDF	F-value	p-value	Significant? (α=0.01)
(Intercept)	1	47	21.554	<.0001	-
RNAi Treatment	4	8	0.156	0.955	No

Roots

Salicin

	Value	Std.Error	DF	t-value	p-value	Significant? (α=0.01)
(Intercept)	2.252	0.828	47	2.991	0.010	-
PtBEBT (*PtACT49*) RNAi	-0.015	1.173	8	-0.014	1.089	No
Empty Vector Control	-0.312	1.172	8	-0.293	0.877	No
DKD RNAi	1.409	1.172	8	1.323	0.290	No
PtSABT (*PtACT47*) RNAi	0.300	1.272	8	0.259	0.902	No

One way ANOVA:

	numDF	denDF	F-value	p-value	Significant? (α=0.01)
(Intercept)	1	47	48.459	<.0001	-
RNAi Treatn	4	8	0.717	0.706	No

Salicortin

	Value	Std.Error	DF	t-value	p-value	Significant? (α=0.01)
(Intercept)	3.884	0.748	47	5.715	0.000	-
PtBEBT (*PtACT49*) RNAi	1.467	1.059	8	1.524	0.224	No
Empty Vector Control	-0.594	1.057	8	-0.618	0.649	No
DKD RNAi	-0.182	1.057	8	-0.190	0.954	No
PtSABT (*PtACT47*) RNAi	-1.228	1.174	8	-1.151	0.359	No

One way ANOVA:

	numDF	denDF	F-value	p-value	Significant? (α=0.01)
(Intercept)	1	47	136.391	<.0001	-
RNAi Treatn	4	8	1.745	0.295	No

Tremuloidin

	Value	Std.Error	DF	t-value	p-value	Significant? (α=0.01)
(Intercept)	1.533	0.382	47	4.408	0.000	
PtBEBT (*PtACT49*) RNAi	-1.156	0.542	8	-2.345	0.072	No
Empty Vector Control	0.017	0.541	8	0.035	1.073	No
DKD RNAi	0.025	0.541	8	0.050	1.061	No
PtSABT (*PtACT47*) RNAi	-1.082	0.692	8	-1.719	0.172	No

One way ANOVA:

	numDF	denDF	F-value	p-value	Significant? (α=0.01)
(Intercept)	1	47	46.107	<.0001	-
RNAi Treatn	4	8	2.399	0.178	No

Tremulacin

	Value	Std.Error	DF	t-value	p-value	Significant? (α=0.01)
(Intercept)	2.537	1.227	47	2.275	0.049	-
PtBEBT (*PtACT49*) RNAi	0.148	1.738	8	0.094	1.028	No
Empty Vector Control	-0.259	1.735	8	-0.164	0.974	No
DKD RNAi	0.863	1.735	8	0.547	0.696	No
PtSABT (*PtACT47*) RNAi	-0.459	1.909	8	-0.265	0.898	No

One way ANOVA:

	numDF	denDF	F-value	p-value	Significant? (α=0.01)
(Intercept)	1	47	23.709	<.0001	-
RNAi Treatn	4	8	0.172	1.050	No

A.6.6.3. Statistical analysis testing for a significant effect of RNAi in individual lines for [salicortin] (mg g^{-1} fr. wt).

Only samples where a significant effect of genotype had been detected were included here. Analysis of indivual lines was achieved using SAS JMP software for a one-way ANOVA and comparison of means using a student t-test of the concentration of [salicortin] mg g fr. wt versus independent line.

[Salicortin] versus line in medium leaves - Oneway Anova

Analysis of Variance

Source	DF	Sum of Squares	Mean Square	F Ratio	Prob > F
Line	14	325.25827	23.2327	2.9842	0.0027
Error	45	350.33370	7.7852		
C. Total	59	675.59197			

Means Comparisons
Comparisons for each pair using Student's t

Level						Mean
PtBEBT (PtACT49) RNAi_11	A					11.090000
PtBEBT (PtACT49) RNAi_9	A	B				10.412500
Wild type_2	A	B				10.217500
Empty Vector Control_11	A	B	C			9.635000
Empty Vector Control_6	A	B	C			9.017500
Empty Vector Control_9	A	B	C			8.627500
Wild type_3	A	B	C	D		8.245000
Wild type_1	A	B	C	D		7.887500
PtBEBT (PtACT49) RNAi_8	A	B	C	D	E	7.720000
PtSABT (PtACT47) RNAi_4		B	C	D	E	6.712500
PtSABT (PtACT47) RNAi_2			C	D	E	5.695000
DKD RNAi_2				D	E	4.562500
DKD RNAi 10				D	E	4.455000
DKD RNAi_4					E	4.197500
PtSABT (PtACT47) RNA_9					E	4.185000

Levels not connected by same letter are significantly different.

Conclusion, lines PtSABT (PtACT47) RNAi 9 and DKD RNAi 4 have significantly lower salicortin concentrations than wild types and empty vector controls.

[Salicortin] versus line in old leaves - Oneway Anova

Analysis of Variance

Source	DF	Sum of Squares	Mean Square	F Ratio	Prob > F
Line	14	612.00677	43.7148	11.7941	<.0001
Error	45	166.79252	3.7065		
C. Total	59	778.79930			

Means Comparisons
Comparisons for each pair using Student's t

Level						Mean
Empty Vector Control_6	A					15.122500
Wild type_3	A	B				13.580000
Wild type_1	A	B				12.992500
PtBEBT (PtACT49) RNAi_11	A	B				12.660000
Empty Vector Control_11		B	C			11.972500
PtBEBT (PtACT49) RNAi_8		B	C			11.402500
Empty Vector Control_9		B	C			11.330000
Wild type_2			C	D		9.870000
PtBEBT (PtACT49) RNAi_9				D	E	8.540000

Level					Mean
DKD RNAi_10	D	E	F		7.612500
PtSABT (PtACT47) RNAi_9	D	E	F		7.610000
DKD RNAi_4	D	E	F	G	6.227500
PtSABT (PtACT47) RNAi_4		E	F	G	5.885000
DKD RNAi_2			F	G	5.695000
PtSABT (PtACT47) RNAi_2				G	4.652500

Levels not connected by same letter are significantly different.

Conclusion, lines *PtSABT* RNAi 4, 2, and DKD RNAi 2 have significantly lower salicortin concentrations compared with wild types and empty vector controls.

A.6.6.4. Statistical analysis of phenolic peaks from transgenic RNAi plants.

A one-way ANOVA and student t-test for comparison of means was performed on individual chromatographic peaks from the phenolic extracts of transgenic RNAi and control plants. Only extracts from old leaves were included in this analysis since a significant effect in salicortin concentration was detected in PtSABT and DKD lines (Figure 3.20, and 3.21). Data used for the analysis was the mean intergrated peak areas normalized by dividing them by the sample mass (mg fr. wt). Analysis was performed using SAS JMP software. For each treatment, data from the three independent lines was combined. Peaks that showed significant differences between treatments are shown below.

Peak # 2 By RNAi treatment - Oneway Anova

Analysis of Variance

Source	DF	Sum of Squares	Mean Square	F Ratio	Prob > F
RNA i treatment	4	1099970102	274992525	2.2694	0.8761
Error	55	1232707015	22412855		
C. Total	59	2332677116			

Means Comparisons
Comparisons for each pair using Student's t

Level		Mean
Empty Vector Control	A	14586.233
PtBEBT (PtACT49) RNAi	A	14517.710
DKD RNAi	A	14234.883
Wild type	A	14085.992
PtSABT (PtACT47) RNAi	A	13666.000

Levels not connected by same letter are significantly different.

Conclusions, the normalized peak area of peak 2 is not significantly different between treatments.

Peak # 3 (Chlorogenic acid-2) By RNAi treatment - Oneway Anova

Analysis of Variance

Source	DF	Sum of Squares	Mean Square	F Ratio	Prob > F
RNA i treatment	4	353981935	88495484	1.1381	0.3483
Error	55	4276611529	77756573		
C. Total	59	4630593463			

Means Comparisons
Comparisons for each pair using Student's t

Level		Mean
PtSABT (PtACT47) RNAi	A	42578.758
Wild type	A	37805.875
Empty Vector Control	A	36144.342
PtBEBT (PtACT49) RNAi	A	36103.011
DKD RNAi	A	35948.150

Levels not connected by same letter are significantly different.

Conclusion, the normalized peak area of peak 3 is not significantly different between treatments.

Peak # 4 By RNAi treatment - Oneway Anova

Analysis of Variance

Source	DF	Sum of Squares	Mean Square	F Ratio	Prob > F
RNA i treatment	4	55826574	13956644	12.6055	<.0001
Error	55	60895167	1107184.9		
C. Total	59	116721741			

Means Comparisons
Comparisons for each pair using Student's t

Level			Mean
Empty vector control	A		3512.0667
PtBEBT (PtACT49) RNAi	A		3402.3001
Wild type	A		3308.8583
PtSABT (PtACT47) RNAi		B	1885.5333
DKD RNAi		B	1753.7000

Levels not connected by same letter are significantly different.

Conclusion, the normalized peak area of Peak 4 was significantly less in *PtSABT* (*PtACT47*) RNAi and DKD RNAi plants compared to wild type plants.

Peak # 5 (Catechin) By RNAi treatment - Oneway Anova

Analysis of Variance

Source	DF	Sum of Squares	Mean Square	F Ratio	Prob > F
RNA i treatment	4	108398151	27099538	1.9267	0.7188
Error	55	379573387	6901334.3		
C. Total	59	487971538			

Means Comparisons
Comparisons for each pair using Student's t

Level		Mean
PtBEBT (PtACT49) RNAi	A	9132.908
Wild type	A	9000.025
Empty Vector Control	A	8645.617
PtSABT (PtACT47) RNAi	A	8478.650
DKD RNAi	A	7926.317

Levels not connected by same letter are significantly different.

Conclusion, the normalized peak area of peak 5 is not significantly different between treatments.

Peak # 6 (Chlorogenic acid-1) By RNAi treatment - Oneway Anova

Analysis of Variance

Source	DF	Sum of Squares	Mean Square	F Ratio	Prob > F
RNA i treatment	4	840595773	210148943	2.5299	0.0507
Error	55	4568613115	83065693		
C. Total	59	5409208888			

Means Comparisons
Comparisons for each pair using Student's t

Level		Mean
DKD RNAi	A	43232.608
Wild type	A	40818.683
PtBEBT (PtACT49) RNAi	A	40205.103
Empty Vector Control	A	39341.108
PtSABT (PtACT47) RNAi	A	38949.258

Levels not connected by same letter are significantly different.

Conclusion, the normalized peak area of peak 6 is not significantly different between treatments.

Peak # 7 By RNAi treatment - Oneway Anova

Analysis of Variance

Source	DF	Sum of Squares	Mean Square	F Ratio	Prob > F
RNA i treatment	4	47035307	11758827	2.8377	0.0828
Error	55	227909558	4143810.1		
C. Total	59	274944865			

Means Comparisons
Comparisons for each pair using Student's t

Level		Mean
Empty Vector Control	A	5463.4167
PtSABT (PtACT47) RNAi	A	5358.8917
Wild type	A	5106.7417
PtBEBT (PtACT49) RNAi	A	5059.1667
DKD RNAi	A	4441.8083

Levels not connected by same letter are significantly different.

Conclusion, the normalized peak area of peak 7 is not significantly different between treatments.

Peak # 8 By RNAi treatment - Oneway Anova

Analysis of Variance

Source	DF	Sum of Squares	Mean Square	F Ratio	Prob > F
RNA i treatment	4	8513547	2128387	1.2974	0.2824
Error	55	90230858	1640561		
C. Total	59	98744405			

Means Comparisons
Comparisons for each pair using Student's t

Level		Mean
Empty Vector Control	A	5146.2500
Wild type	A	5136.0500
PtBEBT (PtACT49) RNAi	A	4923.8500

Level		Mean
PtSABT (PtACT47) RNAi	A	4839.2333
DKD RNAi	A	4802.9750

Levels not connected by same letter are significantly different.

Conclusion, the normalized peak area of peak 8 is not significantly different between treatments.

Peak # 9 By RNAi treatment - Oneway Anova

Analysis of Variance

Source	DF	Sum of Squares	Mean Square	F Ratio	Prob > F
RNA i treatment	4	33728950	8432237	1.9308	0.1182
Error	55	240201509	4367300		
C. Total	59	273930458			

Means Comparisons
Comparisons for each pair using Student's t

Level			Mean
Empty Vector Control	A		6290.5417
PtBEBT (PtACT49) RNAi	A		5984.3417
Wild type	A	B	5591.2000
PtSABT (PtACT47) RNAi	A	B	5404.9417
DKD RNAi		B	4079.2750

Levels not connected by same letter are significantly different.

Conclusion, the normalized peak area of peak 9 is significantly less in DKD RNAi plants.

Peak # 10 By RNAi treatment - Oneway Anova

Analysis of Variance

Source	DF	Sum of Squares	Mean Square	F Ratio	Prob > F
RNA i treatment	4	134494040	33623510	2.7998	0.0846
Error	55	660511266	12009296		
C. Total	59	795005306			

Means Comparisons
Comparisons for each pair using Student's t

Level		Mean
Wild type	A	11194.425
PtBEBT (PtACT49) RNAi	A	11017.925
DKD RNAi	A	10482.883
PtSABT (PtACT47) RNAi	A	10414.433
Empty Vector Control	A	10617.950

Levels not connected by same letter are significantly different.

Conclusion, the normalized peak area of peak 10 is not significantly different between treatments.

Peak # 12 By RNAi treatment - Oneway Anova

Analysis of Variance

Source	DF	Sum of Squares	Mean Square	F Ratio	Prob > F
RNA i treatment	4	30376384	7594096	1.5463	0.0921
Error	55	117776189	2141385		
C. Total	59	148152573			

Means Comparisons
Comparisons for each pair using Student's t

Level		Mean
DKD RNAi	A	8605.2000
PtSABT (PtACT47) RNAi	A	8333.5250
Wild type	A	7738.1583
PtBEBT (PtACT49) RNAi	A	7632.4167
Empty Vector Control	A	7571.4250

Levels not connected by same letter are significantly different.

Conclusion, the normalized peak area of peak 12 is not significantly different between treatments.

Peak # 13 By RNAi treatment - Oneway Anova

Analysis of Variance

Source	DF	Sum of Squares	Mean Square	F Ratio	Prob > F
RNA i treatment	4	415039974	103759994	3.8158	0.0289
Error	55	837294748	15223541		
C. Total	59	1252334722			

Means Comparisons
Comparisons for each pair using Student's t

Level		Mean
Empty Vector Control	A	14838.875
DKD RNAi	A	13803.350
Wild type	A	12644.925
PtBEBT (PtACT49) RNAi	A	12006.342
PtSABT (PtACT47) RNAi	A	11026.358

Levels not connected by same letter are significantly different.

Conclusion, the normalized peak area of peak 13 is not significantly different between treatments.

Peak # 14 By RNAi treatment - Oneway Anova

Analysis of Variance

Source	DF	Sum of Squares	Mean Square	F Ratio	Prob > F
RNA i treatment	4	147198689	36799672	2.9602	0.1745
Error	55	408048095	7419056.3		
C. Total	59	555246784			

Means Comparisons
Comparisons for each pair using Student's t

Level		Mean
Wild type	A	10261.600
PtSABT (PtACT47) RNAi	A	9874.867
DKD RNAi	A	9748.950
PtBEBT (PtACT49) RNAi	A	9643.650
Empty Vector Control	A	9576.575

Levels not connected by same letter are significantly different.

Conclusion, the normalized peak area of peak 14 is not significantly different between treatments.

Peak # 15 By RNAi treatment - Oneway Anova

Analysis of Variance

Source	DF	Sum of Squares	Mean Square	F Ratio	Prob > F
RNA i treatment	4	185887150	46471787	2.3757	0.3814
Error	55	584118834	10620342		
C. Total	59	770005983			

Means Comparisons
Comparisons for each pair using Student's t

Level		Mean
DKD RNAi	A	13332.342
Empty Vector Control	A	11959.150
PtSABT (PtACT47) RNAi	A	11940.667
Wild type	A	11546.083
PtBEBT (PtACT49) RNAi	A	10875.325

Levels not connected by same letter are significantly different.

Conclusion, the normalized peak area of peak 15 is not significantly different between treatments.

Peak # 16 By RNAi treatment - Oneway Anova

Analysis of Variance

Source	DF	Sum of Squares	Mean Square	F Ratio	Prob > F
RNA i treatment	4	1024032076	256008019	1.8285	0.1364
Error	55	7700365276	140006641		
C. Total	59	8724397353			

Means Comparisons
Comparisons for each pair using Student's t

Level		Mean
PtSABT (PtACT47) RNAi	A	31295.842
PtBEBT (PtACT49) RNAi	A	29352.015
Wild type	A	27829.575
Empty Vector Control	A	26732.700
DKD RNAi	A	26379.750

Levels not connected by same letter are significantly different.

Conclusion, the normalized peak area of peak 16 is not significantly different between treatments.

Peak # 17 By RNAi treatment - Oneway Anova

Analysis of Variance

Source	DF	Sum of Squares	Mean Square	F Ratio	Prob > F
RNA i treatment	4	378405009	94601252	5.9691	0.0005
Error	55	871664225	15848440		
C. Total	59	1250069234			

Means Comparisons
Comparisons for each pair using Student's t

Level			Mean
Empty Vector Control	A		13518.217
PtBEBT (PtACT49) RNAi	A		13422.725
Wild type	A		12021.392
PtSABT (PtACT47) RNAi		B	7587.508
DKD RNAi		B	7248.742

Levels not connected by same letter are significantly different.

Conclusion, the normalized peak area of Peak 17 was significantly less in PtSABT (PtACT47) RNAi and DKD RNAi plants compared to wild type plants.

Peak # 18 By RNAi treatment - Oneway Anova

Analysis of Variance

Source	DF	Sum of Squares	Mean Square	F Ratio	Prob > F
RNA i treatment	4	14729072	3682268	1.7280	0.1570
Error	55	117204430	2130990		
C. Total	59	131933502			

Means Comparisons
Comparisons for each pair using Student's t

Level		Mean
PtSABT (PtACT47) RNAi	A	4905.5167
DKD RNAi	A	4766.7583
Empty Vector Control	A	4691.5417
Wild type	A	4334.6833
PtBEBT (PtACT49) RNAi	A	4009.5183

Levels not connected by same letter are significantly different.

Conclusion, the normalized peak area of peak 18 is not significantly different between treatments.

Peak # 19 (Grandidentatin) By RNAi treatment - Oneway Anova

Analysis of Variance

Source	DF	Sum of Squares	Mean Square	F Ratio	Prob > F
RNA i treatment	4	688688030	172172007	66.7879	<.0001
Error	55	141784008	2577891.1		
C. Total	59	830472038			

Means Comparisons
Comparisons for each pair using Student's t

Level			Mean
Empty Vector Control	A		12841.458
PtBEBT (PtACT49) RNAi	A		11556.250
Wild type	A		11361.367
PtSABT (PtACT47) RNAi		B	6959.267
DKD RNAi		B	6791.725

Levels not connected by same letter are significantly different.

Conclusion, the normalized peak area of Peak 17 was significantly less in PtSABT (PtACT47) RNAi and DKD RNAi plants compared to wild type plants.

Peak # 21 By RNAi treatment - Oneway Anova

Analysis of Variance

Source	DF	Sum of Squares	Mean Square	F Ratio	Prob > F
RNA i treatment	4	2586321	646580	1.5849	0.1141
Error	55	9919794	180360		
C. Total	59	12506115			

Means Comparisons
Comparisons for each pair using Student's t

Level		Mean
PtBEBT (PtACT49) RNAi	A	3111.3000
Empty Vector Control	A	3064.4167
PtSABT (PtACT47) RNAi	A	2967.5583

Level		Mean
DKD RNAi	A	2842.4000
Wild type	A	2804.8417

Levels not connected by same letter are significantly different.

Conclusion, the normalized peak area of peak 21 is not significantly different between treatments.

Peak # 22 By RNAi treatment - Oneway Anova

Analysis of Variance

Source	DF	Sum of Squares	Mean Square	F Ratio	Prob > F
RNA i treatment	4	83564195	20891049	1.8122	0.1396
Error	55	634044699	11528085		
C. Total	59	717608894			

Means Comparisons
Comparisons for each pair using Student's t

Level		Mean
PtSABT (PtACT47) RNAi	A	12681.425
PtBEBT (PtACT49) RNAi	A	11899.042
Wild type	A	11767.467
Empty Vector Control	A	11240.108
DKD RNAi	A	10590.550

Levels not connected by same letter are significantly different.

Conclusion, the normalized peak area of peak 22 is not significantly different between treatments.

Peak # 23 By RNAi treatment - Oneway Anova

Analysis of Variance

Source	DF	Sum of Squares	Mean Square	F Ratio	Prob > F
RNA i treatment	4	93387760	23346940	2.6028	0.0722
Error	55	229187390	4167043.5		
C. Total	59	322575150			

Means Comparisons
Comparisons for each pair using Student's t

Level		Mean
PtSABT (PtACT47) RNAi	A	11892.417
Empty Vector Control	A	11559.283
DKD RNAi	A	9857.583
PtBEBT (PtACT49) RNAi	A	9467.108
Wild type	A	9195.217

Levels not connected by same letter are significantly different.

Conclusion, the normalized peak area of peak 23 is not significantly different between treatments.